SUSANA DA COSTA SILVA MACHADO

CHARACTERIZATION OF TRIB2-MEDIATED DRUG RESISTANCE AND ITS VALIDATION AS A NOVEL DIAGNOSTIC MARKER

2021

SUSANA DA COSTA SILVA MACHADO

CHARACTERIZATION OF TRIB2-MEDIATED DRUG RESISTANCE AND ITS VALIDATION AS A NOVEL DIAGNOSTIC MARKER

PhD Programme in

Mechanisms of Disease and Regenerative Medicine

Work developed under the supervision of:

Dr Wolfgang Link

Dr Bibiana Ferreira

UNIVERSIDADE DO ALGARVE
DEPARTAMENTO DE CIÊNCIAS BIOMÉDICAS E MEDICINA

2021

CHARACTERIZATION OF TRIB2-MEDIATED DRUG RESISTANCE AND ITS VALIDATION AS A NOVEL DIAGNOSTIC MARKER

Declaração de autoria de trabalho

Declaro ser a autora deste trabalho, que é original e inédito. Autores e trabalhos consultados estão devidamente citados no texto e constam da listagem de referências incluída.

_____

Susana Machado

Dedicated to my family due to their continuous support, and Daniel for his encouragement and unconditional love

"From then on, my thesis hung over me like a curse, and with bloodshot eyes, I worked like a madman."

Natsume Sōseki, Kokoro

Acknowledgements

A terminar a tese de doutoramento resta-me registar os meus sinceros agradecimentos às pessoas que contribuiram de maneira diversa para que esta etapa se tornasse realidade.

Aos meus orientadores Wolfgang Link e Bibiana Ferreira pelo acompanhamento e estímulo durante o meu doutoramento.

Aos meus professores que me acompanham desde o mestrado, em especial ao Prof. Bragança pelo seu apoio e acompanhamento.

Aos meus pais Agostinho e Berta e ao meu irmão Rui, por serem o meu porto seguro e me acompanharem nas minhas aventuras.

A todos o meus colegas e ex-colegas, pelas vossas manifestações de solidariedade e encorajamento. À Vanessa Henriques, Andreia Lamy, Inês e João Santos, foi um prazer trabalhar com vocês no laboratório! Ao Gonçalo, Prata, Ricky e Joana (Inem), vocês foram excelentes colegas de laboratório e agradecida pela vossa amizade dentro e fora do laboratório.

Ao Gil e Ana Jesus, por me terem aturado numa fase muito difícil, e me terem ajudado em tudo! Sem vocês não tinha mantido o que restava da minha saúde mental!

Ao Tomás pelo teu apoio e longas conversas de nerds fantabolásticas. À Cristina, que me fizeste rir com as tuas histórias maravilhosas!

Aos meus amigos Mefis, Dudu, Yupi, Mi, Tijolo e Vanessa que me acompanham desde a licenciatura, e sempre me receberam de braços abertos.

Ao meu namorado Daniel, por sempre termos sido uma equipa, contra tudo e todos, e pelo suporte emocional. À Suki, a estrelinha no céu que me alegrava nos piores dias.

E a todos os meus amigos cujos nomes não se encontram mencionados, mas que vocês sabem quem são, e estiveram sempre disponíveis. Obrigada!!!

A todos o meu profundo agradecimento!

List of Publications

Publications produced during my PhD:

1. **Machado, S**.; Silva, A.; De Sousa-Coelho, A.L.; Duarte, I.; Grenho, I.; Santos, B.; Mayoral-Varo, V.; Megias, D.; Sánchez-Cabo, F.; Dopazo, A., et al. Harmine and Piperlongumine Revert TRIB2-Mediated Drug Resistance. *Cancers (Basel)* 2020, *12*, doi:10.3390/cancers12123689.
2. **Machado S**, Raposo C, Ferreira BI, Link W. Image-based Identification of Chemical Compounds Capable of Trapping FOXO in the Cell Nucleus. Methods Mol Biol. 2019;1890:163-170. doi:10.1007/978-1-4939-8900-3_14

3. Henriques V, **Machado S**, Link W, Ferreira BI. Monitoring the Transcriptional Activity of FOXO Transcription Factors by Analysing their Target Genes. Methods Mol Biol. 2019;1890:103-113. doi:10.1007/978-1-4939-8900-3_9

4. Cautain B, Castillo F, Musso L, Ferreira BI, de Pedro N, Rodriguez Quesada L, **Machado S**, Vicente F, Dallavalle S, Link W. Discovery of a Novel, Isothiazolonaphthoquinone-Based Small Molecule Activator of FOXO Nuclear-Cytoplasmic Shuttling. PLoS One. 2016;11(12):e0167491. Published 2016 Dec 9. doi:10.1371/journal.pone.0167491

5. Ferreira BI, Lie MK, Engelsen AST, **Machado S**, Link W, Lorens JB. Adaptive mechanisms of resistance to anti-neoplastic agents. Medchemcomm. 2016;8(1):53-66. Published 2016 Oct 21. doi:10.1039/c6md00394j

6. Hill R, Madureira PA, Ferreira B, Baptista I, **Machado S**, Colaço L, Dos Santos M, Liu N, Dopazo A, Ugurel S, Adrienn A, Kiss-Toth E, Isbilen M, Gure AO, Link W. TRIB2 confers resistance to anti-cancer therapy by activating the serine/threonine protein kinase AKT. Nat Commun. 2017;8:14687. Published 2017 Mar 9. doi:10.1038/ncomms14687

Publications 4 and 6 correspond to original articles performed in collaboration with colleagues under the supervision of Dr Wolfgang Link. Publication 5 corresponds to a review article in collaboration with colleagues under the supervision of Dr Wolfgang Link. Publications 2 and 3 correspond to review chapters in collaboration with lab members and the first author, respectively, under the supervision of Dr Wolfgang Link. Publication 1 is an original article reporting the results in this thesis.

Publications produced during my PhD unrelated to the PhD project:

Pinto, J.P.; Machado, R.S.R.; Magno, R.; Oliveira, D.V.; **Machado, S.**; Andrade, R.P.; Bragança, J.; Duarte, I.; Futschik, M.E. StemMapper: a curated gene expression database for stem cell lineage analysis. *Nucleic acids research* **2018**, *46*, D788-d793, doi:10.1093/nar/gkx921.

Awards

FCT PhD Fellowship- ProRegeM PhD Programme (PD/BD/114258/2016)

Abstract

Intrinsic and acquired resistance to conventional and targeted chemotherapeutics is the fundamental reason for treatment failure in many cancer patients. Identifying molecular mechanisms involved in drug resistance or sensitization to targeted therapy is of enormous clinical importance. Critical transcription factors such as forkhead box O (FOXO) proteins and p53 have been shown to mediate the action of multiple anti-cancer drugs. Our lab discovered a novel mechanism of drug resistance facilitated by TRIB2 by activating AKT and, consequently, the inactivation of both FOXO and p53. Furthermore, this lab has established TRIB2 as a potential biomarker for melanoma, and its expression correlated with disease stage (I-IV). As TRIB2 may potentially be used as a biomarker and confers resistance to several standard front-line therapeutics to treat melanoma, these results are extremely relevant for the clinical management of melanoma. While accounting for less than 5% of all skin cancer patients, melanoma is the deadliest form of skin cancer, responsible for over 90% of all skin cancer deaths.

Furthermore, metastatic melanoma incidence has increased over the past three decades, with a mortality rate that continues to rise faster than almost all other cancers. Genetic analyses of melanoma have uncovered several key pathways in disease onset and progression, most prominently are the Ras/Raf/MEK/ERK and the PI3K/AKT/FOXO signalling pathways. In the decades 70 and 80, the established treatment for metastatic melanoma included high-dose interleukin-2 or dacarbazine (DTIC) administration associated with response rates of between 10-20% with severe side effects during treatment. The limited success prompted investigators to further characterize and understand the disease, leading to the development of immunotherapy, namely immune checkpoint inhibitors (pembrolizumab, nivolumab and ipilimumab), and targeted therapy, namely the BRAF inhibitors vemurafenib and dabrafenib and the MEK inhibitor trametinib, which are approved to treat melanoma patients with mutated BRAF (about 50% of patients). Simultaneously, several PI3K, AKT, mTOR, and MEK inhibitors have been tested in clinical trials but, intrinsic or acquired resistance limits

the efficacy of all these treatments. Our lab has previously shown that the tumour suppressor FOXO is the central downstream transcriptional mediator of the PI3K/AKT pathway after PI3K inhibition, which is in accordance with other studies that also show that FOXOs are crucial for the anti-cancer action of several drugs, in particular, PI3K pathway inhibitors. Therefore, proteins capable of inactivating FOXO factors are good candidates for mediating tumour formation, progression and resistance to these agents. Strikingly, our lab previously established TRIB2 as an oncogenic protein that suppresses FOXO factors in melanoma and induces resistance to the dual PI3K/mTOR inhibitor BEZ235 (dactolisib). We hypothesize that TRIB2 mediates therapy resistance by altering the gene expression profile of the cells, and we can pharmacologically reverse these effects of TRIB2.

To characterize the downstream events of TRIB2 activity, we analyzed the gene expression profiles of isogenic cell lines with different TRIB2 statuses by RNA sequencing. Using a connectivity map-based computational approach, we identified drug-induced gene-expression profiles that invert the TRIB2-associated expression profile. The natural alkaloids harmine and piperlongumine produced inverse gene expression profiles and synergistically increased BEZ235-induced cell toxicity. Notably, both agents promote FOXO nuclear translocation without interfering with the nuclear export machinery and induce transcription of FOXO target genes. Our results highlight the great potential of this approach for drug repurposing and suggest that harmine and piperlongumine or similar compounds might help overcome TRIB2-mediated therapy resistance in cancer patients.

Keywords: TRIB2; cancer; drug resistance; FOXO; BEZ235; harmine; piperlongumine

Resumo

Os pacientes oncológicos sujeitos a quimioterapia convencional e dirigida, nem sempre obtêm um resultado clínico positivo. Uma das principais razões é a resistência ao tratamento intrínseca e adquirida. Como tal, é de extrema importância clínica identificar e caracterizar os mecanismos moleculares envolvidos na resistência ao tratamento oncológico e promover a resensitização do paciente à terapêutica dirigida.

Diversos factores de transcrição, dos quais as proteínas forkhead box O (FOXO) e p53 são as mais conhecidas, têm sido identificados como principais responsáveis pela modulação da eficácia de diversos fármacos anti-cancro. O nosso laboratório identificou previamente um novo mecanismo de resistência à terapêutica oncológica originada pela proteína TRIB2. O TRIB2 activa a proteína AKT, o que leva à inibição dos factores de transcrição FOXO e p53. Adicionalmente, o nosso laboratório demonstrou que o TRIB2 mostra potencial como biomarcador em melanoma, em que a expressão de TRIB2 correlaciona-se com o avançar do estadio da doença (I-IV). Tendo em conta que o TRIB2 poderá ser um biomarcador e também confere resistência a diversas estratégias terapêuticas no tratamento do melanoma, estes resultados são extremamente relevantes para o futuro da terapêutica em melanoma (a incidência de novos casos de melanoma nos Estados Unidos da America é de 73870). Embora só 5% dos pacientes com cancro de pele sejam diagnosticados com melanoma, esta doença é no entanto a mais fatal de todos os cancros de pele, responsável por mais de 90% de falecimentos de pacientes com cancro de pele.

Além do mais, a incidência de melanoma metastático tem aumentado nas últimas três décadas, caracterizada por uma taxa de mortalidade superior a todos os restantes cancros. Análises genéticas ao melanoma permitiram a identificação de diversas vias de sinalização envolvidas na origem e na progressão da doença, principalmente as vias de sinalização Ras/Raf/MEK/ERK e PI3K/AKT/FOXO. Nas décadas de 70 e 80, a terapêutica standard para o melanoma metastático incluía administração de doses elevadas de interleucina 2 or dacarbazina (DTIC), usualmente com taxas de resposta clínica positiva de 10 a 20%, mas como efeitos secundários severos durante o tratamento. A sua eficácia limitada impulsionou o estudo e a

caracterização da doença, o que levou ao surgimento de immunoterapia, nomeadamente inibidores de immune checkpoints (pembrolizumab, nivolumab e ipilimumab), e terapia dirigida, nomeadamente os inibidores de BRAF, como o vemurafenib e dabrafenib, e os inibidores de MEK como o trametinib, que se encontram-se aprovados para o tratamento de melanoma em pacientes com mutações em BRAF, que ocorrem em cerca de 50% dos pacientes diagnosticados com melanoma. Adicionalmente, também estão a ser estudados em ensaios clínicos, diversos inibidores the PI3K, AKT, mTOR e MEK, no entanto, a eficácia destas terapêuticas é de momento limitada devido à presença de resistência ao tratamento intrínsica e adquirida em diversos pacientes. Como tal, é necessário o desenvolvimento de novas estratégias terapêuticas, que visam reverter esta resistência.

O nosso laboratório demonstrou previamente que o suppressor de tumor FOXO é o principal mediador de transcrição regulado pela via sinalização PI3K/AKT, após a inibição de PI3K. Estes resultados encontram-se de acordo com a literatura que demonstra que os factores de transcrição FOXO são os principais moduladores da eficácia de fármacos, nomeadamente os inibidores da via de sinalização PI3K. Portanto, proteínas que sejam capazes de inactivar FOXO, são potenciais candidatos como responsáveis pela formação e progressão de tumores, e de aparecimento de resistência ao tratamento destas patologias.

Notavelmente, o nosso laboratório estabeleceu previamente TRIB2 como uma proteína oncogénica que inibe os factores de transcrição FOXO em melanoma, e outros estudos demonstraram que TRIB2 também se comporta como um oncogene em diversos tumores sólidos, como os cancros do pulmão, colorectal e fígado. Tanto o nosso laboratório como outros estudos, demonstrou-se que TRIB2 confere resistência a diversos fármacos para o tratamento de cancro, incluindo inibidores de PI3K/mTOR , gemcitabina, dacarbazina e temozolomida. A resistência mediada por TRIB2 é causada por activação de AKT por TRIB2. Mecanisticamente, TRIB2 tem preferência em se ligar directamente a AKT1 cataliticamente inactivo (resíduo treonina 308 não fosforilado), o que induz a fosforilação de AKT no resíduo serina 473 em células humanas, indicando o aumento da actividade catalítica de AKT. A activação de AKT via TRIB2, resulta na inibição de FOXO, o que por sua vez altera a expressão de

genes alvo de FOXO, incluindo a redução da expressão de genes envolvidos na regulação da apoptose. Consequentemente, a apoptose resultante da terapêutica oncológica, é diminuida na presença de elevados níveis de TRIB2. Um exemplo de um fármaco cuja eficácia é diminuida na presença de TRIB2, é o derivado de imidazoquinolina, conhecido como BEZ235. Este composto é um inibidor de PI3K e mTOR, que consiste numa molécula de baixo peso molecular que compete com o ATP pelo sítio cataliticamente activo nestas cinases. A eficácia de BEZ235 tem sido avaliada em vários ensaios clínicos, e muitos outros inibidores de PI3K e mTOR têm sido aprovados para uso clínico para vários tipos de cancro. Interferir com a actividade de TRIB2 poderá ser uma potencial estratégia terapêutica para o tratamento de vários tipos de cancro, especialmente no contexto de superar a resistência ao tratamento.

Neste estudo, pretendemos caracterizar os efeitos de TRIB2 a nível molecular e identificar estratégias farmacológicas que possam interferir com a sua actividade. Para avaliar a contribuição dos efeitos de TRIB2 em células humanas, procedemos à criação de linhas celulares humanas de osteosarcoma (U2OS) isogénicas, com níveis de expressão de TRIB2 elevada e baixa, respectivamente. Estas linhas celulares também foram tratadas com BEZ235 para avaliar os efeitos de TRIB2 na resistência ao tratamento. Seguidamente, procedemos à sequenciação de RNA para analisar o perfil de expressão génica induzido por TRIB2, nas células não tratadas e tratadas com BEZ235. A sobreexpressão de TRIB2 resultou na alteração da expressão de genes envolvidos na proliferação, apoptose e migração celulares, incluindo genes alvo de FOXO e p53. Na tentativa de identificar potenciais fármacos ou compostos que possam interferir na actividade de TRIB2, utilizámos o perfil de expressão génica induzido por TRIB2 para identificar compostos que induzissem um perfil de expressão génica oposto ao do TRIB2, utilizando uma ferramenta denominada de connectivity Map. Entre os compostos identificados, procedemos à validação dos compostos naturais alcalóides, harmina e piperlongumina, que não só apresentam um perfil de expressão génica oposta ao TRIB2, como também demonstraram um efeito sinérgico com o tratamento BEZ235, induzindo toxicidade cellular na presença de TRIB2, comparando com o tratamento BEZ235 sozinho. Notavelmente, harmina e a piperlongumina promoveram a translocação nuclear de FOXO, sem interferir com os mecanismos de exportação nuclear, e que foi consistente com FOXO sendo

transcripcionalmente activo, resultando na indução da transcrição de genes alvo de FOXO.

Os nossos resultados indicam o potencial desta estratégia terapêutica, recorrendo ao reaproveitamento de fármacos, e sugere que harmina, piperlongumina e outros compostos similares possam vir a ser úteis na clínica para superar a resistência induzida por TRIB2 no tratamento oncológico em pacientes.

Palavras-chave: TRIB2; cancro; resistência ao tratamento; FOXO; BEZ235; harmina; piperlongumina

Contents

List of figures

List of Tables

Abbreviations

1. INTRODUCTION

Introduction

1.1 Cancer

Cancer defines as a group of diseases that develops when some cells in the organism become old, abnormal or damaged. Instead of dying, they continue to proliferate and spread to nearby tissues [1]. In 2018, cancer was responsible for an estimated 9.6 million deaths worldwide, making it the number one cause of death worldwide, with lung, colorectal, stomach, liver and breast cancers the top causes of cancer death [2]. In Portugal, the cancers with the highest estimated age-standardized (ASR) incidence and mortality rates in 2018 were breast, prostate, colorectum and lung cancers, following the trend worldwide (Figure 1.1).

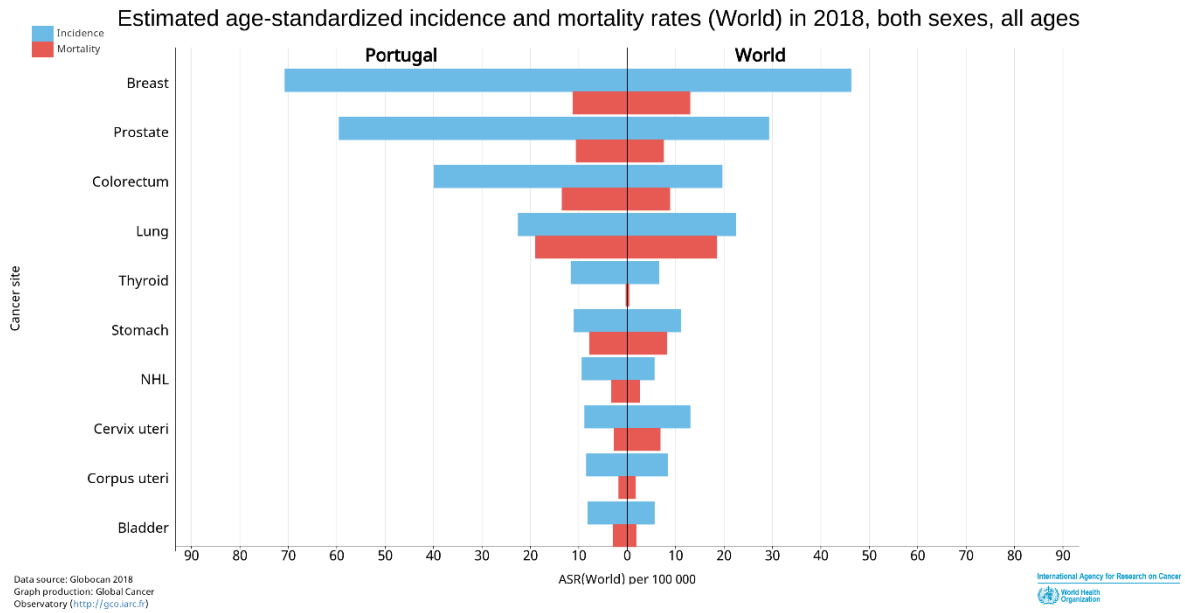

Figure 1.1. Incidence and mortality rates for various cancers in Portugal and Worldwide. Adapted from: World Health Organization (WHO). Data from "Cancer Today – IARC" from 2018. Accessed 4th June 2020.

Additionally, the worldwide economic burden is increasing significantly, with a total annual financial cost of cancer in 2010 reaching an estimated US$ 1.16 trillion [2]. Cause of death statistics help countries adjust priorities in their health systems, and thus, due to cancer mortality and economic burden, fighting and preventing cancer has become a priority worldwide to increase cancer prevention and treatment efficiency.

However, while progress in cancer screening, early diagnosis and treatment have been significant, cancer continues to be in the top causes of death worldwide [2]. Therefore, it is vital to continue understanding what causes cancer to prevent it, how it develops, and what cancer types exist to build more adequate treatments. Primary prevention consists of adopting lifestyles and health precautions to prevent or decrease the probability of developing a disease or injury, and avoiding or modifying exposure to risk factors can help reduce the cancer burden [2]. Cancer is very heterogenous and with geographical, economic, and social differences among countries. However, significant risk factors have been identified despite geographical nuances and include tobacco, alcohol, lack of sufficient physical activity, and an unhealthy diet. Risk factors include modifiable dietary risk factors, and their decreased exposure seems to correlate with reducing the probability of a diagnosis of cancer associated with these risks [3].

Cancer will become fatal if untreated and targets all types of tissues. The major histological types of cancer include carcinoma, sarcoma, melanoma, myeloma, lymphoma, leukaemia and mixed types, and depending on which cancer and its stage, treatment protocols will vary accordingly [4]. Cancer therapies vary according to the type of cancer and its stage. Thus, a cancer diagnosis is crucial to treating the patient accordingly, either curing the patient or prolonging and improving life quality [2]. Anti-cancer treatment includes destroying, controlling, and removing tumour tissue. The objective is to destroy tumours, prevent tumour reoccurrence and spread and relieve symptoms when all treatment options are depleted [5].

1.1.1 How cancer develops

Cancer develops when normal cells acquire several mutations in a multistep process that give them survival advantages, and their survival and proliferation is promoted by the altered microenvironment and eventually become malignant [6].

In 2000, Hanahan and Weinberg proposed six hallmarks of cancer that help explain how a normal cell can be responsible for cancer formation, and in 2011 added two emerging hallmarks of cancer and two enabling characteristics [7]. The six hallmarks of cancer comprise sustaining proliferative signalling, evading growth suppressors, resisting cell death, enabling replicative immortality, and activating invasion and metastasis. More recently, studies suggest that two additional emerging hallmarks are involved in at least some cancers, if not all of them, that deregulate cellular energetics and avoid immune destruction. Additionally, the two enabling characteristics (genome instability and mutation and tumour-promoting inflammation) facilitate neoplasia by enabling the occurrence of the hallmarks of cancer [7].

Briefly, Figure 1.2 displays a general outline depicting a linear sequence of events explaining a solid tumour's origin and progression. A mutated cell in an epithelium starts dividing, originating a mass of benign abnormal cells (hyperplasias). As the tumour grows, the interior of the tumour mass lacks nutrients and oxygen, which leads to angiogenesis, increasing tumour growth (carcinoma *in situ*). Eventually, the tumour will be able to spread to nearby tissues and migrate through the circulation (invasive carcinoma), and finally seed new tumours in distant tissues (metastasis) [8].

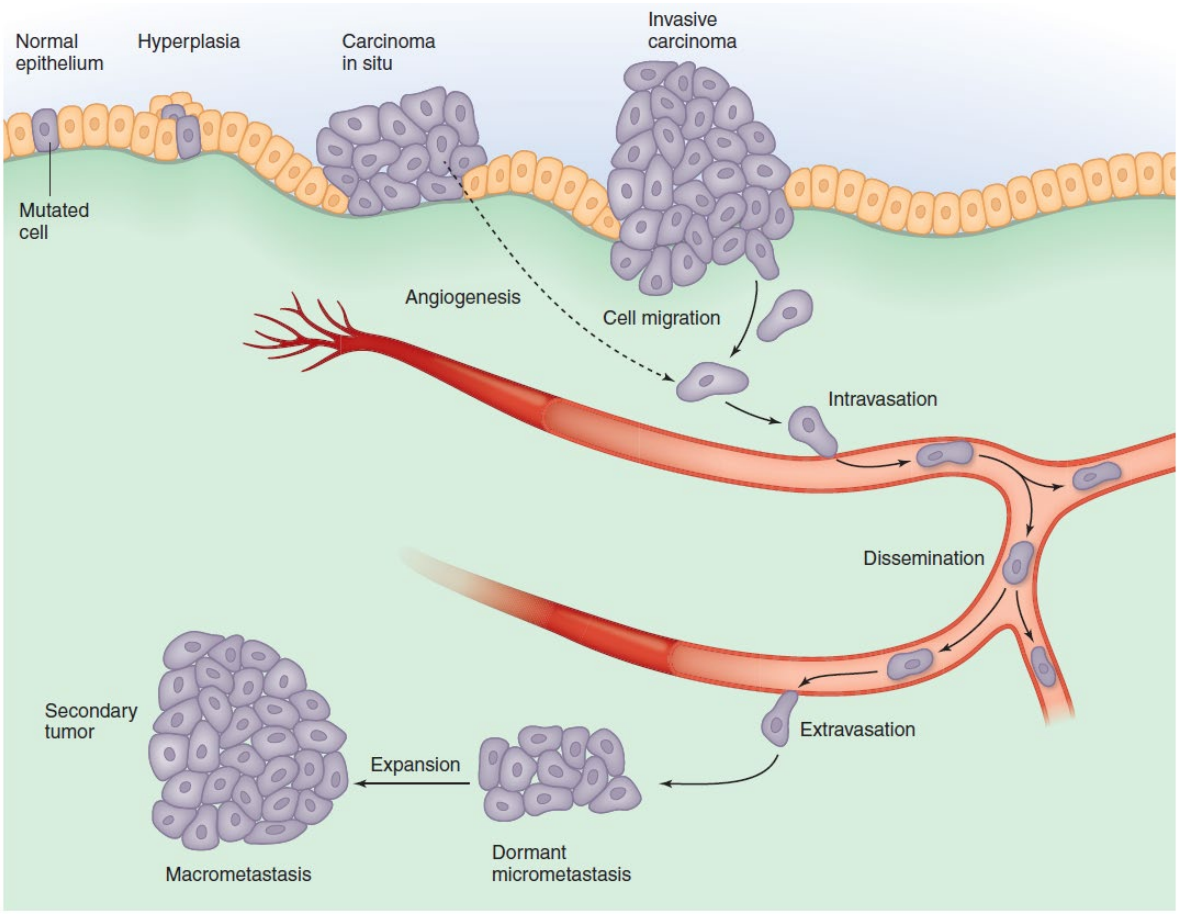

Figure 1.2. Cancer progression. Cancer originates from a single abnormal cell that will divide and originate hyperplasia. Then angiogenesis is upregulated to allow the tumour to grow (carcinoma in situ) and become an invasive carcinoma when it becomes able to migrate and metastasize to distant tissues. Adapted from: DOI: 10.1101/cshperspect.a006098 [8].

1.2 Signalling pathways in cancer

Cancer originates from genetic and epigenetic changes that allow cancer cells to proliferate, survive and migrate by escaping cellular mechanisms that control cellular growth, survival and metabolism [8]. As such, cancers often correlate with dysregulated signalling pathways involved in cell proliferation and survival, including activation of oncogenes, inactivation of tumour suppressors, or hyperactivation of signalling pathways [8]. The most frequently altered signalling pathways in cancer include the Janus kinase-signal transducer and activator of transcription (JAK-STAT), the Wnt/β-catenin, the mitogen-activated protein kinase (MAPK), and the PI3K/AKT signalling pathways [9-11].

JAK-STAT regulates many immunological processes, including tumour recognition and tumour immune escape, and induces the PI3K/AKT signalling pathway [9]. The Wnt/β-catenin signalling pathway, which comprises the canonical β-catenin-dependent pathway and the non-canonical β-catenin-independent pathway, affects cellular functions such as cell proliferation, differentiation, regeneration, organogenesis and tumorigenesis [10, 12]. Both MAPK and PI3K/AKT signalling pathways modulate several cellular functions, namely cell growth, proliferation, survival, and migration, and are frequently involved in tumour progression and anti-cancer drug resistance [13].

1.2.1.1 MAPK signalling pathway

The MAPK and the PI3K/AKT signalling pathways get activated by growth factors and cytokines that bind to and activate the various receptor tyrosine kinases (RTKs). Ligands change the receptor conformation, allowing its dimerization or oligomerization to allow trans-autophosphorylation of the tyrosine kinase domain (the cytoplasmic domain) [14]. This process will recruit and activate specific proteins in the cytoplasm that contain the Src homology 2 (SH2) domain or a phosphotyrosine binding (PTB) domain [11, 14, 15].

In the context of the RAS-RAF-MAPK signalling pathway (Figure 1.3), after RTK activation, for instance, the epidermal growth factor receptor (EGFR), the growth factor receptor bound protein 2 (GRB2) activates after binding to the cytoplasmic domain of the RTK [16]. Then, a guanine nucleotide exchange factor (GEF) protein called Son of Sevenless (SoS) has a proline-rich domain that will bind to the Src homology 3 (SH3) domain of GRB2, becoming activated. RAS anchors to the cytoplasmic side of the cellular membrane and, after SoS is activated and close to RAS, SoS will bind to and stimulate RAS to exchange the GDP for GTP, activating it [11, 16, 17].

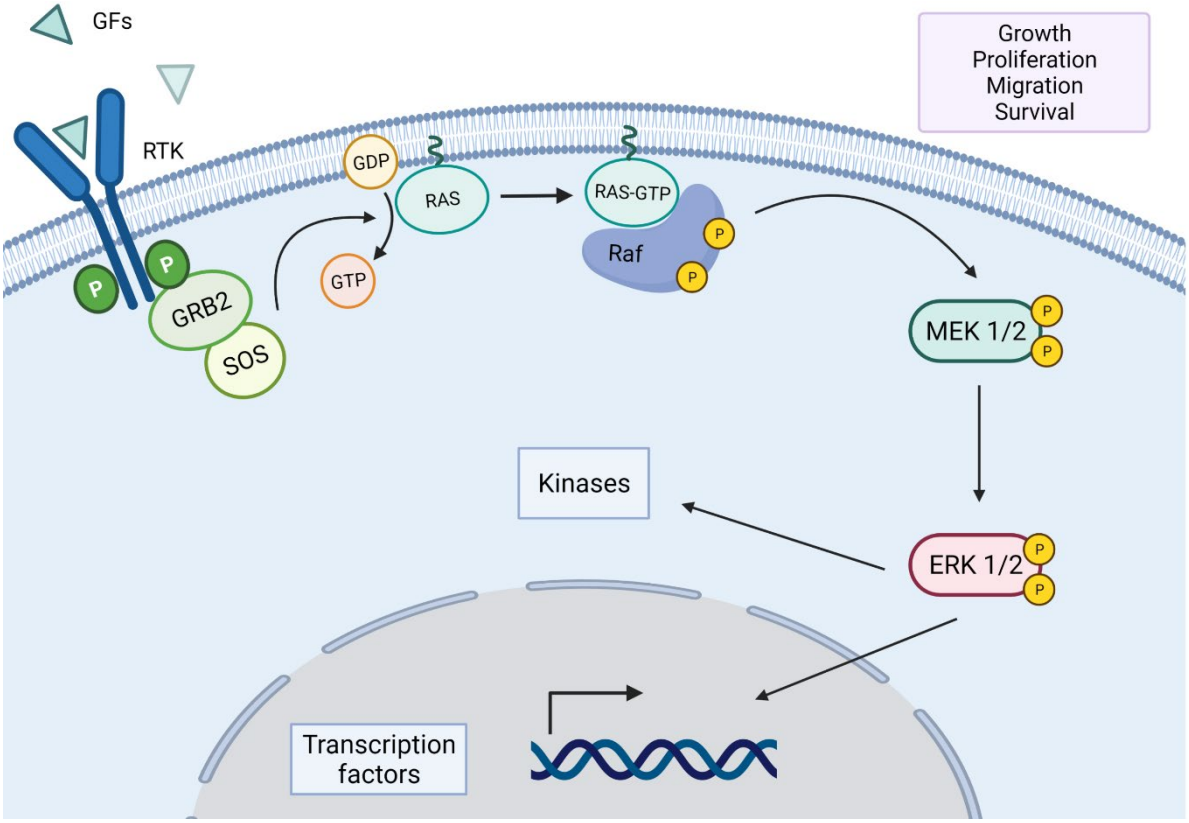

Figure 1.3. The RAS-RAF-MAP kinase signalling pathway. The activation of the RTK by a growth factor recruits GRB2 to its intracellular domain and activates it. GRB2 then recruits and activates SoS. SoS binds to the nearby RAS and activates it, resulting in RAS activating RAF (MAPKKK) to activate MEK (MAPKK). MEK will activate ERK1 and ERK2. The ERKS will then phosphorylate other kinases (cytoplasm) and transcription factors (nucleus) to regulate transcription.

Then, scaffold proteins help RAS bind to its effector proteins, such as RAF. RAF becomes phosphorylated after binding to RAS, and, as RAF is a serine/threonine kinase, it will phosphorylate its target, the MEK protein. MEK is a dual-specificity kinase that phosphorylates serine/threonine and tyrosine residues, such as the extracellular signal-regulated kinase (Erk), Erk1 and Erk2, become activated after phosphorylation. Erk1 and Erk2 will then phosphorylate other kinases in the cytoplasm as well as transcription factors (TF) in the nucleus (Figure 1.3) [11, 16].

Around 30% of human cancers display mutated RAS proteins [18]. Although mutations in RAS genes appear virtually everywhere in their sequences, the most frequent mutations are the point mutations in three residues in the catalytic domain of all the RAS genes [11, 18]. This type of mutation helps the RAS protein to be

constitutively active, inducing constitutive activation of the MAPK and PI3K/AKT pathways, as both signalling pathways cross-talk (Figure 1.4). RAF protein family comprises A-RAF, B-RAF, and C-RAF. B-RAF is often mutated in 90% of cancers, such as in melanoma and papillary thyroid carcinomas, in which the substitution of a Valine for a Glutamic Acid in codon 600 (V600E) is the most common mutation. This mutation forces B-RAF to be catalytically constitutively active [16, 19].

1.2.1.2 PI3K/AKT signalling pathway

Besides RAF, RAS can also activate phosphatidylinositol 3-kinase (PI3K). Activated PI3K will then convert phosphatidylinositol-(4,5) diphosphate (PIP2) to phosphatidylinositol-(3,4,5) triphosphate (PIP3) (Figure 1.4). PI3K is a kinase that includes a catalytic subunit to allow the binding to RAS (p110) and a regulatory subunit that contains an SH2 domain to allow the binding to the phosphotyrosines of RTKs (p85) (Figure 1.5). PI3K binds to an activated RTK, becoming close to the GTP-active RAS. RAS binds to and activates PI3K, allowing the PI3K to convert the close-by PIP2 into PIP3 [20].

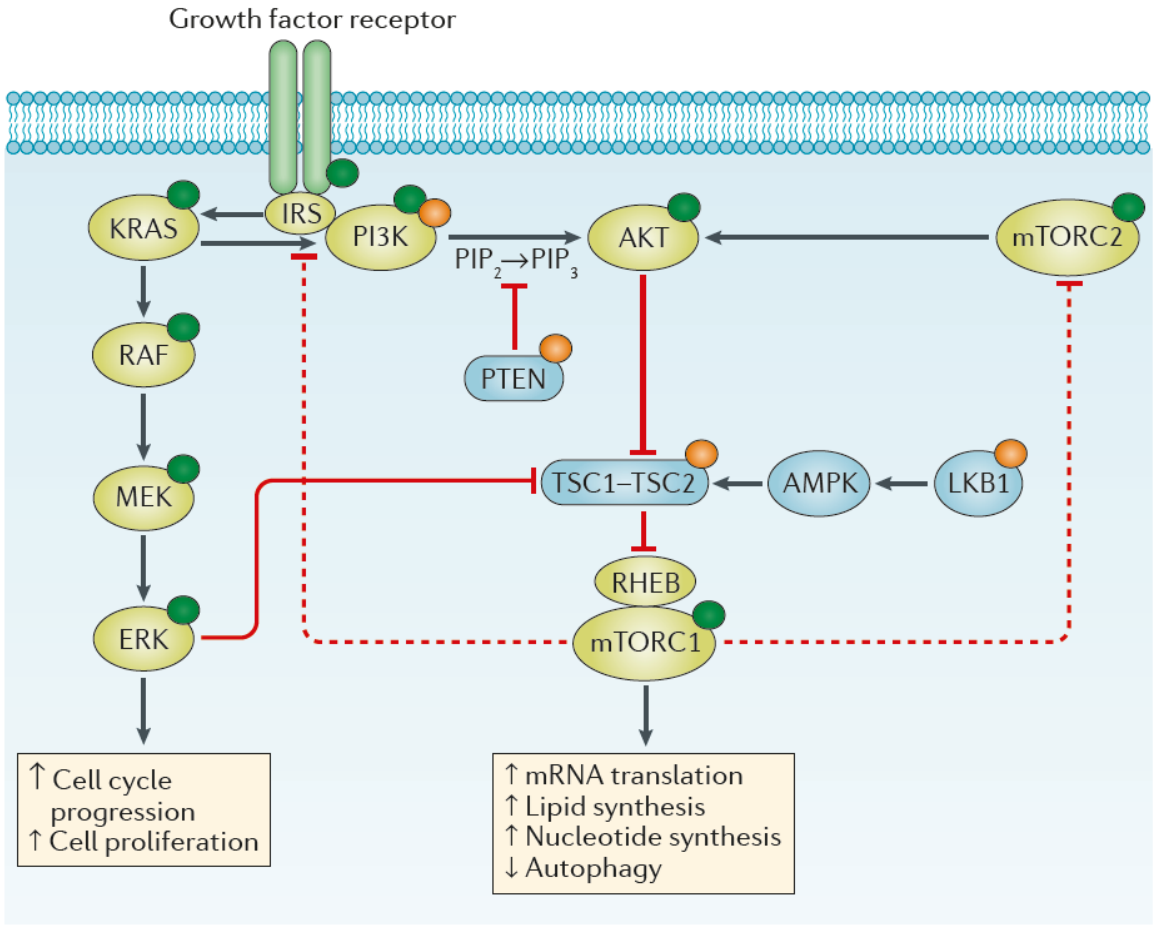

Figure 1.4. The PI3K/AKT signalling pathway. Growth factor receptors and G-protein coupled receptors (not shown), after ligand binding, activate the PI3K/AKT signalling pathway. The activated membrane receptor recruits and activates PI3K with adapter proteins such as insulin receptor substrate (IRS) [21] or RAS. Activated PI3K phosphorylates PIP2 to convert it to PIP3. PIP3 recruits AKT leading to its phosphorylation and activation. AKT dissociates the complex TSC1-TSC2, inducing the activation of mTORC1, promoting cell proliferation and growth. Adapted from: doi:10.1038/nrclinonc.2018.28. [22].

PI3K is a family of lipid kinases divided into three classes (I, II and III) based on their structure and substrate specificity, with class I further subdivided into IA and IB to account for differences in regulation. Class IA PI3Ks are heterodimers comprised of a p110 catalytic subunit (Figure 1.5) and a p85 regulatory subunit. Genes Phosphatidylinositol-4,5-Bisphosphate 3-Kinase Catalytic Subunit Alpha (PIK3CA), Phosphatidylinositol-4,5-Bisphosphate 3-Kinase Catalytic Subunit Beta (PIK3CB) and

Phosphatidylinositol-4,5-Bisphosphate 3-Kinase Catalytic Subunit Delta (PIK3CD) encode three catalytic isoforms: p110α, p110β and p110δ, respectively. The genes Phosphoinositide-3-Kinase Regulatory Subunit 1 (PIK3R1), Phosphoinositide-3-Kinase Regulatory Subunit 2 (PIK3R2) and Phosphoinositide-3-Kinase Regulatory Subunit 3 (PIK3R3), encode three isoforms of the regulatory subunit: p85α (and splicing variants p50α and p55α), p85β and p85γ, respectively. Class IB PI3Ks are heterodimers comprised of the catalytic subunit p110γ, encoded by Phosphatidylinositol-4,5-Bisphosphate 3-Kinase Catalytic Subunit Gamma (PI3KCG) gene, and a regulatory subunit p101, encoded by Phosphoinositide-3-Kinase Regulatory Subunit 5 (PIK3R5), or p87, encoded by Phosphoinositide-3-Kinase Regulatory Subunit 6 (PIK3R6). The activation of signalling pathways by different PI3K isoforms results in different cellular signalling and cancer progression outcomes. Therefore, isoform-specific PI3K inhibitors decrease off-target side effects while the pan-PI3K inhibitors decrease the probability of compensatory feedback loops [23, 24].

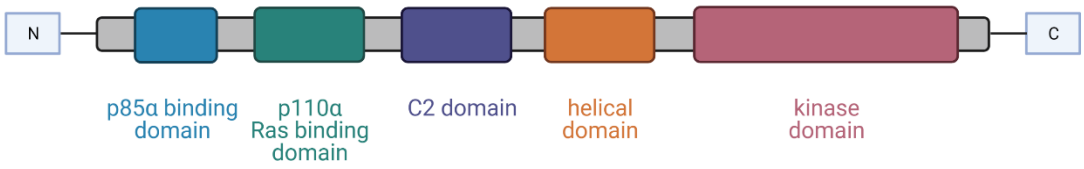

Figure 1.5. Domain structure of the p110α catalytic subunit of PI3K. The regulatory domain (blue) interacts with the p85 regulatory subunit of PI3K which is responsible for the binding to activated RTKs. The Ras binding domain (green) binds to the Ras oncoprotein. The kinase domain enables the enzymatic capacity to to phosphorylatelipids in the plasma membrane.

The lipid bilayer contains several types of lipids in its constitution, including phospholipids. Some phospholipids contain an inositol group (polyalcohol) in their polar heads facing the cytoplasm in cells. Phosphoinositol kinases (PI) can add

phosphate groups to inositol, generating PIP2, and PIP2 can receive another phosphate by the action of PI3K, generating PIP3 (Figure 1.6). This PIP3 will attract and tether proteins to induce these proteins to interact with their effectors in the signalling cascade [20, 25].

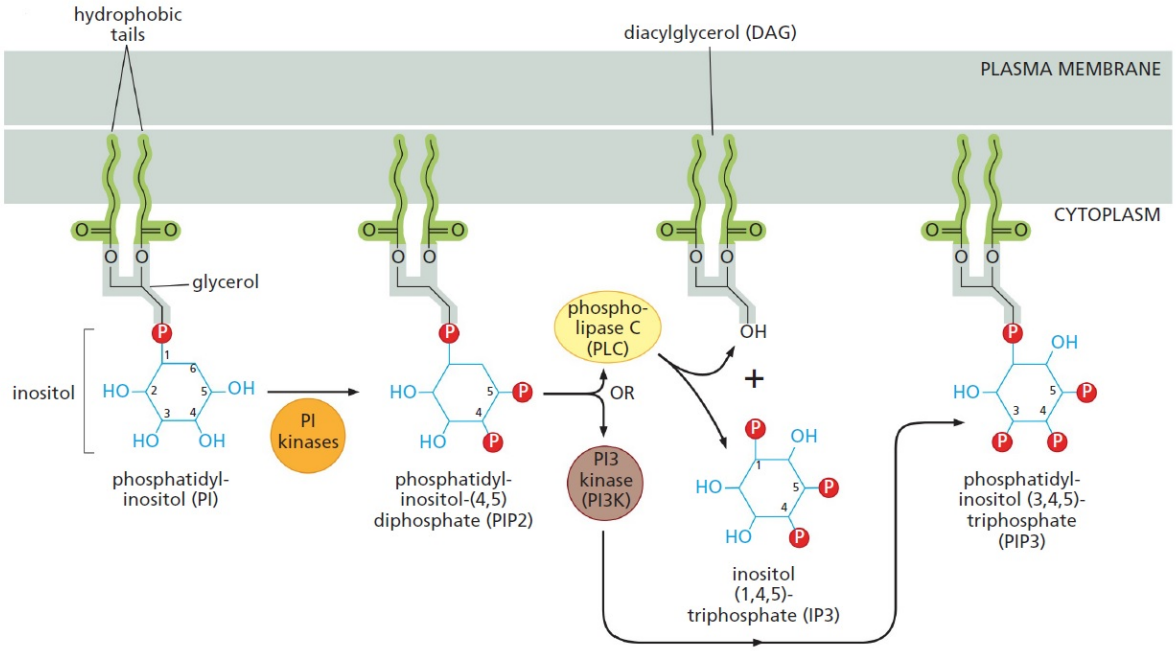

Figure 1.6. The role of PI in the PI3K/AKT signalling pathway. Phosphatidylinositol (PI) kinases add phosphates to PI at the 4th and 5th positions. Then either PI is cleaved by phospholipase C (PLC) to generate diacylglycerol (DAG) and inositol (1,4,5)-triphosphate (IP3), or receives another phosphate at the 3rd position by PI3K to yield PIP3. DAG activates PKC and IP3 acts as a second messenger. PIP3 attracts proteins to the plasma membrane, where they will interact with other proteins of the signalling pathway. Adapted from: ISBN: 978-0-8153-4219-9 [11].

PIP3, anchored at the plasma membrane (Figure 1.7), attracts several cytosolic proteins that contain pleckstrin homology (PH) domains, including protein kinase B (PKB), also known as AKT, a serine/threonine kinase. AKT tethering near the plasma membrane leads to partial AKT activation via phosphorylation by phosphoinositide-dependent kinase 1 (PDK1) at T308, and full activation with another phosphorylation

event by integrin-linked kinase (ILK), mechanistic target of rapamycin complex (mTORC), DNA-dependent protein kinase (DNA-PK) or potentially phosphoinositide-dependent kinase 2 (PDK2) at S473. AKT will then phosphorylate its effector proteins to inhibit apoptosis and promote cell growth and proliferation (Figure 1.4, Figure 1.7) [21, 26, 27].

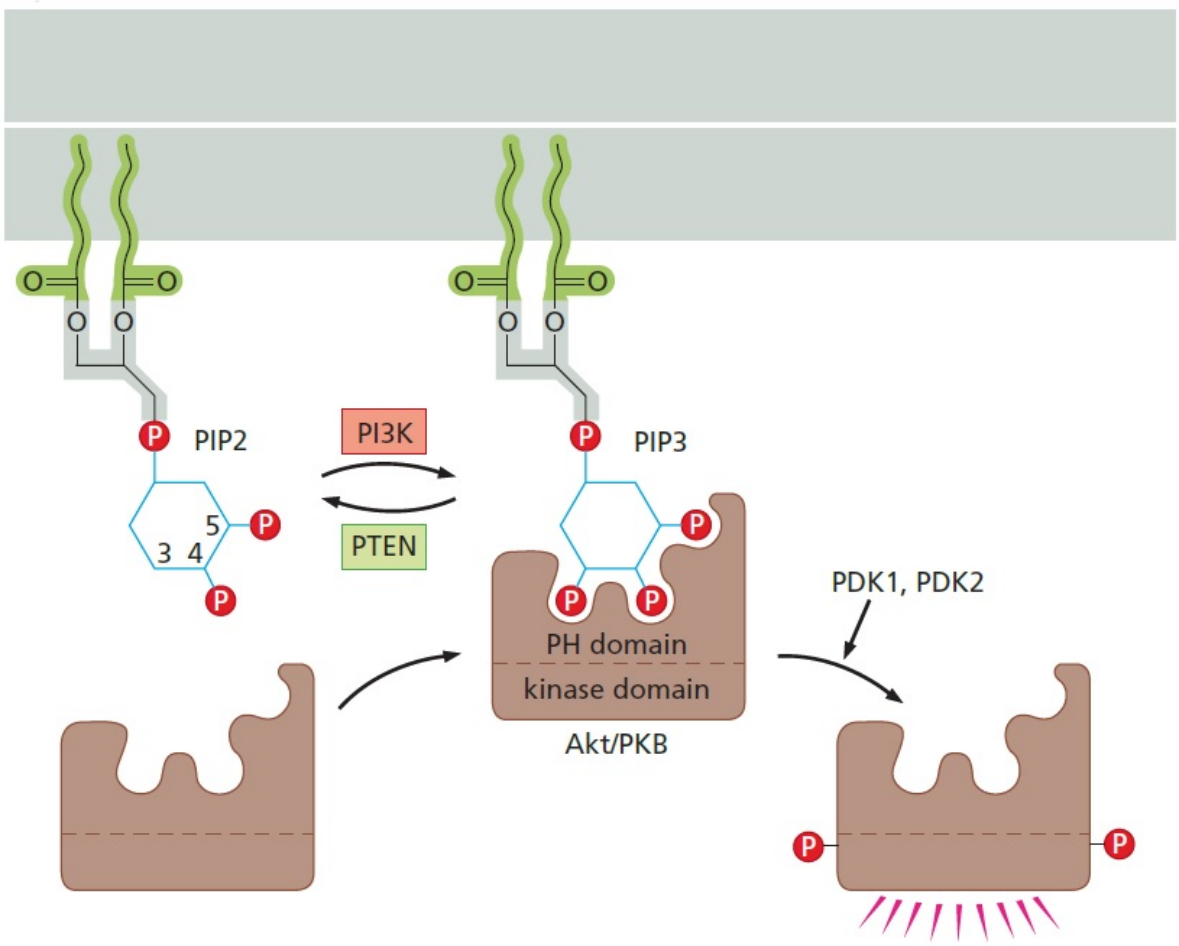

Figure 1.7. The activity of PI3K and Phosphatase And Tensin Homolog (PTEN) regulate PIP3 levels. PI3K converts PIP2 to PIP3, which will tether AKT by its PH domain. Then AKT becomes active after phosphorylation of PDK1 and PDK2, leading to regulation of cellular processes such as apoptosis and cellular growth and proliferation. The presence of PTEN will convert PIP3 to PIP2, which leads to a decrease in the PI3K/AKT signalling. Adapted from: ISBN: 978-0-8153-4219-9 [11].

The serine/threonine kinase AKT is involved in cell survival and avoidance of apoptosis, cell growth and proliferation, glucose metabolism and neovascularization

[28]. AKT is very similar to protein kinase A (PKA) and protein kinase C (PKC) and comprises three isoforms, AKT1, AKT2 and AKT3 (Figure 1.8). All isoforms have a PH domain, a catalytic domain (kinase activity), and a regulatory domain. AKT fully activation occurs upon phosphorylation at a threonine in the catalytic domain and a serine in the regulatory domain (Figure 1.8) [29]. AKT1 is phosphorylated at T308 and S473, while AKT2 is at T309 and S474, and AKT at T305 and S472 (Figure 1.8).

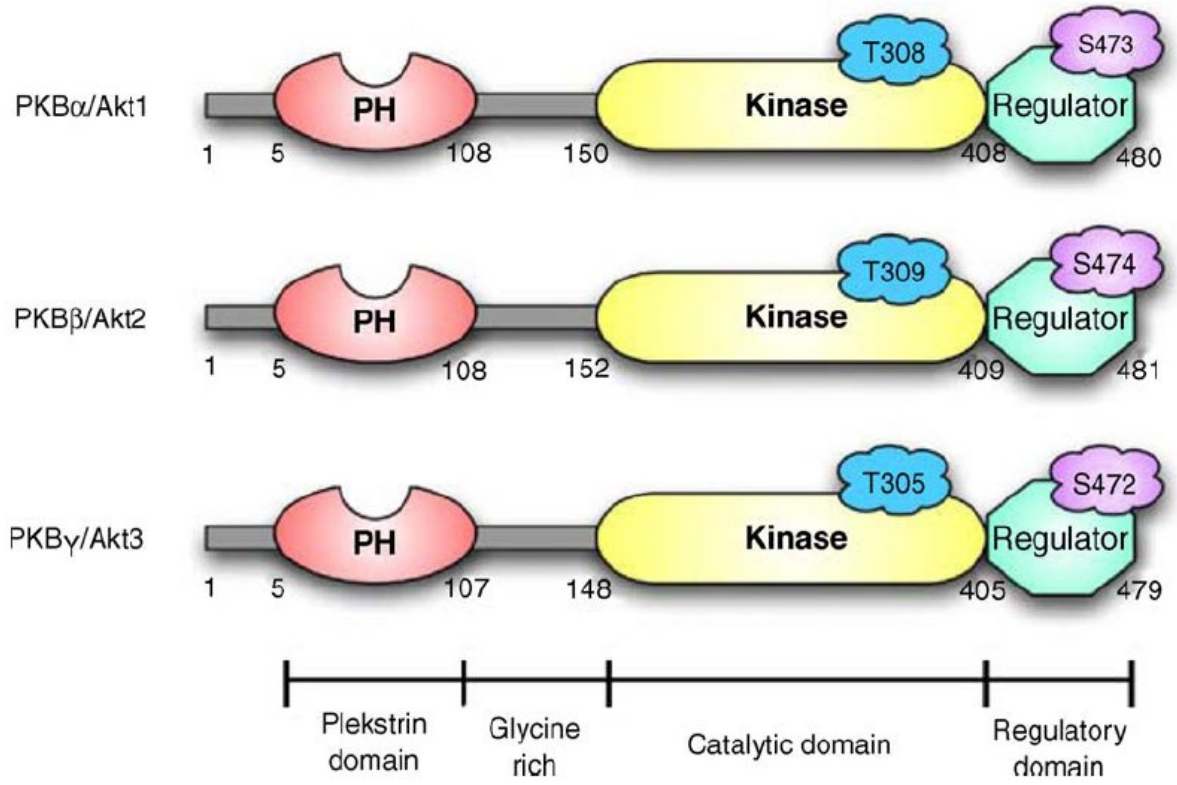

Figure 1.8. Structure of AKT isoforms. AKT contains a PH domain to bind to PIP3, a catalytic domain that becomes active when phosphorylated at the residue threonine, and a regulatory domain that becomes active upon phosphorylation at the residue serine. Adapted from: doi:10.1016/j.biocel.2005.08.017. [29].

Different genes encode these AKT isoforms, and although they are very similar structurally and very conserved among mammals, their expression patterns differ significantly. For instance, the brain and testis express mainly AKT3, and although ubiquitous, the brain, lung, heart and thymus display higher expression levels of AKT1 and AKT2 [29]. Moreover, their functions are not redundant in physiological and

pathological environments and change with biological context. Most studies describe AKT1 to induce tumour initiation, increase cell proliferation by modulating p21, p27 and cyclin D1, and modulate Tumour Protein P53 (p53) to inhibit apoptosis and decrease cell migration in breast cancer. AKT2 induces tumour progression and metastasis by regulating β-integrins, epithelial-to-mesenchymal transition (EMT) proteins and F-actin, and AKT3 is involved with negative ER status. Furthermore, AKT1 is usually mutated while AKT2 is often amplified, and responses to survival and therapy can differ with different isoforms [30].

PIP3 attracts both AKT and PDK1, and AKT binding to PIP3 induces a conformational change that permits PDK1 to phosphorylate T308 (AKT1), T309 (AKT2) or T305 (AKT3) (Figure 1.7) [29]. Then, phosphorylation at S473 (AKT1), S474 (AKT2) or S472 (AKT3) fully activates AKT. AKT can be phosphorylated at the S473 by several kinases such as PDK1, phosphoinositide-dependent kinase 2 (PDK2), ILK, ILK-associated kinase, PI3K-related kinase (PIKK) family, mammalian target of rapamycin complex 2 (mTORC2) and AKT autophosphorylation [30]. Additionally, AKT activity can be modulated by heat shock protein 90 (HSP90), heat shock protein 27 (HSP27), ERK1, ERK2 and SH3 domain-containing RING finger protein 1 (SH3RF1) [28, 31].

After activation, AKT dissociates from the plasma membrane and will travel through the cytoplasm and can also shuttle to the nucleus to phosphorylate numerous targets [30]. AKT phosphorylates various proteins with the RxRxxS/T consensus motifs, such as proline-rich Akt substrate of 40 kDa (PRAS40), Cyclin Dependent Kinase Inhibitor 1A (p21), Cyclin Dependent Kinase Inhibitor 1B (p27), vimentin, palladin, among many others [28], to regulate cellular processes such as cell proliferation, migration and survival.

Forkhead box O (FOXO) and p53 are major downstream effectors of AKT. PRAS40 is a component of the mammalian target of rapamycin complex 1 (mTORC1) and disassociates from mTORC1 after growth factor stimulation [32]. PRAS40 is a protein that can translocate between the cytoplasm and nucleus and is described to form complexes with other proteins together with FOXO transcription factors (FOXOs) or p53 [31].

AKT signalling promotes cell proliferation through modulating genes involved with the cell cycle, such as the cell cycle inhibitors p21 and p27. AKT1 phosphorylates p21 at the T154, causing p21 to translocate to the cytoplasm, increasing cell proliferation. Contrarily, AKT2 binds to p21 preventing AKT1 phosphorylation, thus maintaining p21 in the nucleus, inhibiting the cell cycle and promoting cell differentiation [33]. AKT1 phosphorylates the S-phase kinase associated protein 2 (SKP2), promoting SKP2 stabilization and cytoplasmic localization [33]. The activated SKP2 phosphorylates p27 at residues T157 and S10 causing p27 translocation to the cytoplasm and p27 degradation [34]. p27 can be degraded at the nucleus and the cytoplasm, but the phosphorylation at S10 induces p27 nuclear export [34]. Similar to AKT-mediated p21 regulation, AKT2 will prevent SKP2 phosphorylation by AKT1, resulting in p27 stabilization and nuclear localization due to the absence of SKP2 phosphorylation events [30, 35]. Additionally, AKT1 also phosphorylates p27 directly at the T157 residue, promoting p27 cytoplasmic localization [36].

EMT allows cancer cells to rearrange the cytoskeleton and increase cell motility to promote metastasis through changes in intermediate filaments (IF) expression levels. After EMT, the IF Vimentin expression increases and plays functions in the cellular cytoskeleton and acts as a signalling molecule if phosphorylated [37]. Zhu *et al.* reported AKT1 to bind to vimentin (head region) and phosphorylate S39, preventing vimentin degradation and promoting an increase of cell migration and invasion properties [38].

Palladin is an actin-bundling protein, hence a regulator of cell morphology, motility and invasion, described to be abnormally expressed in several cancers with PI3K/AKT pathway hyperactivated [39, 40]. AKT1 phosphorylates palladin at the S507 residue, which facilitates the formation of actin bundles and inhibits cell migration in breast cancer, but does not affect paladin transcription levels, only its activity level. Studies describe that AKT2 upregulates palladin and promotes protein stabilization *in vitro*, while it does not affect palladin activation level by phosphorylation [30, 40].

AKT also promotes cell survival by inhibiting apoptosis. AKT anti-apoptotic activity occurs partially by inhibition of the release of cytochrome C from mitochondria [41], but also inhibits pro-apoptotic factors such as BCL2 Associated Agonist Of Cell

Death (BAD), procaspase-9 and FOXOs, and activate anti-apoptotic factors such as the proto-oncogenic E3 Ubiquitin Protein Ligase (MDM2) [42].

Although AKT has numerous downstream effectors, the major canonical downstream effectors include mTOR, GSK3, MDM2, FOXO, and p53, which affect cellular growth, anabolic metabolism, survival, proliferation, migration and glucose uptake (Figure 1.9) [43, 44].

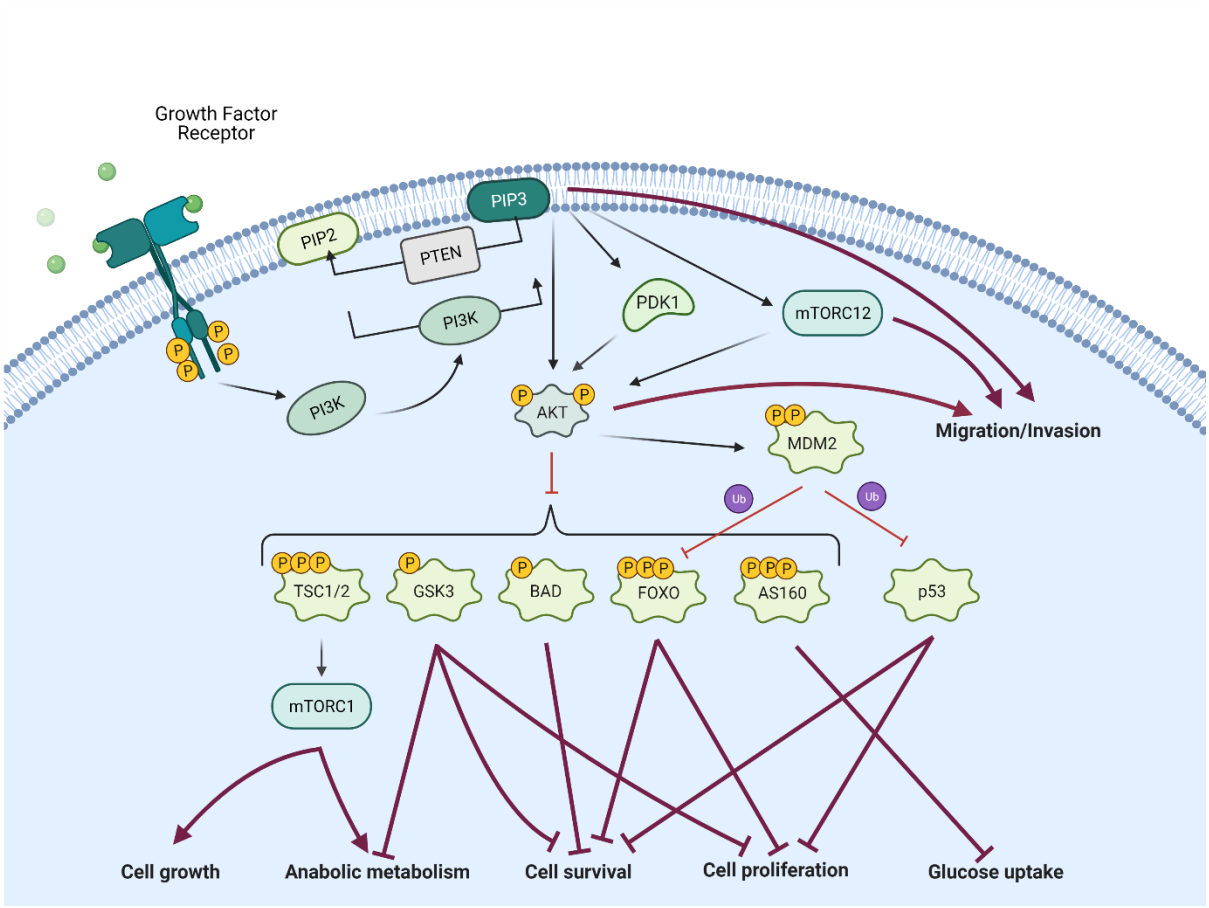

Figure 1.9. The major AKT downstream effectors. AKT induces cell growth, proliferation and migration, improves cell survival and promotes anabolic metabolism and glucose uptake by inhibiting TSC2, GSK3, BAD, FOXO, AS160, and p53, and inducing MDM2 leading to degradation of FOXO and p53.

The mTOR is a serine/threonine kinase that comprises the catalytic subunit of the two complexes, mTOR complex 1 (mTORC1) and mTOR complex 2 (mTORC2).

mTORC1 comprises mTOR, Regulatory Associated Protein Of MTOR Complex 1 (Raptor) and mTOR Associated Protein, LST8 Homolog (mLST8). mTORC1 mediates cell growth and energy metabolism, and AKT indirectly activates it through phosphorylation. AKT phosphorylates tuberous sclerosis complex 2 (TSC2), which is part of the TSC complex. TSC2 activation by AKT disrupts the complex TSC/inhibiting Ras Homolog, MTORC1 Binding (RHEB), by acting as a GTPase-activating protein (GAP) protein. Then RHEB-GTP accumulates and binds to mTORC1, activating it [43, 45]. mTORC2 consists of mTOR, RPTOR Independent Companion Of MTOR Complex 2 (Rictor), MAPK Associated Protein 1 (Sin1) and MTOR Associated Protein, LST8 Homolog (mLST1). mTORC2 affects cell survival and cytoskeleton maintenance by activating AKT by phosphorylation at S473 [43, 45].

AKT also modulates cell growth and development, tumorigenesis, and glycaemic regulation by inhibiting the serine-threonine protein kinase Glycogen Synthase Kinase 3 (GSK3) via phosphorylation, kinase [43, 45]. GSK3 interacts with several PI3K/AKT signalling pathway members, with the potential to participate in feedback mechanisms [46].

Another AKT target is MDM2 Proto-Oncogene, E3 Ubiquitin Protein Ligase (MDM2), an oncogene that regulates protein ubiquitination and degradation of several proteins involved in tumorigeneses, such as the degradation of FOXO1 and FOXO3 [47]. AKT induces MDM2 by phosphorylating MDM2 at S166 and S183, promoting MDM2 nuclear translocation and leading to p53 and FOXO inhibition [48-50]. The tumour suppressor p53 is the most frequently mutated gene in cancer and a regulator of cell senescence and cell death upon oncogenic stress. AKT stabilizes p53 protein by inhibition of MDM2 [50].

The FOXOs are involved with cell migration, differentiation, proliferation, survival and oxidative stress [43, 45], and AKT phosphorylates FOXOs, FOXO1, FOXO3 and FOXO4 [51-53]. One of the mechanisms that regulate FOXOs activity is the phosphorylation of FOXOs, which induces their nuclear export, preventing the transcription of their target genes [43, 45, 51-53].

PI3K/AKT is the signalling pathway more often altered in human cancer, and its oncogenic activation directs cellular metabolism to increase the supply of anabolic requirements of cancer cells. Moreover, FOXOs are the most crucial downstream

transcriptional regulators of the PI3K/AKT pathway. Zanella *et al*. identified protein FOXO repressors in a large-scale genetic screening that included TRIB2 [43, 54, 55]. TRIB2 has a role in leukaemia progression, and several solid tumours such as lung cancer, liver cancer and melanoma show elevated levels of TRIB2. TRIB2 expression correlates with disease stage and clinical prognosis in melanoma, suggesting TRIB2 as a potential biomarker and great clinical relevance in melanoma treatment [56, 57].

1.3 Melanoma

Melanoma is a very aggressive pathology, acquires many mutations and is highly heterogeneous. Until recently, melanoma treatment showed marginal efficacy towards advanced melanoma, but lately, new treatments options such as targeted therapeutics and immunotherapy have improved clinical outcomes. However, melanoma patients still develop drug resistance with these new approaches, and it is imperative to develop more efficient treatment protocols according to the melanoma subtype and stage and improve diagnosis [58].

Melanoma is a type of skin cancer that arises from transformed melanocytes, specialized pigment cells that produce melanin. Melanoma comprises several subtypes, including superficial spreading melanoma, nodular melanoma, lentigo maligna melanoma, amelanotic melanoma and acral lentiginous melanoma. Additionally, mucosal melanoma, melanoma of the eye and desmoplastic melanoma may occur [59]. The primary tumour often originates from the skin but sometimes is detected in other organs (mucosa, eye and others). Among all the skin cancers, melanoma is the rarest. However, if its detection does not occur at earlier stages, when it is easily treatable, it will grow and metastasize very quickly, causing a fatal outcome up to 80% of skin cancer patients [60, 61]. Survival rates at stages 0, I and II (localized melanoma) are 99%, stage III (regional melanoma) is 65%, and stage IV (metastatic melanoma) is 25%, according to the data collected by the American Cancer Society 2009-2015, showing that survival rates decrease significantly with melanoma progression [62, 63].

1.3.1 Melanoma, risk factors and prevention

In 2018, melanoma estimated incidence in Europe was 50.1% (144209 cases in Europe compared to 287723 cases worldwide) and mortality of 44.7% (27147 death numbers in Europe compared to 60712 worldwide). The ratio of mortality/incidence numbers in Europe, North America, Australia and New Zealand is considerably lower than the rest of the world, indicating that despite the elevated incidence and mortality numbers, the living and healthcare conditions can help melanoma patients to improve treatment outcomes [64]. In Portugal, melanoma 5-year prevalence in 2018 was 4279 cases, with estimated 1329 incident case numbers and 356 death numbers, and the melanoma incidence and mortality rates in Portugal are in line with the European average [65].

As worldwide incidence increases, avoiding risk factors is essential to decrease the disease burden. Risk factors for melanoma are ultraviolet light exposure, moles, fair skin, light hair, family melanoma history, history of previous melanoma or other skin cancers, compromised or weakened immune system, and age [66-70].

1.3.2 Melanoma stages and diagnosis

The early and improved diagnosis of melanoma also improves survival rates. The ABCDEF rule, expanded from the original ABCD mnemonic (1985), is used to detect and interpret melanoma lesions, according to the following guidelines: asymmetry (A), border irregularity (B), colour variation in the pigmented area and among pigmented areas (C), more than 6mm diameter (D), evolving pigmented area (phenotypic changes over time) (E), and the pigmented area that most differs from all the other pigmented areas is the primary suspect of a melanoma lesion, also known as the “ugly duckling sign” or “Funning looking” (F), incorporated in 2015 [71].

Melanoma developmental stages (Figure 1.10) classify according to their location and progression. Melanoma initiates with the generation of benign nevi that consists of limited growth of altered melanocytes. Spontaneous mutations arise throughout the melanoma stages, and B-Raf proto-oncogene, serine/threonine kinase (BRAF) mutations may appear at this first stage facilitating constitutive activation of the MAPK signalling pathway that facilitates cell proliferation [72]. Melanoma can be divided into four molecular subtypes: mutant BRAF, mutant RAS, mutant NF1, and triple wild-type melanoma [73]. BRAF mutations occur in 50% of cutaneous melanoma patients, and BRAF-mutated melanoma is more aggressive, more likely to metastasize to the brain, and presents shorter overall survival in patients [74]. Mutant neuroblastoma RAS viral oncogene homolog (NRAS) occurs in 30% of melanoma patients, and it is the second most frequent mutation in cutaneous melanoma, unlike Kirsten rat sarcoma viral oncogene homolog (KRAS) and Harvey rat sarcoma viral oncogene homolog (HRAS) with 1,3% and 1.5% incidence, respectively. Both mutated BRAF and NRAF lead to constitutive activation of the MAPK pathway [73]. Neurofibromin 1 (NF1) inhibits GAP activity in the RAS signalling pathway, and mutant NF1 occurs in 10-15% of patients, with 46% of those patients display wild-type BRAF or RAS. Mutant BRAF or RAS melanomas that also present mutant NF1 can lead to resistance to MEK inhibitors [73].

The next step is the dysplastic nevus formation, either from the benign nevi or new lesions, consisting of pre-malignant lesions with an asymmetrical shape and irregular borders with various diameters and colours. Phosphatase and tensin homolog (PTEN) and cyclin dependent kinase inhibitor 2A (CDKN2A) loss may occur from this stage forward, promoting cell proliferation and survival [72]. In melanomas displaying resistance to MEK and BRAF inhibitors, the PI3K/AKT signalling activating mutations allow the proliferation and survival of cell subpopulations unresponsive to MAPK pathway inhibitors, eventually promoting resistance to multiple therapies [75]. PTEN is a tumour suppressor that inhibits PI3K activity [21], and mutated PTEN is detected in 7% of metastatic melanomas, leading to increased PI3K/AKT pathway signalling [73]. PTEN and BRAF mutations are often concurrent, suggesting that activation of the MAPK and PI3K/AKT are essential for melanoma progression [73, 75]. Melanomas rarely present activating mutations in PI3K, with an incidence of mutant

PIK3CA in 5% of patients, but they often co-occur with BRAF or NRAS mutations, leading to increased melanogenesis and increased resistance to BRAF inhibitors [73]. Another key player of the PI3K/AKT signalling is mTOR that acts upstream and downstream of AKT, with mTOR mutations occurring in around 3.6%-12% of melanoma cases [73]. Among the patients with cutaneous melanoma, 21.4% present mutated or lost CDKN2A. CDKN2A encodes two proteins inhibitors of G1 progression, $p16^{INK4A}$ and $p14^{ARF}$, that suppress the initiation of the metastatic process [73].

On the radial growth phase, cells no longer present random atypia (cancerous cell phenotype) and become able to proliferate in the epidermis and penetrate the dermis in small groups without cell growth. T-Cell Surface Glycoprotein CD1a (CD1), an antigen-presenting molecule [76], acts as an oncogene and its expression increases from this stage onwards. In the vertical growth phase, cells invade the dermis and proliferate, forming tumours. During this stage, changes occur in the expression of essential proteins related to cell migration and differentiation, such as loss of E-cadherin expression, responsible for maintaining cell adhesion and epithelial phenotype [77], and decreased expression of Transient Receptor Potential cation channel subfamily M member (TRPM1), a tumour suppressor, used as a diagnostic and prognostic marker for melanocytic differentiation [78]. This stage is also accompanied by increased expression of N-cadherin, a cell adhesion molecule that promotes cancer cell migration [79], $\alpha V\beta 3$ integrin that promotes angiogenesis [80], Matrix Metallopeptidase 2 (MMP2), which is secreted by tumours to degrade the extracellular matrix promoting cell migration [81], and baculoviral IAP repeat containing 5 (survivin), that is a member of the IAP family that inhibits cell death [82]. In the last stage, metastatic melanoma, cells can migrate to and proliferate on other tissues, and TRPM1 is no longer expressed in these cells [72].

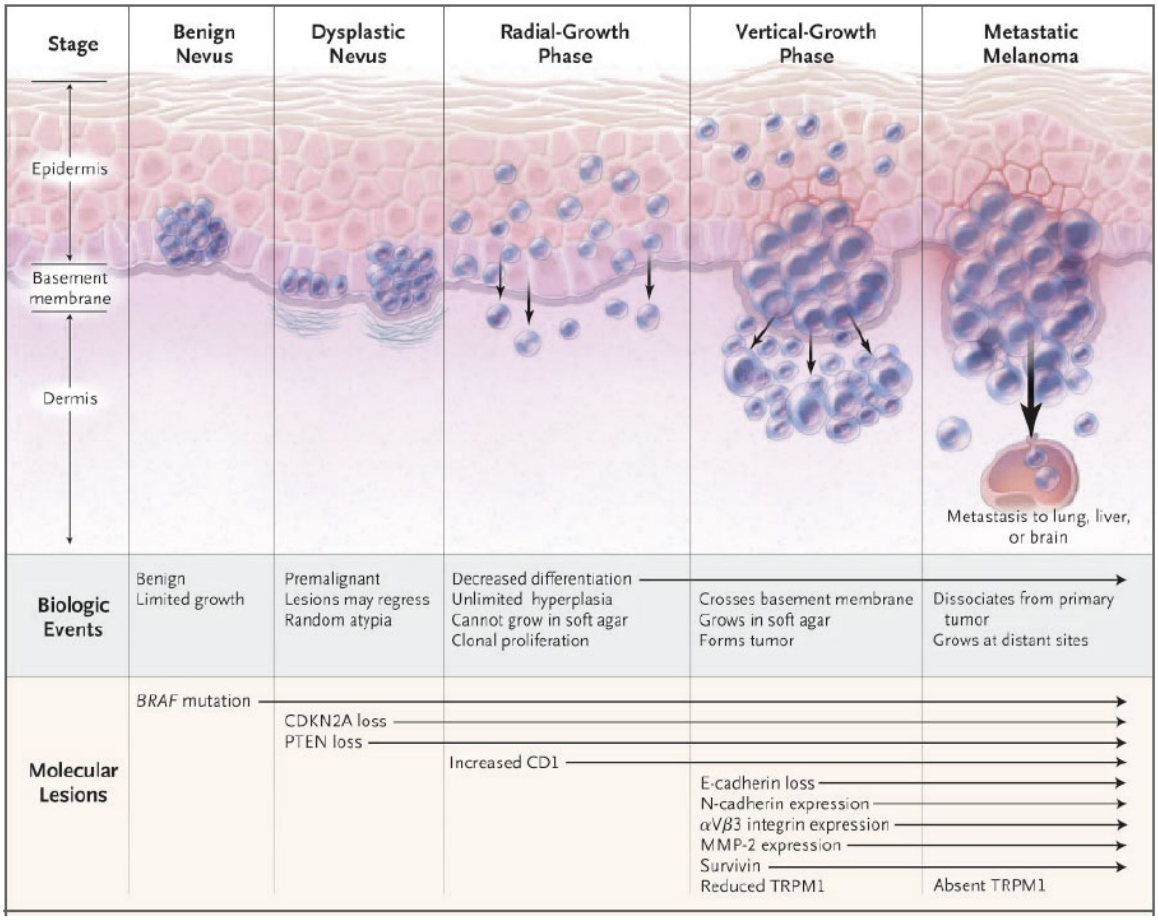

Figure 1.10. Melanoma development stages. The benign nevus stage is characterized by limited growth and BRAF mutation, causing activation of the MAPK signalling pathway. The dysplastic nevus is premalignant, and the lesions result from loss of PTEN and CDKN2A. The radial-growth phase displays decreased differentiation, increased clonal proliferation and increased expression of CD1. The vertical-growth and metastatic melanoma phases display tumour formation, loss of cell adhesion and increased metastatic potential. Adapted from: DOI: 10.1056/NEJMra052166 [72].

1.3.3 The altered PI3K/AKT signalling in melanoma

The discovery of common mutations in melanoma, such as in BRAF, NRAS and NF1, indicate that the dysregulation of RAF-MEK-ERK signalling promotes melanoma progression and led to the development of drugs targeting these proteins, such as mutant BRAF. However, patients often develop resistance a few months after initial targeted therapy. The advent of immunotherapy with immune checkpoint inhibitors successfully improved clinical outcomes, but many patients are unresponsive to this therapy or develop resistance [83].

Inherent activation of the PI3K/AKT signalling pathway in melanoma has been reported by discovering the loss of PTEN or activating mutations in PIK3CA in a subset of melanoma. Moreover, mutant BRAF in melanoma induces melanogenesis and mutated PIK3CA and loss of PTEN help accelerate melanogenesis. Additionally, PI3K/AKT signalling activation promotes resistance to BRAF/MEK inhibitors and immune checkpoint inhibitors. Therefore, targeting the PI3K/AKT signalling pathway is one of the efforts to overcome treatment resistance in melanoma [83].

The PI3K/AKT signalling pathway is activated in melanoma multiple ways during the dysplastic nevus stage (pre-malignant) of melanoma (Figure 1.10). Among the melanoma patients, up to 30% present mutant NRAS, and around 7% display loss of PTEN function, with NRAS and PTEN mutations being mutually exclusive, possibly as they both activate the PI3K/AKT pathway [73]. On the other hand, PTEN mutations commonly co-exist with BRAF mutations leading to MAPK and PI3K/AKT signalling activation. Moreover, the concomitant presence of PTEN and BRAF mutations renders melanoma tumours resistant to apoptosis after treatment with BRAF inhibitors [84]. Activation of the PI3K/AKT signalling can result from mutations in PIK3CA, present in 5% of melanoma patients, and mutated AKT1 and AKT3 (substitution E17K) in 1-2% of melanoma patients. In 5% of melanomas, mTORC2 is also found to be mutated [73, 83]. Moreover, mutated C-KIT present in acral and mucosal melanomas only occurs in the absence of BRAF and NRAS mutations and activates the MAPK pathway and affects the PI3K/AKT signalling. Epigenetically activated RTKs induced resistance to BRAF inhibitors by compensatory activation of the PI3K/AKT signalling [73, 83].

The various ways PI3K/AKT signalling can be activated and induce melanoma progression and resistance is the rationale for developing strategies for therapeutic targeting of this signalling pathway.

1.3.4 Melanoma treatment

Usually, melanoma originates *de novo* from normal skin (70%) and only in 30% of the cases is originated from pre-existing moles (acquired or congenital). As such, prophylactic removal of naevi is not frequent. Instead, patients are monitored and only when new naevi appear or existing ones change appearance, patients subject to naevi excision for further analysis [63].

Patients are subjected to primary tumour excision surgery for tumour identification and staging. To ensure that the primary tumour is completely removed and decrease recurrence risk, a subsequent surgery will remove the scar from the previous excision surgery, or if this is not possible, adjuvant radiotherapy is considered. Patients might undergo adjuvant surgery to improve cure rates if metastatic lymph nodes are detected [63].

Tumours staged from IIB to IV are eligible for chemotherapy and radiotherapy. High-dose of Interferon-alpha 2b (IFN-α2b) has been approved as an adjuvant in patients with regional lymph node metastasis at stage IIB-III after surgery. IFN are immunomodulators with anti-angiogenic, anti-proliferative and pro-apoptotic properties [63, 85].

After patient stratification, the treatment of choice to target tumours staged IV is chemotherapy, immunotherapy or targeted therapy. Therapeutic agents include immune checkpoint inhibitors, BRAF and MEK inhibitors and cytotoxic agents. Immune checkpoint inhibitors allow T-cells to recognize and target cancer cells (such as Ipilimumab, Nivolumab) by improving tumour cell recognition by cytotoxic T lymphocytes (CTLs) and induce tumour cell lysis [86, 87]. BRAF and MEK inhibitors decrease the pro-survival signalling, for instance, Vemurafenib, Dabrafenib,

Trametinib and Selumetinib [88-91]. Cytotoxic agents are more toxic to cancer cells (such as Dacarbazine, Temozolomide and Fotemustine) than healthy cells [63, 85, 92-95].

The first-line therapeutic strategies recommended for advanced or metastatic melanoma approved by the FDA are displayed in Figure 1.11 [96].

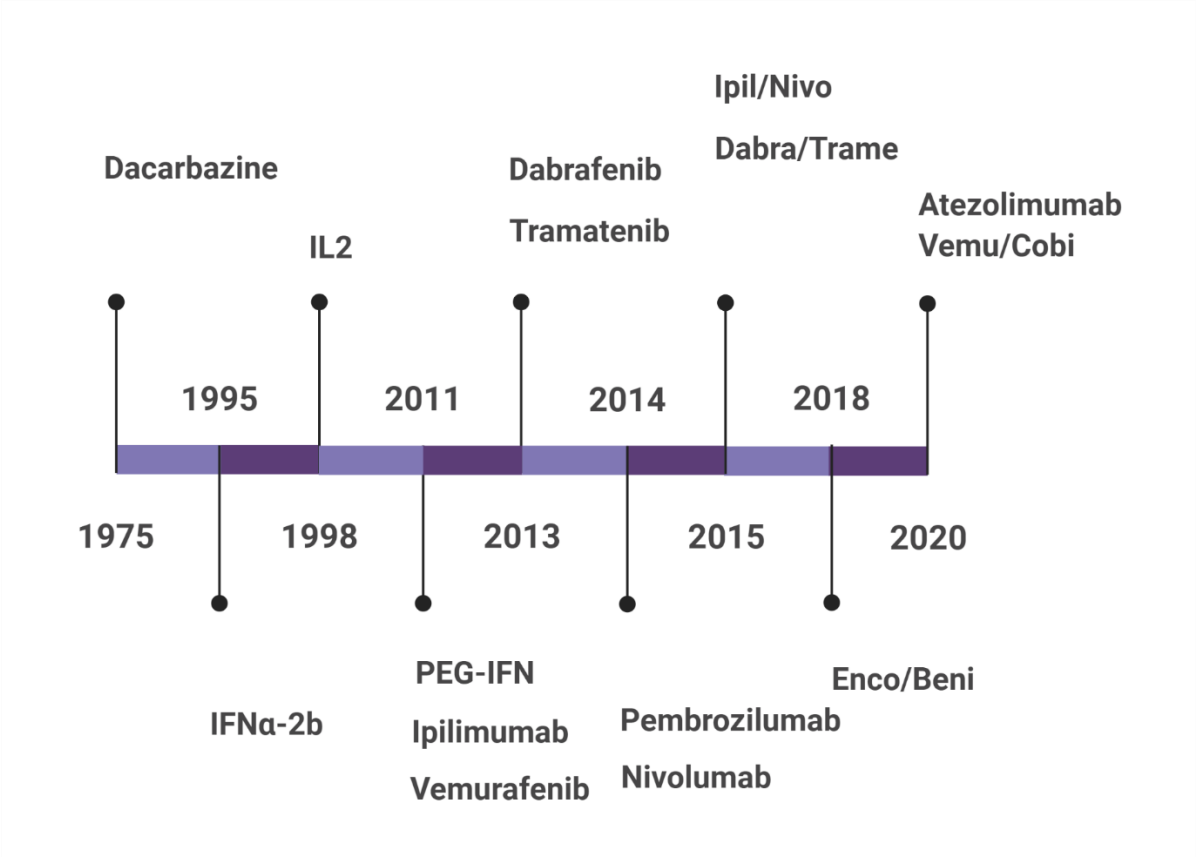

Figure 1.11. Timeline of FDA-approved treatments for advanced or metastatic melanoma. Ipil, Nivo, Dabra, Trame, Enco, Beni, Vemu and Cobi refer to ipilimumab, nivolumab, dabrafenib, trametinib, encorafenib and benimetinib, vemurafenib, and cobimetinib, respectively.

1.3.4.1 Targeted therapy

The first approved treatment strategy for advanced melanoma was chemotherapy (Figure 1.11). The alkylating agent dacarbazine showed limited

success with a 5-year survival of only up to 10% of patients and complete clinical response in less than 5% of patients [92].

Many cancers were discovered to present mutations in their signalling pathways, promoting tumorigenesis. Targeted therapy consists of treating patients with small molecules or antibodies that target mutated proteins responsible for tumour progression [97]. An advantage of targeted therapy is that patients with specific mutations can be treated with the appropriate targeted drugs while preventing treatment of patients that will not clinically respond to the targeted therapy [85].

BRAF is found mutated in around 50% of cutaneous melanomas, inducing activation of the MAPK signalling pathway, resulting in cancer cell growth and proliferation. The most frequent BRAF mutations are $BRAF^{V600E}$ and $BRAF^{V600K}$ [85, 97]. So far, the three approved drugs targeting BRAFV600E mutation are vemurafenib, dabrafenib and encorafenib (Figure 1.11) [97]. These drugs improved the overall survival, tumour regression, and clinical response rate compared to patients treated with chemotherapy [85, 97-100].

MEK is a downstream target of BRAF, making it a desirable therapeutic target, and various MEK1 and MEK2 inhibitors were FDA-approved, such as trametinib, cobimetinib and binimetinib, for monotherapy and combination therapy (Figure 1.11) [97]. Trametinib improved response rate and overall survival compared to chemotherapy-treated patients [97, 101]. Additionally, FDA approved in 2014 the combined treatment of trametinib and dabrafenib (BRAF inhibitor) to treat advanced melanoma with BRAF mutations, as well as in 2015, the combined therapy with cobimetinib (MEK inhibitor) and vemurafenib (BRAF inhibitor) to treat metastatic melanoma with BRAF mutation [85, 102, 103].

Melanoma often displays an activated PI3K/AKT/mTOR signalling pathway, inducing cell proliferation, survival and migration, resulting in resistance to treatment [104]. Several PI3K inhibitors, such as BKM120, GSK2636771, INCB050465 (Parsaclisib), IPI-549, and the AKT inhibitor MK2206, are being studied in undergoing clinical trials combined with other therapeutic strategies [85, 105-109]. However, several of these drugs present drawbacks, such as poor tolerability due to toxic effects, especially for pan-PI3K inhibitors, or tumours develop resistance due to compensatory signalling mechanisms [105, 110]. Melanoma cells with BRAF

mutations are more susceptible to mTOR inhibition. Thus, combined treatment with mTOR inhibitors with PI3K, AKT or MAPK inhibitors is another strategy attempting to revert resistance to BRAF inhibitors. Clinical trials are ongoing with mTOR inhibitors, everolimus and temsirolimus combined with a BRAF inhibitor, respectively [85].

Despite improved overall survival in melanoma patients with targeted drugs, patients often developed resistance to the treatment due to mutations and abnormal expression levels downstream of the signalling pathways [85].

1.3.4.2 Immunotherapy

Immunotherapy is a cancer treatment strategy that improves the immune response against cancer. Even though the percentage of patients that respond positively to immune therapy is lower than targeted therapies, the therapeutic response is significantly more prolonged. Treatment of advanced melanoma often occurs resistance to treatment and adverse events leading to skin and gastrointestinal toxicity, but immunotherapy generally displays fewer adverse events [111]. Some cancers do not benefit as much from immunotherapy, such as pancreatic cancer, due to being strongly immunosuppressive and with a low mutational load [112]. Nevertheless, immunotherapy to treat advanced melanoma has been a significant breakthrough, due to melanoma being highly immunogenic and antigenic [112, 113], with FDA approving drugs showing long-term anti-tumour effects, namely Nivolumab, Ipilimumab, Pembrolizumab, IFNα-2b, PEG-IFN, T-VEC, IL2 and ONTAK (Figure 1.11).

The main current immune checkpoint inhibitors target cytotoxic T-lymphocyte associated protein 4 (CTLA-4), programmed cell death 1 (PD-1), programmed cell death 1 ligand 1 (PD-L1) and lymphocyte activation gene-3 (LAG-3). In melanoma, CTLA-4 becomes activated in cytotoxic T lymphocytes (CTLs) residing in the tumour microenvironment instead of only in specific regulatory T cells, leading to CTL suppression and increasing immune tolerance. Ipilimumab is a monoclonal antibody that targets CTLA-4 inducing CTL tumour infiltration and was FDA-approved in 2011 to treat metastatic melanoma. Another CTLA-4 inhibitor is tremelimumab, undergoing

clinical trials for monotherapy and combined treatment [85, 111]. Antigen-presenting cells (APCs), tumour cells and tumour microenvironment often express PD-1 receptors. Inflammatory signalling induces the ligands PD-L1 and PD-L2 to bind to PD-1, preventing PD-1 from activating T-cells, suppressing the immune response. The FDA-approved Nivolumab and Pembrolizumab (Figure 1.11) are anti-PD-1 antibodies, preventing PD-L1/2 binding to the receptor, thus inducing the immune response by T-cell activation, ultimately reducing tumour progression [85], with significantly improved progression-free survival over targeted monotherapy [85, 114].

IFNα-2b is a cytokine that activates the immune response by modulating various immune cells, inhibits angiogenesis, cell proliferation and tumorigenesis, and promotes MHC I expression in melanoma [85]. In 1995 IFNα-2b was approved by the FDA to treat advanced melanoma as an adjuvant. Despite IFNα-2b improving melanoma patient survival and decreasing the recurrence risk, only a small subset of cancer patients respond to IFNα-2b treatment. Thus, other immunomodulatory therapies have appeared, such as the FDA approved in 2011 PEG-IFN, consisting of IFNα-2b combined with polyethylene glycol (PEG) molecule, as an adjuvant to treat advanced melanoma (stage III) [85, 114, 115]. IL2 is a cytokine that shows anti-tumoral activity due to expanding effector T cells (Teffs) and Tregs. In 1998 the FDA approved IL2 to treat metastatic melanoma, and IL2 treatment shows around 20% overall response and is still undergoing clinical trials for combined treatment, including chemotherapy, radiotherapy and targeted therapies [85, 114]. Ontak is an FDA-approved drug (1999) that consists of the fusion between the diphtheria toxin and IL2 and acts by eliminating IL2 receptor-expressing Tregs cells from peripheral blood. However, the clinical response of melanoma patients to ontak is not consistent among clinical trials [85, 116].

Oncolytic virus treatment consists of generating a virus that only replicates in specific cancer cells, causing tumour lysis and release of tumour-specific antigens, resulting in a tumour-specific immune response [85]. In 2015 FDA approved talimogene laherparepvec (T-VEC), the first oncolytic virus to treat melanoma. T-VEC is still being studied in clinical trials alone or combined with other treatment strategies and produced a 28% clinical response with manageable side effects [85, 117].

Adoptive T cell transfer (ACT) therapy consists of isolating from tumour tissue or peripheral blood of the patient, autologous reactive and tumour-specific T cells, expanded *ex vivo*, and infused back to the patient with IL2 treatment. Additionally to the natural host T cells, patients can also be administered with chimeric antigen receptors (CARs) T cells, engineered T cell receptors (TCRs) or tumour-infiltrating lymphocytes (TILs), which comprise CD4+ and CD8+ T cells that induce tumour regression [97]. So far, clinical trials with ACT with CARs are in progress with limited success. It is a possibility that the efficacy of CARs therapy may be affected by the inhibitory effects of the tumour microenvironment resultant from inhibitory immune checkpoints. Combined treatments with CAR-T cells and PD-1 or CTLA-4 antibodies, as well as other immune checkpoint inhibitors, are under evaluation [85, 118].

Overall, the clinical outcomes for patients with melanoma significantly improved with the development of targeted therapy, especially BRAF and MEK inhibitors, and immunotherapy, such as immune checkpoint inhibitors. However, targeted therapy presents short-term therapeutic effects, and immunotherapy presents a lower response rate, and both therapeutic strategies can result in acquired resistance [119-121]. Combinatorial therapies with targeted therapy and immunotherapy improved therapeutic effects but increased toxicity, and patients still develop resistance to treatment [122].

Oncogenic activation of the PI3K/AKT signalling pathway contributes to melanoma progression and resistance to treatment [123], and mTOR was described to be an effective point for targeting the cell growth in PI3K/AKT signalling *in vitro*. BEZ235 is a PI3K/mTOR dual inhibitor that has been under several clinical trials for various cancers in monotherapy and combined therapy, and similar to various targeted drugs, BEZ235 showed significant anti-tumour effects. Nonetheless, patients suffered from toxicity, and BEZ235 can promote resistance by compensatory ERK signalling pathway activation [24]. Moreover, we have shown that cancer with elevated TRIB2 generates resistance to BEZ235 [56]. However, we describe a novel approach to reduce this resistance, consisting of combined treatment with compounds that synergize with BEZ235 to increase the BEZ235 therapeutic effect and reduce resistance.

1.4 Resistance to cancer treatment

Frequently, several tumours, including melanoma, kidney cancer and hepatocellular carcinoma, present intrinsic resistance to chemotherapy, leading to poor clinical outcomes upon treatment. Other tumours, or in later stages as in metastatic melanoma, display acquired resistance, in which they first present sensitivity to treatment but later become unresponsive. Cancer treatment has progressed significantly, but cancer relapse and recurrence still occur, frequently with fatal outcomes. Drug resistance has caused poor clinical outcomes such as increased mortality and risk of relapse. As such, there are continuous efforts to identify and characterize resistance mechanisms [124-126].

1.4.1 Mechanisms of drug resistance

During tumour progression and treatment, intrinsic and acquired resistance mechanisms can co-exist. Acquired resistance mechanisms can differ from intrinsic, or they can develop from an advantageous selection of intrinsic mechanisms [126]. Besides the influence of the tumour heterogeneity, resistant cell subpopulations, induction of autophagy and cross-talk between the microenvironment and tumour stroma promote resistance. Resistance mechanisms such as drug targets alterations, increased drug efflux, more efficient detoxifying mechanisms, avoidance of cell death, enhanced DNA damage repair mechanisms and increase of cell proliferation [126, 127].

Targeted therapy consists of using drugs that target specific proteins, thus improving selectivity and decreasing side effects. Nevertheless, this type of treatment is prone to develop resistance due to drug target mutation or epigenetic changes leading to altered expression levels [126]. Cells can rapidly downregulate a drug target expression following treatment, such as doxorubicin *in vitro* treatment that

caused downregulation of topoisomerase IIα, rendering doxorubicin less efficient. Receptor tyrosine kinase inhibitors can become ineffective when their targets become mutated following treatment, as mentioned previously for the BCR activator of RhoGEF and GTPase-ABL proto-oncogene 1, non-receptor tyrosine kinase (BCR-ABL) fusion protein. Moreover, cells may bypass the drug inhibition if the drug target is involved in a signalling pathway activated by multiple molecules. One example is the mutation of epidermal growth factor receptor (EGFR) in anaplastic lymphoma kinase (ALK) fusion gene-positive in lung adenocarcinoma [126, 127].

The ATP-binding cassette (ABC) superfamily of proteins translocates various substrates out of the cells, including toxins and drugs. The ATP-binding cassette subfamily B member 1 (MDR1) gene, also known as ABCB1, produces the phenolic glycoprotein (PgP), an efflux pump. Overexpression of PgP leads to resistance to anti-cancer treatment, as well as with other transporters, namely multidrug resistance-related protein (MRP1, ABCC1) and breast cancer-related protein (BCRP, ABCG2) [127].

The drug metabolization process in the cells comprises phase I reactions, namely oxidation and reduction, and phase II reactions, namely consumption and conversion. Increased activity of these reactions leads to drug resistance [127]. Increased activity of the phase I enzyme P450 in breast cancer causes docetaxel inactivation. In phase II reactions, increased activity of glutathione S-transferase (GSTπ) induces drug degradation. Some cancers display upregulated GSTπ, promoting resistance to treatment [127, 128].

Cell death processes comprise apoptosis, necrosis, necroptosis and autophagy, and inhibiting these processes promotes tumour progression. Apoptosis has often been described to be involved in cancer resistance. Cancers often display downregulated pro-apoptotic genes, such as BAX and B-cell lymphoma-extra large (BCLxl), upregulated anti-apoptotic genes such as BCL2, and alterations in the expression of ligands, cell death receptors, and remaining players of the extrinsic and intrinsic apoptotic pathways. Moreover, p53 mutations can inhibit p53-mediated apoptosis [127, 128].

Chemotherapeutic drugs, such as 5-fluorouracil (5-FU) or cisplatin, act by promoting DNA damage in cancer cells to induce cell death. However, many cancers

display upregulated genes involved in DNA repair mechanisms. Colon cancer cell lines resistant to 5-FU presented upregulated DNA repair genes RAD23 Homolog B, Nucleotide Excision Repair Protein (RAD23B), Flap Structure-Specific Endonuclease 1 (FEN1) and FA Complementation Group G (FANCG), and upregulated p53-target genes involved in DNA damage repair mechanisms [127]. Furthermore, oncogenic mutations in the DNA repair mechanisms may result in cancer cells becoming more dependent on another DNA repair pathway to promote further mutations. For example, cancer cells can become less dependent on BRCA1 DNA Repair Associated (BRCA1) and BRCA2 DNA Repair Associated (BRCA2), involved in the double-strand DNA repair mechanism, to be more reliant on Poly(ADP-Ribose) Polymerase 1 (PARP1), involved in DNA repair and cell proliferation [127, 128].

Chemotherapeutic agents, such as cisplatin, generate enough DNA damage to induce cell death. However, cancer cells that are resistant to apoptosis frequently enter premature senescence after chemotherapy. Paradoxically, cancer cells, at a later stage, can recover from tumour-induced senescence, likely due to inhibition of p53 activity, and cause tumour relapse. Moreover, senescence reversal is accompanied by more proliferative cell clones and increased expression of stem cell markers, indicating more aggressive tumour growth [129].

1.4.2 Resistance to targeted therapy in melanoma

The major altered signalling pathways that most contribute to melanoma progression are the MAPK and the PI3K/AKT signalling pathways, affecting various cellular processes, and targeted therapies attempt to inhibit these signalling pathways, which led to the development of BRAF inhibitors, such as vemurafenib and dabrafenib, and MEK inhibitors such as trametinib [98, 100]. Then combined therapies have surged to improve the clinical response of the monotherapies. However, 50% of patients relapse within seven months after the initial positive clinical response, and they develop more aggressive metastases at novel sites [130].

Mutations in RAS, NF1 and RTKs cause constitutive activation of BRAF activity. Aberrant splicing in oncogenic BRAF can cause resistance to treatment. Several patients treated with vemurafenib later developed resistance to treatment. They displayed a subset of cells resistant to the drug because they express a 61kDa isoform of BRAFV600E (p61BRAF^{V600E}) that lack the RAS-binding domain, essentially allowing the p61BRAF^{V600E} to dimerize independently of RAS activity status [131]. Duplication of the kinase domain of BRAF or upregulation of BRAF levels can also cause resistance to treatment. Resistance can also arise downstream of BRAF inhibition. Some mutations in MEK1 or upregulation of MAP3K8 can increase activation of MEK1 downstream of BRAF. Mutations of negative regulators of extracellular signal-regulated kinase (ERK), such as dual specificity phosphatase 4 (DUSP4) and dual specificity phosphatase 6 (DUSP6), or proteins that inhibit ERK modulators, can increase ERK signalling, leading to treatment resistance. Parallel signalling pathways can also promote resistance. For example, mutated PTEN causes aberrant activation of the PI3K/AKT signalling pathway, inducing cellular proliferation and apoptosis inhibition. Ultimately it decreases the efficacy of BRAF inhibitors [132].

The microenvironment contains the extracellular matrix and factors that can induce tumour angiogenesis and recruit stromal cells and growth factors to promote tumour growth [133]. Macrophages and fibroblast-derived factors can promote resistance to inhibitors of the MAPK signalling pathway in melanoma. Another mechanism of extrinsic resistance is the ligand HGF that can also be secreted by stromal cells, in addition to cancer cells, promoting tumorigenic effects and resistance to BRAF inhibitors [134, 135]. Both cancer cells and the microenvironment adapt to the pressure caused by targeted treatment. For example, during targeted therapy in melanoma cells, normal stroma contained fibroblasts with hyperactivated MAPK signalling pathway that ultimately led to increased ERK signalling in some melanoma cells, causing resistance to treatment [136]. Likewise, melanoma cells in contact with more aged fibroblasts are more invasive [137]. Also, inhibitors of the MAPK signalling pathway administered to patients caused an increase in tumour-associated macrophages that secreted tumour necrosis factor (TNFα), ultimately leading to upregulation of MITF, causing resistance to treatment. Furthermore, TNFα inhibits apoptosis in melanoma cells treated with BRAF inhibitors, contributing to melanoma

invasion and vascularization. Moreover, co-administration of MAPK inhibitors with TNFα inhibitors delayed the development of resistance [130].

1.4.3 Resistance to immunotherapy in melanoma

The development of immunotherapy introduced the targeting of immune checkpoints and tumour-specific antigens to induce an immune response against cancer cells. As previously discussed, the clinical response to melanoma treatment improved with antibodies that target the immune checkpoints CTLA-4, PD-1 and PD-L1 [130]. However, the therapeutic strategy itself can further increase the resistance. For example, the immune response against tumours becomes less efficient with decreasing mutational burden [138]. Moreover, during the tumour progression, tumours tend to lose part of their non-silent mutations that might lead to immune adaptation by reducing the load of antigenic epitopes [130]. The mutated BRCA2 gene, involved in DNA repair, is enriched in melanoma responsive to PD-1 inhibitor treatment [139]. For patients who displayed intrinsic resistance to PD-1 inhibitors, the tumours presented a transcription signature with upregulated genes involved in a mesenchymal phenotype, angiogenesis regulation and wound healing. Similarly, patients with acquired resistance to PD-1 inhibitors by oncogenic activation of the MAPK signalling pathway also showed a similar transcriptional profile [130].

Another mechanism of resistance includes acquired mutations in the interferon gamma (IFNγ) receptor pathway, affecting the immune recognition of the tumour cells. Initially, INFγ helps the immune response against tumour cells by recruiting immune cells. At later stages, allows the tumour cells to evade the immune response by modulating the expression of genes that affect T cell function or deplete T cells, such as upregulation of indolamine 2.2 dioxygenase (IDO), PD-L1 and carcinoembryonic antigen cell adhesion molecule-1 (CEACAM1) [130, 140].

Additionally, the accumulation of regulatory T cells that express FOXP3+ constitute another mechanism of resistance through inhibition of the immune response by secretion of chemokines, downregulation of the effector T cell activation

and proliferation, and inducing the production of TNFα [141]. TNFα promotes the downregulation of melanoma-specific genes, resulting in less differentiated melanoma cells, leading to immune evasion. Moreover, progressive selection of non-immunogenic cell clones (immunoediting) could result from T cells-mediated immunoselection during tumour progression [130].

1.5 The role of FOXOs in cancer progression

1.5.1 The FOXO family

Forkhead box (FOX) family of proteins are classified as transcription factors that mediate a wide range of biological functions, including ageing, tissue homeostasis, maintenance of glucose and lipid metabolism, autophagy, and protection from oxidative stress, and are also involved in human diseases including cancer and diabetes [142].

FOXO transcription factors, a subfamily of the FOX family of proteins, are usually present in the nucleus, in the absence of stimulation by growth factors and the presence of cell quiescence, where they modulate the transcription of several target genes that decrease cellular proliferation, survival and stress resistance, and increase cellular differentiation. When growth factors stimulate cells, occurs cytosolic translocation of FOXO proteins and subsequent proteasomal degradation. This inhibition of FOXO transcriptional activity leads to an increase in cell survival. It promotes overriding DNA damage-checkpoints contributing to an increase of cellular proliferation, which is advantageous to cancer progression, and as such, many cancers hyperactivate pro-survival signalling, such as the PI3K/AKT pathway [143].
The vertebrate FOXO family possibly arose as a result of successive gene duplications according to bioinformatic analyses, and human FOXOs comprise FOXO1 (FKHR), FOXO3 (FKHRL1), FOXO4 (AFX), and FOXO6, that are involved in tumour suppression pathways (Figure 1.12) [142-144]. FOXO1 is highly expressed in adipose tissue, FOXO4 in cardiac tissue, FOXO3 in the neuronal tissue and FOXO6 in the developing brain. Moreover, FOXOs rearrangement is commonly present in several cancers (chromosomal translocation that originates fused proteins), altering their function together with their expression levels [143, 144].

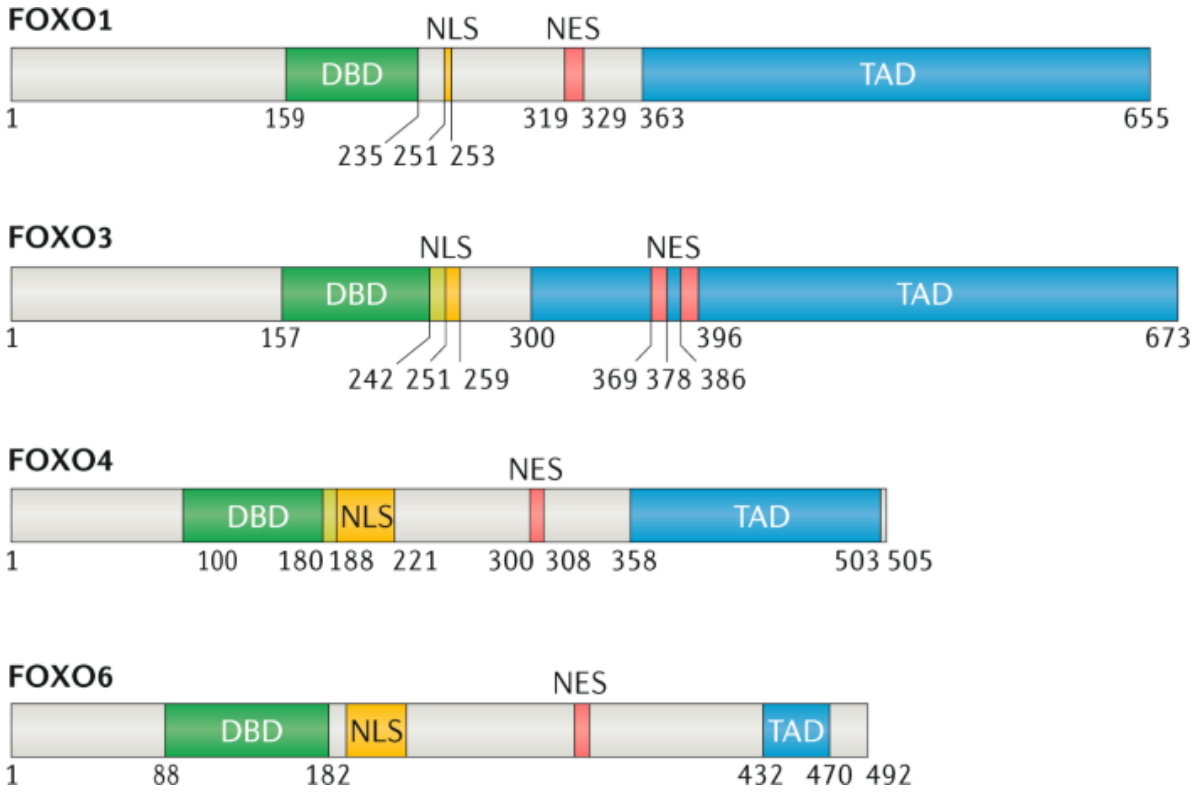

Figure 1.12. The FOXO family members in mammals. The FOXO family members present in mammals are FOXO1, FOXO3, FOXO4 and FOXO6. They present different amino acid lengths, but all members display conserved domains for their phosphorylation, acetylation and post-translational activity. The numbers represent amino acid positions, DBD refers to DNA-binding domain, NLS refers to nuclear localization signal, NES refers to nuclear export signal, and TAD refers to transactivation domain. Adapted from: doi:10.1038/s41573-020-0088-2. [144].

The structure of FOXO proteins contains a forkhead DNA-binding domain (DBD), a nuclear localization signal (NLS), a nuclear export signal, and a transactivation domain (TAD) (Figure 1.12). FOXO transcriptional activity modulation results from post-translational modifications in the FOXO proteins such as ubiquitination, phosphorylation, methylation and acetylation, with phosphorylation the most prevalent (Figure 1.13) [144]. These post-transcriptional modifications control FOXOs DNA-binding affinity, binding to other proteins, transactivation, and cellular localization. FOXOs are only transcriptionally active in the nucleus, but they can also indirectly modulate the activity of other targets in other subcellular localizations. For example, FOXOs in the cytoplasm can modulate autophagy, affect ERK1/2 activity and

alter stress resistance in the mitochondria [52, 145, 146]. FOXOs also interact with a wide range of different proteins, which can be explained by disordered regions outside the forkhead domain, allowing the FOXO proteins to adopt different conformations [142, 143].

FOXOs display a range of functions, in which many are shared between all FOXO proteins, denoting a redundant effect. However, some functions are specific to a FOXO protein, restricted to two or three members, or family members may even display antagonistic functions. The wide range of functionalities results from the FOXO family members recognising similar DNA sequences (same function), different DNA sequences (specific or exclusive functions), or the ability to interact with various proteins. Schmitt-Ney *et al.* describe FOXOs to exhibit autonomous expression as they locate in different chromosomes, but they also regulate the expression of the other members [142]. FOXOs transcriptional regulation in the nucleus can occur through FOXO binding to DNA directly, FOXO binding to other transcription factors, or FOXO binding to DNA after an interactor previously binds to a nearby DNA sequence, altering its conformation, hence allowing FOXO interaction [142].

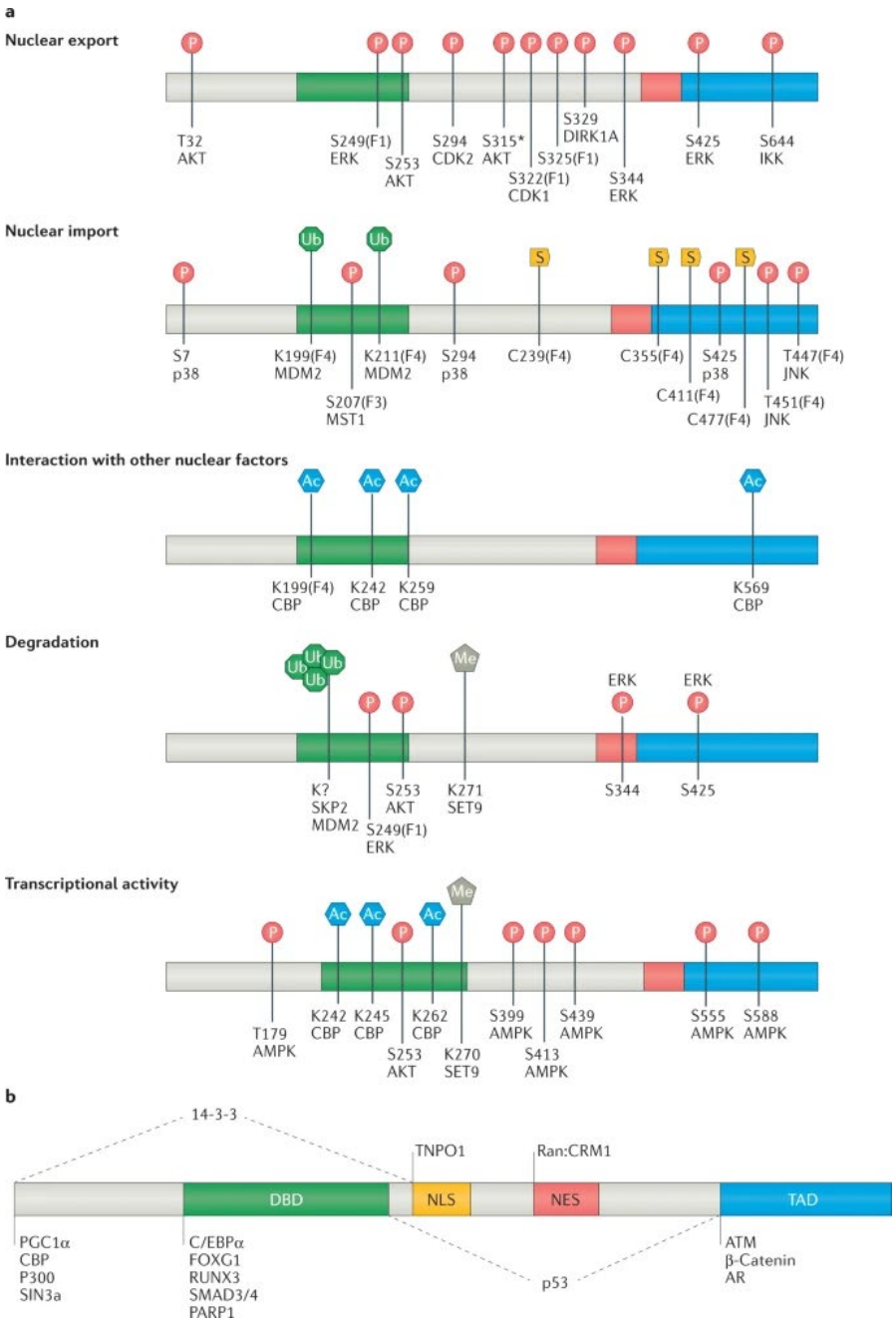

Figure 1.13. Outline of FOXOs post-translational modifications. a) The cellular effects caused by post-translational modifications in FOXOs and their position along with the FOXO domains. Post-translational modifications include phosphorylation (P), ubiquitylation (Ub), acetylation (Ac), methylation (Me) and intermolecular disulfide bonds (S). Modifications on specific FOXO isoforms are designate as F1 (FOXO1), F4 (FOXO4), F6 (FOXO6) and F3 or not stated (FOXO3). The asterisk denotes the absence of modifications in FOXO6. b) Proteins that interact with FOXOs, at the specified domains or positions. The FOXO domains comprise the DNA-binding domain (DBD), nuclear export signal (NES), nuclear localization signal (NLS) and a transactivation domain (TAD). Adapted from: doi:10.1038/s41573-020-0088-2. [144].

1.5.2 FOXO targets

Studies show that FOXOs can bind to an extended range of target genes, confirmed by chromatin immunoprecipitation and direct sequencing. The presence of many of these target genes varies with tissue type, indicating a wide functional diversity, but many are also present in all tissues and conserved among different species, indicating highly conserved FOXO targets. Additionally, FOXOs also regulate their target genes indirectly [147]. The known FOXO targets are involved in various cellular processes, including cell cycle, apoptosis, autophagy, stem cell maintenance and terminal differentiation, DNA repair, glucose and lipid metabolism, stress resistance, pluripotency, immune response and other cellular processes (Figure 1.14) [147, 148].

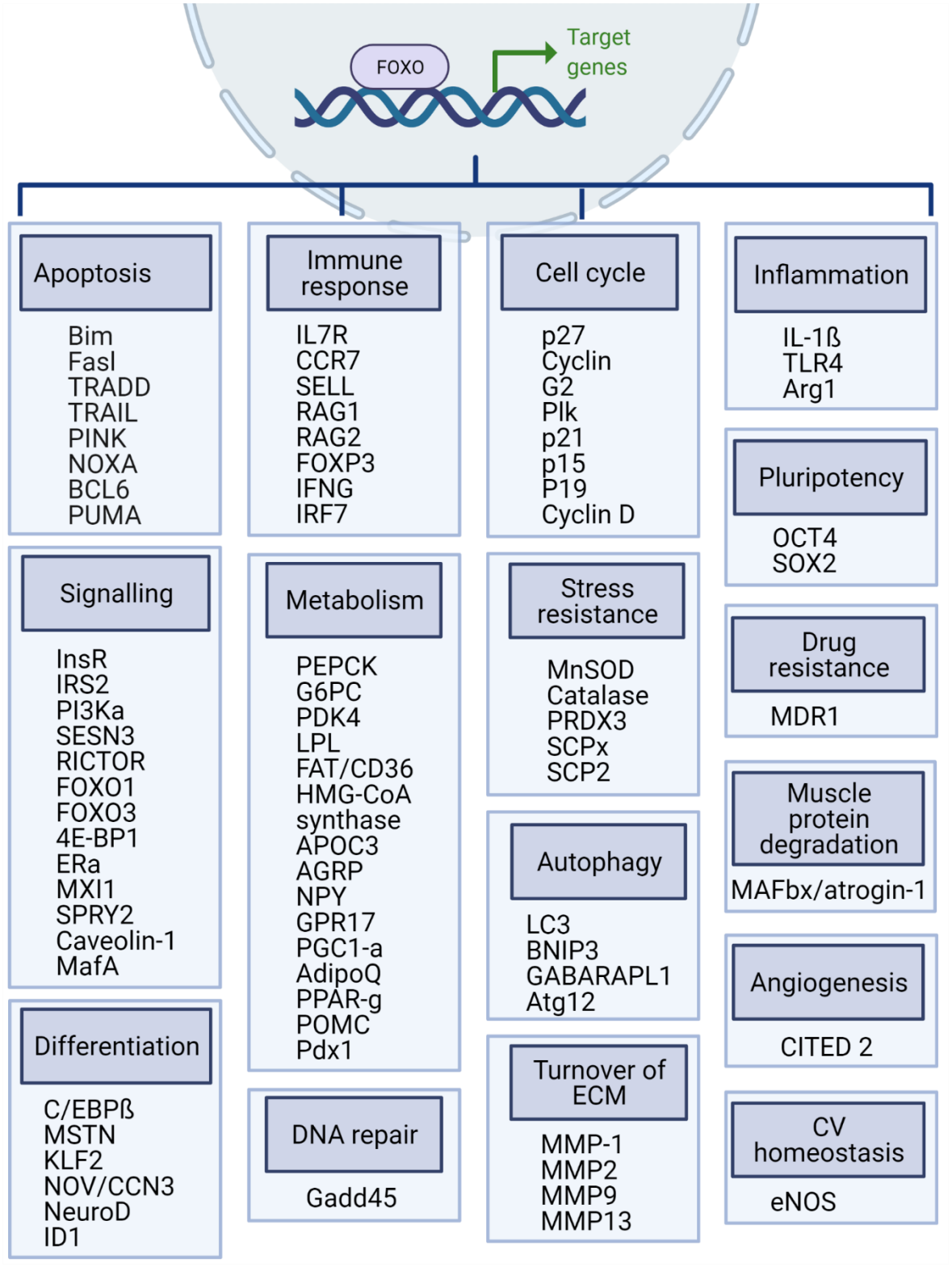

Figure 1.14. Overview of various FOXO target genes involved in diverse cellular functions. 4E-binding protein 1 (4E-BP1), agouti-related protein (AGRP), adiponectin (AdipoQ), arginase 1 (Arg1), B-cell lymphoma 6 (BCL6), BCL2/adenovirus E1B 19 kDa protein-interacting protein 3 (BNIP3), catalase (CAT), cyclin D1 (CCND1), cyclin G2 (CCNG2), C-C chemokine receptor 7 (CCR7), CCAAT/enhancer binding protein beta (C/EBPβ), cardiovascular (CV), extracellular matrix (ECM), endothelial nitric

oxide synthase (eNOS), estrogen receptor alpha (Erα), fatty acid translocase CD36 (FAT/CD36), Fas ligand (FasL), glucose-6α phosphatase (G6PC), GABA type A receptor-associated protein like 1 (GABARAPL1), G protein-coupled receptor 17 (GPR17), 3-hydroxy-3-methylglutaryl-CoA synthase (HMG-CoA synthase), inhibitor of DNA binding 1 (ID1), interleukin 1 beta (IL1β), interferon gamma (IFNG), interleukin 7 receptor (IL7R), interferon regulatory factor 7 (IRF7), insulin receptor substrate 2 (IRS2), Krüppel-like factor 2 (KLF2), lipoprotein lipase (LPL), v-maf musculoaponeurotic fibrosarcoma oncogene homologue A (MafA), multidrug-resistance 1 (MDR1), manganese-dependent superoxide dismutase (MnSOD), matrix metalloproteinase (MMP), myostatin (MSTN), neurogenic differentiation (NeuroD), neuropeptide Y (NPY), nephroblastoma overexpressed (NOV/CCN3), pyruvate dehydrogenase kinase-4 (PDK4), pancreatic and duodenal homeobox 1 (PDX1), phosphoenolpyruvate carboxykinase (PEPCK), Peroxisome proliferator-activated receptor gamma coactivator 1-alpha (PGC-1α), PTEN-induced putative kinase 1 (PINK1), proopiomelanocortin (POMC), peroxisome proliferator-activated receptor gamma (PPAR-γ), peroxiredoxin 3 (PRDX3), recombination activating gene (RAG), regulatory-associated protein of mTORC1 (RAPTOR), retinoblastoma-like 2 (RBL2), rapamycin insensitive companion of mTOR (RICTOR), sterol carrier protein x (SCPx), sterol carrier protein 2 (SCP2), Sprouty2 (SPRY2), selectin L (SELL), sentrin-specific peptidase 1 (SENP), sestrin 3 (SESN3), superoxide dismutase 2 (SOD2), Toll-like receptor 4 (TLR4), tumour necrosis factor superfamily member 10 (TNFSF10), TNF receptor-associated death domain protein (TRADD), TNF-related apoptosis-inducing ligand (TRAIL). Adapted from: doi:https://doi.org/10.1002/ijc.30840. [148].

1.5.3 The relationship between FOXO and signalling pathways in cancer

The importance of FOXOs in tumourigenesis is a result of the regulation of FOXOs activity by insulin and growth factor-induced signalling pathways, the role of FOXOs regulation by ROS, FOXO regulation of angiogenesis, FOXOs regulation of cell cycle arrest, the interaction between FOXO and p53, and FOXO mutations in cancer [143].

The PI3K/AKT signalling pathway plays a critical role during development and tumourigenesis, promoting cell survival, proliferation and invasiveness, and, as mentioned previously, FOXOs are downstream targets of AKT. AKT, one of the significant interactors of FOXOs, phosphorylates FOXO1, FOXO3 and FOXO4 at three

sites, promoting FOXO proteins to translocate to the cytoplasm. AKT phosphorylates FOXOs at an N-terminal conserved sequence (typical to all FOXO proteins), at a C-terminal of the DNA-binding domain sequence, containing the nuclear localization signal sequence (NLS), and at a nuclear export signal sequence (NES). On the other hand, the NES is not present in FOXO6, resulting in AKT phosphorylating FOXO6 in two sites and not translocating to the cytoplasm as the other FOXO members [142, 143].

The PI3K/AKT signalling pathway has an oncogenic effect in cancer, often due to mutations in several steps of the signalling pathway, including PI3K, RAS or PTEN, which leads to FOXO function inhibition. Cell treatment with PI3K inhibitors, such as LY294002 (reversible inhibitor of PI3K), promotes FOXO transcriptional activity, inducing apoptosis and cell cycle arrest (tumour suppressor role), confirming the importance of the PI3K/AKT in tumorigenesis [143].

Another signalling pathway involved in FOXO regulation is the MAPK/ERK signalling pathway, leading to FOXO3 phosphorylation and subsequent degradation after MDM2 polyubiquitination [149]. Furthermore, the IKK/NF-κB signalling pathway, known to regulate inflammation and innate immune response, has also been associated with several cancers. FOXO phosphorylation (S644) by IKKα and IKKβ and IKKε degrades FOXO and excludes it from the nucleus, promoting cancer cell proliferation and survival [143].

Several micro-RNAs also affect FOXO expression levels in cancer. The miR-96 overexpression in breast and bladder cancers target FOXO1 and FOXO3 to increase cell proliferation. Upregulation of miR-182 targets FOXO1 to increase cancer cell growth and Melanocyte Inducing Transcription Factor (MITF) to increase cancer cell invasiveness in melanoma cells. Farhan *et al.* report several micro-RNAs to target FOXO1, including miR-27a, miR-96 and miR-182 in human breast cancer cell line, the miR-96, miR-182 and miR-183 in Hodgkin's lymphoma and endometrial cancer, miR-135b in an osteosarcoma cell line, miR-370 in prostate cancer, miR-411 in lung cancer and miR-1269 in hepatocellular carcinoma, promoting cancer cell growth, proliferation and survival [143].

FOXOs regulate the transcription of genes that produce antioxidant proteins, such as Superoxide Dismutase 2 (MnSOD), that reduce ROS formation, thus

preventing oxidative damage. On the other hand, the regulation of FOXOs results from post-translational modifications that are responsive to ROS levels and will affect the anti-oxidant function of FOXOs. In PI3K/AKT and ERK1/2 signalling pathways, stimulation of RTKs by their natural ligands results in a transient increase of ROS due to nicotinamide adenine dinucleotide phosphate (NADPH) oxidases activity, necessary for modulation of these signalling cascades and exogenously-induced ROS levels that also stimulate these signalling pathways. Consequently, these signalling cascades will modulate FOXO activity by promoting FOXO degradation and inhibition of its transcriptional activity [143, 150].

Angiogenesis is essential for tumour growth to induce cell proliferation, migration and invasion. The production of angiogenic factors, including vascular endothelial growth factor (VEGF), initiates angiogenesis, and FOXO proteins can stimulate pro- and anti-angiogenic factors.

FOXOs modulate cell cycle arrest by regulating genes such as p21 and p27. The E2F Transcription Factor 1 (E2F-1) transcription factor complexes with FOXO1 and FOXO3 inhibiting cell proliferation and survival, a mechanism that is often blocked in cancer. FOXOs can also regulate p19 through MYC, promoting p53 activity and cell cycle arrest [143, 151].

FOXO and p53 have shown a few similar functions, such as regulating the cell cycle and the DNA-damage repair mechanisms. Furthermore, similar mechanisms regulate their activity, namely post-translational modifications (such as phosphorylation and acetylation), share several target genes, and signalling pathways crosstalk in several ways. Examples include FOXO3 that can bind directly to p53 to stabilize it, FOXO3 can regulate the transcription of regulators upstream of p53, such as Sirtuin 1 (SIRT1), or p53 can regulate upstream regulators of FOXO3, such as Serum/Glucocorticoid Regulated Kinase 1 (SGK), and p53 can directly regulate transcription of FOXO3 under DNA damage in fibroblasts [143, 152].

Cancers seldom display mutated FOXOs, and instead, cancers usually present deregulated FOXO function and abnormal expression. Loss of function mutations in FOXO isoforms will most probably not affect cellular functions, as FOXO family members present redundant functions, and it is improbable to occur mutations in all FOXO members simultaneously [153]. Contrarily, PI3K pathway and p53 mutations

are frequent because they often result in pro-survival signalling, advantageous to tumour progression [154, 155]. However, some cancers display FOXO mutations, such as FOXO fusion proteins, resulting from chromosomal translocations and somatic point mutations, often behaving as oncogenes. For example, PAX3-FOXO1, first detected in alveolar rhabdomyosarcoma (ARMS), was originated from a chromosomal t(2, 13) translocation and elevated levels of PAX3-FOXO1 in ARMS together with other genetic lesions, promotes cell proliferation and transformation [143].

1.5.4 Anti-cancer drugs that target FOXO signalling

As FOXO proteins display such a central role in tumorigenesis, it stimulates the development of anti-cancer drugs that target FOXOs directly and the signalling pathways that regulate FOXOs. Except for ligand-inducible nuclear receptors, transcription factors are challenging to target pharmacologically. The reason lies in their 3D structure that displays flat surfaces to bind to other proteins and DNA, which hinders the interference by small molecules that target these transcription factors. Additionally, although FOXOs are desirable targets as they are involved in cancer, ageing, and degenerative pathologies, they display numerous functions, and their regulation is tightly controlled, which hinders FOXO targeting. Moreover, different isoforms and different FOXO members may compensate for the loss of activity of one FOXO member [144, 156].

Nevertheless, with increasing knowledge regarding their structure, function, activity and how they bind to DNA, drugs have been reported to target several transcription factors, including p53, Signal Transducer And Activator Of Transcription 1 (STAT1), Nuclear Factor, Erythroid 2 Like 2 (NRF2), GLI Family Zinc Finger 1 (GLI) and Notch Receptor 1 (NOTCH). Pharmacologically modulating FOXOs may be possible by targeting nuclear import and export, upstream regulatory players, FOXO protein interactions, DNA binding and post-translational modifications that affect FOXO activity [144, 157].

The regulation of FOXO by enzymes (Figure 1.15) enabled the development of drugs targeting upstream regulators of FOXO, as enzymes are less complex to inhibit by small molecules than transcription factors. However, the cellular effects may not be limited to just FOXO modulation as they are upstream in the signalling pathways [144]. Kinases, phosphatases, histone acetyltransferases (HATs) and histone deacetylases (HDACs) regulate FOXO activity, as kinases phosphorylate substrates, phosphatases remove phosphate groups, HATs and HDACs increase and decrease DNA expression, respectively [144]. The first activators of FOXO were pan-PI3K enzymatic inhibitors, such as LY294002 and wortmannin, and compounds that inhibit PI3K and mTOR simultaneously strongly induce FOXO nuclear localization, such as dactolisib (BEZ235). These compounds prevent the phosphorylation of AKT, impeding its activation [144].

Inhibitors of AKT, such as AKT inhibitor VIII, AKT inhibitor X and capivasertib (AZD5363), increase FOXO activity, targeting AKT directly by allosteric or competitive inhibition, preventing AKT phosphorylation. Additionally, full activation of AKT requires phosphorylation at T308 by PDK1, so AKT activity decreases upon treatment with the PDK1 inhibitors, such as celecoxib. AKT inhibition with these drugs induces FOXO nuclear localization [144]. Other chemotherapeutics induce FOXO activity by increasing ROS levels, such as cisplatin, doxorubicin and SN-38. Drugs can also increase FOXO activity by activating upstream FOXO activators such as JNK and AMPK. Paclitaxel and vinblastine activate FOXO3 by activating the c-Jun N-terminal kinase (JNK) pathway [158]. Other drugs activate protein kinase AMP-activated catalytic subunit alpha 1 (AMPK), increasing FOXO activity in breast cancer, hepatocytes and erythrocytes, such as metformin [144].

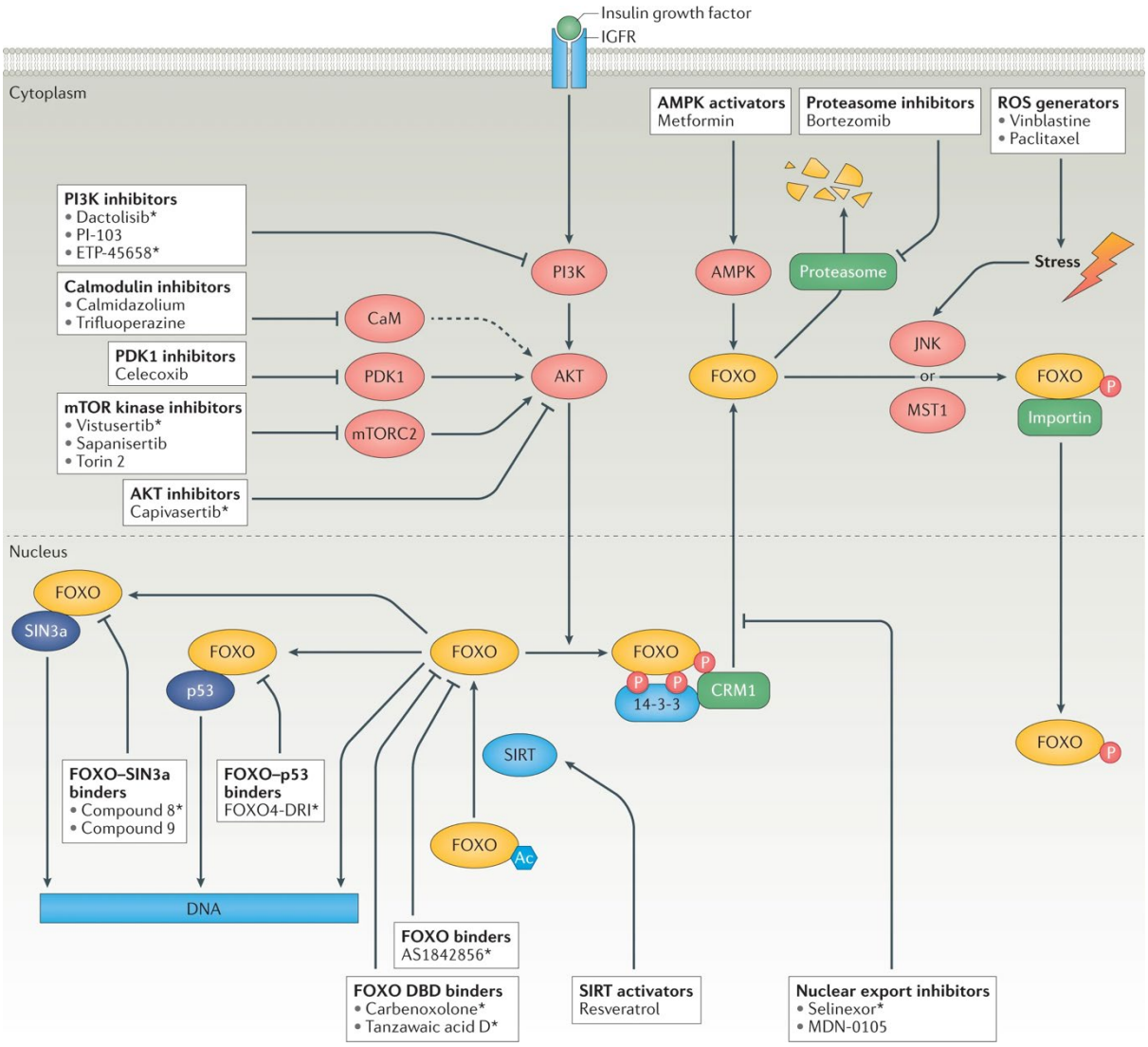

Figure 1.15. Drugs that modulate FOXO activity directly and indirectly through upstream and downstream regulators. Compounds that inhibit PI3K, calmodulin, PDK1, mTOR, AKT, FOXO nuclear export and proteasome degradation, and compounds that activate AMPK, promote FOXO nuclear localization and its transcriptional activity. Compounds that destabilize FOXO-DNA or FOXO-p53 and FOXO-SIN3a complexes, and induce FOXO nuclear export, inhibit FOXO activity. Ac (acetylation), DBD (DNA-binding domain), P (phosphorylation), ROS (reactive oxygen species). Adapted from: doi:10.1038/s41573-020-0088-2. [144].

FOXO activity can also be regulated by modulating FOXO subcellular localization, as FOXO transcriptional activity is limited to the nucleus. FOXO translocation to the nucleus induced by ROS relies on a cysteine-dependent complex with transportin 1 (TNPO1) [144], while energetic stress in the absence of growth

factors drives the nuclear import of FOXO through an unknown import protein. On the other hand, phosphorylated FOXO by AKT is exported from the nucleus by the nuclear export receptor CRM1 [144, 159-161]. Attempts to retain FOXO at the nucleus, where it is transcriptionally active, might prevent the inhibition of FOXO activity and prevent treatment resistance. Leptomycin B (LMB) was the first compound discovered to inhibit CRM1 by binding covalently to CRM1 at the export signal binding domain at the C528 [162]. LMB is too toxic for clinical use but is very useful to investigate nuclear export [144, 148]. Nuclear export inhibitors that target CRM1 are under development, with selinexor recently FDA-approved [163], to investigate their potential as tumour suppressors in the clinic [144]. Calissi *et al*. describes various small-molecule nuclear export inhibitors that promote nuclear localization of FOXO, such as psammaplysene A, compounds A–D, octahydrocurcumin, plumbagin, MDN-0105, S109, and the selective inhibitors sverdinexor and selinexor [144]. Sverdinexor and selinexor bind reversibly to CRM1 at C528, and selinexor helps trap FOXO in the nucleus. Selinexor increased nuclear localization of FOXO1 and increased cisplatin efficiency in ovarian carcinoma models, either sensitive and resistant to cisplatin [144].

FOXOs bind to other proteins generating protein complexes, allowing the modulation of the activity of downstream mediators. The development of drugs that target these complexes enables the modulation of FOXO activity. For example, the peptide FOXO4-DRI targets a sequence in FOXO that binds to p53, preventing the formation of the complex FOXO4-p53, responsible for the survival of senescent cells. This peptide induces death in doxorubicin-induced senescent cells but protects healthy cells, reverting doxorubicin resistance [144]. In another example, insulin represses FOXO1, leading to FOXO1-dependent inhibition of glucose-6-phosphatase and glucokinase induction. The dual action of FOXO1 results from the direct binding of FOXO1 to different co-factors. Targeting FOXO1-SIN3A prevents the upregulation of glucokinase expression without affecting lipogenesis [144].

FOXOs act primarily as transcription factors; thus, disrupting the protein-DNA binding would be valuable in modulating FOXO activity. Some molecules, such as carbenoxolone, inhibited FOXO3 by binding to its DBD and resensitized neuroblastoma cells to chemotherapy [144].

Drugs targeting the processes of post-translational modifications can be another strategy to modulate FOXO activity. For example, AS1842856, a hydroquinone-carboxylic acid, binds to dephosphorylated FOXO1, precluding its inactivation [144].

FOXOs respond to chemotherapy and small molecule inhibitors. Anti-cancer treatments with inhibitors of PI3K, AKT and BCR-ABL, as well as 5-fluorouracil, paclitaxel and resveratrol, resulted in apoptosis mediated by FOXO [164]. As such, dysregulation of FOXO proteins can promote resistance to anti-cancer drugs; for example, lower expression of FOXO3 in cancer cells causes resistance to paclitaxel and epirubicin. However, due to the tight regulation and plasticity of growth factor signalling, cancer treatment with small molecule inhibitors that target oncogenic kinases, such as PI3K and AKT, can result in robust feedback mechanisms to maintain the signalling. For example, FOXO1 and FOXO3 upregulate MDR1, causing breast cancer and leukaemia resistance, or doxorubicin and phenylbutyrate treatments in B-cell lymphoma upregulate FOXO4 by upregulating PIK3CA, RICTOR, and SESN3 as a feedback mechanism [144, 164]. Paclitaxel treatment in ovarian cancer cells increases ROS levels, increasing FOXO activity. Paradoxically increased FOXO activity mediates the expression of MnSOD, increasing resistance to ROS levels, which leads to a decrease in the toxicity of the drug. Also, doxorubicin treatment in breast cancer leads to FOXO3 nuclear translocation, upregulating PIK3CA and activating the PI3K/AKT signalling pathway, resulting in doxorubicin resistance [164].

Combined treatments that also target PI3K/AKT signalling or FOXO to prevent feedback mechanisms may be a potential strategy to overcome drug resistance resulting from increased FOXO transcriptional activity that paradoxically promotes resistance. For example, prostate cancer cells treated with paclitaxel and PI3K inhibitors developed resistance because FOXO nuclear translocation leads to ERK feedback activation. However, treatment with a FOXO1 mimicking peptide prevented ERK activation by FOXO and blocked resistance. Similarly, a peptide blocking the FOXO4-p53 interaction in senescent cells induced apoptosis and clearance of senescence cells from the body [144, 164]. However, FOXO-specific inhibitors are difficult to find. Therefore, further development and characterization of FOXO-specific inhibitors seem to be promising [164].

The discovery and development of various compounds that affect FOXO activity underwent significant progress. As such, despite the need to continue to improve clinical efficacy with fewer side effects, FOXO targeting is paving the way for future clinical treatments against cancer and other diseases associated with ageing.

1.5.4.1 BEZ235

BEZ235, also known as Dactolisib, NVP-BEZ235 and RTB101, is an imidazoquinoline derivative (Figure 1.16), capable of inhibiting all isoforms of class I PI3K and mTOR. BEZ235 binds to the ATP-binding pocket of the p110 subunit of PI3K, specifically to V882 and S805. BEZ235 also binds to the catalytic site of mTOR. Previous studies showed that BEZ235 inhibition of PI3K and mTOR led to decreased cancer proliferation and growth in cell lines and xenografts by inhibiting the PI3K/AKT signalling pathway, regardless of the type of cancer [165].

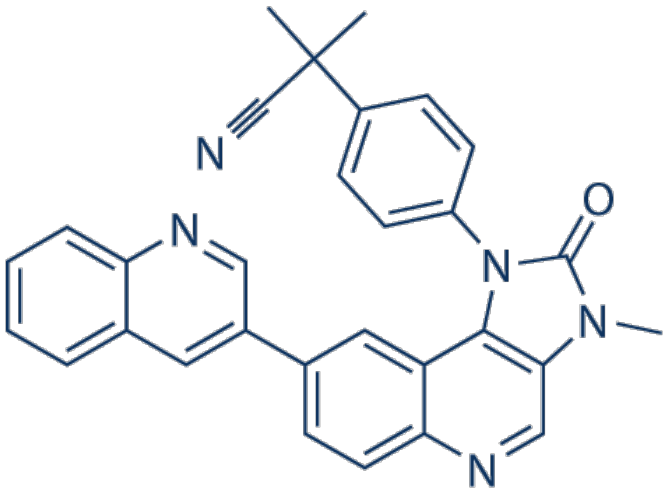

Figure 1.16. The chemical structure of BEZ235. BEZ235 is a dual ATP-competitive PI3K and mTOR inhibitor. Adapted from: doi:10.1038/sj.bjc.6604995. [166].

BEZ235 has been evaluated in several clinical trials. The phase I/II study of BEZ235 in patients with advanced solid malignancies, including patients with advanced breast cancer, as a single agent or combined with trastuzumab (CBEZ235A2101). Another phase I study of BEZ235, administered orally in adult Japanese patients with advanced solid tumours (CBEZ235A1101). The phase Ib study for the maximum tolerated dose of oral BEZ235 and BKM120 combined with paclitaxel or trastuzumab in patients with advanced solid tumours and HER2+ metastatic breast cancer (CBEZ235A2118). Additionally, BEZ235 has also been studied in clinical trials for acute lymphocytic leukaemia (ALL) and acute myeloid leukaemia (AML), with phase I to determine the recommended dose (NCT01756118) [165]. Currently, BEZ235 is in the preclinical phase for precursor cell lymphoblastic leukaemia-lymphoma. Others described BEZ235 to synergize with Dexamethasone, Cytorabine, Doxorubicin, Nilotinib, GX15-070 in preclinical B-ALL models [167].

By inhibiting PI3K and mTOR, BEZ235 inhibits the PI3K/AKT signalling pathway, thus inducing FOXO activity. Our lab has also previously established that TRIB2 is a FOXO repressor by inducing AKT activity and confers *in vitro* and *in vivo* resistance to BEZ235-treatment by acting downstream of BEZ235 inhibition [56].

1.6 The Tribbles proteins

Our lab previously performed a systematic large-scale loss-of-function screening to identify endogenous suppressors of FOXO. The objective is to restore FOXO function by pharmacologically targeting those FOXO-repressor proteins. TRIB2 was one of the identified genes with a role in melanoma progression by inhibiting FOXO activity, both *in vitro* and *in vivo* [55].

1.6.1 Historical overview of the Tribbles family

The human Tribbles family comprise the three members TRIB1, TRIB2 and TRIB3, and these genes are orthologs of the pseudokinase Tribbles (Trbl) in the Drosophila. Trbl in Drosophila promotes slbo and String degradation by the proteasome pathway, leading to cell proliferation, differentiation, and migration changes. Slbo and String are the Drosophila homologues for the human CEBPA and CDC25 phosphatase, respectively [168].

The discovery of Trbl resulted from screens in Drosophila that identified genes that affected oogenesis and gastrulation during embryonic development, namely slbo and String, respectively. Mutant Trbl leads to early mitosis and impaired protein degradation, causing gastrulation defects, and interacts with the proto-oncogene AKT. Similarly, Trbl functions seem conserved in different species; in humans, TRIB2 regulation is affected by the cell cycle, degrades other proteins through ubiquitin and proteasomal mechanisms, very likely CDC25 phosphatases as well. Additionally, human TRIB2 affects the capacity of AKT phosphorylating FOXO3, and thus FOXO3 subcellular localization, TRIB3 binds to AKT, affecting AKT activation by mTORC2. Additionally, both the human and murine brains express TRIB3, and its expression inversely correlates with PARKIN, a protein that causes Parkinson disease when mutated [168].

1.6.2 Pseudokinases

Most signalling pathways include essential components such as protein kinases. These proteins contain a kinase domain fold that specifically phosphorylates serine, threonine or tyrosine residues, and this domain is highly conserved evolutionarily. Kinase function dysregulation may lead to several pathologies, such as neurological, immunological, metabolic and cancer diseases [168-170].

Pseudokinases comprise around 10% of the kinases in the human kinome and regulate many cellular functions, but are less characterized, display missing residues and display low or no catalytic activity. Despite lacking canonical catalytic activity, pseudokinases can still bind to other proteins and participate in signal transduction. Examples of pseudokinases include JAK2 (includes kinase and pseudokinase domains), RAF/MEK and the Tribbles [170].

1.6.3 The pseudokinase structure of the Tribbles and biological functions

The Tribbles are serine/threonine pseudokinases considered to lack (TRIB1) or display low (TRIB2) catalytic activity *in vitro*.

According to Eyers *et al*. [168], the Tribbles are present only in the animal kingdom, with TRIB2 the most ancestral member, followed by TRIB1 and, more recently, TRIB3 likely due to gene duplications from TRIB2. The Tribbles possibly arose due to novel requirements in biological functions in more complex organisms, favouring their roles in substrate regulation by ubiquitination.

Studies regarding Tribbles structure suggest three domains, the N-terminal Proline-Glutamic acid-Serine-Threonine (PEST), the pseudokinase and the C-terminal E3-ligase targeting domains (Figure 1.17A). The PEST sequence is present in many short-lived proteins, such as TRIB1 and TRIB2, and regulate protein degradation [168,

171]. The pseudokinase domain structure was discovered for TRIB1 (Figure 1.17B) and extrapolated for TRIB2 and TRIB3, and this pseudokinase domain lacks the sequence DFG (metal binding) and displays an unusual N-lobe as well as canonical C-lobe. The C-terminal domain interacts *in cis* with a pocket formed contiguous to the unusual region in the tribble pseudokinase domain and contains two regulatory sequences, the HPW[F/L] and the DQXVP[D/E] motifs, that target the MAPKK/MEK family members and bind to E3 ubiquitin ligases such as COP1 to promote degradation of its targets, respectively (Figure 1.17A) [168, 170, 172].

A

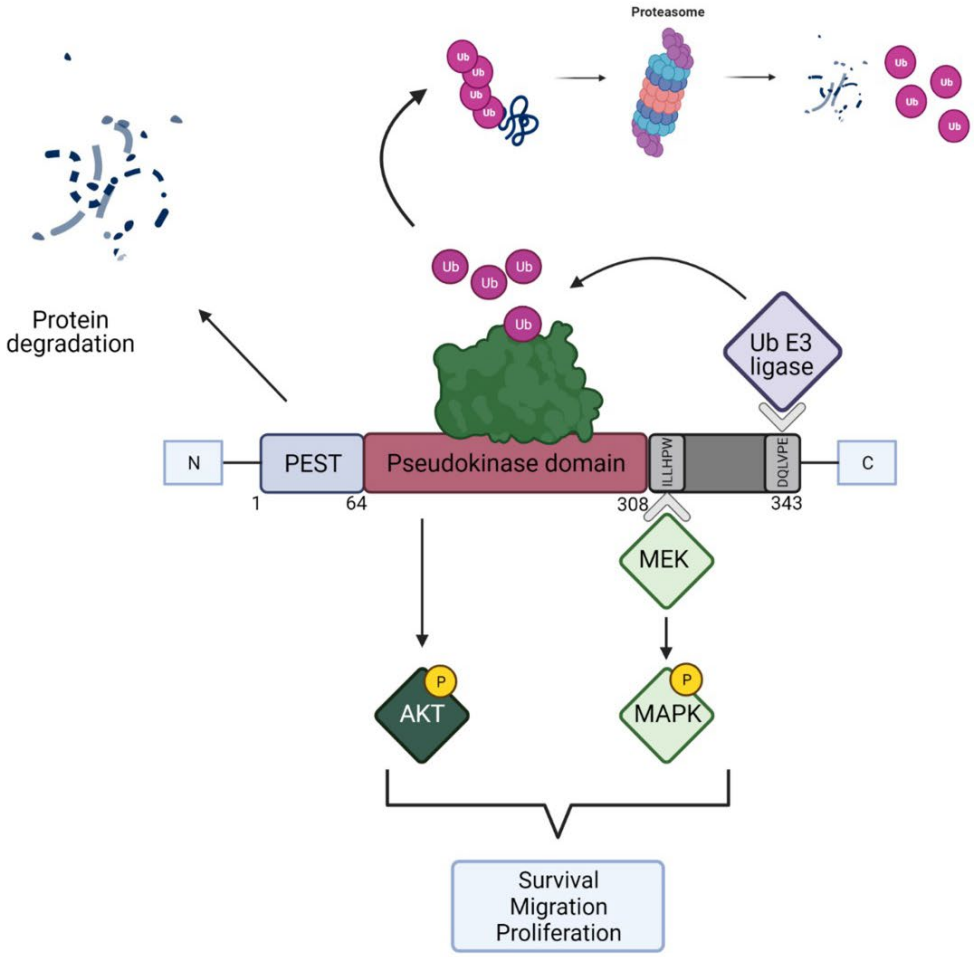

B

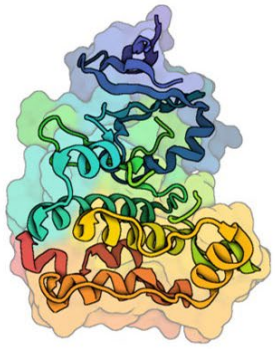

Figure 1.17. A) Structure of Tribbles family. Tribbles comprise three domains, the N-terminal PEST domain involved in protein stability, the pseudokinase domain that shows no or low catalytic activity, and the C-terminal domain containing two conserved motifs HPW[F/L] and DQXVP[D/E. The first motif allows the Tribbles to modulate the MAPK/MEK family, and the latter allows binding to E3 ubiquitin ligases, priming target proteins for degradation. B) TRIB1 pseudokinase domain. TRIB1 structure adapted from: doi:10.1016/j.str.2015.08.017. [172]. Data bank (PDB) protein ID 5CEK.

One of the best examples of Tribbles-induced protein degradation is the TRIB1-mediated CCAAT Enhancer Binding Protein Alpha (CEBPA) degradation. CEBPA binding to the pseudokinase domain induces a conformational change in TRIB1, causing allosteric changes resulting in the COP1 binding sequence becoming available and recruiting COP1, leading to CEBPA ubiquitination and degradation (Figure 1.18) [170, 172].

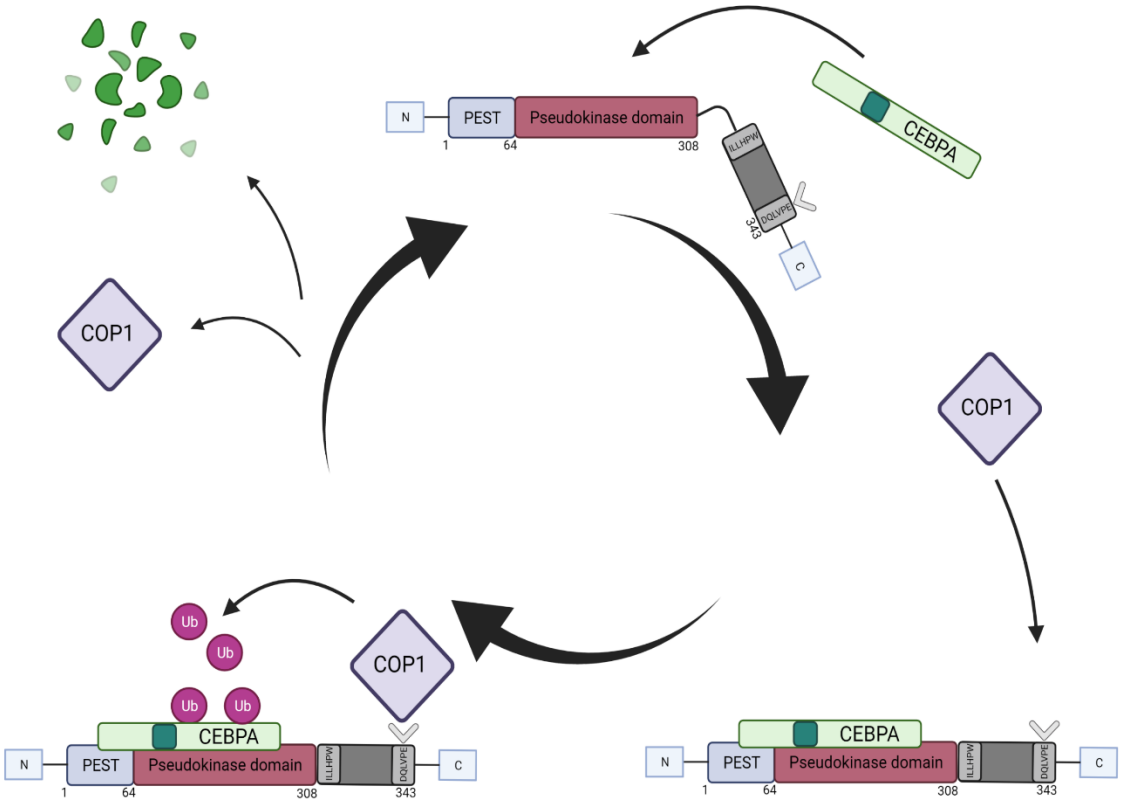

Figure 1.18. TRIB1-mediated CEBPA degradation mechanism. CEBPA binds to the TRIB1 pseudokinase domain, inducing a conformational change that releases COP1-binding domain autoinhibition. COP1 binds to its COP1-binding domain and ubiquitinates CEBPA, priming it for proteasome degradation. COP1 is released, and COP1-binding domain availability becomes inhibited again.

The Tribbles can also alter cancer progression. For example, the oncoprotein PML-RARα induces the progression of acute promyelocytic leukaemia (APL). TRIB3 stabilizes the PML-RARα protein, which also helps prevent senescence by p53, promoting disease progression [173].

Additionally, the Tribbles affect prosurvival signalling, such as the PI3K/AKT signally pathway. TRIB3 prevents AKT phosphorylation, increasing FOXO activity, leading to neuronal cell death [173], and TRIB2 phosphorylates AKT, leading to FOXO inhibition drug resistance [56, 170].

Therefore, the Tribbles can regulate protein degradation and cellular signalling. For example, the Tribbles family has a role in hematopoiesis, but each member also has specialized functions. TRIB1 is involved with cell cycle, liver metabolism and immunoglobulin production, while TRIB2 is involved with the pluripotency of embryonic stem cells and thermogenesis. Moreover, TRIB3 plays a role in adipogenesis, glucose regulation, cell cycle, apoptosis and autophagy in the brain and lipid metabolism [170].

The first description of Tribbles functions was that TRIB3 promoted insulin resistance by inhibiting AKT and stimulated lipolysis through COP1 E3 ligase. Afterwards, TRIB2 was described to affect the differentiation and function of hematopoietic cells and cause AML. Moreover, the Tribbles showed different expression patterns in hematopoiesis (lineage-specific) with TRIB1/TRIB3 expression inversely correlating with TRIB2 expression. Furthermore, the underlying mechanism for TRIB1 and TRIB2 in hematopoiesis is their degradation of CEBPA, which affects the differentiation of monocytes, macrophages, eosinophils and neutrophils. On the other hand, TRIB3 seems to maintain senescence in hematopoietic stem cells [170, 174-176].

The Tribbles also regulate many other proteins, such as MEK1, MAPKs, Wnt/β-catenin and Nuclear Factor Kappa B Subunit 1 (NF-κB), thus spanning their impact on many cellular functions [170]. While kinases serve their biological functions through their catalytic activity, it seems the Tribbles biological functions rely solely on the non-canonical mechanisms (protein degradation and scaffold protein), as they do not seem to display biologically significant catalytic activity.

While TRIB1 structural studies confirm no catalytic activity, one study showed TRIB2 to bind to ATP and autophosphorylate [177], but it remains controversial as another study [178], screening the catalytic activity of several pseudokinases, showed no ATP binding for TRIB2. Moreover, there is no proof of any biological function

associated with the catalytic activity of TRIB2, indicating that the residual catalytic activity may not be essential for the Tribbles to regulate their targets [170].

Consequently, the Tribbles, albeit unable to function as canonical kinases, are still modulators of cellular functions, including transcription, proliferation and metabolism, by interacting directly with other proteins involved in signalling pathways [168, 170].

1.6.4 Tribbles dysregulation: oncogenic and tumour suppressive roles

Dysregulated Tribbles may cause several pathologies, such as liver and metabolic syndromes, neurodegenerative and inflammatory disorders. TRIB3 upregulation promotes Parkinson disease progression by inducing neuronal cell death and delays diabetic kidney disease progression by reducing the expression of genes involved with inflammation. TRIB1 was associated with specific plasmid lipids involved with cardiovascular disease progression [168, 170].

Dysregulated Tribbles also occur in cancer, with altered signalling pathways involved in cell survival, migration, and other cellular processes, promoting cancer treatment resistance [56, 104]. Additionally, the Tribbles family show tumour suppressive and tumour promoting properties depending on the biological environment and family member, as reported by Richmond *et al*. that compiled a list of cancers affected by the Tribbles family and their mechanisms [170].

An example of oncogenic behaviour by the Tribbles is the degradation of CEBPA. TRIB1 and TRIB2 promote CEBPA p42 degradation, originating and accumulating a truncated isoform denominated CEBPA p30. The high ratio of p30/p42 CEBPA promotes the progression of AML, including the AML subtype, APL, that expresses PML-RARα. TRIB3 also stabilises PML-RARα and inhibits p53-mediated senescence in APL [170, 172, 173, 179, 180]. Moreover, the Tribbles modulate the RAS-Raf-MEK-ERK MAPK signalling pathway by interacting with MEK1, resulting in

ERK phosphorylation. Phosphorylated ERK with a high ratio of p30/p42 CEBPA promotes resistance and cell proliferation in AML. Additionally, TRIB2 increases BCL2 Apoptosis Regulator (BCL2) expression levels, promoting resistance in AML by inhibiting apoptosis and inducing cell proliferation [170, 180, 181].

On the other hand, TRIB3 also displays tumour suppressor properties. Qu *et al*. showed that elevated levels of TRIB3 in endometrial cancer cells suppressed cell proliferation and invasion while promoting apoptosis via inhibition of the AKT signalling pathway [182]. Although TRIB3 is the most studied Tribble, especially in the metabolic context, it is still challenging to characterize it as it displays both tumour suppressor and oncogenic behaviours. For example, Wennemers *et al*. reported hypoxia to induce higher TRIB3 mRNA levels in breast cancer, which correlates with a worse prognosis [183]. Endoplasmic reticulum (ER) stress, hypoxia, and nutrient starvation induce TRIB3 via the unfolded protein response, as TRIB3 inhibits Activating Transcription Factor 4 (ATF4) and DNA Damage Inducible Transcript 3 (CHOP) by a negative feedback mechanism [184]. Posteriorly, Wennemers *et al*. [184] also reported similar results, with TRIB3 mRNA levels in another cohort of breast cancer patients. However, surprisingly, TRIB3 mRNA levels did not correlate with TRIB3 protein levels, and higher TRIB3 protein levels were associated with a better prognosis in breast cancer patients via AKT inhibition after radiation or hypoxia treatments [184]. Others suggest that the Tribbles functions correlated better with protein levels than transcriptional levels [170].

1.6.5 Potential use of Tribbles as biomarkers

Cancers are very heterogeneous, and treatment outcome is not consistent with all patients with the same cancer type. Biomarkers are then vital tools for cancer diagnosis and staging, establishing prognosis and indicating more adequate treatment protocols. As such, there is a need for the identification and characterization of novel biomarkers.

As mentioned previously, the Tribbles regulate several cellular functions related to cell survival and proliferation, and their dysregulation and differential expression can contribute to cancer, metabolic dysfunctions and neurodegenerative diseases [168, 170], making them potential biomarkers for these pathologies.

Previously, our lab reported TRIB2 as a potential biomarker for melanoma development [57]. Induction of melanoma progression occurs by inhibition of FOXO due to elevated TRIB2 expression. TRIB2 was the second best to detect human melanoma compared with other melanoma biomarkers, and its expression levels correlated with disease stage and clinical prognosis [57]. Similarly, TRIB2 levels also correlated with worse clinical outcomes in primary pancreatic and colon patient samples [170].

The Tribbles could also be potential biomarkers in AML. TRIB1 is upregulated and mutated in Acute Megakaryocytic Leukaemia (AMKL) and AML with 8q amplifications. Subtypes of AML with low CEBPA or with mutations in Fms Related Receptor Tyrosine Kinase 3-tyrosine kinase domain (FLT3-TKD) display high levels of TRIB2 expression, but its expression decreases in AML subtypes with mutated NPM1 and Fms Related Receptor Tyrosine Kinase 3 (FLT3). TRIB1 and TRIB2 elevated expression induce AML in HOX-dependent leukaemias and APL, and TRIB3 expression increases with APL progression [185]. Elevated TRIB2 protein levels also induced expression of BCL2, an anti-apoptotic protein that promotes AML chemoresistance in an AML cell line U937 and 25% of primary patient samples. Treatment of the AML cell line with venetoclax, a BCL2 inhibitor, sensitized cells to chemotherapy. Other cancers that also display elevated TRIB2 and BCL2 levels, including melanoma, breast and lung cancer, suggest that TRIB2 could be a biomarker for cancers regulated by BCL2 [170, 186, 187].

TRIB3 expression correlated with disease stage and worse prognosis in renal cell carcinoma by inducing cell proliferation and invasion and gastric cancer by stimulating angiogenesis (VEGF-A) [170].

These results indicate that the Tribbles may be potential biomarkers in several cancers, as Tribbles expression levels correlate with disease stage and promote chemoresistance by modulating downstream effectors of cell proliferation, survival and invasion.

1.6.6 Tribbles as therapeutic targets

The Tribbles not only show potential as biomarkers but also as therapeutic targets. Nevertheless, as mentioned previously, the Tribbles are not easy to target because they are pseudokinases [168]. The crystal structure of TRIB1 was determined, unlike TRIB2 and TRIB3, hence delaying the development of drugs targeting the Tribbles. However, we expect all the Tribbles to behave similarly mechanistically. Knowing how TRIB1 changes its conformational structure upon binding to CEBPA to degrade it (Figure 1.18) [172] suggests that it may be possible to target the Tribbles by affecting their conformational structure to inhibit or promote their protein-binding capabilities or by disrupting the interaction of a Tribble with its target protein with peptides or antibodies. For example, Pep2-S160 disrupts the binding between TRIB3 and PML-RARα [170].

Cancer research in targeted therapy generated a vast array of anti-cancer compounds, including kinase inhibitors. Kinase inhibitors compete with ATP at the docking site or bind to allosteric sites to block the protein's catalytic activity [188]. Moreover, many of these clinically approved kinase inhibitors are being re-purposed for pseudokinases, including the Tribbles. For example, the ErbB kinase inhibitors afatinib, neratinib and osimertinib bind to and promote degradation of TRIB2 *in vitro* by destabilizing the C-terminal domain [170, 189].

Jamieson *et al*. [190] screened several kinase inhibitors and selected those that induced thermal stabilization of TRIB1, indicative of successful interaction with TRIB1 and subsequent changes to its conformational structure. Many of these compounds were initially used to target TEK Receptor Tyrosine Kinase (TIE2), VEGF receptor 2 (VEGFR2), EGFR and Erb-B2 Receptor Tyrosine Kinase 2 (ErbB2), also known as HER2, hence suggesting that we can repurpose them to target TRIB1. These compounds act by preventing substrate binding or inhibit TRIB1 autoinhibition [190].

Metformin is used to manage diabetes type 2 and acts by serum reducing glucose levels. Melanoma is a pathology dependent on glucose metabolism. *In vitro* and *in vivo* studies showed that metformin decreases tumour growth and prevents

metastasis by inducing cell cycle arrest and immune response, upregulating miRNA expression, activating p53 and AMPK and decreasing TRIB3 levels [191].

Drug repurposing has some advantages, as it is more economical than developing new drugs and existing FDA-approved drugs already present a known list of clinical effects and side effects on large populations, and the studies above suggest that several compounds may be used as adjuvants in cancer treatment that inhibit the effects of the Tribbles in cancer progression.

1.7 TRIB2-mediated resistance mechanism

We have previously characterized a novel molecular mechanism of therapy resistance in melanoma mediated by the kinase-like protein *Tribbles homologue 2* (*TRIB2*) [56]. The three human Tribbles (TRIB) pseudokinases are homologues of the Drosophila melanogaster pseudokinase termed Tribbles, which controls ovarian border cell and neuronal stem cell physiology [168, 192]. The human TRIB1, 2 and 3 orthologues contain a catalytically impaired pseudokinase domain. Instead of directly phosphorylating target proteins, the Tribbles act as adaptors in critical cellular processes, affecting the activity of activating transcription factor 4 (ATF4) and the MAPK, nuclear factor kappa-light-chain-enhancer of activated B cells (NF-kB) and PI3K/AKT signalling pathways. Tribbles proteins are unique in combining a kinase domain with an adjacent C-terminal motif (COP-1) that engages the ubiquitin E3 ligase machinery and controls the stability of the target proteins [193].

TRIB2 affects several cellular functions, namely cellular differentiation, proliferation, apoptosis, inflammation, immunity, reproduction and drug resistance. Moreover, TRIB2 is involved in neurological, metabolic, autoimmune and inflammatory diseases. TRIB2 also has a role in several cancers, including melanoma, leukaemia, liver and ovarian cancers, by inducing cell proliferation and cell cycle arrest. A more recent discovery, TRIB2 promotes embryonic stem cell (ESC) self-renewal, chondrogenesis and reprogramming of somatic cells [194].

1.7.1 The role of TRIB2 in cancer

TRIB2 often acts as an oncogene but can also function as a tumour suppressor. In AML and T cell acute lymphoblastic leukaemia (T-ALL), MEISI, E2F1 and NOTCH1 regulate TRIB2 activity, promoting tumour progression [194, 195]. Additionally, TRIB2 degrades CEBPA and upregulates BCL2, also contributing to AML progression [185].

Notch1 upregulates TRIB2, inducing degradation of CEBPA, promoting cell proliferation and survival in T-ALL [175]. TRIB2 also activates the ERK signalling pathway in chronic myelogenous leukaemia (CML), resulting in cell proliferation and drug resistance [196]. In myeloid leukaemia, TRIB2 induces the degradation of E3 ubiquitin ligases COP1, βTrCP and Smad ubiquitination regulatory factor 1 (Smurf1), inhibiting the Wnt signalling pathway, thus reducing cell proliferation [168, 197]. Furthermore, TRIB2 can respond to stress by activating the p38 stress signalling pathway, thus functioning as a tumour suppressor [194].

TRIB2 promotes liver cancer progression by interacting with βTrCP, accelerating Yes-associated protein (YAP) stabilization (Hippo signalling pathway), and by preventing the degradation of transcription factor 4 (TCF4) and β-catenin, thus decreasing the activity of the Wnt signalling pathway [194, 198]. Additionally, TRIB2 prevents oxidative damage and reduces ubiquitin availability by activating poly (rC) binding protein 2 (PCBP2) and regulating the ubiquitin proteasome system (UPS) [194, 199].

TRIB2 also promotes lung cancer progression by interacting with Tripartite Motif Containing 21 (TRIM21), which leads to CEBPA degradation, thus inducing cell proliferation [200]. TRIB2 promotes colorectal cancer progression by binding to activating enhancer-binding protein 4 (AP4), thus reducing p21 expression [201]. Glioblastoma develops resistance to temozolomide (TMZ) chemotherapy and radiotherapy in the presence of TRIB2, as TRIB2 interacts with Mitogen-Activated Protein Kinase Kinase Kinase 1 (MEKK1) [194, 202].

The overexpression of TRIB2 in malignant melanomas inhibits FOXO, inducing cancer cell proliferation, survival and tumour progression [55-57]. Moreover, circular RNAs (circRNA)-0084043 interact with miR-429 to increase TRIB2 expression in melanoma [203]. In pancreatic cancer, TRIB2 induces AKT, inhibiting FOXO and p53 and leading to PI3K inhibitors resistance [194].

Several long non-coding RNAs (lncRNA) were recently suggested to modulate TRIB2 to promote tumour progression. ZEB1-AS1 seems to regulate the axis miR-505-3p/TRIB2 in pancreatic cancer, X inactivate-specific transcript (XIST) to regulate miR-125b-5p inducing TRIB2 expression in laryngeal squamous cell carcinoma, and Tripartite motif (TRIM) protein to affect the axis TRIB2/MAPK to induce interleukin 6

(IL6) and disrupt the balance of TH1/TH2, IFNγ and interleukin 4 (IL4) in T cells [194, 204-206]. Due to the relevance of TRIB2 in cancer progression, TRIB2 is a desirable target for cancer treatment. In AML cells, afatinib induced the degradation of TRIB2 [207]. The cell proliferation in lung adenocarcinoma cells decreased when the presence of miR-511 and miR-1297 reduced TRIB2 expression [208]. Furthermore, miR-206 and miR-140 decreased TRIB2 expression, thus reducing cell proliferation and survival [209]. TRIB2 promotes osteosarcoma progression, and miR-509-5p reduces cell proliferation and migration by targeting TRIB2 [194, 210].

1.7.2 The role of TRIB2 in stem cell fate

Embryonic stem cells derive from the inner cell mass of preimplantation embryos, and induced pluripotent stem cells (iPSCs) derive from somatic cells after treatment with the reprogramming factors POU Class 5 Homeobox 1 (OCT4), SOX2, Nanog Homeobox (Nanog), and Kruppel Like Factor 4 (Klf4)(OSKM) [211]. TRIB2 induced cell colony formation, increased alkaline phosphatase activity, and maintained embryonic stem cells (ESC) self-renewal capacity. Moreover, TRIB2 facilitates the reprogramming of somatic cells through modulation of OCT4 and a decrease in TRIB2 levels correlated with ESC differentiation [194, 212].

The degradation of CEBPA by TRIB2 inhibits adipocyte differentiation [213]. Additionally, the MLL-TET1 (MT1) fusion protein increases TRIB2 transcription and protein levels, reducing CEBPA protein levels, hindering the myeloid progenitor cells differentiation, and TRIB2 expression maintains leukemic cells undifferentiated [214]. Moreover, the lncRNA MEG3 was described to upregulate enhancer zeste homolog 2 (EZH2) methyltransferase, which lead to TRIB2 downregulation epigenetically, thus inhibiting chondrogenesis of mesenchymal stem cells (MSC)s [194, 215].

1.8 Aims

There is an absolute need for advances to overcome drug resistance in cancer therapy, as intrinsic and acquired resistance to cancer treatment is the primary cause of treatment failure. TRIB2 promotes resistance to anti-cancer therapy, and melanoma patients with elevated TRIB2 status revealed worse clinical prognoses than patients with lower TRIB2 status [56, 57].

Thus, the main goal of this study is to improve the treatment of melanoma presenting TRIB2-induced resistance. Therefore, we explored the mechanism of TRIB2-mediated resistance and addressed the possibility to overcome TRIB2 resistance pharmacologically.

1.8.1 Hypothesis 1: TRIB2 mediates resistance through transcriptional changes

Our lab has shown that TRIB2 expression inhibits FOXO activity, which affects the transcription of FOXO and p53 target genes, such as FASLG, BIM, PUMA and BCL2 Associated X, Apoptosis Regulator (BAX) [55, 56]. These data suggest that TRIB2-mediated drug resistance results from changes in the expression levels of genes involved in cellular processes, including apoptosis, proliferation, and migration.

The first aim of this study was to test the hypothesis of whether TRIB2-mediated therapy resistance was mediated by changes in the transcriptional regulation of genes. In order to achieve this, we performed RNA-sequencing of isogenic osteosarcoma (U2OS) cell lines with different TRIB2 expression levels (low TRIB2 vs High TRIB2) to evaluate the impact of TRIB2 on gene expression.

1.8.2 Hypothesis 2: TRIB2 resistance can be reverted pharmacologically

As TRIB2 overexpression elicited a transcriptional signature consistent with increased cancer cell proliferation, survival and migration, we propose that TRIB2-mediated resistance could decrease by reversing the transcriptional signature.

In order to test this second hypothesis, we compared our TRIB2 gene expression signature with gene expression signatures from the gene expression database cMAP and selected drugs that induced gene expression profiles opposite TRIB2. These drugs were validated by their effect on cell viability, their effect on FOXO and AKT phosphorylation status, expression levels of FOXO and p53 target genes in several cell lines.

2 Material and Methods

Material and Methods

2.1 Cell Culture

The human osteosarcoma cell line U2OS and the human melanoma cell line UACC-62 were purchased from the American Type Culture Collection (ATCC) and maintained in DMEM supplemented with 10% FBS (Sigma, PT) and antibiotics (Gibco, US). All cell cultures were maintained in a humified incubator at 37°C with 5% CO2 and passaged when confluent using trypsin/EDTA.

2.1.1 Generation of U2OS-TRIB2 cell line

U2OS parental cells, at 70-90% confluency, were transfected with pEGFP-N1 (U2OS-empty) and pEGFP-N1-TRIB2 (U2OS-TRIB2) plasmids, according to Lipofectamine 2000 (Thermofisher Scientific, Portugal) supplier instructions on a 6-well plate, and based on the protocol for the generation of other previous U2OS reporter cells [160]. The plasmid DNA:lipid complexes were prepared with 1µg plasmid, 5µL lipofectamine and Opti-MEM® Reduced Serum Medium to a final volume of 200µL, and incubated for 5 minutes at room temperature (RT). Cells were treated with the DNA:lipid complexes, pEGFP-N1 or pEGFP-N1-TRIB2, for 4H. After the incubation, the transfection media was replaced with fresh culture media. After 72H, the transfected cells were transferred to 10 cm culture plates.

The selection of stable clones was performed by adding G418 (VWR, Portugal) at a final concentration of 600µg/mL to U2OS parental cells and the transfected cells. Cells were under selection for around two weeks, replacing the medium and G418 every two days. The control cells (untransfected cells) and transfected cells that did

not integrate the resistance gene died during the selection process, resulting in the survival of only the G4180-resistant cells. The successful transfection of U2OS-TRIB2 and U2OS-empty cell lines was confirmed by GFP detection under a fluorescent microscope. Cells were further validated at the protein level by western-blot, which detected GFP on the transfected cells and the TRIB2 of the U2OS-TRIB2 cells (Figure 3.1).

2.1.2 Generation of U2nesRELOC and U2foxRELOC cell lines

The U2nesRELOC and the U2foxRELOC systems are FOXO translocation assays previously established [216, 217].

The U2foxRELOC cell line was previously generated from the U2OS cell line that stably expresses GFP-FOXO3a protein and has been previously used to study the FOXO nuclear-cytoplasmic shuttling using image-based cell screening [158, 216].

The U2nesRELOC assay is based on U2OS cells stably expressing green fluorescent protein (GFP)-labelled Rev protein, which contains a strong heterologous NES (pRevMAPKKnesGFP) [216].

2.1.3 Generation of hTRIB2 KO cell line

Dr Bibiana Ferreira generated the hTRIB2 KO cell line using CRISPR/Cas9 to genetically disrupt the TRIB2 locus in the UACC-62 melanoma cell line. The two gRNAs, targeting exon 1, were cloned into a plasmid containing Cas9 and pSpCas9(BB)-2A-Puro (PX459) V2.0. Plasmids were transfected into the UACC-62 cell line with Lipofectamine 2000 (Thermofisher Scientific, Portugal), according to supplier recommendations, and cells were selected following 48H of treatment with

1µg/µl puromycin (VWR, Portugal). Single-cell clones were expanded and analysed by western blot (Figure 3.42).

2.1.4 Generation of UACC62-FOXO and UACC62-TRIB2KO-FOXO

Parental UACC-62 and UACC-62 TRIB2 KO cell lines were cultured as described above without antibiotics and were transfected with pEGFP-C3-FOXO3 using Lipofectamine 2000 (Thermofisher Scientific, Portugal). The cell clones were treated with 1 µg/ml G418 for weeks, and the GFP positive clones were selected.

2.2 RNA sequencing

U2OS-empty and U2OS-TRIB2 cell lines were grown until 70-80% confluency and treated with BEZ235 100nM and the drug vehicle control dimethyl sulfoxide (DMSO) (0,1% v/v) for 72H.

Total RNA was extracted by using TRI-reagent (Sigma, PT). The library preparation and RNA sequencing were performed at the CNIC Genomics Unit (Madrid, Spain). All samples were prepared in biological triplicates, and RNA was sequenced with the GAIIx sequencer, with the single-end 75-bp elongation sequencing protocol.

2.2.1 Mapping and determination of DEGs and gene enrichment analysis

Raw data from the RNA sequencing entailed the four conditions in triplicates. These conditions are U2OS-TRIB2 cells treated with BEZ235 and treated with DMSO, and U2OS-empty cells treated with BEZ235 and treated with DMSO (Figure 3.4).

Sequencing adaptor contaminations were removed from reads using Cutadapt software [218], and the resulting reads were mapped and quantified on the transcriptome (Ensembl GRCh37.v72) using RSEM v1.2.3 [219]. Only genes with at least one count per million in at least three samples were considered for statistical analysis. Data were then normalized, and differential expression tested for the comparisons depicted in Figure 3.4, using the Bioconductor package EdgeR [220]. We considered as differentially expressed those genes with a Benjamini-Hochberg adjusted p-value ≤0.05.

2.2.2 EnrichR analysis

Many of the enrichment analysis tools are based solely on the gene ontology source and generally use the Fisher exact test to compute enrichment analysis, displaying some bias towards list size. Enrichr is a user-friendly enrichment analysis web-based tool that generates various visualization summaries of the collective functions of the gene lists [221].

Enrichr computes three types of enrichment scores to assess the significance of the overlap between the input list and the gene sets in each gene set library. These tests are: 1) the Fisher exact test, a test that implemented in most gene list enrichment analyses; 2) the z-score, a correction test, that computes the deviation from the expected rank by the Fisher exact test; and 3) a combined score that multiplies the log of the p-value computed with the Fisher exact test by the z-score computed by

our correction to the test. We selected the combined score to correct Fischer's exact test [221, 222].

2.3 Wound healing assays

The wound healing assays were performed by growing U2OS-empty and U2OS-TRIB2 cells on 24-well plates up to 80% confluent and treated with BEZ235 or 0.1% DMSO (BEZ235 vehicle control) accordingly. Cells were starved for 12H (DMEM 0% FBS). The wells were scratched with a 200µL pipette tip (Figure 2.1) and washed with PBS 1x to remove cell debris. DMEM 0.5% FBS was added to each well (0H) and incubated up to 24H. The low serum culture media was used only to promote cell migration and minimize cell proliferation while maintaining cells integrity.

Microscope images were taken at the exact three coordinates on each well at 0H and 24H time points (Figure 2.1). We included the following controls in each experiment: the "control" cells were not starved and were maintained in DMEM 10% FBS as a control for cell proliferation and migration after starvation. The control "untreated" cells were starved and maintained in DMEM 0.5% FBS as a control for cell migration in drug-treated cells.

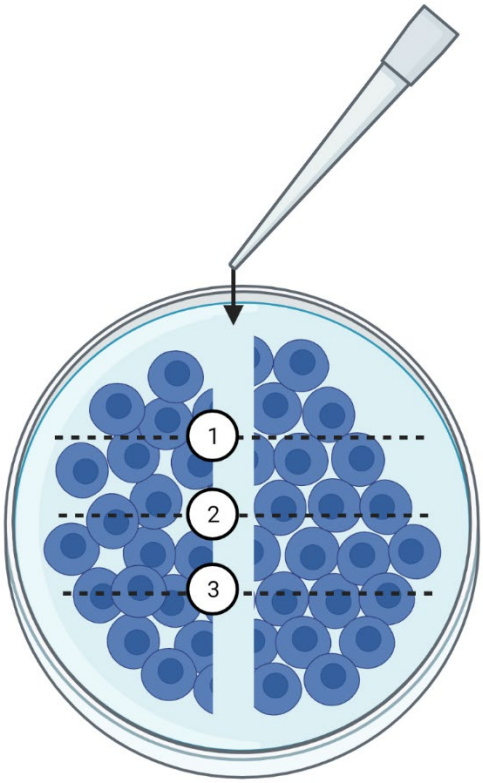

Figure 2.1. Representation of the scratch performed and the position of the microscope images. After cells reached confluency, a pipette tip was used to scratch the cells vertically. The numbers represent the coordinates used to generate microscope images of the cells at both time points (0H and 24H). The dashed lines represent the grid used to define the coordinates (1, 2 and 3).

The scratch width on each well at time-points 0H and 24H was measured with the "length" tool of the Axiovision software and measurements displayed on the cells microscope images. The more cells migrated, the smaller the width.

The area of the scratch on each well over time was determined with the "MRI Wound healing tool" plugin for ImageJ (Fuji) [223]. The wound closure percentage for each coordinate per well was calculated as below and averaged.

$$Wound\ closure\ \% = \frac{Area\ (t = 0h) - Area\ (t = 24h)}{Area\ (t = 0h)} x\ 100$$

2.4 Dual-luciferase reporter assays

We performed dual-luciferase reporter assays to determine if TRIB2 overexpression would affect the promoter activity of its target genes.

U2OS-empty cells and U2OS-TRIB2 cells were seeded at 30000 cells per well in 24-well plates and grown for 24H. Cells were transfected with pGL4.70 vector (Renilla luciferase) and either pGL4.10-empty or pGL4.10-hKISS1p1975 vector, for 4H, with the transfection reagent Lipofectamine2000, according to supplier instructions. The vector:lipid complexes were prepared with either 100µg pGL4.10-KISS1 vector or pGL4.10-empty vector, 4ng pGL4.70 vector, 5µL lipofectamine and Opti-MEM® Reduced Serum Medium to a final volume of 200µL, and incubated for 20 minutes at RT. The reporter vectors were a kind donation from Sabine Heger (Institute of Clinical Biochemistry, Hannover Medical School, Germany) [224]. The same protocol was performed with HEK293T-empty cells.

After transfection, fresh culture media was added to the cells, and cells were treated with BEZ235 100nM or 0,1% DMSO for 24H.

According to supplier instructions, luciferase activity was assessed after the treatment period with Dual-Luciferase Reporter Assay (Promega, Portugal). Briefly, cells were washed with PBS1x, added 100µL Promega Lysis Buffer (PLB) per well, and incubated protected from light at RT for 15 minutes with mixing movement. Samples were transferred to microcentrifuge tubes and stored on ice and protected from light. After the incubation period, 20µL of each sample was transferred to a 96-well plate for luminescence measuring, 100µL of Luciferase Assay Reagent (LARII) was added to each sample. Firefly luciferase activity was immediately measured. Then 100µL of STOP&GLO Reagent was transferred to each sample, and Renilla luciferase was immediately measured.

The firefly luciferase measurements for each sample were normalized by dividing them with their respective renilla luciferase measurements. The fold change of each condition was obtained by dividing the normalized luciferase values with the control (U2OS-empty treated with 0,1% DMSO).

The same protocol in U2OS-empty and U2OS-TRIB2 cells was performed with the pGL3-hKRT14, pGL3-empty and pRL-CMV renilla vectors. The reporter vectors were a kind donation from Eleonora Candi (Department of Experimental Medicine, University of Rome “Tor Vergata”, and IDI-IRCCS, Via dei Monti di Creta, Rome, Italy) [225].

2.5 Connectivity Map analysis

Connectivity Map (cMAP) is an extensive reference collection of gene expression data from cultured human cells perturbed with many chemicals and genetic reagents (perturbagens) that promises to identify connections among drugs, diseases and genes [226, 227].

The novelty of cMAP is to compare the database of drug-induced gene expression signatures with a disease-specific gene signature. The user submits a list of genes affected by a specific disease, and the tool returns a list of drugs or compounds with known mechanisms of action that induce similar or opposite effects on the cells, which allows to understand the potential underlying mechanisms of that disease and to identify possible therapeutic drug candidates [226, 228].

cMAP analysis was performed by querying experiments with drugs that generated transcriptional signatures similar and reversed to TRIB2 transcriptional signature. Drugs were selected with P-value < 0.05 and lower enrichment scores. The enrichment scores are calculated based on the Kolmogorov-Smirnov statistic, a non-parametric rank statistic known as gene set enrichment analysis (GSEA), to interpret gene expression data [226, 229].

2.6 Quantitative Real-Time PCR

Quantitative real-time PCR (RT-qPCR) was performed to determine the transcription levels of genes affected by TRIB2, BEZ235, harmine (HAR) and piperlongumine (PIP), with primer sequences listed in Table 1. Cells were treated with each drug alone, 24H after plating, at cell confluency of 70-90% on 10cm plates (20101, SPL, Portugal). After treatment duration, cells were collected to extract RNA with the E.Z.N.A. Total RNA Kit I (R6834-02, VWR, Portugal), according to supplier instructions. The RNA integrity and concentration was determined by absorbance with NanoDrop 2000 (Thermofisher, Portugal). The samples were stored at -20ºC until further use.

According to supplier instructions, cDNA synthesis was performed with NZY First-Strand cDNA Synthesis Kit (MB12502, Nzytech, Portugal). Briefly, a master mix with 10µL NZYRT 2× Master Mix, 2µL NZYRT Enzyme Mix, 2µg RNA, and DEPC-treated H_2O up to a volume of 20µL per reaction was prepared. The running conditions on the thermocycler were: 25 °C for 10 min, 50 °C for 30 min, 85 °C for 5 min, chill on ice to add 1 µL of NZY RNase H (E. coli), and incubation at 37 °C for 20 min. The cDNA product was diluted 10x with Milli-Q H_2O and stored at -20ºC until further use.

Quantitative PCR was performed on a CFX96 Real-Time System (C1000™ Thermal Cycler, Biorad, Portugal) using Applied Biosystems' SYBR™ Green PCR Master Mix (4309155, Thermo Fisher scientific, Portugal). The samples were prepared with a master mix with 5µL 2x SYBR Green, 2.8µL MilliQ H_2O, 0.5µL of forward primer, 0.5µL of reverse primer and 1.25µL cDNA per reaction for every analyzed gene. The running conditions were: 50ºC for 2 minutes, 95ºC for 2 minutes, 40x GOTO cycle comprised of 95ºC for 15 seconds, 58ºC for 15 seconds and 72ºC for 1 minute, and a melting curve cycle comprised of 65ºC and 95ºC with an increment of 0.05 every 5 seconds. Relative quantification of gene expression was determined by the $2^{-\Delta\Delta Ct}$ method [230].

Table 1. Quantitative real-time PCR primer sequences

Gene	**Forward primer 5'-3'**	**Rev primer 5'-3'**
ANO2	AGGGATCCATCTTTGTCCGG	CTGGAGAATGGGTAGGAGAGG
FasL	GGCCTGTGTCTCCTTGTGAT	GCTTCTCCAAAGATGATGCTG
FMNL2	ATGGGGTCAGAAGTGGTAGC	GGTGGCATAGGTGGTGTTAC
GAPDH	CAATGACCCCTTCATTGACC	TTGATTTTGGAGGGATCTCG
GATA3	TAACATCGACGGTCAAGGCA	ATGGACGTCTTGGAGAAGGG
GNRH1	TACTGACTTGGTGCGTGGAA	CTTTCAGGTCTCGGAGGGG
KISS1	TGGCAGCTACTGCTTTTCCT	CAGTAGCAGCTGGCTTCCTC
LMCD1	TATTCCACCCTCACTGCTCG	TGAGCTCCATGTACTGCAGT
MYCN	CACAAGGCCCTCAGTACCTC	GGATGGGAAGGCATCGTTTG
OCT4	CAGGTTGGAGTGGGGCTAG	GCAGAGCTTTGATGTCCTGG
P21	CAGCAGAGGAAGACCATGTG	GGCGTTTGGAGTGGTAGAAA
P27	CCGGCTAACTCTGAGGACAC	CTTCTGAGGCCAGGCTTCTT
PCYT1A	ATCAAGGAGGCAGGCATGTT	TTGTCAACCCTCTCCTGCAA
PLK1	GAGACCTACCTCCGGATCAA	GGAGACGGGCAGGGATATAG
PUMA	GACCTCAACGCACAGTACGA	TGGGTAAGGGCAGGAGTC
SESN2	GCTGCTGGATGAGAAGTTCC	TCTTCGGGTGGTCTTCTCTG
TNFAIP6	GAAGACACTCAAGGATGGGGA	GCTGCTTGTAAGTTGCGAGA
TRIB2	CACAGGTCTACCCCCATCAC	CCCGATACAAGAAACGCAAT
ZNF3	GAAGGAGTGGAAGCGTTTGG	AGTCCCTTCGCCACACTTAG

2.7 MTT assay

Cell viability was determined using the MTT colourimetric assay. In a 96-well plate, 4000 cells per well were seeded and treated the following day with the respective drugs for 48H and 72H. Cell media was removed and replaced with 100ul

of fresh media containing MTT (0793, VWR, Portugal) solution to a final concentration of 0.5mg/mL. After 3H of incubation, the media was aspirated and replaced with 100ul of DMSO to dissolve the formazan crystals.

Absorbances were measured at 560nm (Abs560) and the reference wavelength 700nm (Abs700). “No cells” control consisted of MTT being added to wells without cells. Absorbances at 560 nm were normalized by subtracting the reference wavelength values (Norm Abs560 = Abs560 sample – Abs700 sample). Cell viability % = (Norm Abs560 sample – Norm Abs560 blank) / (Norm Abs560 control – Norm Abs560 blank) x 100.

2.8 Drug synergy assay

We determined dose-response curves for BEZ235 (Dactolisib) (Novartis, USA), HAR (ACRO302972500, VWR, Portugal) and PIP (CAYM11006-25, VWR, Portugal) in the U2OS-TRIB2 cells to generate equipotent concentration ratios of BEZ235/HAR and BEZ235/PIP. Twenty-four hours after plating, U2OS-TRIB2 cells were treated with 20 serial dilutions of the compounds for 48H and 72H. We determined cell viability at each time point with MTT assays. On GraphPad, we generated normalized dose-response plots (log [drug (μM)] vs cell viability (%)) and non-linear regression to calculate GI50 values.

We then evaluated the synergistic effect on cell viability of BEZ235 and HAR co-treatment by treating U2OS-TRIB2 cells with five serial dilutions of each drug alone, and both drugs combined a constant BEZ:HAR ratio by a 2-fold increase. The same protocol was performed for BEZ235 and PIP synergy experiments. Cell viability was determined using an MTT assay.

Synergy values were obtained with the CompuSyn software [231], based on the Chou Talalay method (http://www.combosyn.com/). Combination index (CI)<1 denotes synergism, CI>1 antagonism, and CI=1 additive.

2.9 FOXO translocation assay

The U2foxRELOC system is a FOXO translocation assay that has been previously established [216, 217]. MSc student Andreia Lamy performed these experiments. Briefly, cells were seeded at a density of 40000 cells per well onto coverslips covering a 24-well plate (SPL Life Sciences Co., Korea). The following day, cells were treated with 0.1% DMSO, 4nM LMB, 16 μM HAR or 13μM PIP for 1H. Cells were fixed with 4% paraformaldehyde for 10 min and washed three times with 1x phosphate-buffered saline (PBS). After 24H, the coverslips were mounted on slides using mounting media coupled with DAPI (Santa Cruz Biotechnology, USA) to stain the nucleus, and slides were stored at 4ºC. All experiments were performed in triplicate. Samples were imaged using 40x lenses on the AxioImager Z2 microscope (Zeiss) imaging system, and images were obtained using AxioVision 4.8.2 software.

2.10 Image and data analysis

MSc student Andreia Lamy and Dr Diego Megias (CNIO, Madrid, Spain) performed the quantification. Quantification of FOXO localization was performed by Definiens Developer v2.5 software (Definiens). Nucleus and cytoplasm segmentation was done with a custom-made rule set using nuclear Dapi signal for the nucleus and then growing the area to identify the cytoplasm. The ratio of green intensity was measured in both the nucleus and cytoplasm. The ratio of Nucleus versus Cytoplasm was calculated to define a threshold for translocation.

2.11 Western-Blot

For the preparation of whole-cell lysate, cells were harvested and lysed in lysis buffer (20 mM Tris pH 7.5, 150 mM NaCl, 1% Triton X-100, 50 mM NaF, 1 mM EDTA, 1 mM EGTA, 2.5 mM sodium pyrophosphate, 1 mM b-glycerophosphate, 10 nM Calyculan A, and EDTA-free complete protease inhibitor cocktail (PIC) (Sigma). Sample buffer was added to 1X final, and samples were boiled at 95ºC for 5 minutes. Samples were resolved on 8–12% SDS-PAGE gels, transferred to nitrocellulose membranes and immunoblotted according to the antibody manufacturer's instructions. Secondary antibodies were added (GE Healthcare) at typically 1:10000 dilution for 1H at RT. Visualization of the signal was achieved using a ChemiDocXRS þ Imaging System (BioRad). Anti FOXO3a (#2497), P-AKT Ser 473 (#4060), total AKT (#9272) and TRIB2 (#13533) were purchased from Cell Signaling Technology (CST, Portugal), P-FOXO Ser 253 (sc-101683), GAPDH FL-335 (sc-25778) and GFP (sc-8334) were purchased from Santa Cruz Biotechnology (SCB, Portugal).

2.12 Trypan Blue exclusion assay

Cells were resuspended and mixed with trypan blue (1:1 v/v). Viable (unstained) and unviable (stained) cells were counted on a hemacytometer and multiplied by two (dilution factor). Cell viability percentage was calculated by dividing the total number of live cells/mL by the total number of cells/mL and multiplied by 100 [232].

3 **Results**

3.1 TRIB2 mediates resistance through transcriptional changes

Interfering with TRIB2 activity might be a therapeutic strategy for treating diverse tumour types and, significantly, to overcome therapy resistance. Here, we use RNA sequencing-based transcriptional profiling of isogenic cells lines with different TRIB2 status in the presence or absence of PI3K/mTOR inhibition to identify sets of differentially expressed genes (DEG), to evaluate if TRIB2-resistance mechanism can result from TRIB2-modulated changes in the transcription signature in cells treated with BEZ235.

Our results show that TRIB2 can mediate the transcriptional signature of the U2OS cell line and, in line with this observation, hinders BEZ235 in regulating several genes, thus decreasing BEZ235 toxicity. TRIB2 overexpression induces changes in gene expression compatible with tumour-promoting effects in the cells, such as an increase in cell survival and migration.

3.1.1 TRIB2 impacts U2OS transcriptional signature

We previously reported TRIB2-mediated resistance to several anti-cancer agents, including the dual PI3K/mTOR inhibitor BEZ235 [56]. To gain insight into the molecular mechanism by which TRIB2 mediates resistance, we analysed global transcriptional changes using next-generation sequencing of total RNA (RNA-seq) in U2OS osteosarcoma cells, a cellular model we have previously used to analyze the function of TRIB2 [55, 56]. The expression of TRIB2 in U2OS is very low at the RNA level and undetectable at the protein level as measured by western blot analysis (Figure 3.1). We have previously confirmed that the TRIB2 protein levels considerably vary among cell lines of different tumour types, with melanoma being cancer that most

strongly expresses TRIB2 (Figure 3.2, Figure 3.3), at the protein level (Figure 3.2) and the mRNA level retrieved from NCI-60 Human Tumour Cell Lines Screen (Figure 3.3).

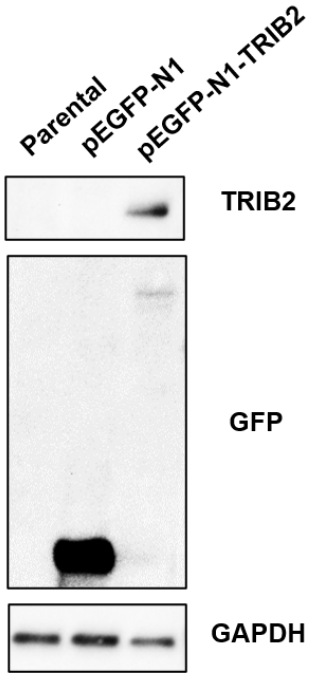

Figure 3.1. Immunoblot of TRIB2 protein levels in U2OS cell lines. TRIB2 and GFP are not detected in the parental U2OS (control). GFP is detected in the U2OS-empty cell line (U2OS transfected with pEGFP-N1 plasmid), and TRIB2 and GFP are detected in the U2OS-TRIB2 cell line (U2OS transfected with pEGFP-N1-TRIB2 plasmid). GAPDH was used as a loading control.

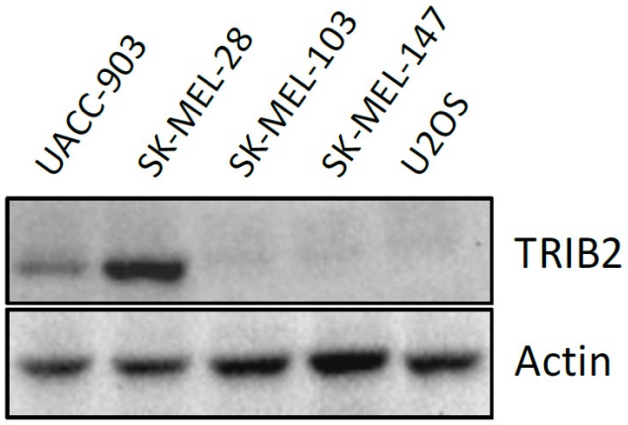

Figure 3.2. Immunoblot of TRIB2 protein levels in a panel of cell lines. The panel included UACC-903, SK-MEL-28, SK-MEL-103, SK-MEL-147 (melanoma cell lines), and U2OS (osteosarcoma cell line). We selected U2OS for further experiments because no TRIB2 protein was detected. Actin was used as a loading control.

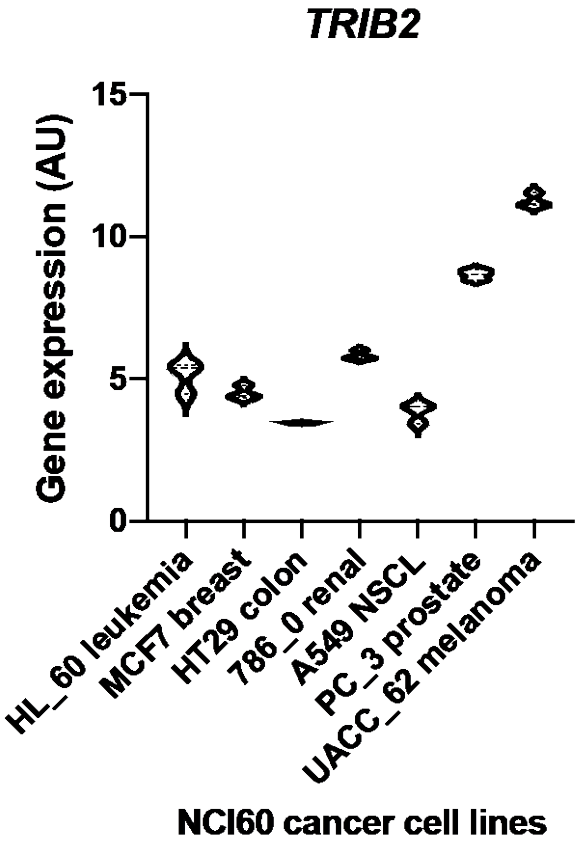

Figure 3.3. TRIB2 expression levels in a panel of cancer cell lines. Expression analysis of TRIB2 mRNA levels in the selected cancer cell lines (NCI60 panel, GDS4296) HL60 (leukaemia), MCF7 (breast cancer), HT29 (colon cancer), 7860 (renal cancer), A549 (NSCL), PC3 (prostate cancer) and UACC-62 (melanoma). NSCL stands for Non-small cell lung cancer.

TRIB2 overexpression in the isogenic U2OS cell line (Figure 3.1) is well within the range of the physiological level of TRIB2 expression. We obtained four lists of differentially expressed genes (DEG) by comparing U2OS cells overexpressing TRIB2 (U2OS-TRIB2) with mock-transfected cells in basal conditions (U2OS parental cells transfected with an empty vector), untreated or upon BEZ235 treatment (Figure 3.4). DEG1 and DEG4 refer to the BEZ235 treatment effects on U2OS cells with no TRIB2 (DEG1) and TRIB2-overexpressing U2OS cells (DEG4), respectively. DEG2 and DEG3 refer to the effects of TRIB2 overexpression in untreated (DEG2) and BEZ235-treated cells (DEG3). DEG5 and DEG6 are subsets of DEG1 and DEG2, respectively.

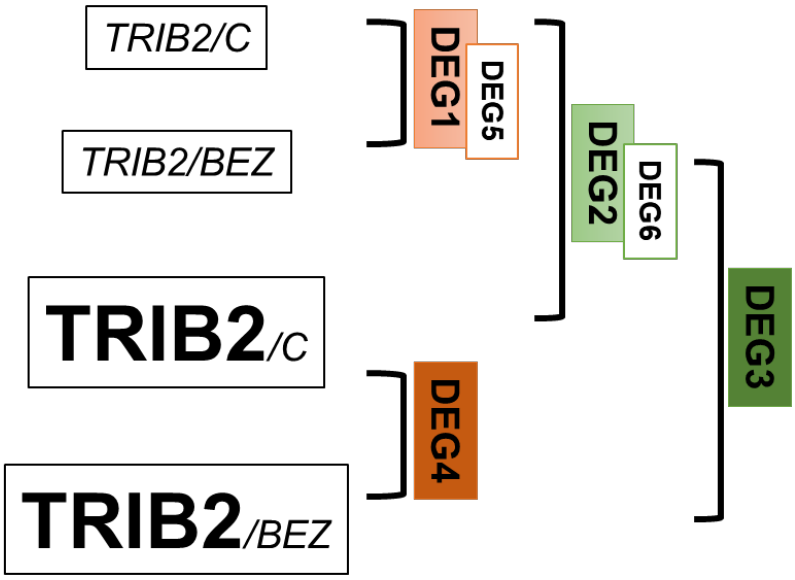

Figure 3.4. Schematic representation of the experimental conditions and the DEGs analysed. DEG1 refers to genes differentially expressed following BEZ235 treatment in cells without TRIB2, and DEG2 refers to genes differentially expressed by TRIB2 overexpression in untreated cells. DEG3 refers to genes differentially expressed following BEZ235 treatment, regardless of TRIB2 levels, while DEG4 represents differentially expressed genes by TRIB2 overexpression, with or without BEZ235 treatment. DEG5 consists of genes exclusively regulated following BEZ235 treatment in cells with low TRIB2 expression, thus a subset of DEG1, while DEG6 refers to genes exclusively regulated by TRIB2 overexpression in untreated cells, hence a subset of DEG2. RNA-seq was performed with isogenic U2OS cell lines that stably express either pEGFP-N1 (No TRIB2) or pEGFP-N1-TRIB2 (TRIB2 overexpressed). Cells were treated with 100nM BEZ235 or vehicle (DMSO) for 72H.

Hierarchical clustering of DEG revealed complete segregation of untreated cells and cells treated with the dual PI3K/mTOR inhibitor BEZ235 independently of TRIB2 status (Figure 3.5).

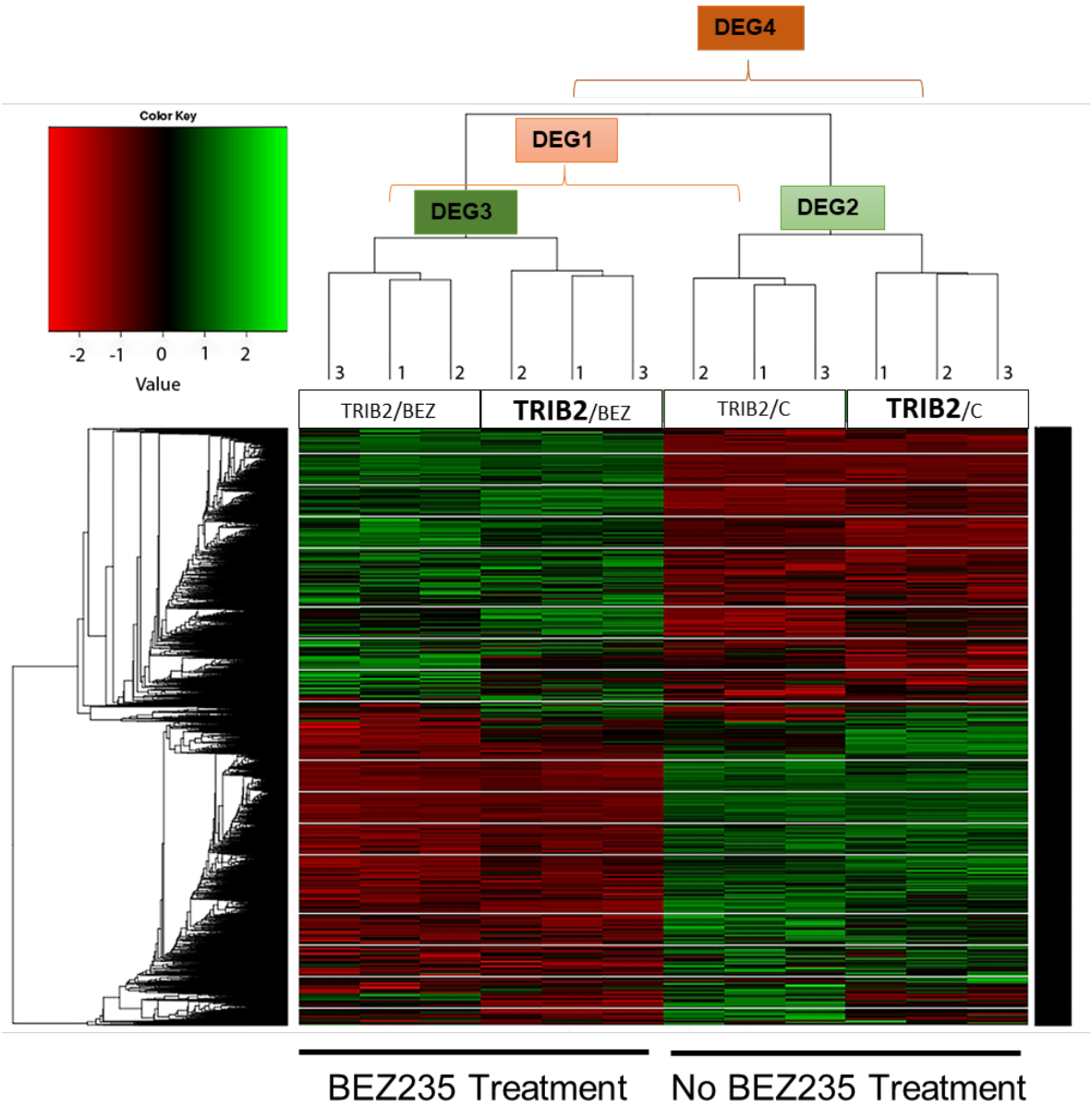

Figure 3.5. Heatmap shows the changes in the transcriptional signatures of U2OS cell lines induced by BEZ235 treatment and TRIB2 overexpression. Upregulated genes are displayed in green, and downregulated genes are displayed in red. **TRIB2** refers to U2OS cell lines overexpressing TRIB2, "BEZ" refers to U2OS cell lines treated with BEZ235, and "C" refers to untreated U2OS cell lines. DEG2 and DEG3 result from comparing the transcriptional signatures of U2OS cells with low and high TRIB2 levels in untreated and BEZ235-treated cells, respectively, while DEG1 and DEG4 result from the comparison between untreated and BEZ235-treated cells with low and high TRIB2 levels, respectively. Genes were considered differentially expressed with a Benjamini-Hochberg adjusted p-value ≤0,05.

TRIB2 overexpression resulted in up-regulation and down-regulation (log2 fold change 0,5 and false discovery rate [FDR] <0,05) of 111 and 164 genes, respectively, constituting a total of 275 genes (DEG2) (Figure 3.6). Treatment with BEZ235 resulted in changes in the expression levels of 2394 genes, 1365 and 1029 upregulated and downregulated genes, respectively (DEG1) (Figure 3.6). Moreover, cells overexpressing TRIB2 and treated with BEZ235 resulted in differential expression of 2630 genes (Figure 3.6). A subset of these genes, 2066 genes, were also affected by BEZ235 treatment, with 1214 upregulated genes and 852 downregulated genes (DEG3). Additionally, other 113 genes were also affected by TRIB2 overexpression, with 79 upregulated genes and 132 downregulated genes (DEG4).

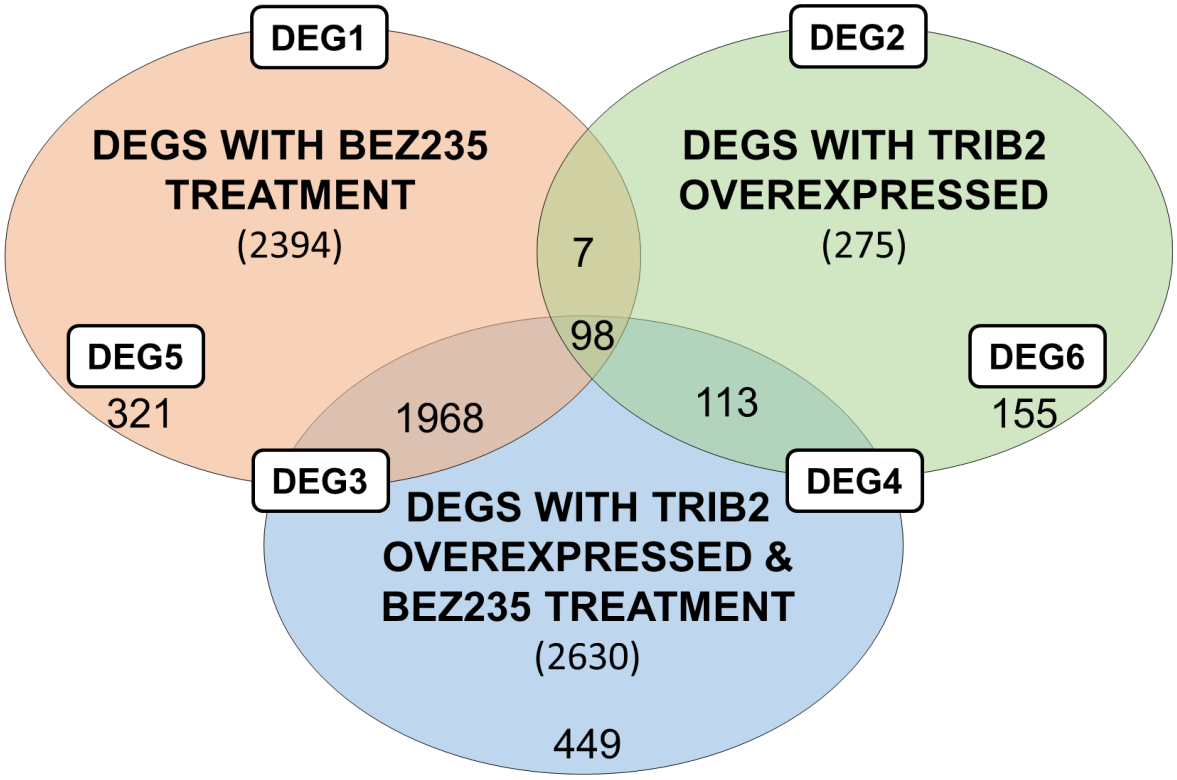

Figure 3.6. The impact of TRIB2 overexpression and BEZ235 treatment on gene expression. Venn diagram displays the number of DEGs by TRIB2 overexpression (green balloon, DEG2), by BEZ235 treatment (pink balloon, DEG1) and by both (blue balloon). The overlapped areas display the number of shared genes affected by combinations of two or three conditions. The lists of genes were obtained assuming a cut-off of log2(fold change) = 0.5 on all significantly differentially expressed genes (adjusted P-value≤0,05).

As expected and validating our approach, we identified TRIB2 as the most upregulated gene in the RNA-seq experimental isogenic cell line, with varying TRIB2 status (Figure 3.7). We verified this by quantitative real-time PCR (RT-qPCR) and western blotting analysis (Figure 3.11 and Figure 3.1). Additionally, TRIB2-mediated downregulation of CEBPA (Figure 3.7) is consistent with previous studies and further confirms the robustness of our approach [197, 233].

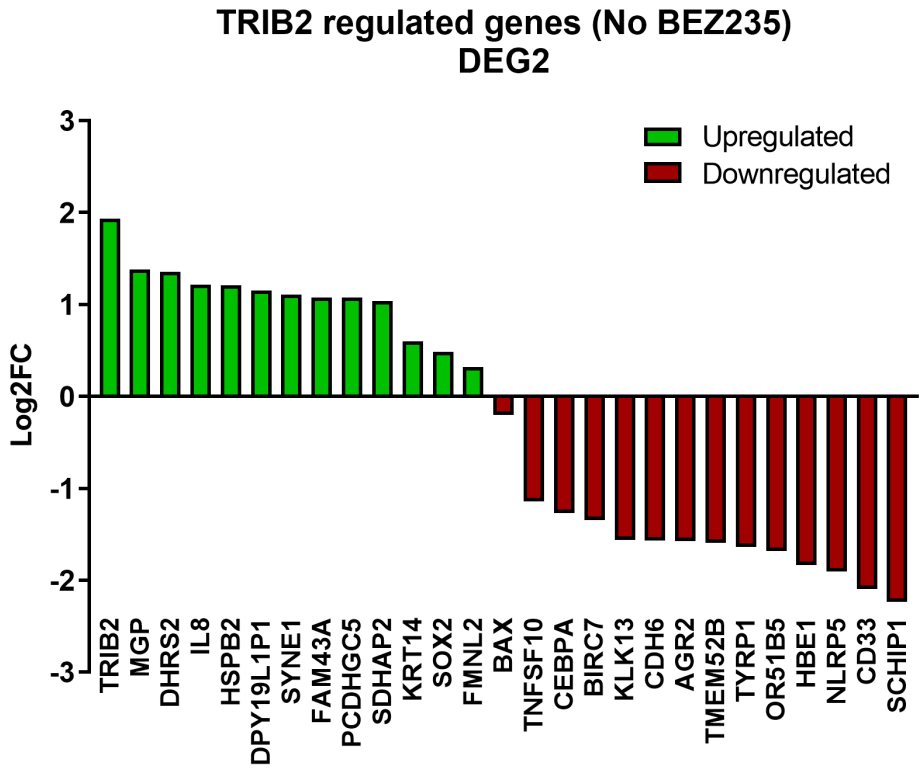

Figure 3.7. Top differentially expressed genes by TRIB2 overexpression in untreated U2OS cells. TRIB2 overexpression changed U2OS cells transcriptional signature and affected the expression of genes involved in cancer progression, such as SOX2, KRT14, CEBPA and BIRC7. The topmost regulated genes were selected, assuming a cut-off of log2(fold change) = 0.5 on all significantly differentially expressed genes (adjusted P-value≤0,05).

We also validated several of the top up- and downregulated genes mediated by TRIB2 overexpression in both untreated (Figure 3.7) and BEZ235 treated cells (Figure 3.8) in the RNA-seq data by RT-qPCR.

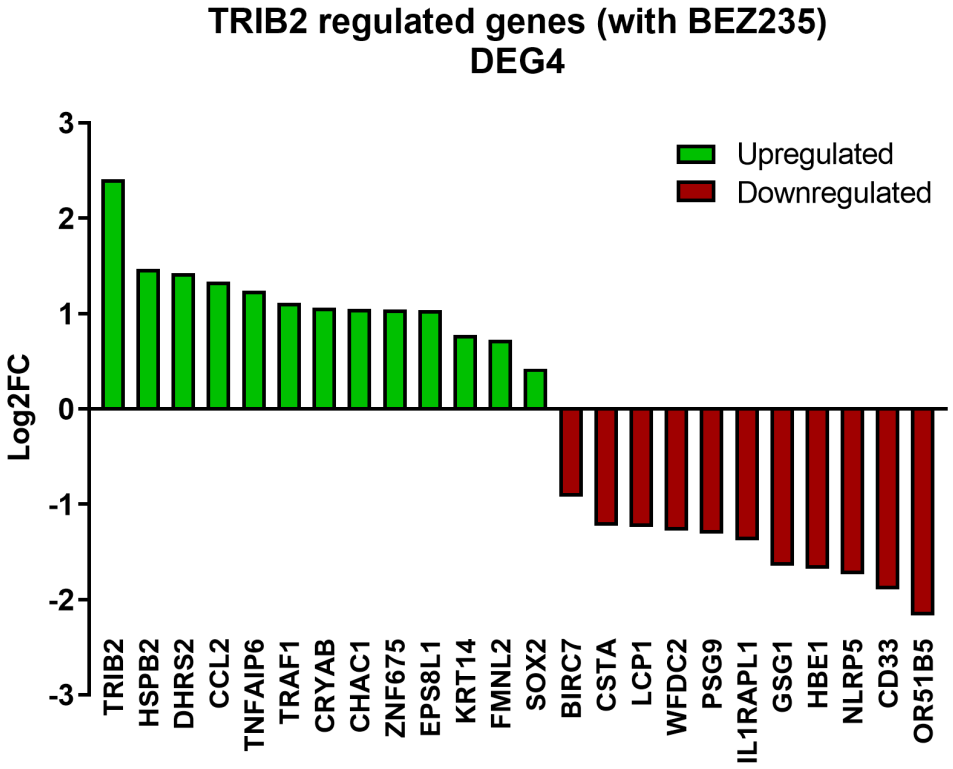

Figure 3.8. Top differentially expressed genes by TRIB2 overexpression in BEZ235-treated cells. TRIB2 overexpression changed the BEZ235-treated U2OS cells transcriptional signature. The top regulated genes were selected, assuming a cut-off of log2(fold change) = 0.5 on all significantly differentially expressed genes (adjusted P-value≤0,05).

The top genes were chosen from the list of differentially expressed genes (Figure 3.6), from which we selected the 10 most upregulated and 10 most downregulated genes by TRIB2, as well as genes described to be involved in cancer proliferation and survival, namely Keratin 14 (KRT14), SRY-Box Transcription Factor 2 (SOX2), Formin Like 2 (FMNL2), BAX, TNFSF10, CEBPA, Baculoviral IAP Repeat Containing 7 (BIRC7), KiSS-1 Metastasis Suppressor (KISS1), Sestrin 2 (SESN2),

MYCN Proto-Oncogene, BHLH Transcription Factor (MYCN) and BCL2 Binding Component 3 (PUMA) [234-244].

KRT14, SOX2, FMNL2 were upregulated by TRIB2 and downregulated by BEZ235 treatment, while BAX, TNFSF10 and CEBPA, were downregulated by TRIB2 (Figure 3.7, Figure 3.8, Figure 3.9, Figure 3.10). Similarly, TRIB2 overexpression correlated with downregulation of BIRC7, while BEZ235 treatment upregulates its expression (Figure 3.7, Figure 3.8). Also, we found KISS1 upregulated after BEZ235 treatment (Figure 3.9, Figure 3.10). Our data also shows that BEZ235 treatment downregulates SESN2 and MYCN (Figure 3.9).

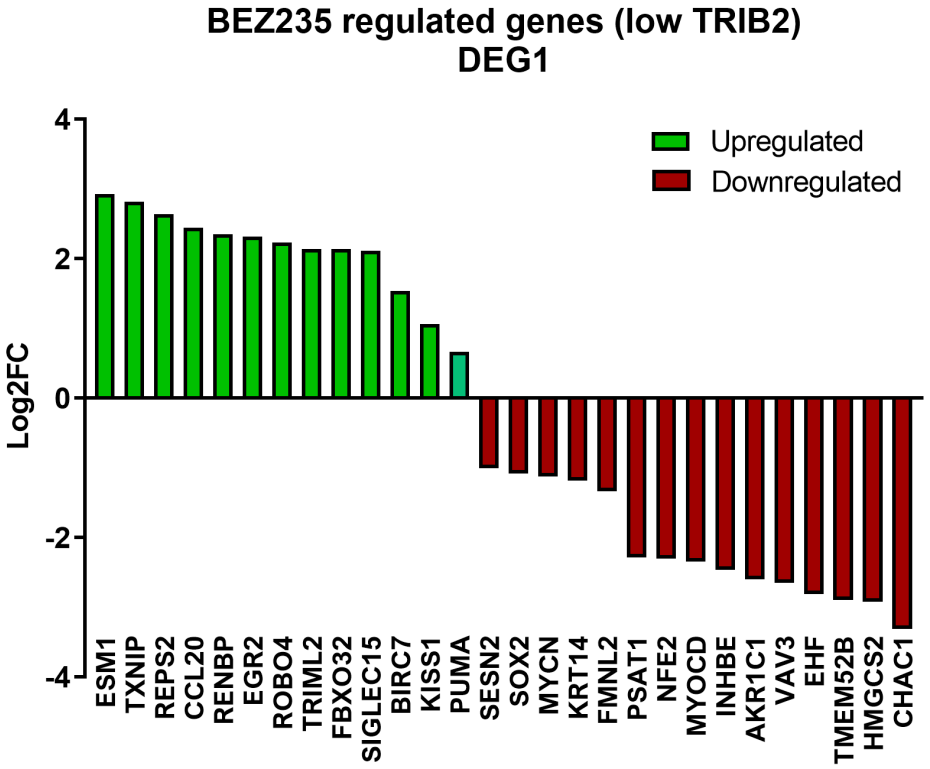

Figure 3.9. Top differentially expressed genes by BEZ235 treatment in U2OS cells with low TRIB2 expression levels. BEZ235 treatment affected the U2OS cells transcription signature and altered the expression of genes involved in cell survival, proliferation and migration, such a KISS1, PUMA, SOX2, SESN2, MYCN and KRT14. The top regulated genes were selected, assuming a cut-off of log2(fold change) = 0.5 on all significantly differentially expressed genes (adjusted P-value≤0,05).

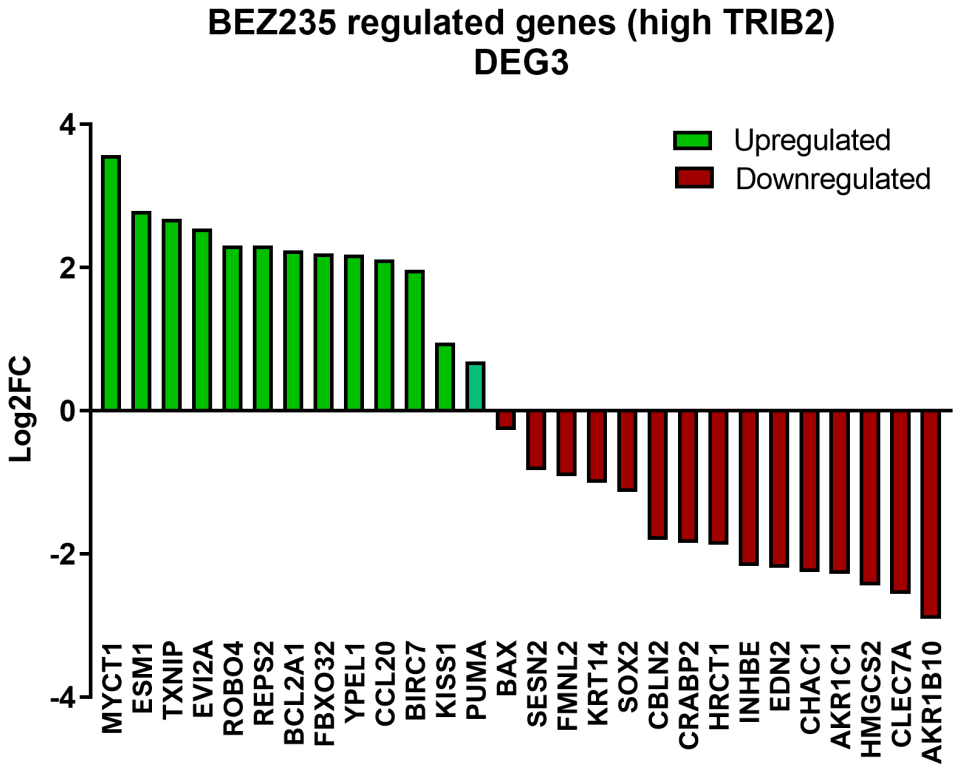

Figure 3.10. Top differentially expressed genes by BEZ235 treatment in U2OS cells with elevated TRIB2 expression level. BEZ235 treatment affected the U2OS cells transcription signature and altered the expression of genes involved in cell survival, proliferation and migration, such a KISS1, PUMA, SOX2, SESN2, MYCN and KRT14. High TRIB2 expression affected the expression of some BEZ235-regulated genes. The top regulated genes were selected, assuming a cut-off of log2(fold change) = 0.5 on all significantly differentially expressed genes (adjusted P-value≤0,05).

3.1.2 TRIB2 overexpression affects BEZ235-induced gene expression

Analysis using qRT-PCR revealed that upregulation of MYCN and SESN2 in U2OS-TRIB2 cells is statistically significant ($p<0,05$) compared to mock-transfected control (MOCK) cells (Figure 3.11). On the other hand, PUMA and KISS1 gene regulation depends on TRIB2 status, downregulated when TRIB2 was overexpressed (Figure 3.12). Moreover, BEZ235 also modulates PUMA, KISS1 and FMNL2 transcriptional levels (Figure 3.12). Interestingly, TRIB2 overexpression appears to

blunt the BEZ235 effect on these cells (Figure 3.12), suggesting that TRIB2 counteracts PI3K/mTOR pathway inhibition.

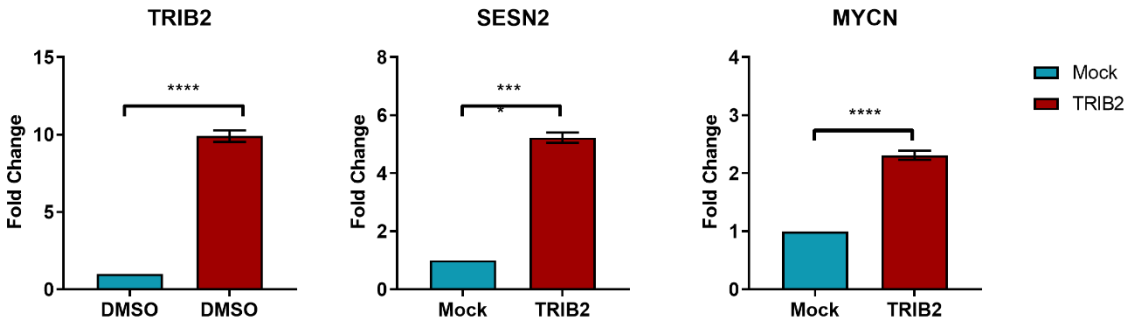

Figure 3.11. Validation of TRIB2 regulated genes by RT-qPCR. mRNA levels detected in U2OS cells with low TRIB2 (MOCK) and with TRIB2 overexpressed. TRIB2, SESN2 and MYCN are upregulated in U2OS cells overexpressing TRIB2. Results represent the mean±SEM generated from 3 independent experiments with triplicates. Statistical significance was determined by unpaired t-test with two-tailed P-value < 0,05, with (****) P < 0,0001.

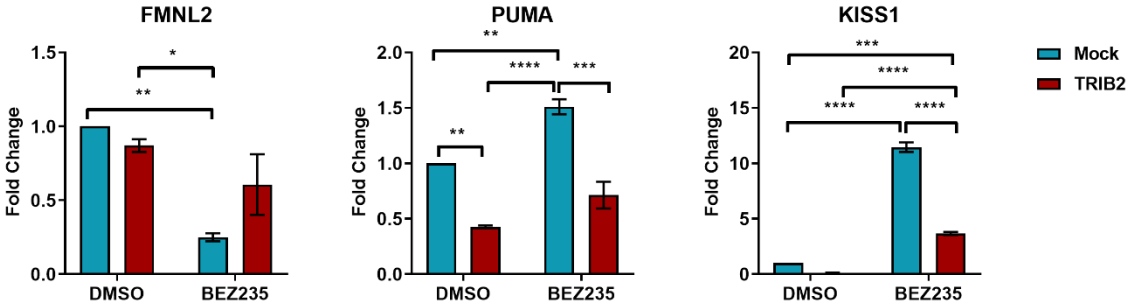

Figure 3.12. Validation of TRIB2 and BEZ235 regulated genes by RT-qPCR. Cells treated with vehicle (DMSO) or BEZ235 100nM for 72H. BEZ235 downregulated FMNL2 and upregulated PUMA and KISS1 on MOCK cells. The presence of TRIB2 decreased BEZ235 modulation of FMNL2, PUMA and KISS1. Results represent the mean±SEM generated from 3 independent experiments with triplicates. Statistical significance was determined by 2-Way ANOVA with Tukey's multiple comparisons test with (*) P < 0,05, (**) P < 0,01, (***) P < 0,001, (****) P < 0,0001.

We performed luciferase assays to evaluate whether BEZ235 treatment and TRIB2 overexpression would affect the candidate genes promoter activity. Figure 3.13 shows that BEZ235 treatment increases KISS1 promoter activity, and TRIB2 overexpression prevents it, according to the RNA-seq data (Figure 3.9, Figure 3.10) and RT-qPCR (Figure 3.12). KRT14 promoter activity decreased with BEZ235 treatment and increased with TRIB2 (Figure 3.13), following the RNA-seq data (Figure 3.7, Figure 3.8, Figure 3.9, Figure 3.10).

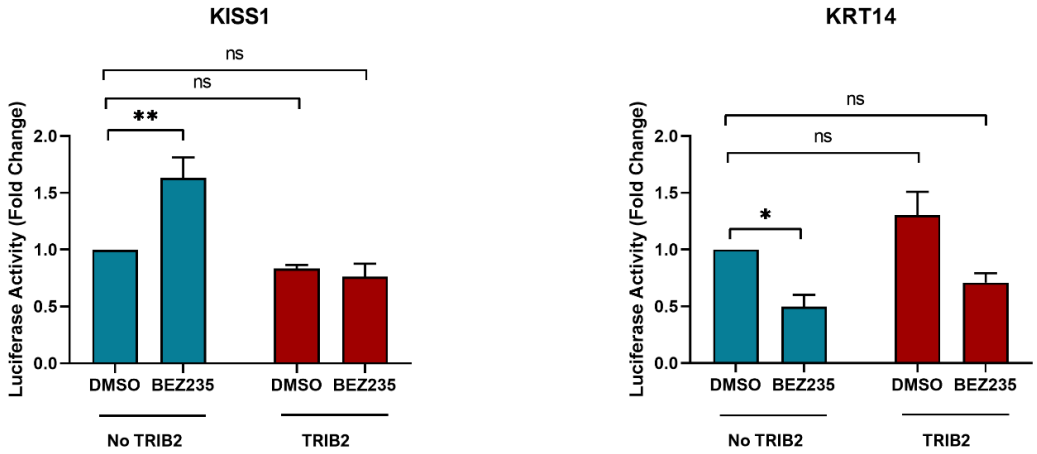

Figure 3.13. The impact of TRIB2 and BEZ235 on the promoter activity of candidate genes. U2OS-empty cells were transiently co-transfected with pGL4.70 (Renilla luciferase) and pGL4.10 or pGL4.10-KISS1 or pGL4.10-KRT14 vectors. U2OS-TRIB2 cells were transiently transfected with the same vectors. After transfection, cells were treated with BEZ235 or 0.1% DMSO for 24H, and a dual luciferase assay was performed. Luciferase values were normalized with the Renilla values. Results represent the mean±SEM generated from 3 independent experiments. Statistical significance was determined by 2-Way ANOVA with Dunnet's multiple comparisons test with (*) P < 0,05, (**) P < 0,01, (***) P < 0,001, (****) P < 0,0001.

To further validate our findings, we analyzed the impact of BEZ235 on KISS1 promoter activity on another cell line and evaluated whether BEZ235 treatment could modulate KISS1 transcription through AKT. BEZ235 treatment upregulated KISS1 promoter activity (Figure 3.14) and decreased AKT phosphorylation status (Figure 3.15), suggesting that BEZ235 inhibition of AKT activity could have led to KISS1 upregulation, consistent with previous results that show that TRIB2 overexpression

prevents KISS1 upregulation by BEZ235 (Figure 3.12) and KISS1 increased promoter activity by BEZ235 (Figure 3.13).

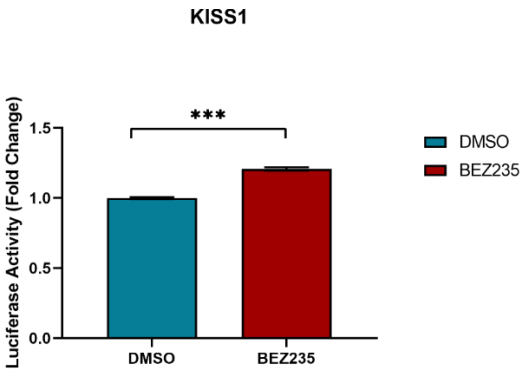

Figure 3.14. BEZ235 treatment upregulated KISS1 promoter activity. HEK293T cells were transiently co-transfected with pGL4.70 (Renilla luciferase) and pGL4.10 or pGL4.10-KISS1. After transfection, cells were treated with BEZ235 or 0.1% DMSO for 24H, and a dual luciferase assay was performed. Luciferase values were normalized with the Renilla values. Results represent the mean±SEM generated from 3 independent experiments. Statistical significance was determined by unpaired T-test with two-tailed P-value with (*) P < 0,05, (**) P < 0,01, (***) P < 0,001, (****) P < 0,0001.

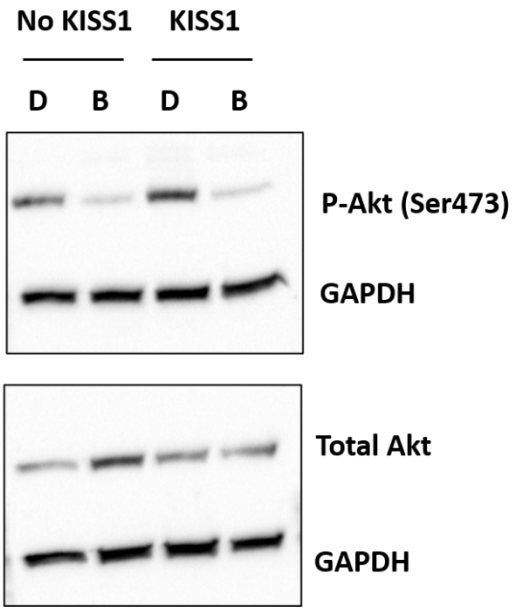

Figure 3.15. Immunoblot of AKT levels in HEK293T cells treated with BEZ235. BEZ235 treatment decreased the phosphorylated AKT protein levels. HEK293T cells were transiently co-transfected with pGL4.70 (Renilla luciferase) and pGL4.10 or pGL4.10-KISS1. After transfection, cells were treated with BEZ235 or 0.1% DMSO for 24H. GAPDH was used as a loading control.

Principal Component Analysis (PCA) of the logarithmized Counts per Million (log CPM) of the RNA-seq data showed that TRIB2 overexpression and BEZ235 treatment have a significant impact on gene expression (Figure 3.16), consistent with the heatmap (Figure 3.5).

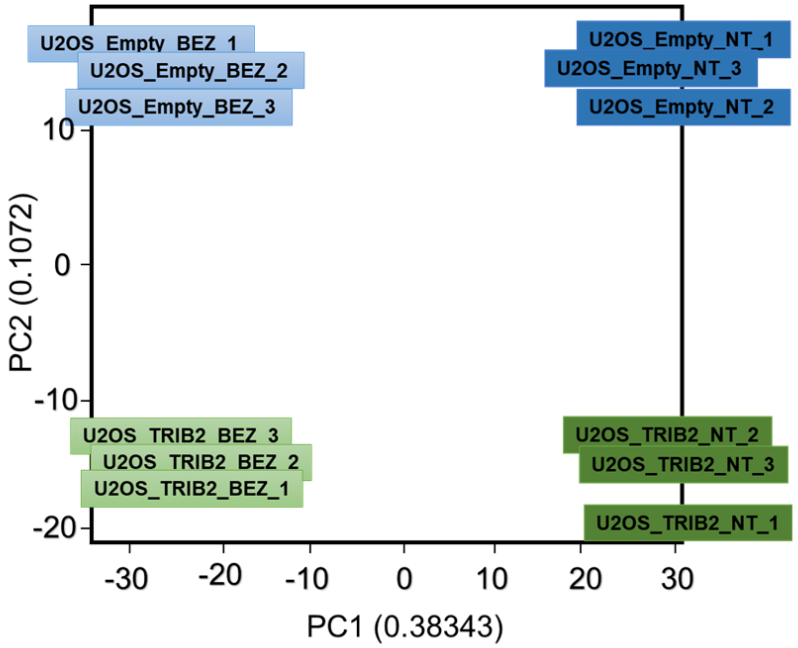

Figure 3.16. PCA analysis showing the variance produced by BEZ235 treatment and TRIB2 overexpression. The *x*- and *y*-axes denote the first and second principal components, respectively. BEZ235 treatment (PC1) and TRIB2 overexpression (PC2) have a significant impact on gene expression.

To evaluate the impact of TRIB2 and BEZ235 on the differential expression of the analysed genes, we generated MA-plots [245] to visualize the distribution of the DEGs (red dots) in terms of read-counts (log CPM) and fold change (logFC), among the gene population (Figure 3.17, Figure 3.18). TRIB2 overexpression in untreated (Figure 3.17A) and BEZ235 treated cells (Figure 3.17B) significantly affected the expression of several genes (red dots). On the other hand, BEZ235 treatment (Figure

3.18) affected more genes than TRIB2 overexpression (Figure 3.17). In both TRIB2-overexpressed and BEZ235-treated cells, most of the logFC magnitudes lie under 2, which means most of these DEGs increased or decreased up to 4 times (Figure 3.17, Figure 3.18).

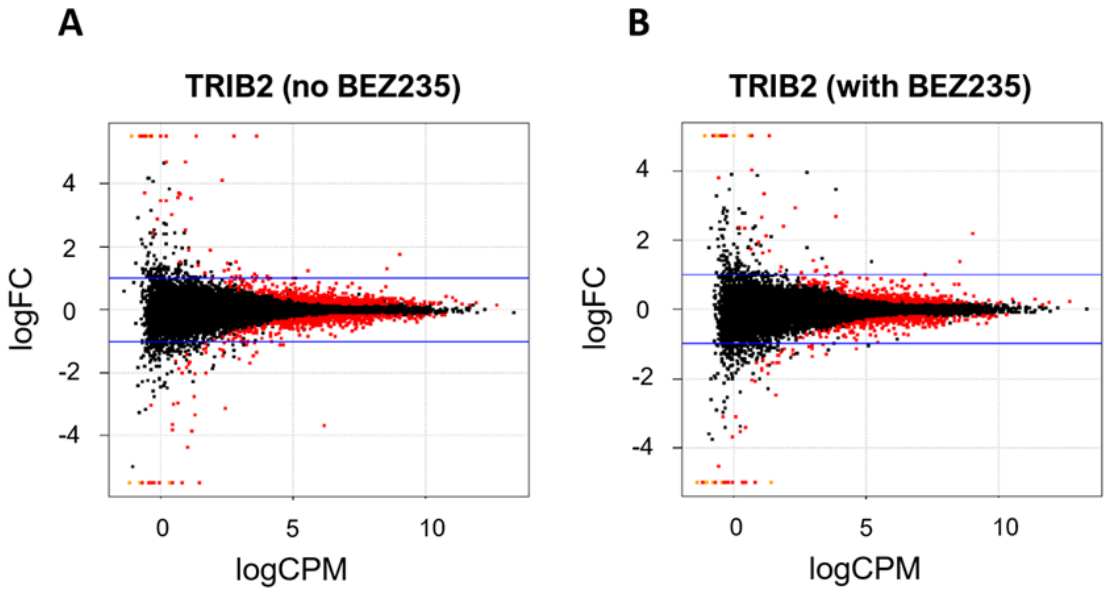

Figure 3.17. The contribution of TRIB2 overexpression to gene expression. High levels of TRIB2 impacts gene expression in untreated (A) and BEZ235-treated (B) U2OS cells. The MA plots show the correlation between read-counts (log CPM) and fold change (log2FC). Red dots indicate differentially expressed genes. Horizontal lines represent the threshold for fold change (-0.5 and 0.5) to indicate significant fold change. The higher the read count and the higher the fold change, the greater the confidence in DEGs.

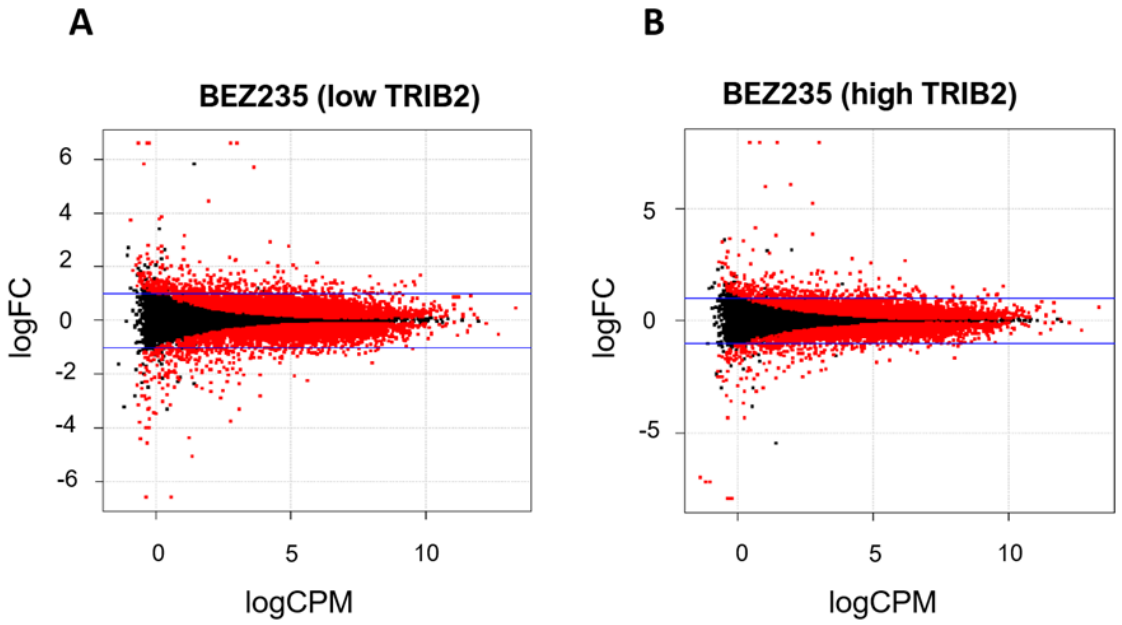

Figure 3.18. The contribution of BEZ235 treatment to gene expression. BEZ235 treatment impacts gene expression in U2OS cells with low (A) and high TRIB2 levels (B). BEZ235 treatment showed more DEGs than TRIB2 overexpression (Figure 3.17). The MA plots show the correlation between read-counts (log CPM) and fold change (log2FC). Red dots indicate differentially expressed genes. Horizontal lines represent the threshold for fold change (-0.5 and 0.5) to indicate significant fold change. The higher the read count and the higher the fold change, the greater the confidence in DEGs.

3.1.3 TRIB2 regulates genes involved in cancer cell proliferation, migration and survival

From the 2396 genes differentially regulated by BEZ235 treatment (DEG1) in cells with low TRIB2, 321 are BEZ exclusive (Figure 3.6) (DEG5). Enrichment analysis of the DEG5 gene list for kinase perturbations from the GEO database (obtained from EnrichR tool [221, 222], resulted in the enrichment of the perturbation of various kinases, including inhibition of PI3Kα mutant, Advanced Glycosylation End-Product Specific Receptor (AGER), also known as RAGE, spleen tyrosine kinase (SYK), Epidermal Growth Factor Receptor (EGFR), ABL Proto-Oncogene 1, Non-Receptor

Tyrosine Kinase (ABL1), Cyclin-Dependent Kinase 19 (CDK19) and Ataxia Telangiectasia Mutated (ATM) (Table 2).

From the 275 genes differentially regulated by TRIB2 overexpression (DEG2) in untreated cells (Figure 3.6), 155 are TRIB2 exclusively regulated (DEG6). Enrichment analysis of the DEG6 gene list for kinase perturbations from the GEO database (obtained from EnrichR tool) resulted in the enrichment of the perturbation of several kinases, including activation of 3-phosphoinositide-dependent protein kinase 1 (PDK1), Glycogen Synthase Kinase 3 beta (GSK3β), two important components of the PI3K/AKT signalling pathway, and IL2 Inducible T Cell Kinase (ITK) (Table 3). This data is in line with previous data describing TRIB2 as part of the PI3K/AKT signalling cascade.

Table 2. Kinase Perturbations Enrichment Analysis grom GEO database (EnrichR tool) BEZ235.

Term	Overlap	*p*-value	Adjusted P	Old *p*-value	Old Adjust	Odds Ratio	Combined Score	Genes
PIK3CA mutant 27 GDS4053	2/300	0.029289	1	0	0	7.407407407	26.15209006	PTCH2; ADRA1A
RAGE knockout 269 GSE22873	2/300	0.029289	1	0	0	7.407407407	26.15209006	MYCN; ADRA1A
SYK drug inhibition 283 GSE43510	2/300	0.029289	1	0	0	7.407407407	26.15209006	INSIG1; GPD1L
SYK drug inhibition 288 GSE43510	2/300	0.029289	1	0	0	7.407407407	26.15209006	FMNL2; INSIG1
EGFR drug activation 20 GDS2146	2/300	0.029289	1	0	0	7.407407407	26.15209006	ADAMTS15; RGMA
ABL1 knockdown 100 GSE27869	2/300	0.029289	1	0	0	7.407407407	26.15209006	CLMP; FMNL2
CDK19 knockdown 148 GSE32108	2/300	0.029289	1	0	0	7.407407407	26.15209006	MYCN;ADRA1A
ATM knockout 74 GSE23116	2/300	0.029289	1	0	0	7.407407407	26.15209006	CLMP; PDZRN3

Table 3. Kinase Perturbations Enrichment Analysis grom GEO database (EnrichR tool) TRIB2.

Term	Overlap	*p*-Value	Adjusted P	Old *p*-Value	Old Adjust	Odds Ratio	Combined Score	Genes
PDK1 knockout 80 GSE26290	5/300	0.002364	0.673825	0	0	5.376344086	32.51222507	OLFM1; RASL10A; FAM
GSK3A knockdown 207 GDS4305	4/300	0.014008	1	0	0	4.301075269	18.35759126	CST1; RBPMS; CDH22; K
ITK knockout 241 GSE12465	4/300	0.014008	1	0	0	4.301075269	18.35759126	RBPMS; P2RX1; GNG11

To understand the relevance of these genes in the context of the Kyoto Encyclopedia of Genes and Genomes (KEGG) pathways, we have performed enrichment analysis on TRIB2 and BEZ235-induced transcriptional signatures with the EnrichR tool. Enrichment analysis of the list of TRIB2 up-regulated transcripts showed significant enrichment for genes involved in pathways in cancer and TNF signalling (Figure 3.19, Figure 3.20), alcoholism (Figure 3.19) and transcriptional misregulation in cancer (Figure 3.20).

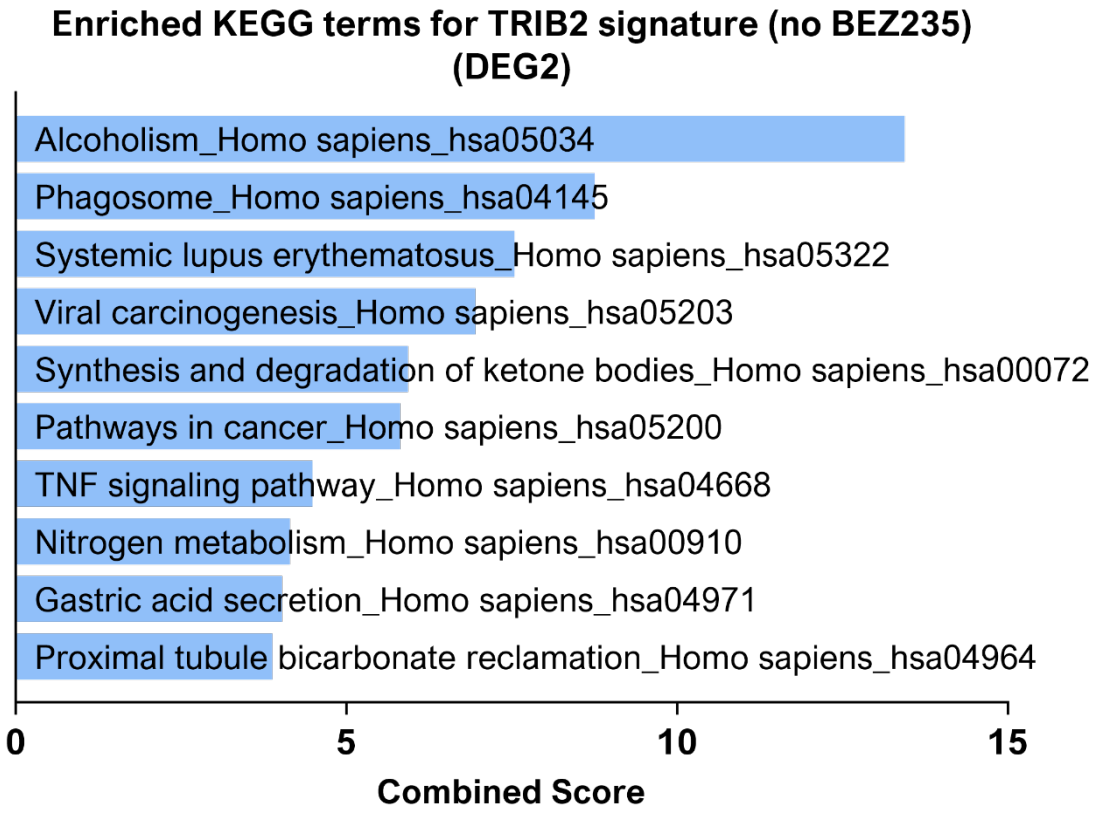

Figure 3.19. Top 10 KEGG terms enrichment analysis in TRIB2 signature in untreated U2OS cells. TRIB2 transcriptional signature was enriched for signalling pathways involved in cancer. KEGG term enrichment analysis was performed using the web tool Enrichr by computing the Combined Score, obtained by multiplying the log of the p-value (the Fisher exact test) by the Z-score. The longer the horizontal bar, the higher the statistical confidence of the term.

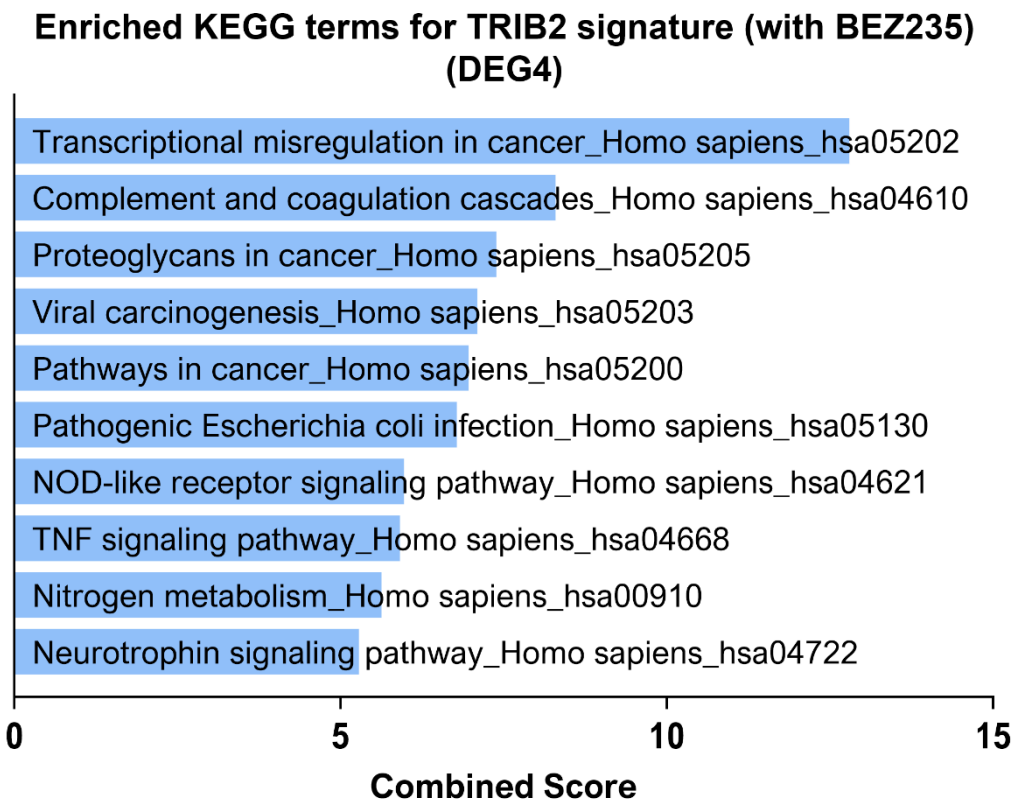

Figure 3.20. Top 10 KEGG terms enrichment analysis in TRIB2 signature in BEZ235-treated U2OS cells. TRIB2 transcriptional signature was enriched for signalling pathways involved in cancer. KEGG term enrichment analysis was performed using the web tool Enrichr by computing the Combined Score, obtained by multiplying the log of the p-value (the Fisher exact test) by the Z-score. The longer the horizontal bar, the higher the statistical confidence of the term.

BEZ235 treatment up-regulated transcripts showed significant enrichment for genes involved in pathways in cancer, TNF signalling and small cell lung cancer (Figure 3.21, Figure 3.22).

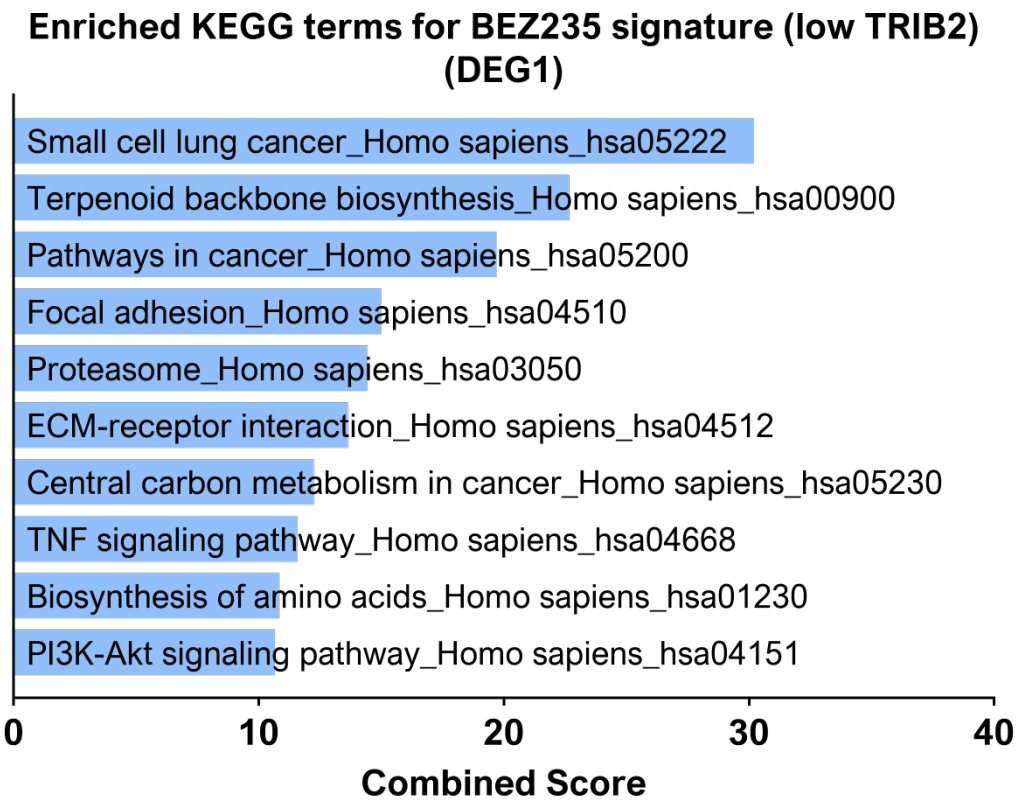

Figure 3.21. Top 10 KEGG terms enrichment analysis in BEZ235 signature in U2OS cells. BEZ235 transcriptional signature was enriched for signalling pathways involved in cancer. KEGG term enrichment analysis was performed using the web tool Enrichr by computing the Combined Score, obtained by multiplying the log of the p-value (the Fisher exact test) by the Z-score. The longer the horizontal bar, the higher the statistical confidence of the term.

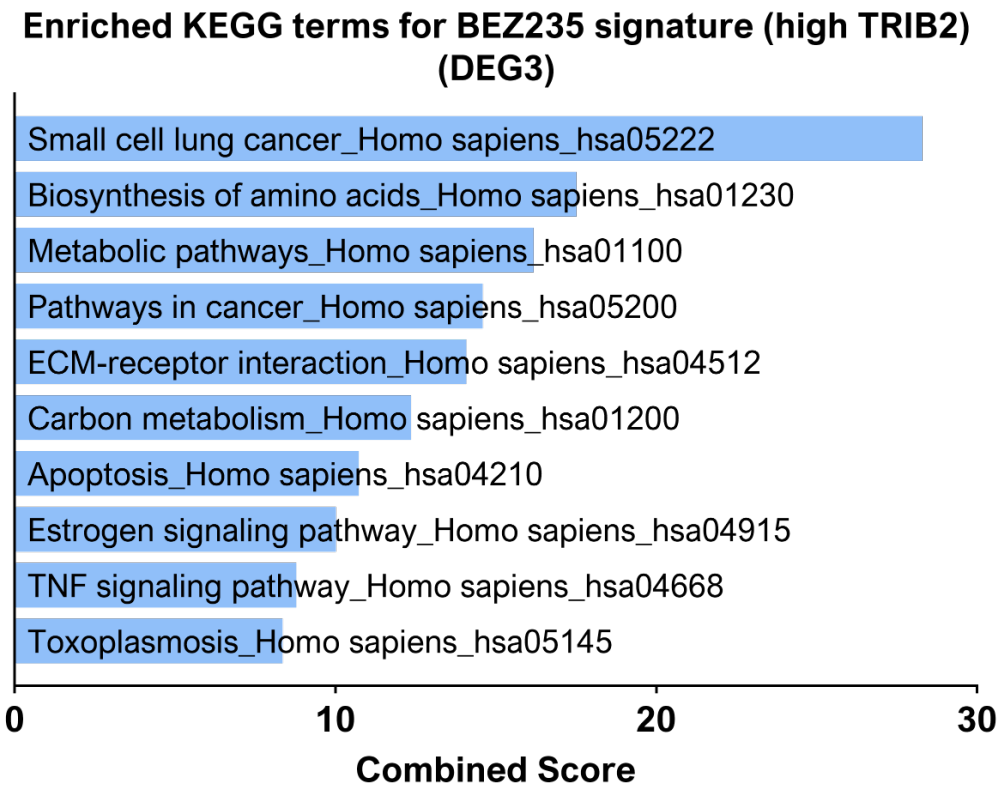

Figure 3.22. Top 10 KEGG terms enrichment analysis in BEZ235 signature in U2OS cells with elevated TRIB2 levels. BEZ235 transcriptional signature was enriched for signalling pathways involved in cancer. KEGG term enrichment analysis was performed using the web tool Enrichr by computing the Combined Score, obtained by multiplying the log of the p-value (the Fisher exact test) by the Z-score. The longer the horizontal bar, the higher the statistical confidence of the term.

TRIB2 overexpression and BEZ235 treatment affect the transcription signature of the U2OS cells.

Considering that BEZ235 is a drug that induces cell senescence and death and can also decrease cell migration [246, 247], and TRIB2 can promote cell proliferation and migration [194, 210], we performed a wound-healing assay to evaluate whether TRIB2 overexpression would affect BEZ235 impact on cell migration (Figure 3.23).

Figure 3.23A shows that after 24H, DMSO-treated U2OS-empty cells (-TRIB2) could migrate and fill the gap (-TRIB2/-BEZ235). When these cells were treated with BEZ235, BEZ235 inhibited cell migration (-TRIB2/+BEZ235), indicated by an empty area with no cells after 24H. However, TRIB2 overexpression on BEZ235-treated cells

restored the cell migration ability in the presence of BEZ235 (+TRIB2/+BEZ235). These results suggest that TRIB2 decreases the tumour-suppressor effect of BEZ235 on the cells.

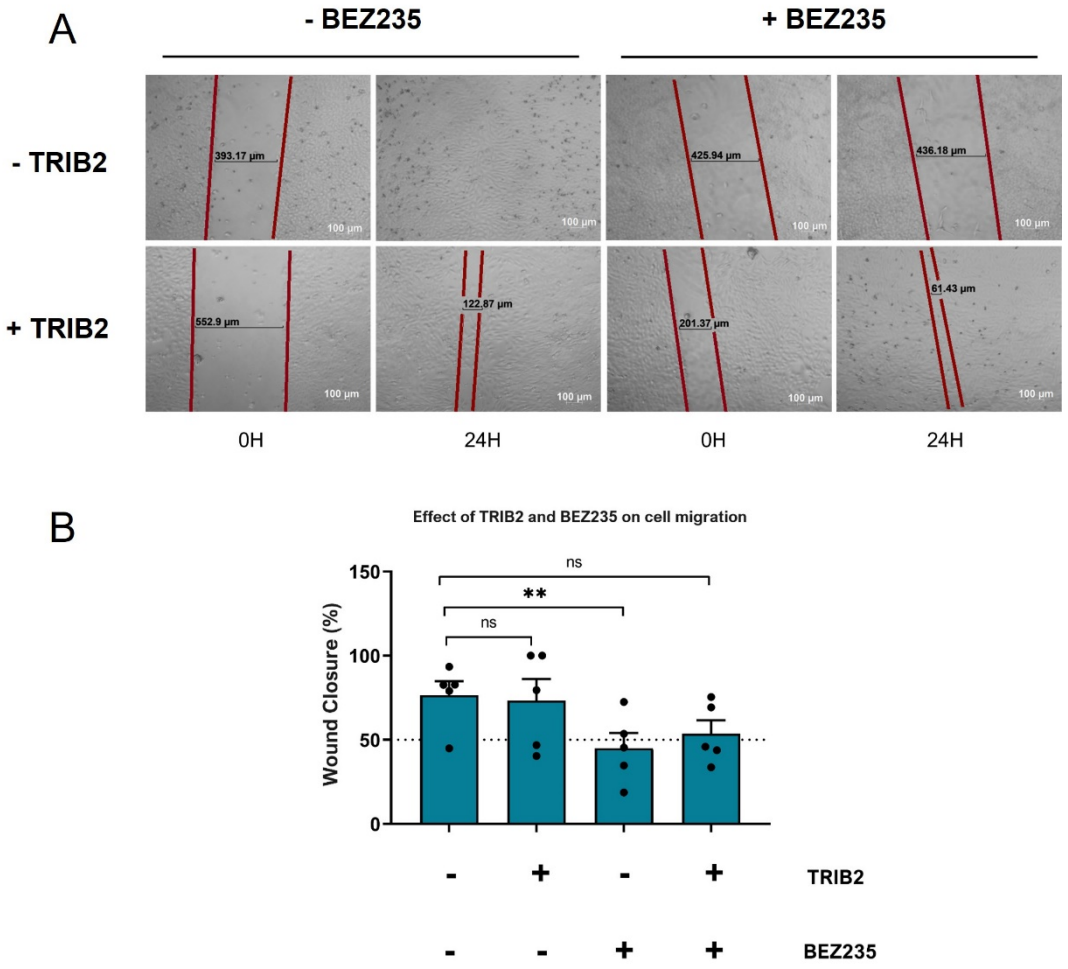

Figure 3.23. TRIB2 overexpression hinders BEZ235-mediated reduced cell migration. A) To evaluate the impact of TRIB2 and BEZ235 on cell migration, we performed a wound-healing assay. U2OS-empty (-TRIB2) and U2OS-TRIB2 (+TRIB2) cells were grown and treated with 100nM BEZ235 (+BEZ235) or 0.1% DMSO (-BEZ235). When the cells were almost confluent, they were starved to halt cell proliferation. At 0H time-point, a vertical scratch was made on each well. Microscope images were taken at time-points 0H and 24H to determine wound areas. B) Quantification of cell migration by wound closure percentage. Increased cell migration correlates with a higher wound closure percentage. Cells treated with BEZ235 exhibited a lower wound closure percentage consistent with decreased cell migration, and TRIB2 hindered the BEZ235 impact on cell migration, increasing wound closure percentage, consistent with increased cell migration. Statistical significance was determined by 2-Way ANOVA with Dunnet's multiple comparisons test with P-value < 0,05, with (ns) P > 0,05, (*) P < 0,05, (**) P < 0,01, (****) P < 0,0001. The mean±SEM from five independent experiments is shown.

We determined the percentage of wound closure after 24H (Figure 3.23B) to quantify the cell migration ability under BEZ235 treatment and TRIB2 overexpression. Wound closure percentage is the decrease in the percentage of an area with no cells at 24H compared to 0H. A wound closure percentage of 100% reflects cells that could migrate and fill the gap, while a wound closure percentage of 0% reflects cells not migrating and the gap area did not decrease. BEZ235 treatment on cells with no TRIB2 (-TRIB2/+BEZ235) significantly decreased the wound closure percentage, which indicates a decrease in cell migration. The presence of TRIB2 hindered the effects of BEZ235 and increased the wound closure percentage (+TRIB2/+BEZ235), restoring the migration capacity of the cells (Figure 3.23B).

Taken together, these data indicate that the TRIB2 signature most significantly affects genes involved in cell survival, migration and proliferation, and we propose that FOXO is a major player, as TRIB2 is a FOXO suppressor (Figure 3.24).

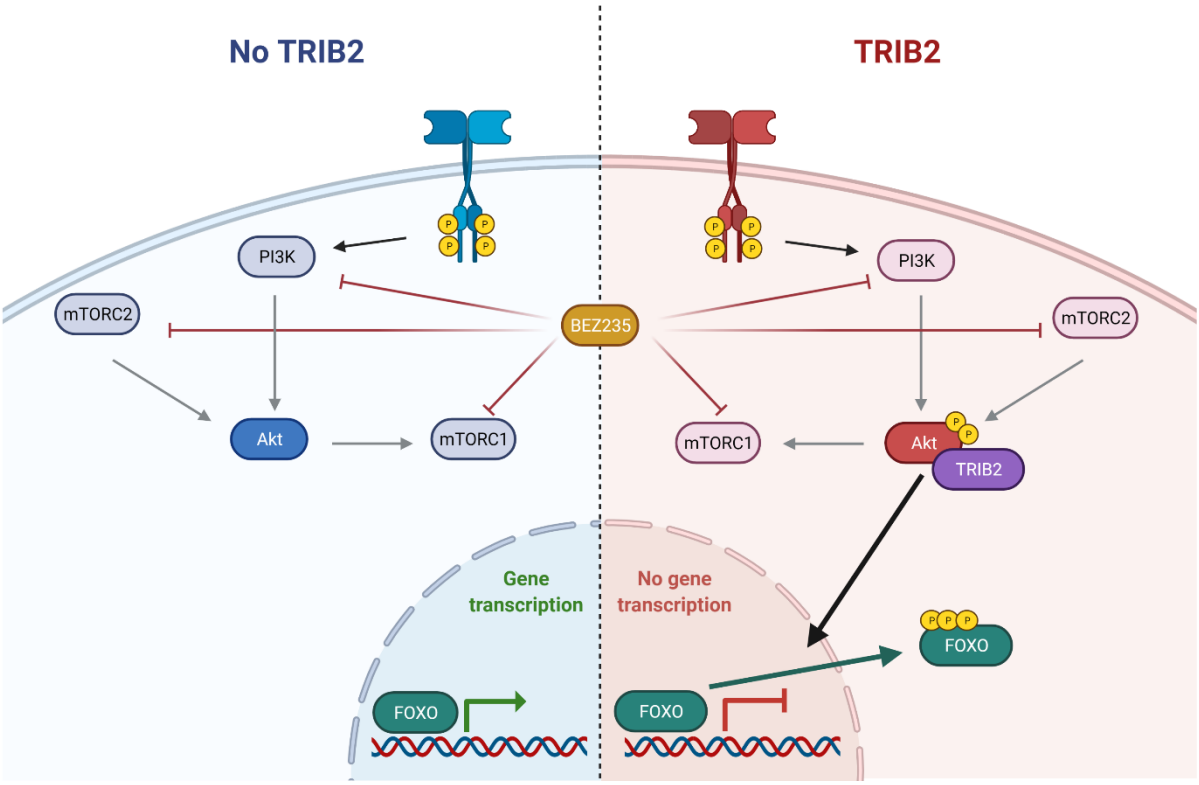

Figure 3.24. Proposed model for TRIB2-mediated resistance. BEZ235 inhibits PI3K and mTOR, leading to AKT inhibition and the tumour suppressor FOXO will remain transcriptionally active (left). In the presence of elevated levels of TRIB2, TRIB2 will induce AKT activity downstream of BEZ235 inhibition, leading to FOXO inhibition, hence decreasing BEZ235 efficacy (right).

3.2 TRIB2 resistance can be reverted pharmacologically

We used the RNA sequencing-based transcriptional profiling of isogenic cells lines with varying TRIB2 status in the presence or absence of PI3K/mTOR inhibition to identify sets of differentially expressed genes (DEG). Then we used the Connectivity Map-based algorithms to identify drugs or chemical compounds capable of inducing reverse transcriptional signatures to TRIB2 to predict the therapeutic response of BEZ235 in the presence of these drugs.

Our results show that several small-molecule compounds, namely harmine (HAR) and piperlongumine (PIP), can affect TRIB2-mediated transcriptional signatures and, in line with this observation, can induce the nuclear translocation of FOXO3 and its consequent activation. We also show that FOXO regains its transcriptional activity upon nuclear localisation, successfully modulating its target genes. Moreover, co-treating cells with both BEZ235 and HAR or PIP induces a synergistic effect, restoring cells sensitivity to BEZ235 toxicity even with elevated levels of TRIB2, suggesting that HAR and PIP revert TRIB2 resistance effects to BEZ235 treatment.

3.2.1 HAR and PIP reverse TRIB2-induced expression profiles

We hypothesise that TRIB2-mediated therapy resistance may be abolished or attenuated by pharmacological treatment capable of reversing TRIB2-mediated transcriptional signatures. Hence, drugs that reverse TRIB2 signatures might resensitize cells to the effect of BEZ235 treatment on cell viability and proliferation.

We took advantage of the TRIB2-induced gene expression profile (DEG2) to match it with Connectivity Map (cMAP) gene expression data and selected bioactive

chemical compounds and FDA-approved drugs that produce an inverse gene expression profile using pattern-matching algorithms of cMAP [227]. cMAP is a gene expression database obtained from experiments on cancer cell lines treated with approximately 5000 small molecule compounds [227]. The list of candidate drugs was obtained by ruling out enrichment scores with P-values greater than 0.05. The enrichment scores are calculated based on the Kolmogorov-Smirnov statistic, a non-parametric rank statistic known as gene set enrichment analysis (GSEA), to interpret gene expression data [226, 229]. The compounds harmine (HAR) [248], piperlongumine (PIP) [249], irinotecan [250] and LM-1685 [251] produced an inverse gene expression profile compared to the profile induced by TRIB2 (Table 4).

Table 4. Drugs with an inverted transcriptional signature of TRIB2. A cMAP query was performed to identify drugs that generated reversed transcriptional signatures of TRIB2 on MCF7, PC3 and MDA-MB-231 cell lines. Drugs were selected according to P-value < 0,05 and lower enrichment score.

Drug	Pubchem ID	Enrichment Score	p-value	Mode of Action
Harmine	5280953	−0.9	0.00016	acetylcholinesterase inhibitor
Piperlongumine	637858	−0.965	0.00276	GSTπ and CBR1 inhibitor
Irinotecan	60838	−0.851	0.00655	Topoisomerase I inhibitor
LM-1685	10068193	−0.792	0.01827	COX-2 inhibitor

Conversely, three compounds with anti-inflammatory properties, maprotiline [252], cromoglicic acid [253] and crachidonyl trifluoromethane [254], produced a similar gene expression profile compared to the profile induced by TRIB2 overexpression (Table 5).

Table 5. Drugs with a similar transcriptional signature of TRIB2. A cMAP query was performed to identify drugs that generated similar transcriptional signatures of TRIB2 on MCF7, PC3 and MDA-MB-231 cell lines. Drugs were selected according to P-value < 0.05 and lower enrichment score.

Drug	Pubchem ID	Enrichment Score	p-value	Mode of Action
Maprotiline	4011	0.9	0.0001	norepinephrine reupt inhibitor
Cromoglicic acid	2882	0.907	0.01795	chloride channels inhibitor
Arachidonyl trifluoromethane	5280436	0.873	0.03292	PLA_2 inhibitor

HAR is a β-carboline alkaloid isolated from the seeds of Peganum harmala and inhibits monoamine oxidase [255]. PIP is a natural amide alkaloid [249, 256] isolated from the Piper longum Linn plant and known to disrupt redox homeostasis by inhibiting glutathione S-transferase π (GSTπ) and carbonyl reductase 1 (CBR1) [256]. We validated the most differentially regulated genes upon HAR and PIP treatment retrieved in the cMAP database by qRT–PCR. Analysis of U2OS-TRIB2 cells treated with HAR showed that the genes LMCD1 and PCT1A are significantly down-regulated (Figure 3.25).

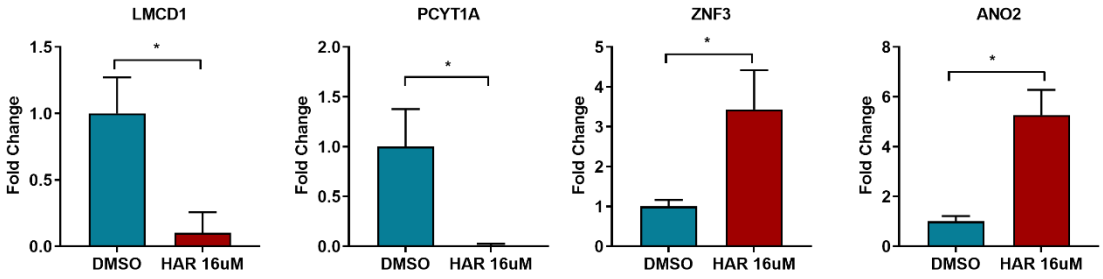

Figure 3.25. Validation of HAR top regulated genes from cMAP analysis by RT-qPCR in U2OS-TRIB2 cells. HAR upregulates ANO2 and ZNF3 and downregulates LMCD1. Results represent mean±SEM from three independent experiments with triplicates. Statistical significance was determined by unpaired t-test with one-tailed P-value, with (*) P < 0,05 and (**) P < 0,01.

Furthermore, PIP significantly down-regulated the expression of the tumour necrosis factor 6 (TNFAIP6) and GATA3 (Figure 3.26). On the contrary, HAR and PIP treatments significantly upregulate ZNF3 and ANO2 and GNRH1 genes, respectively (Figure 3.25, Figure 3.26).

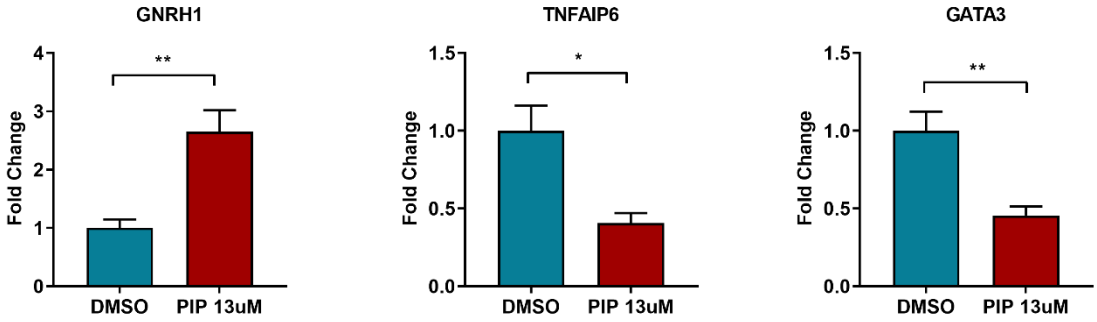

Figure 3.26. Validation of PIP top regulated genes from cMAP analysis by RT-qPCR. PIP upregulates GNRH1 and downregulates TNFAIP6 and GATA3. Results represent mean±SEM from three independent experiments with triplicates. Statistical significance was determined by unpaired t-test with one-tailed P-value, with (*) $P < 0,05$ and (**) $P < 0,01$.

To test the hypothesis that HAR and PIP sensitize cells resistant to anti-cancer drugs, we first sought to determine the most effective concentrations for the combined treatment with the PI3K/mTOR inhibitor BEZ235 and HAR or PIP. We used an MTT assay that measures metabolic activity as an indicator of cell viability of U2OS-TRIB2 cells treated with serial two-fold dilutions of either BEZ235, HAR or PIP for 48H (Figure 3.27) and 72H (Figure 3.28). The dose-response plots at 72H show that growth inhibition by 50% compared to DMSO (GI50) as measured using MTT assay, produced by treatment with HAR, PIP and BEZ235, were 12.89μM, 2μM and 95.37nM, respectively.

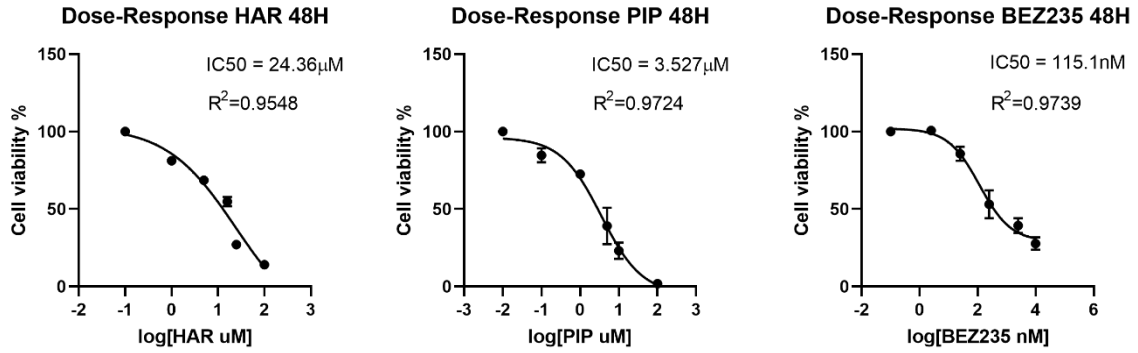

Figure 3.27. Dose-response curves of HAR, PIP and BEZ235 in U2OS-TRIB2 cell line for 48H. Cells were treated with 6 serial dilutions of HAR, PIP or BEZ235 for 48H, and cell viability was determined. Results were normalized and fitted with non-linear regression (log inhibitor vs response with variable slope and 4 parameters). Results were generated from three independent experiments with triplicates.

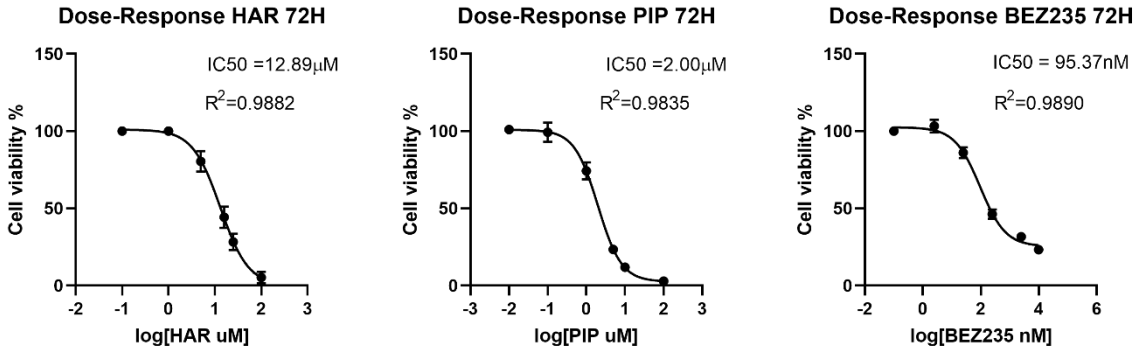

Figure 3.28. Dose-response curves of HAR, PIP and BEZ235 in U2OS-TRIB2 cell line for 72H. Cells were treated with 6 serial dilutions of HAR, PIP or BEZ235 for 72H, and cell viability was determined. Results were normalized and fitted with non-linear regression (log inhibitor vs response with variable slope and 4 parameters). Results were generated from three independent experiments with triplicates.

To determine whether co-treatment of BEZ235 with HAR or PIP could synergistically affect BEZ235-treated cells, we inferred cell viability by MTT assay in U2OS-TRIB2 cells. Co-treatment of BEZ235 and HAR significantly decreased cellular metabolic activity at all concentrations, and combined ratios at 125nM

BEZ235/11.4μM HAR and 250nM BEZ235/22.8μM HAR showed synergy, as depicted by a combination index below 1 (Figure 3.29).

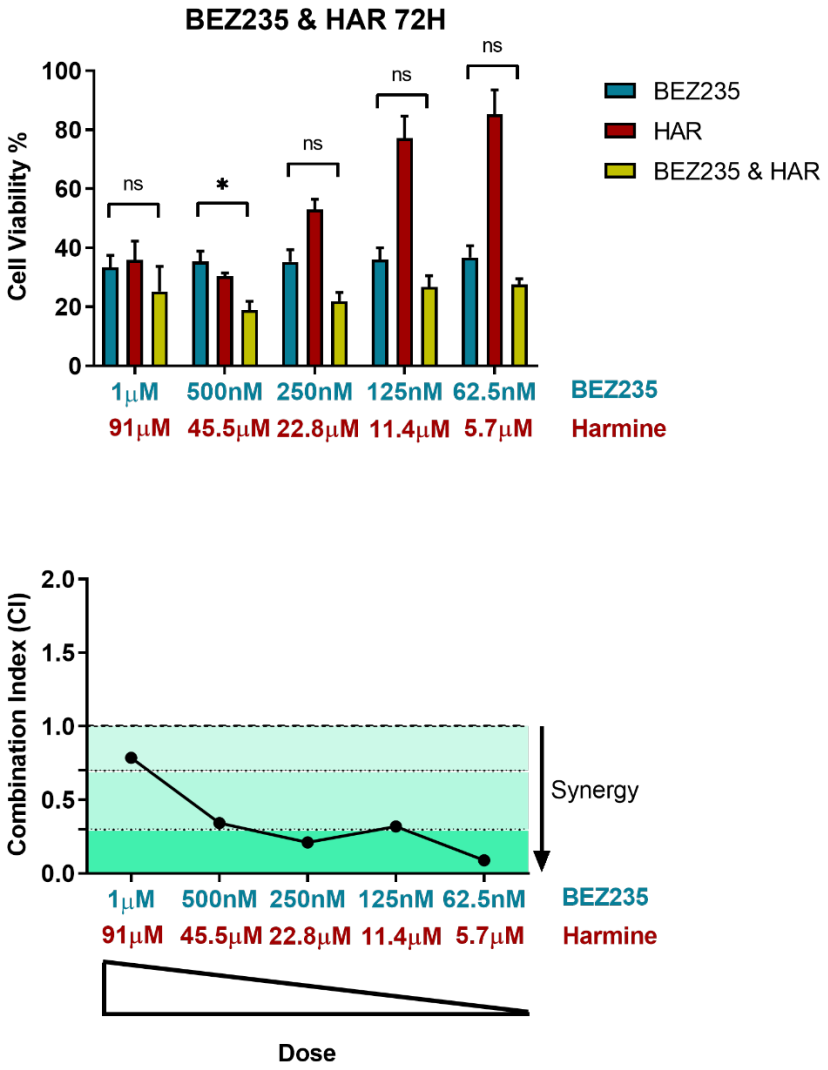

Figure 3.29. Evaluation of synergistic potential between BEZ235 and HAR at 72H. U2OS-TRIB2 cells were treated with BEZ235 or HAR alone, and BEZ235 and HAR combined for 72H. Cell viability was determined by measuring cellular metabolic activity using an MTT assay. BEZ235 and HAR displayed synergy in all concentrations. Synergy is determined by the Chou Talalay method. The combination index (CI)<1 denotes synergism, CI>1 antagonism, and CI=1 additive. Statistical significance was determined by 1-Way ANOVA with Sidak's multiple comparisons test with P-value < 0,05, with (ns) P > 0,05, (*) P < 0,05, (**) P < 0,01, (****) P < 0,0001. The mean±SEM from three independent experiments is shown.

Co-treatment of BEZ235 and PIP also significantly decreased cell viability, with synergy detected at 250nM BEZ235/2.5μM PIP and 500nM BEZ235/5μM PIP (Figure

3.30). These results suggest that HAR and PIP, together with BEZ235, synergistically increase the cytostatic/cytotoxic effects of BEZ235.

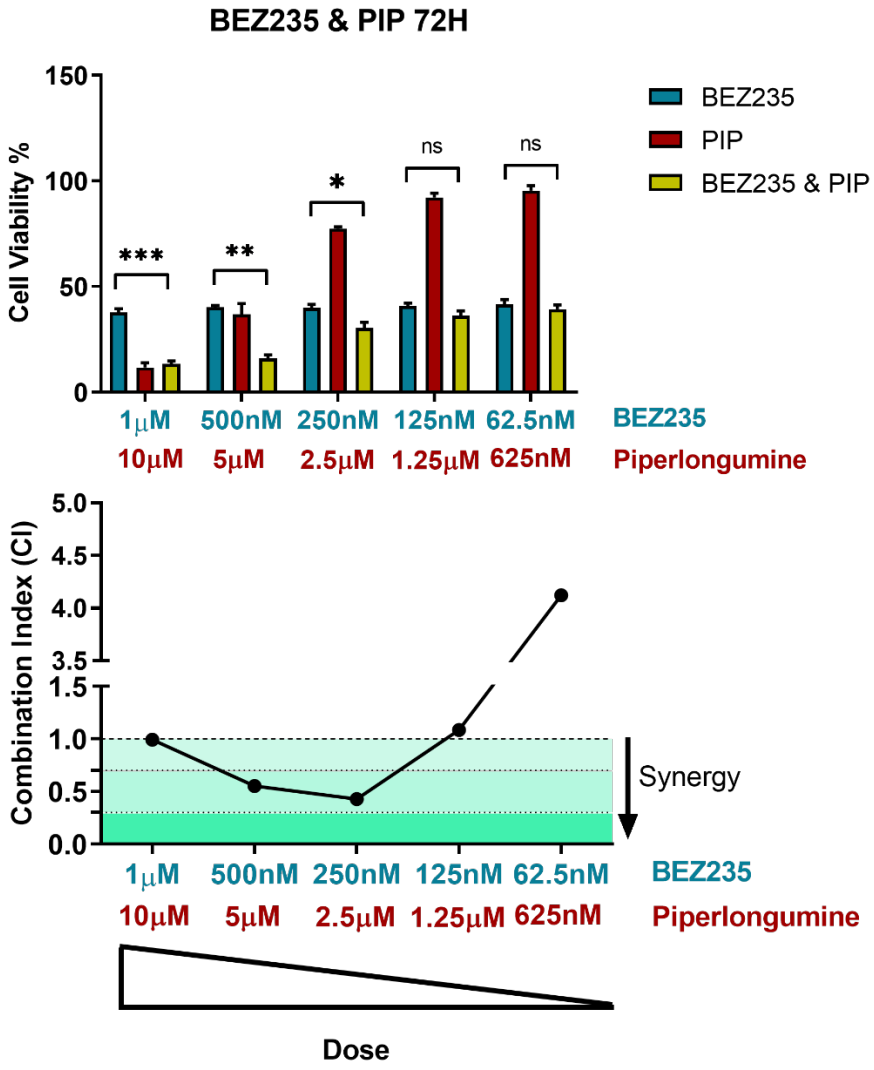

Figure 3.30. Evaluation of synergistic potential between BEZ235 PIP at 72H. U2OS-TRIB2 cells were treated with BEZ235 or PIP alone, and BEZ235 and PIP combined for 72H. Cell viability was determined by measuring cellular metabolic activity using an MTT assay. BEZ235 and PIP displayed synergy at combined concentrations of 250nM (BEZ235)/2.5μM (PIP) or higher. Synergy is determined by the Chou Talalay method. The combination index (CI)<1 denotes synergism, CI>1 antagonism, and CI=1 additive. Statistical significance was determined by 1-Way ANOVA with Sidak's multiple comparisons test with P-value < 0,05, with (ns) P > 0,05, (*) P < 0,05, (**) P < 0,01, (****) P < 0,0001. The mean±SEM from three independent experiments is shown.

At 48H, co-treatment of BEZ235 and HAR also significantly decreased cell viability at all concentrations, and combined ratios at 125nM BEZ235/11.4μM HAR and 250nM BEZ235/22.8μM HAR showed synergy, as depicted by a combination index below 1 (Figure 3.31).

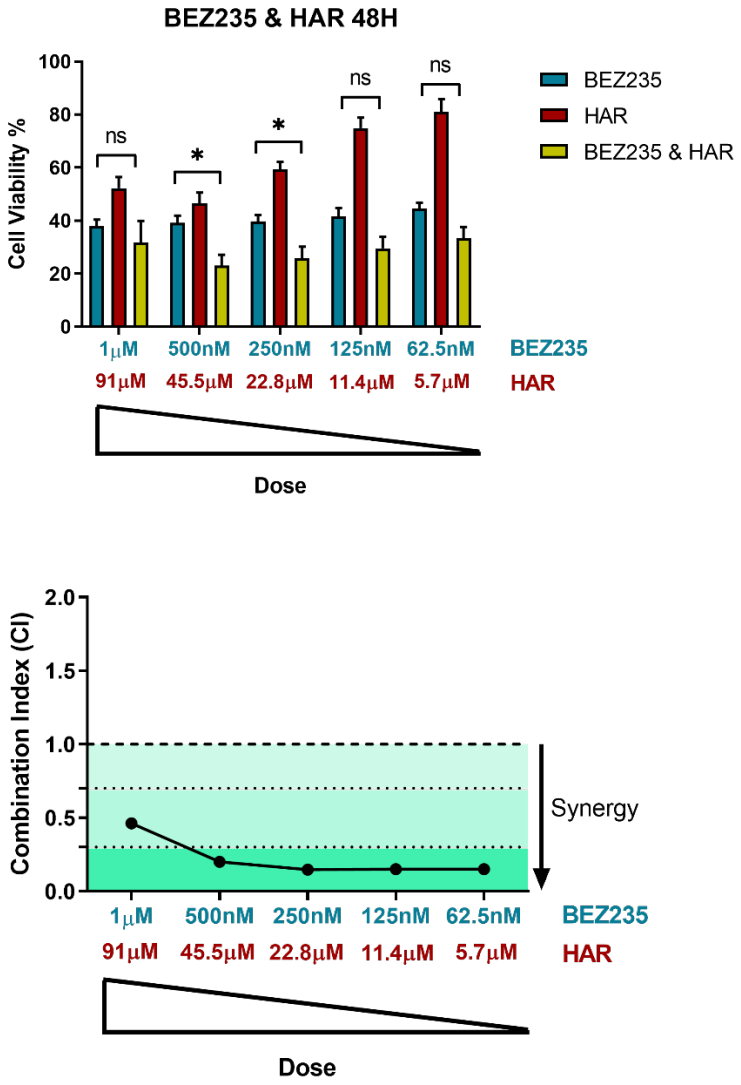

Figure 3.31. Evaluation of synergistic potential between BEZ235 and HAR at 48H. U2OS-TRIB2 cells were treated with BEZ235 or HAR alone, and BEZ235 and HAR combined for 48H. Cell viability was determined by measuring cellular metabolic activity using an MTT assay. BEZ235 and HAR displayed synergy in all concentrations. Synergy is determined by the Chou Talalay method. The combination index (CI)<1 denotes synergism, CI>1 antagonism, and CI=1 additive. Statistical significance was determined by 1-Way ANOVA with Sidak's multiple comparisons test with P-value < 0,05, with (ns) P > 0,05, (*) P < 0,05, (**) P < 0,01, (****) P < 0,0001. The mean±SEM from three independent experiments is shown.

Similarly, co-treatment of BEZ235 and PIP for 48H significantly decreased cell viability, inferred from cellular metabolic activity, with synergy detected at 250nM BEZ235/2.5μM PIP and 500nM BEZ235/5μM PIP (Figure 3.32).

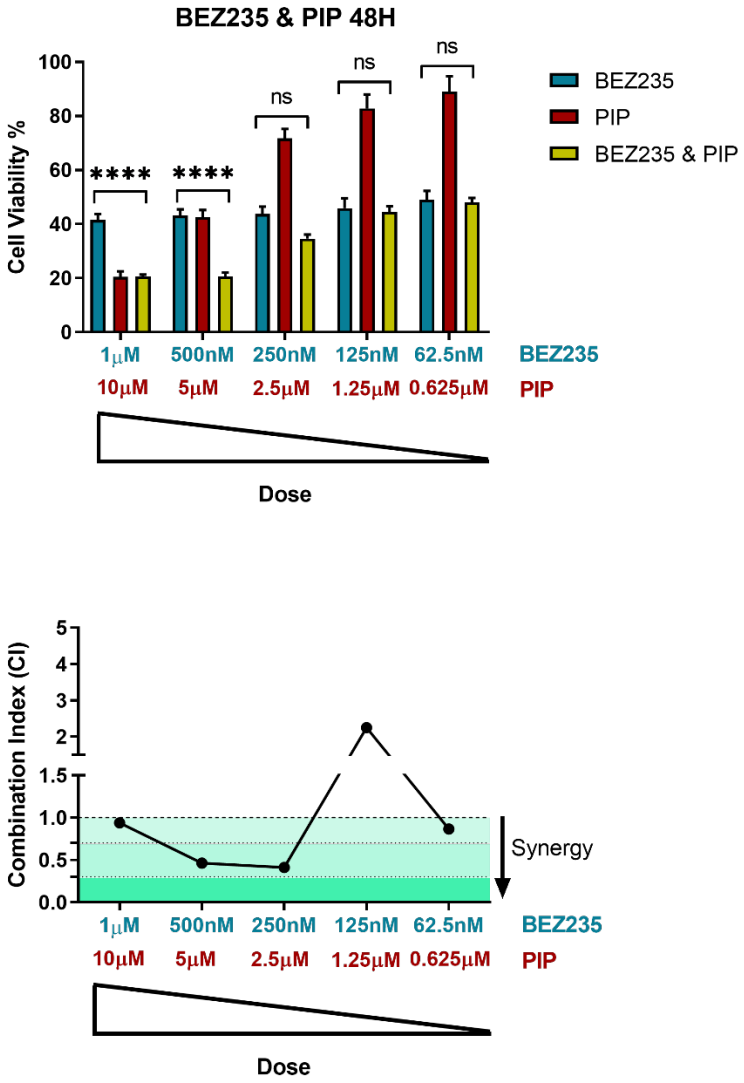

Figure 3.32. Evaluation of synergistic potential between BEZ235 PIP at 48H. U2OS-TRIB2 cells were treated with BEZ235 or PIP alone, and BEZ235 and PIP combined, with 48H treatment. Cell viability was determined by measuring cellular metabolic activity using an MTT assay. BEZ235 and PIP displayed synergy at combined concentrations of 250nM (BEZ235)/2.5μM (PIP) or higher. Synergy is determined by the Chou Talalay method. The combination index (CI)<1 denotes synergism, CI>1 antagonism, and CI=1 additive. Statistical significance was determined by 1-Way ANOVA with Sidak's multiple comparisons test with P-value < 0,05, with (ns) P > 0,05, (*) P < 0,05, (**) P < 0,01, (****) P < 0,0001. The mean±SEM from three independent experiments is shown.

To evaluate if the decrease in cellular metabolic activity at the synergic concentrations, determined by the MTT assays, was in part due to cell death, we performed a cell death assay by Trypan Blue on the U2OS-TRIB2 cells treated with 250nM BEZ235 and 22.8µM HAR (the chosen synergic concentration) or 250nM BEZ235 and 2.5µM PIP (the chosen synergic concentration) for 72H. In line with the MTT results, we found that combined drug treatment induces increased cell death compared to DMSO control (Figure 3.33). Nevertheless, it also suggests that these drugs may also act by preventing cell proliferation (cytostasis) (Figure 3.34), as cell death did not increase as much as cellular metabolic activity decreased. Indeed, BEZ235 has been reported to exhibit more cytostatic effects than cytotoxicity effects on other cell lines [257]. Similarly, HAR exhibits cytostatic effects on cells [258], while PIP is known to have a strong cytotoxic effect [259].

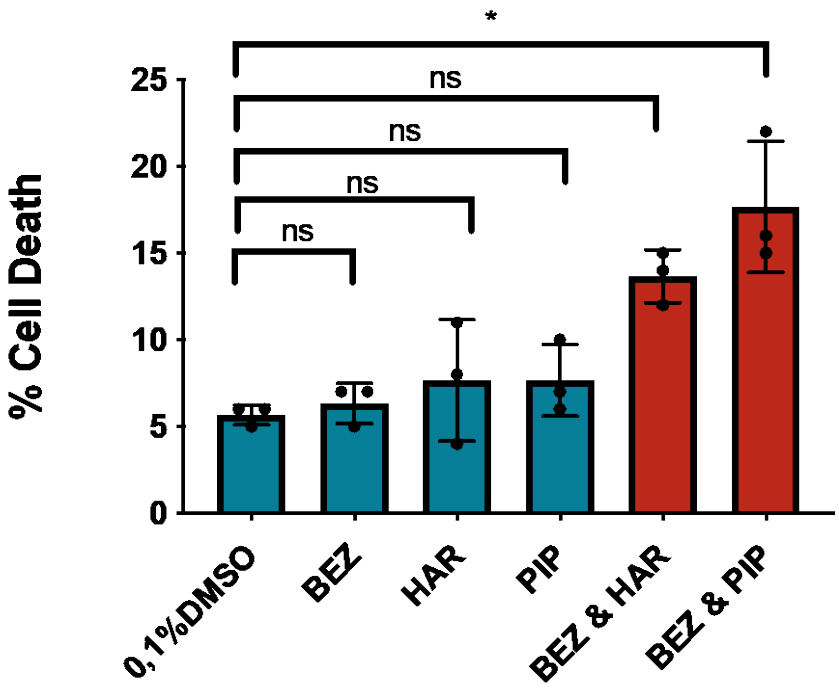

Figure 3.33. The impact of synergic combined treatment on cell death. Cell death assay by trypan blue exclusion assay was performed on U2OS-TRIB2 cells treated with 250nM BEZ235 and 22.8µM HAR (the chosen synergic concentration) or 250nM BEZ235 and 2.5µM PIP (the chosen synergic concentration) for 72H. The trypan blue exclusion assay displays an increase of cell death when cells are treated with combined drugs, compared to DMSO control, in line with the MTT results. P-values were obtained from unpaired t-test with Welch correction, (*) $P < 0,1$. The mean±SEM from three independent experiments is shown.

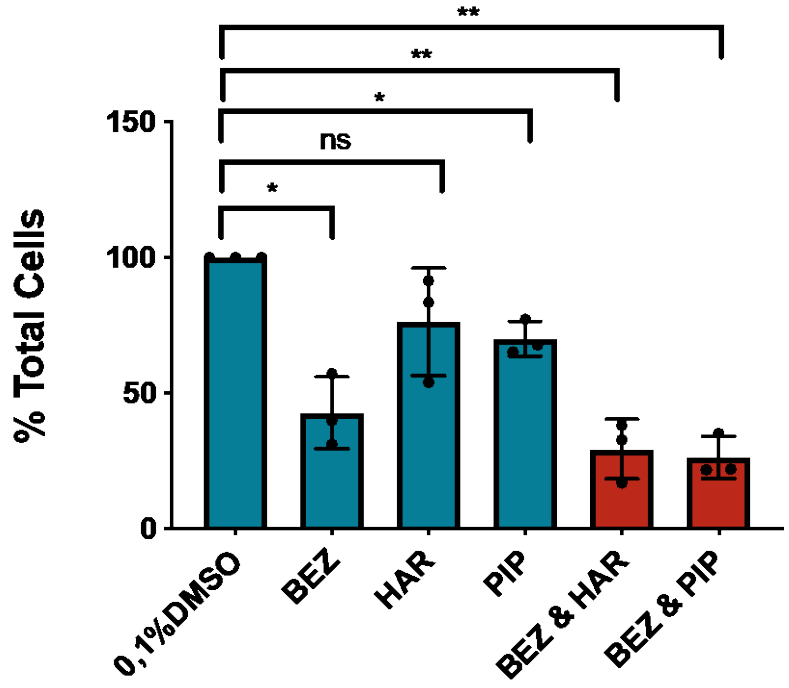

Figure 3.34. The impact of synergic combined treatment on cell growth. Cell death assay by trypan exclusion assay was performed on U2OS-TRIB2 cells treated with 250nM BEZ235 and 22,8μM HAR (the chosen synergic concentration) or 250nM BEZ235 and 2,5μM PIP (the chosen synergic concentration) for 72H. The cell death assay displays a decrease in the total number of cells for each condition compared to the DMSO control. P-values were obtained from unpaired t-test with Welch correction, (*) P < 0,1, (**) P < 0,01. The mean±SEM from three independent experiments is shown.

To evaluate if the synergistic effect of HAR and BEZ235 or PIP and BEZ235 would affect TRIB2 modulation of its target genes, we performed RT-qPCR on cells with low and high levels of TRIB2, treated with BEZ235 alone (250nM), or combined with HAR (22.8μM) or PIP (2.5μM), and evaluated the expression levels of genes regulated by both TRIB2 and HAR or PIP. TRIB2 overexpression prevented BEZ235 from significantly downregulating LMCD1, but when cells were treated with BEZ235 and HAR, LMCD1 was further downregulated regardless of TRIB2 levels (Figure 3.35). Our results indicate that HAR and PIP may help cells regain sensitivity to BEZ235 toxicity in the presence of high levels of TRIB2.

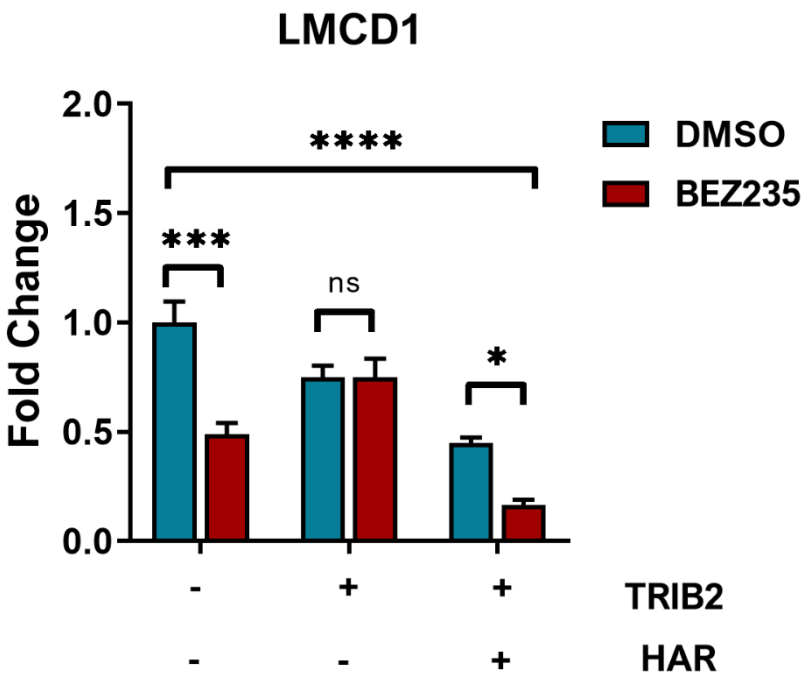

Figure 3.35. The synergy between BEZ235 and HAR contributes to BEZ235-regulation of LMCD1 regardless of TRIB2 levels. RT-qPCR analysis of LMCD1 gene in U2OS-TRIB2 cells treated with 250nM BEZ235 and 22.8μM HAR (the chosen synergic concentration) or 250nM BEZ235 and 2.5μM PIP (the chosen synergic concentration) for 72H. Statistical significance was determined by 2-Way ANOVA and Tukey multiple comparisons test to evaluate the contribution of TRIB2, and 2-Way ANOVA and Sidak multiple comparison tests, to evaluate the contribution of BEZ235 to gene expression with (*) P< 0,05, (***) P < 0,001, (****) P < 0,0001).

3.2.2 HAR and PIP promote FOXO nuclear translocation

We previously identified TRIB2 as a FOXO suppressor protein promoting cytoplasmatic localization of FOXO3, leading to its inactivation [55]. We treated a previously established reporter cell line (U2foxRELOC) with HAR or PIP to test if HAR and PIP would exert an opposite effect on FOXO. U2foxRELOC stably expresses a fluorescently labelled FOXO3 fusion protein and enables an image-based approach

to monitor the subcellular localization of FOXO3 [158]. The cell treatment with the nuclear export inhibitor Leptomycin B (LMB) shifted the reporter protein almost entirely into the cell nucleus. Treatment of these cells with HAR and PIP for 1H is sufficient to promote FOXO nuclear localization similar to the positive control LMB (Figure 3.36).

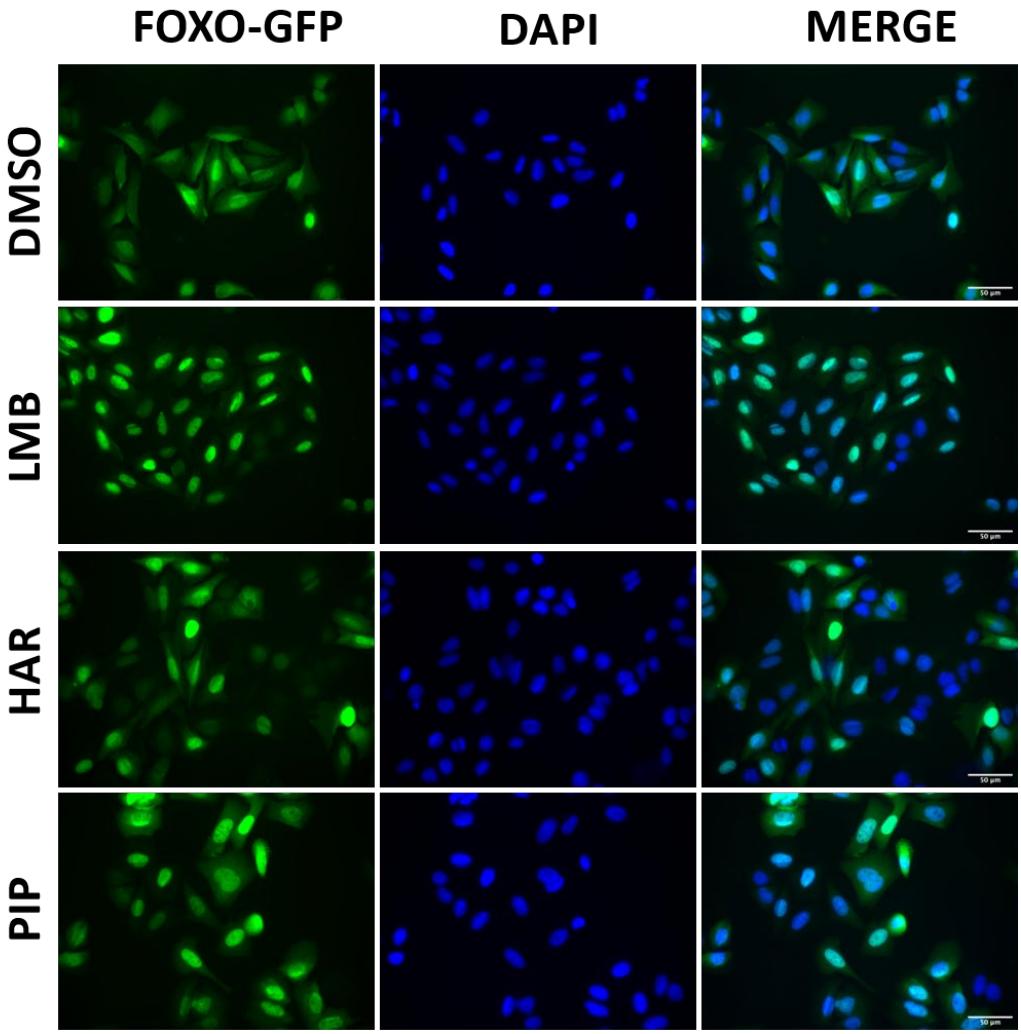

Figure 3.36. HAR and PIP induce FOXO nuclear translocation. U2foxRELOC cells were treated with 16μM HAR or 13μM PIP for 1H. DMSO and Leptomycin B (LMB) were the negative and positive controls for FOXO localization, respectively. DMSO-treated cells continued to display FOXO mainly in the cytoplasm, while LMB, HAR and PIP-treated cells displayed FOXO mainly in the nucleus. The cells were mounted on slides with mounting media coupled with DAPI. Samples were imaged using 40x magnification. Scale bar indicates 50μm. All experiments were performed in triplicate.

These results were automatically quantified by computing the intensity of the green fluorescence within the area stained with DAPI, which defined the cell nucleus and the extended cytoplasm. As shown in Figure 3.37, both compounds scored 20% more positive cells than the negative control (DMSO).

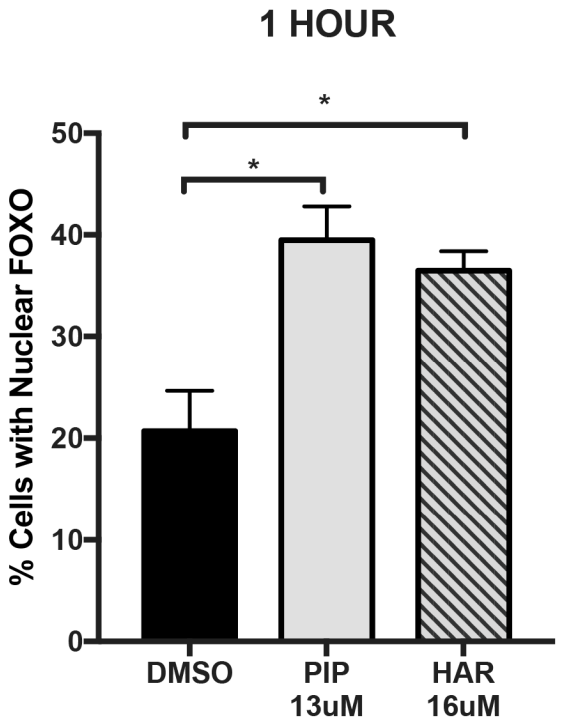

Figure 3.37. Quantification of FOXO nuclear translocation by HAR and PIP. The quantification of FOXO localization was performed by determining the ratio of the green intensity measured in both the nucleus and cytoplasm. Cells treated with HAR or PIP for 1H showed a 2-fold increase of nuclear FOXO compared to DMSO-treated cells. Statistical significance was determined by one-way ANOVA with Dunnet's multiple comparison test and (*) P-value<0,05.

Next, we wanted to determine if the nuclear translocation of FOXO3 was due to the inhibition of the nuclear export receptor CRM-1 known to recognize the nuclear export sequence (NES) in the FOXO proteins. U2nesRELOC cells [216] were treated with 16μM of HAR or 13μM of PIP for 1H and analysed the subcellular distribution by measuring the fluorescent signal. U2nesRELOC cells were generated from the parental U2OS cell line expressing pRevMAPKKnesGFP reporter protein. Compounds

that interfere with the CRM-1 export receptor accumulate NES-containing proteins in the nucleus [216].

The results obtained from this experiment showed that treatment with HAR or PIP does not affect the nuclear export through CRM-1 (Figure 3.38), suggesting that these agents may interfere with the regulatory network upstream of FOXO3.

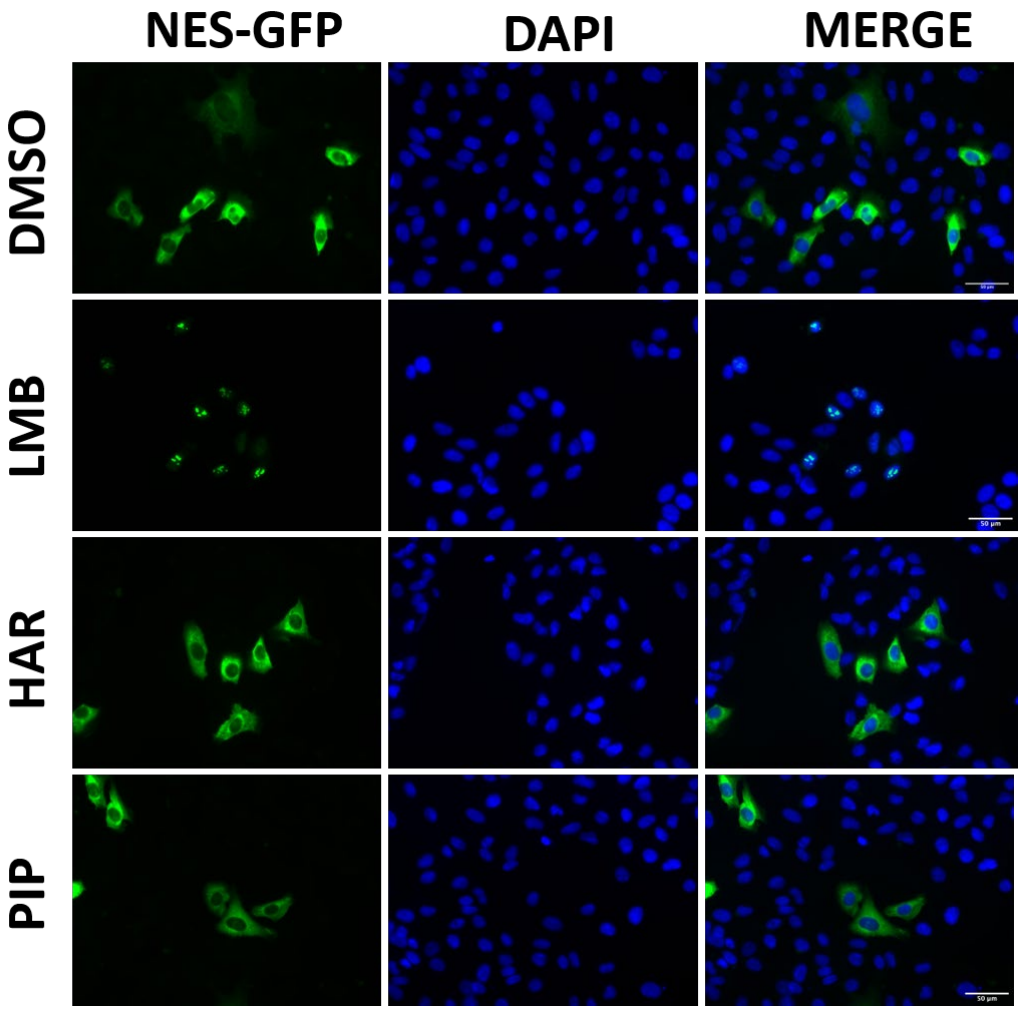

Figure 3.38. HAR and PIP do not inhibit nuclear export mediated by CRM-1. U2nesRELOC cells were treated with 16 and 13μM of HAR or PIP, respectively, for 1H. DMSO and LMB were used as negative and positive controls for FOXO localization, respectively. DMSO-treated cells continued to display FOXO mainly in the cytoplasm, while LMB, HAR and PIP-treated cells displayed FOXO mainly in the nucleus. The cells were mounted on slides with mounting media coupled with DAPI. Samples were imaged using 40x magnification. Scale bar indicates 50μm. All experiments were performed in triplicate.

Since FOXO nuclear translocation is often accompanied by loss of phosphorylation on S253, a target residue of the upstream kinase AKT [53], we monitored both FOXO and AKT phosphorylation status upon HAR and PIP treatment. Figure 3.39 indicates that the exposure of cells to HAR for 1H already decreased the total amount of FOXO. More extended treatment periods provided a similar pattern of AKT and FOXO3 regulation (Figure 3.39). These data show that HAR treatment may decrease FOXO protein stability and suggest that FOXO phosphorylation by AKT might not be the predominant mechanism of HAR-induced translocation of FOXO.

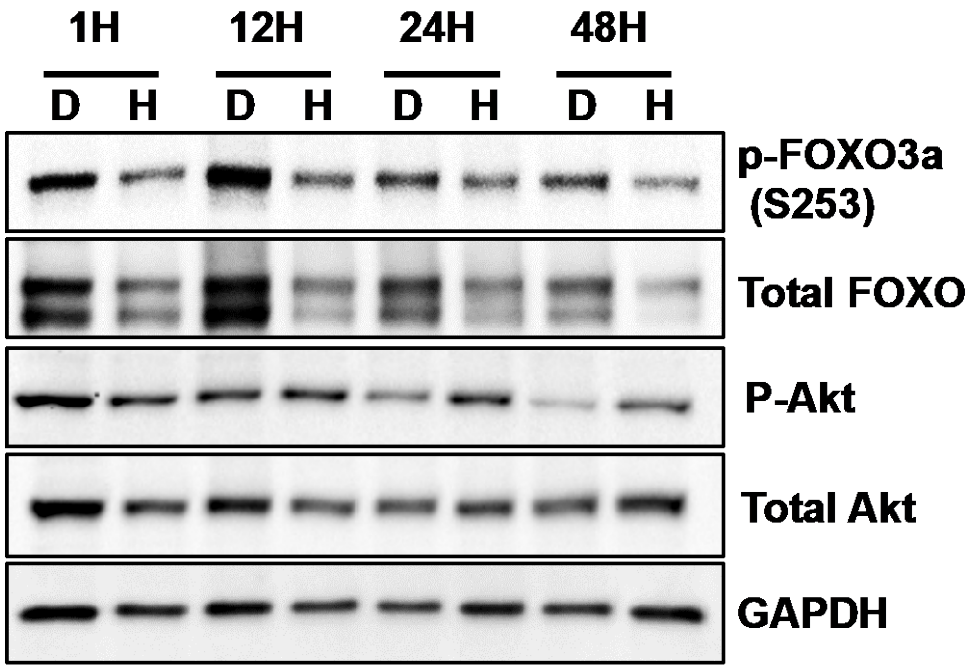

Figure 3.39. The impact of HAR treatment in FOXO and AKT activity. HAR treatment affected the total FOXO protein levels. U2foxRELOC cell line was treated with 16μM HAR (H) for 1H, 12H, 24H and 48H, and western blot was performed to evaluate the levels of FOXO3a and P-FOXO3a, Akt and P-Akt. DMSO (D) was used as a control for HAR and PIP treatments, and GAPDH as the loading control. Representative image of two independent experiments.

Whereas PIP treatment for 1H strongly induced the phosphorylation of AKT, more prolonged exposure to PIP reverted the effect and lead to decreased levels of AKT phosphorylation after 12H (Figure 3.40). Although PIP treatment also decreased the amount of FOXO3 protein, the net effect on FOXO phosphorylation is evident, suggesting that PIP impairs FOXO phosphorylation and this effect seems to be regulated by the activation status of AKT.

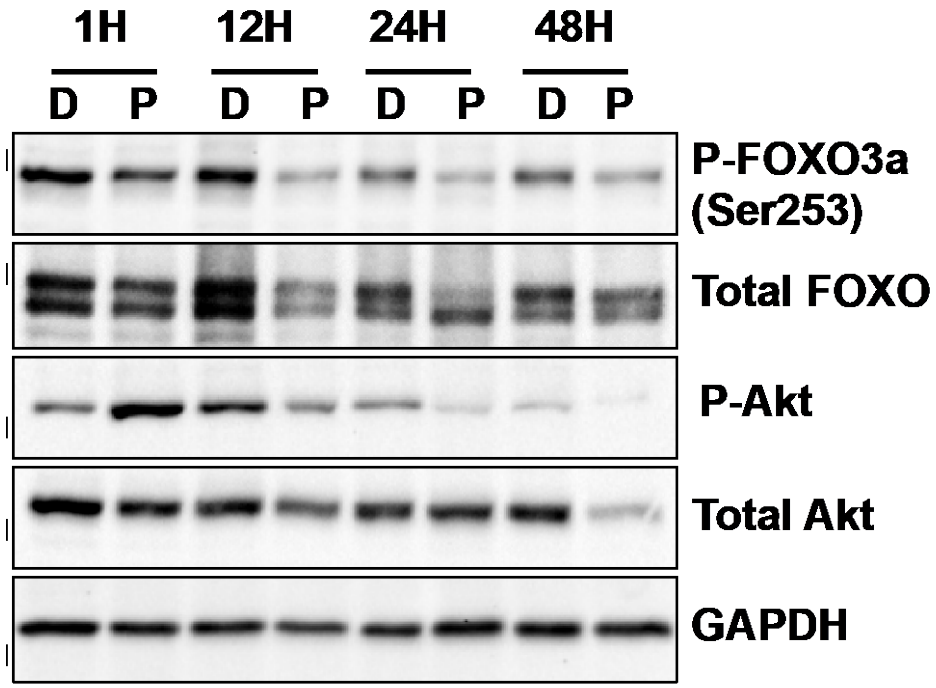

Figure 3.40. The impact of PIP treatment in FOXO and AKT activity. PIP treatment affected AKT and FOXO phosphorylation. U2foxRELOC cell line was treated with 13μM PIP (P) for 1H, 12H, 24H and 48H and western blot was performed to evaluate the levels of FOXO3a and P-FOXO3a, Akt and P-Akt. DMSO (D) was used as a control for HAR and PIP treatments and GAPDH as a loading control. Representative image of two independent experiments.

Next, we investigated if the nuclear localization of FOXO induced by HAR or PIP would affect the transcription of FOXO target genes. We treated U2foxRELOC cells with HAR or PIP and performed RT-qPCR analysis using specific primers for known FOXO target genes. HAR and PIP treatment upregulated p21 and PUMA (Figure 3.41), known to be regulated by FOXO3 [260, 261]. However, as other transcription factors, including p53, might regulate p21 and PUMA, we cannot exclude

that additional mechanisms can contribute or even represent HAR and PIP's predominant mode of action.

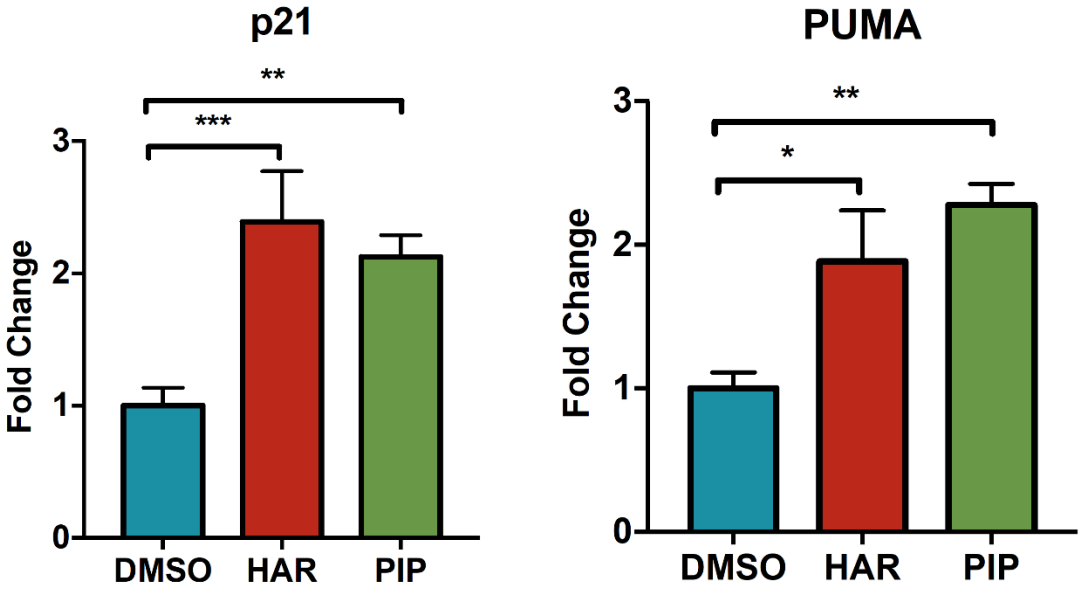

Figure 3.41. HAR and PIP treatments affect the transcription of FOXO target genes. U2foxRELOC cells were treated with HAR 16μM, PIP 13μM or DMSO (control) for 6H. PUMA and p21 mRNA levels were determined by RT-qPCR. Graphics represent the mean±SEM from four independent experiments with triplicates. Statistical significance was determined by 1-Way ANOVA with Tukey multiple comparison test and with (*) $P < 0,05$, (**) $P < 0,01$ and (***) $P < 0,001$.

3.2.3 Validation of TRIB2-mediated resistance with a CRISPR/Cas9 TRIB2 KO cell line

We analysed and validated the obtained data using a different cell line. Hence, an alternative isogenic cell system was generated, which completely abolished the expression of TRIB2. We identified the human malignant melanoma cells UACC-62 as the cell line with the highest endogenous TRIB2 levels in a panel of cell lines for TRIB2 mRNA levels (Figure 3.2).

CRISPR-Cas9 system was used to disrupt the TRIB2 locus in UACC-62 genetically, effectively generating TRIB2 knockout (KO) cells as confirmed by the absence of TRIB2 protein in western blot analysis (Figure 3.42).

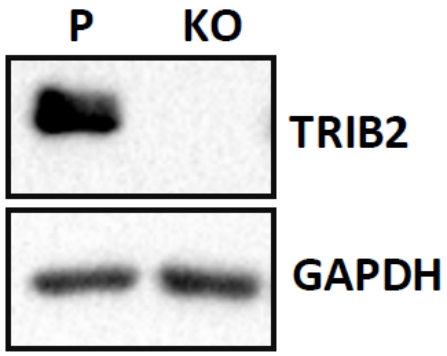

Figure 3.42. Immunoblot of UACC-62 TRIB2 KO cell line. GAPDH was used as a loading control. Representative image of two independent experiments.

We performed an MTT assay (as described previously) and calculated GI50 values on parental UACC-62 cells following treatment with BEZ, HAR and PIP for 72H. We obtained values of 20.4nM, 9,06uM and 2,14uM for BEZ235, HAR and PIP, respectively (Figure 3.43).

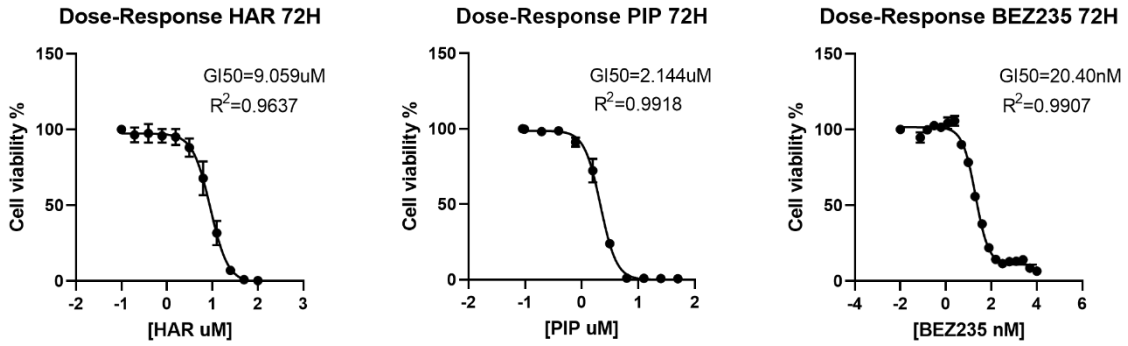

Figure 3.43. Dose-response curves of HAR, PIP and BEZ235 in UACC-62 parental cell line for 72H. UACC-62 parental cells were treated with serial dilutions of HAR, PIP or BEZ235 for 72H, and cell viability percentage was determined to generate dose-response plots. Results were normalized and fitted with non-linear regression (log inhibitor vs response with variable slope and 4 parameters). Results were generated from three independent experiments with triplicates.

Following, we assessed cell death by trypan blue exclusion assay using the GI50 values obtained previously. These results show that co-treatment with BEZ235 and HAR (or PIP) tend to increase cell death, albeit not statistically significant, which suggests that the dominant effect of these drugs on the cells may be through arresting cell proliferation (cytostasis) and not solely cell death (cytotoxicity) (Figure 3.44), as with U2OS-TRIB2 cells.

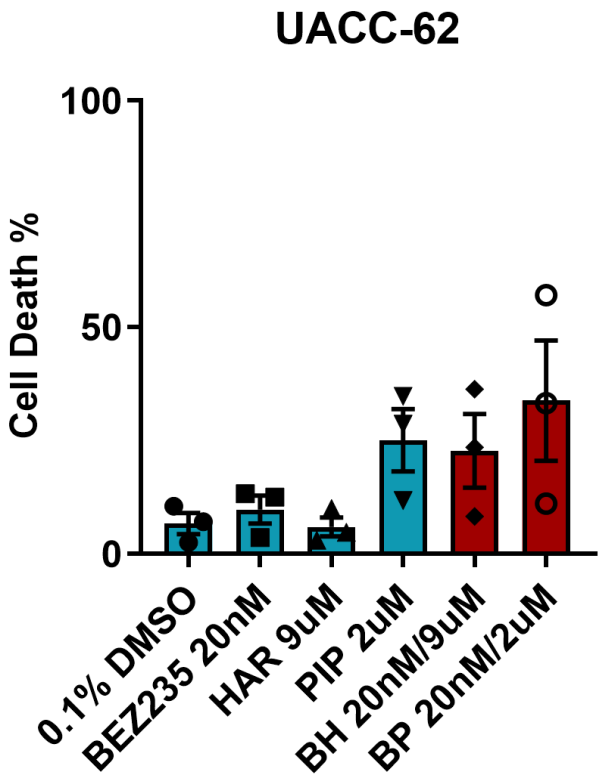

Figure 3.44. The impact of combined treatment on cell death in UACC-62 cells. Cell death assay by trypan exclusion was performed on parental UACC-62 cells treated with 20nM BEZ235 and 9μM HAR or 20nM BEZ235 and 2μM PIP for 72H. The trypan blue exclusion assay displays increased cell death when cells were treated with combined drugs, compared to DMSO control. P-values were obtained from unpaired t-test with Welch correction, (*) P < 0,1. The mean±SEM from three independent experiments is shown.

Next, we validated the previously observed synergy effect between these drugs in the U2OS cell line. We obtained a CI value of 0,5 using the 78,1nM BEZ / 25uM HAR treatment combination in the UACC-62 cell line (Figure 3.45), which indicates a

synergistic effect between both drugs (Figure 3.45). Moreover, we observed a significant reduction in cell viability upon combined HAR and BEZ treatment at 39,1nM BEZ / 12,5uM HAR and 19,5nM BEZ / 6,25uM HAR drug combinations, compared to each treatment alone (Figure 3.44).

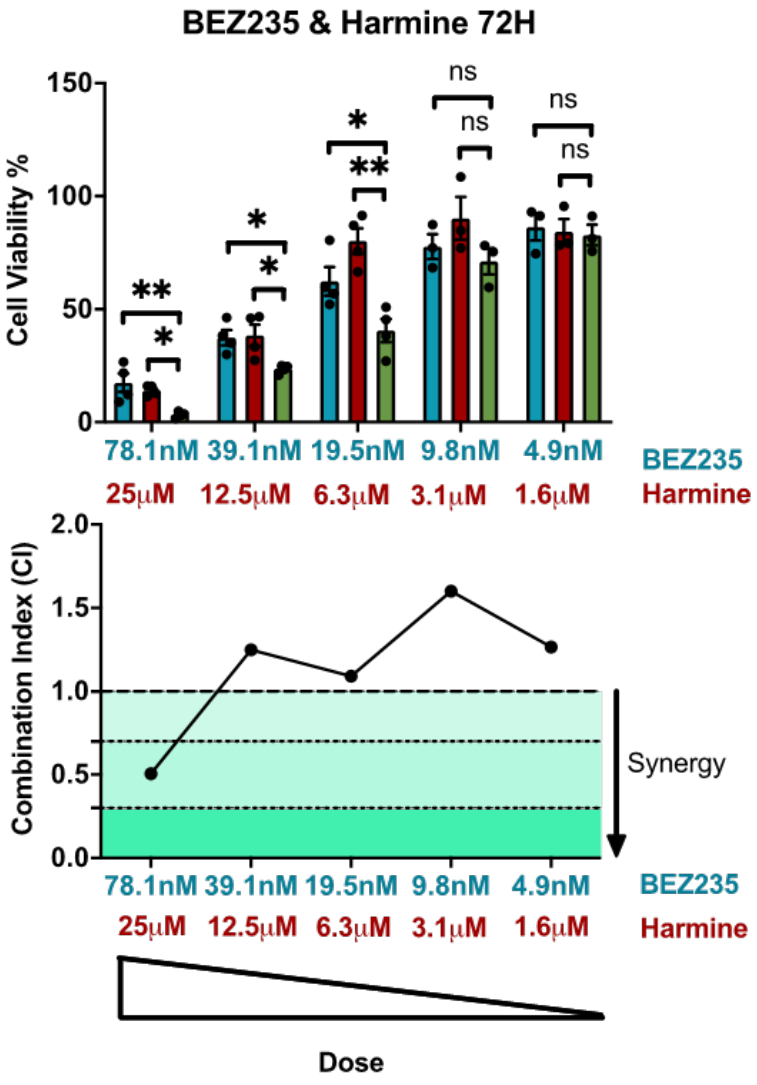

Figure 3.45. Evaluation of synergistic potential between BEZ235 and HAR in UACC-62 parental cell line at 72H. BEZ235 and HAR displayed synergy in all concentrations, while BEZ235 and PIP displayed synergy in all concentrations except the 125nM (BEZ235) / 1,25 μM (PIP) combination. Parental UACC62 cells were treated with BEZ235, HAR, and BEZ235 and HAR combined for 72H. Cell viability inferred by MTT assay. Statistical significance was determined by 1-Way ANOVA with multiple testing with SIDAK's multiple comparisons test with (*) $P < 0,05$ and (**) $P < 0,01$. Synergy is determined by the Chou Talalay method. Combination index (CI)<1 denotes synergism, CI>1 antagonism, and CI=1 additive. The mean±SEM was obtained from three independent experiments.

Combined treatment of 39,1nM BEZ and 3,13uM PIP also showed a statistically decrease in cell viability compared with single-drug treatments (Figure 3.46). Collectively, these data indicate that these drugs display cytotoxicity, but their dominant effect may be cytostatic, similar to the results obtained from the experiments in U2OS-TRIB2 cells (Figure 3.30 and Figure 3.32).

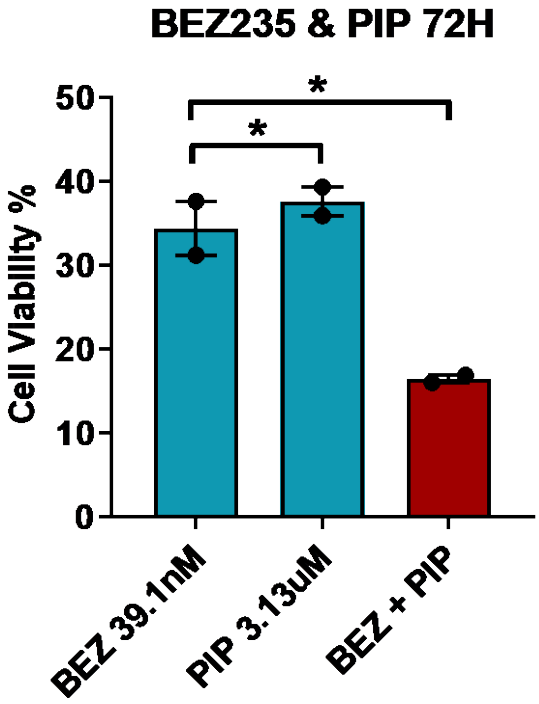

Figure 3.46. Parental UACC62 cells were treated with BEZ235, PIP or BEZ235 and PIP combined, with 72H treatment. Co-treatment with BEZ235 and PIP significantly decreased cell viability compared to cells treated with either BEZ235 or PIP. Cell viability inferred by MTT assay. Statistical significance was determined by 1-Way ANOVA with multiple testing with SIDAK's multiple comparisons test with (*) $P < 0,05$. The mean±SEM was obtained from three independent experiments.

We evaluated whether BEZ235, HAR and PIP would affect the FOXO and AKT activity levels in the presence and absence of TRIB2 by western blot (Figure 3.47), similarly to the U2OS-TRIB2 cells (Figure 3.39, Figure 3.40).

Western blot analysis of parental and TRIB2-KO UACC-62 cell lines revealed that phosphorylation of AKT and FOXO decreased in untreated UACC-62 cells without

TRIB2 (Figure 3.47). Unlike U2OS cells, UACC-62 cells did not show altered levels of total FOXO3 protein levels upon compound treatment. Exposure of the isogenic cell lines to BEZ235 almost completely abolished AKT phosphorylation, while HAR and PIP reduced it significantly after 2H of treatment. Notably, the effect of HAR and PIP treatment on AKT and FOXO phosphorylation was more pronounced in TRIB2 KO cells compared to parental cells. These data agree with the previously established role of TRIB2 as an activator of AKT [56] and as a FOXO repressor [55]. TRIB2 protein levels increased with BEZ235 and HAR treatments. Previous data from our lab (data not shown), cell treatment with inhibitors of the PI3K/AKT signalling pathway resulted in impairment of the proteasome-dependent TRIB2 degradation.

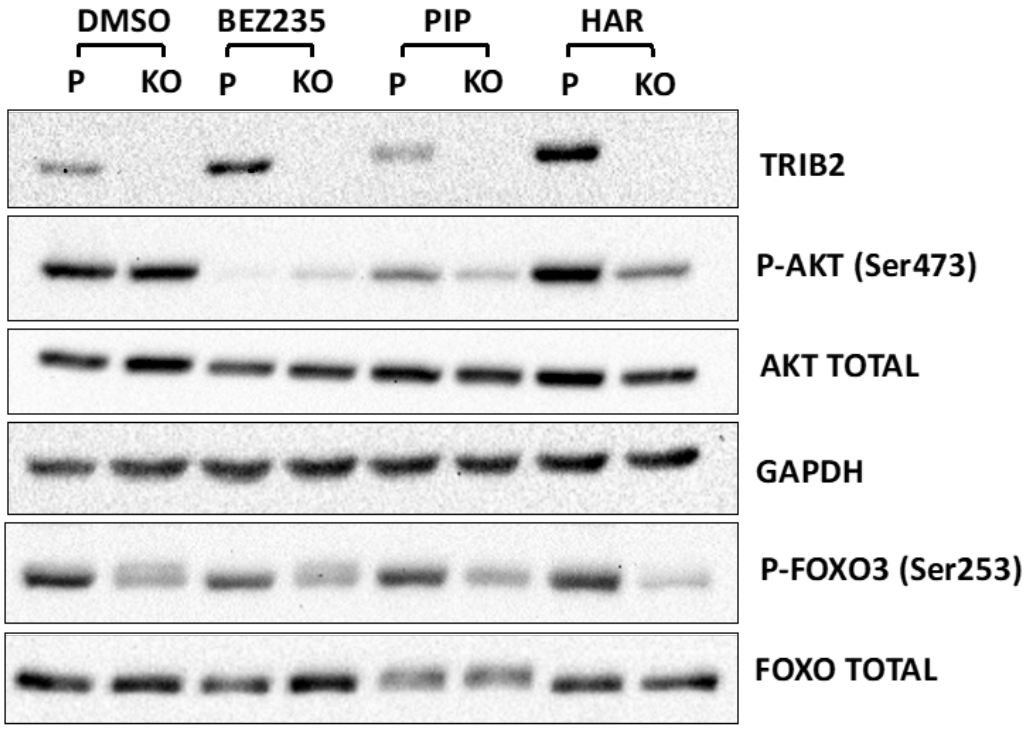

Figure 3.47. Parental UACC62 cells (P) and UACC-62 TRIB2 KO cells (KO) were treated with 16μM HAR or 13μM PIP for 2H. Proteins from lysates were immunoblotted with phospho-specific antibodies as indicated. Representative image of two independent experiments.

A decrease in FOXO phosphorylation levels by BEZ235, HAR or PIP in UACC-62 cells is consistent with an increase in FOXO activity. To confirm if FOXO is

transcriptionally active, we treated UACC-62 isogenic cell lines with BEZ235 (100nM) for 72H and analysed the transcript level of FOXO target genes. BEZ235 treatment significantly increases the transcriptional levels of the FOXO targets PLK1 and OCT4 in cells lacking TRIB2 expression compared to cells that express TRIB2 (Figure 3.48). These results are consistent with previous results showing that PUMA is upregulated with BEZ235 treatment in U2OS cells with no TRIB2 (Figure 3.12). Additionally, we previously showed that U2foxRELOC cells induced p21 and PUMA transcription upon HAR and PIP treatment, respectively (Figure 3.41). Together, these data indicate that HAR, PIP and BEZ235 induce FOXO transcriptional activity, indicated by the upregulation of p21, PUMA, PLK1 and OCT4.

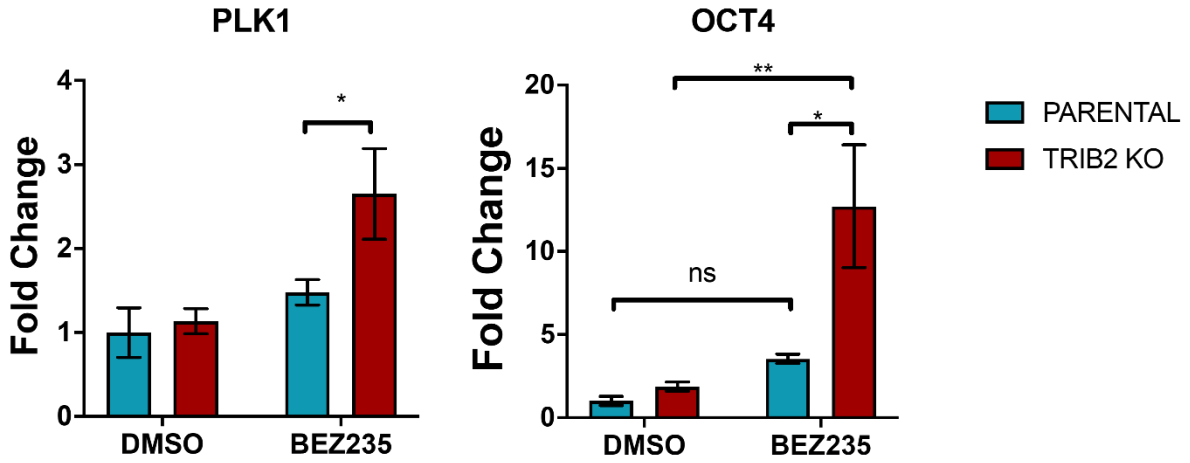

Figure 3.48. Parental UACC62 cells were treated with 100nM BEZ235 or 0.1% DMSO (control) for 72H. The upregulation of the FOXO target genes PLK1 and OCT4 was potentiated with TRIB2 KO. Statistical significance was determined with 2-Way ANOVA with multiple testing with SIDAK's and Tukey's multiple comparisons test with (*) $P < 0,05$ and (**) $P < 0,01$.

Our data suggests so far that TRIB2 decreases BEZ235 efficacy by indirectly inhibiting FOXO transcriptional activity, at least partially by promoting FOXO cytoplasmic localization. To evaluate whether TRIB2 levels in untreated cells affect FOXO localization, the isogenic UACC-62 cell lines (parental and TRIB2 KO) were transfected with a GFP-FOXO3 reporter plasmid.

Interestingly, UACC-62 parental cells tolerated the overexpression of FOXO3 better than the cells without TRIB2. FOXO3 was detected in the cytoplasm and the cell nucleus in the parental cells, while localization in the few surviving TRIB2 KO cells was less consistent, with more cells with nuclear fluorescence (Figure 3.49). These results, which are in line with our previous results, suggest that TRIB2 overexpression may contribute to FOXO inhibition by cytoplasmic localization, which can be the underlying reason for decreasing BEZ235 efficacy.

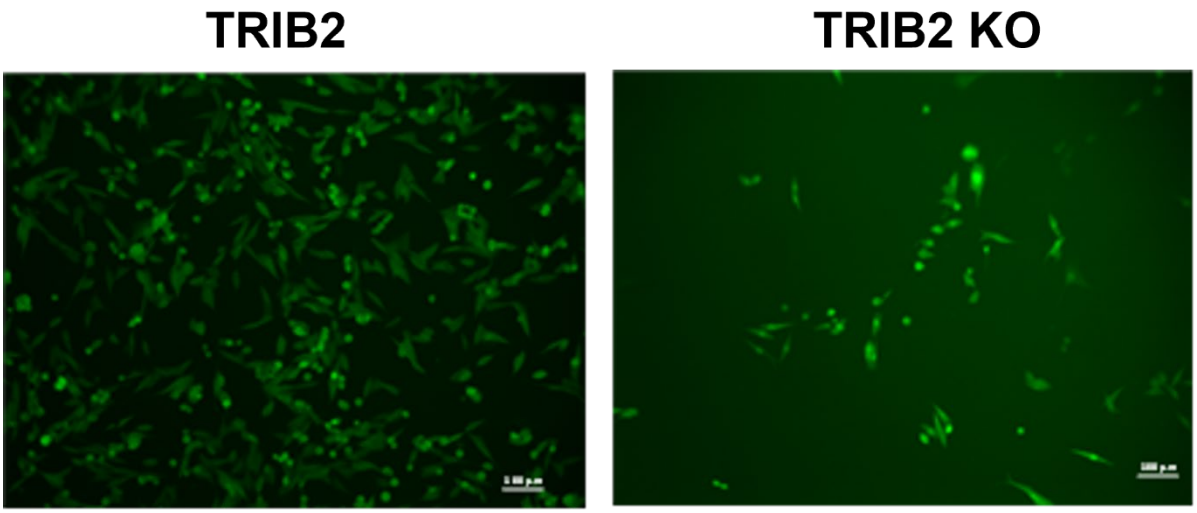

Figure 3.49. TRIB2 KO promotes more FOXO nuclear accumulation. Subcellular localization of GFP-FOXO3 stably transfected into parental UACC62 cells (left panel) and UACC-62 TRIB2 KO cells (right panel). Samples were imaged using 40x magnification. Scale bar indicates 100μm.

So far, our results suggest that HAR and PIP treatments seem to improve BEZ235 efficacy by inducing FOXO nuclear localization, where it is transcriptionally active, and we demonstrated this effect in the different cell lines U2OS, U2foxRELOC and UACC62. Similarly, we previously performed a screening for compounds that activate FOXO, and we demonstrated that an isothiazolonaphthoquinone compound (LOM612) induced endogenous FOXO1 and FOXO3a nuclear localization in a dose-dependent manner [161], resulting in the upregulation of FOXO targets such as p27 and FasL (Figure 3.50) [161]. The upregulation of p27 and FasL inhibits cell cycle progression and induces apoptosis, respectively, thus promoting tumour suppressor

activity [262, 263]. Taken together, our results suggest that compounds that activate FOXO by promoting its nuclear localization, such as HAR and PIP, have significant clinical potential for cancers characterized by inactivated FOXO (Figure 3.51).

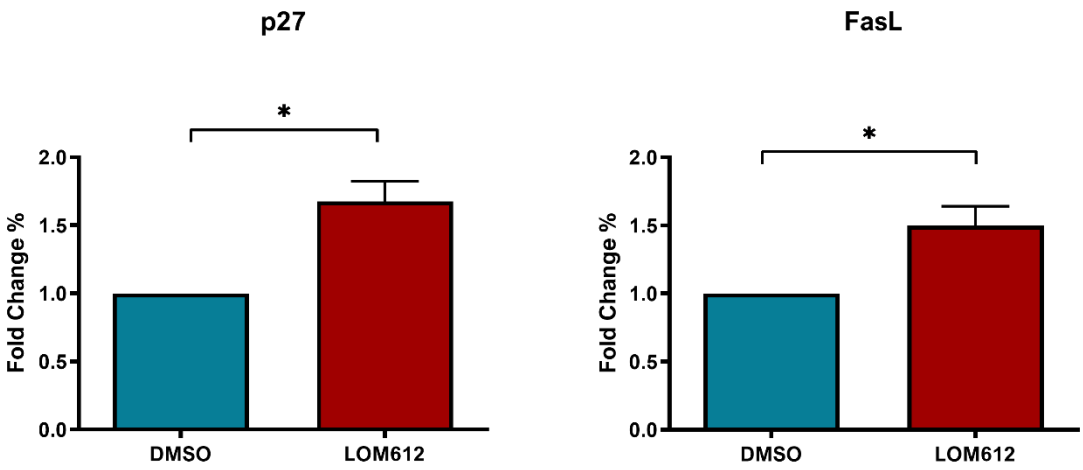

Figure 3.50. LOM612 treatment in U2OS cell line induced activation of FOXO. FOXO upregulated p27 and FasL after LOM612 treatment. Results represent mean±SEM from three independent experiments with triplicates. Statistical significance was determined by unpaired t-test with one-tailed P-value, with (*) $P < 0,05$ and (**) $P < 0,01$.

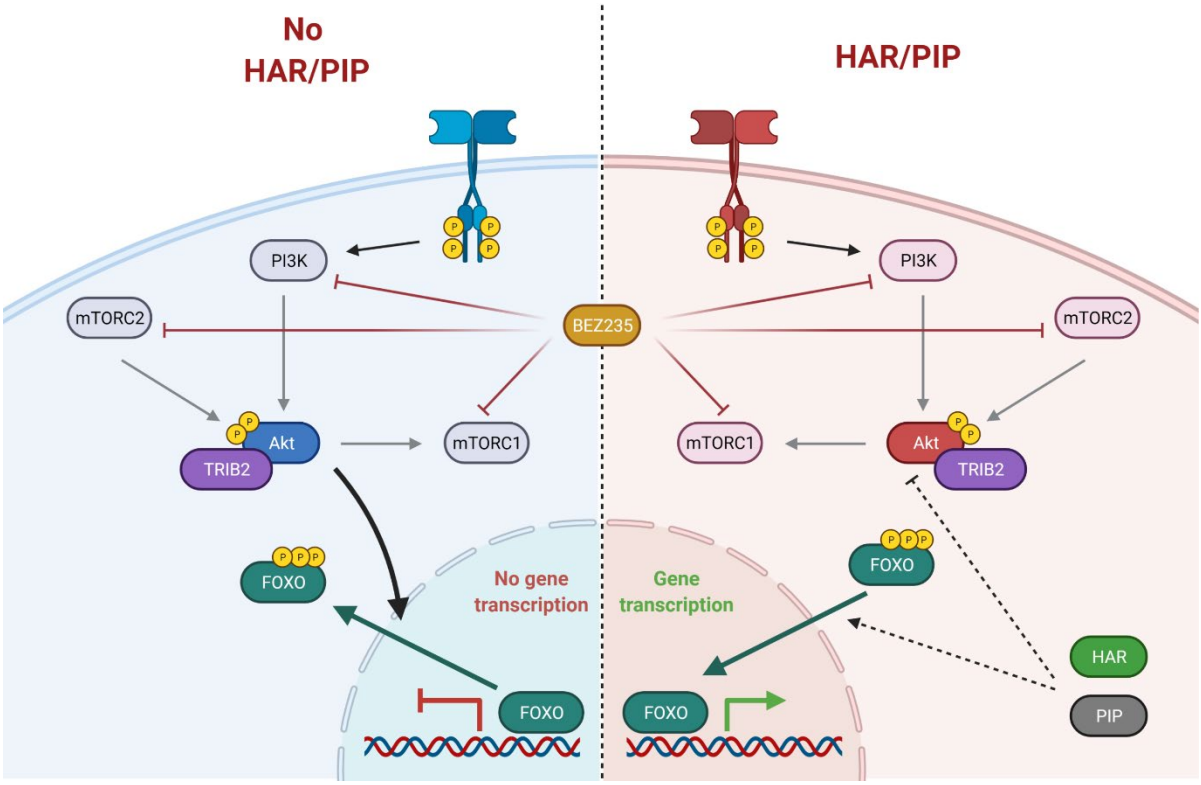

Figure 3.51. Proposed model for the reversal of TRIB2-mediated resistance by HAR and PIP. In the presence of elevated levels of TRIB2, TRIB2 will induce AKT activity downstream of BEZ235 inhibition, leading to FOXO inhibition by inducing FOXO translocation to the nucleus, hence decreasing BEZ235 efficacy (left). The presence of HAR or PIP upon BEZ235 treatment decreases TRIB2-mediated resistance to BEZ235 (right). We propose that HAR and PIP induce FOXO translocation to the nucleus and activate its transcriptional activity, although the exact mechanisms need further investigation.

4 Discussion

Discussion

Identifying molecular mechanisms involved in drug resistance is of enormous clinical importance, and our lab discovered a novel mechanism of drug resistance facilitated by TRIB2 by activating AKT. However, the exact mechanism is still unknown.

In this study, we propose that TRIB2 mediates resistance to the dual PI3K/mTOR inhibitor BEZ235 through transcriptional changes in cells. We used RNA sequencing-based transcriptional profiling of isogenic U2OS cells lines with different TRIB2 status in the presence or absence of PI3K/mTOR inhibition (BEZ235) to identify sets of differentially expressed genes. RNA-seq analysis showed that the overexpression of TRIB2 and exposure to the PI3K/mTOR inhibitor BEZ235 altered the transcriptional signatures of the U2OS osteosarcoma cell line. The inhibition of the PI3K/AKT signalling by BEZ235 treatment affects the expression level of over 2000 genes which is in line with previous studies [264], whereas the ectopic expression of TRIB2 affects ten times fewer genes. A possible explanation might be that while BEZ235 treatment completely abolishes PI3K/AKT signalling, TRIB2 only affects components of this signalling pathway that act downstream of AKT. TRIB2 is a pseudokinase that lost the ability to phosphorylate its targets but can act as a scaffold or promote protein degradation due to the MEK and E3 ubiquitin ligase binding domains. Additionally, these C-terminal domains regulate the interaction of target proteins to the pseudokinase domain, such as CEBPA degradation. Likewise, TRIB2 with its COP1-binding domain binds to AKT and leads to its phosphorylation at S473 [265]. Thus, this mode of action leads to the interaction of TRIB2 with specific target proteins.

We determined that TRIB2 overexpression attenuates BEZ235-induced gene expression and regulates genes involved with processes associated with tumour progression, such as cell proliferation, survival and migration. In general, TRIB2 overexpression increased the expression of genes, promoting tumour progression while repressing those genes known to prevent tumour progression [242-244]. Notably, in line with previous studies, PI3K/mTOR inhibition by BEZ235 treatment

produced an opposite transcriptional signature [264, 266]. Still, TRIB2 overexpression blunted the modulation of several BEZ235-regulated genes, suggesting that TRIB2 hinders BEZ235 from regulating specific genes and prevents BEZ235 from promoting tumour suppressor effects, increasing cancer cell survival to treatment, which is consistent with reports stating that TRIB2 expression correlated with increased resistance to different chemotherapeutic drugs [56, 185, 195, 196, 202, 267].

Promoter activity assays confirmed that TRIB2 indirectly drives changes in the transcription levels of genes involved with cancer cell migration and invasion [234, 268], which agrees with similar studies that showed that TRIB2 regulates the promoter activity of genes to induce pluripotency of embryonic stem cells and increases cell proliferation in colorectal cancer [212, 268]. In addition, it has been reported that reduced TRIB2 promoter activity decreased enzalutamide resistance in prostate cancer [269]. Genes regulated by TRIB2 overexpression and BEZ235 treatment were enriched for perturbed kinases involved with cancer progression and chemoresistance and enriched for KEGG pathways in cancer. Similar studies showed that paclitaxel-resistant and ibrutinib-resistant cell lines displayed enriched and activated PI3K/AKT signalling. BEZ235 was the most successful compound in paclitaxel-resistant cells to show anti-tumour effects [270, 271].

We also evaluated the impact of TRIB2 and BEZ235 on cell migration in U2OS cells, as increased cell migration ability is an indicator for tumour aggressiveness. BEZ235 treatment decreased cell migration, but TRIB2 presence increased cell migration even with concomitant BEZ235 treatment. These results are consistent with our previous data and others that report BEZ235 to decrease cell proliferation and migration in melanoma, AML and squamous cell carcinoma [55, 246, 247].

Many genes regulated by TRIB2 and BEZ235 have an oncogenic or tumour-suppressive role, regulating cancer cell survival, migration and proliferation. Several TRIB2-regulated genes were FOXO targets, which is not surprising considering TRIB2 is a FOXO repressor [55]. However, we cannot rule out additional mechanisms, as TRIB2 can also interact with the MAPK/ERK components and the Wnt pathways [265, 272].

Our data suggest that elevated levels of TRIB2 induce transcriptional changes in genes relevant to cell growth, proliferation, migration and survival, hindering

BEZ235 treatment from regulating genes necessary to arrest the cell cycle and induce toxicity (Figure 3.24).

Several cancers present dysregulated TRIB2 expression. TRIB2 is a known FOXO suppressor, and TRIB2 expression promotes cancer progression and confers resistance to several anticancer therapies [56, 185, 195, 196, 202, 267]. Therefore pharmaceutical means to interfere with TRIB2 activity might overcome drug resistance and improve clinical outcomes in cancer patients.

Thus TRIB2 is a promising therapeutic target that is, so far, poorly explored. TRIB2 can bind target proteins, prime them for degradation, or act as a scaffold protein, affecting the activity of the target proteins, such as AKT and CEBPA. Despite TRIB2 not presenting known catalytic activity *in vivo*, having lost the ability to phosphorylate proteins, it can bind to ATP [56, 175, 177]. Recently reported, the FDA-approved EGFR inhibitors, afatinib, neratinib and osimertinib, bind to and uncouple the c-terminal domain from the pseudokinase domain in TRIB2, promoting TRIB2 destabilization and degradation in breast cancer and non-small cell lung cancer. However, covalent drugs can accumulate significantly in the cells, and the side effects of these drugs are frequent [207, 265].

Furthermore, miRNAs are being investigated as potential therapeutics in cancer and could be helpful to target TRIB2. miR-509-5p was reported to directly inhibit TRIB2, decreasing proliferation and invasion in osteosarcoma [210]. miR-99 is a tumour suppressor that inhibits TRIB2 in cervical carcinoma cells, similar to miR-511, miR-1297, miR-206 and miR-240 in lung adenocarcinoma [208, 209, 273]. However, the delivery of therapeutic miRNAs is still problematic. Delivery by systemic circulation leads to clearance from the body, off-target side-effects, and once inside the cells, miRNAs can accumulate in endosomal vesicles. Local delivery improves bioavailability but may not be accessible according to the localization of the tumour. Therefore formulation strategies are under development to improve the delivery of miRNAs *in vivo* [274].

More recently, proteolysis targeting chimaeras (PROTACs) are under investigation to promote the degradation of considered undruggable targets. PROTACs display excellent selectivity to their targets and promote proximity between a recruited ubiquitin E3 ligase and a target protein, inducing the ubiquitination and

degradation of the target protein [275]. Moreover, hydrophobic tagging (HyT) is being used to promote the degradation of target proteins. The human epidermal growth factor receptor 3 (HER3) inhibitor TX2–121-1 leads to HER3 proteasomal degradation. It will be exciting to determine if PROTACs and HyT can be adapted to target TRIB2, as they can affect the non-catalytic functions of proteins [276, 277]. A screening process must be performed on a generated library of various protein degraders to identify functional PROTACs to generate TRIB2-targeting PROTACs. This process is a challenge, especially for proteins with limited or unknown direct inhibitors of the targeted protein, which is the case for TRIB2 [278].

Currently, there are efforts to explore systematic approaches to identify novel therapeutics based on molecular features of diseases, with the development of large-scale technologies, such as microarray gene expression signatures and high-performance computing [279]. A study showed that the increased capacity of a drug to reverse cancer-associated gene expression profiles correlated with greater efficiency in preclinical models in liver, colon and breast cancers [280].

We propose that TRIB2-mediated resistance can be reverted pharmacologically. Our hypothesis relies on the observation that TRIB2 overexpression increased the expression of genes that promote tumour progression while repressing those genes known to prevent tumour progression. Notably, in line with previous studies, PI3K/mTOR inhibition by BEZ235 treatment showed an opposite transcriptional signature compared to TRIB2 signature [264, 266]. We identified several small-molecule compounds capable of inducing inverse signatures compared to TRIB2, suggesting their potential to interfere with TRIB2 downstream effects. We used the cMAP tool, a gene expression database that allowed us to query compounds that induced transcriptional signatures opposite TRIB2. Numerous investigations illustrated the potential of this approach to identify novel indications for approved drugs or compounds with known modes of action [281-283]. Accordingly, we found that the naturally occurring alkaloids HAR and PIP can revert TRIB2-dependent transcriptional signatures, and several of the genes regulated by HAR and PIP affect cell proliferation, migration and cell death [104].

As HAR and PIP were reported to lead to decreased AKT activity [284, 285] and TRIB2 increases AKT activity, we propose that reversing TRIB2-induced

transcriptional signatures by HAR and PIP might improve BEZ235 treatment efficacy. We found that HAR and PIP act synergistically with the PI3K/mTOR inhibitor BEZ235 affecting cell viability. Thus, cells with high levels of TRIB2 treated with either of these compounds would be more prone to enter apoptosis or become more senescent upon treatment with PI3K/mTOR inhibitors. Moreover, TRIB2 no longer hindered gene regulation by BEZ235 in the presence of HAR and PIP. In line with our data, sanguinarine, a plant alkaloid such as HAR and PIP, has been reported to sensitize cancer cells resistant to cytostatics and induce cell cycle arrest in several phases, decreasing tumour proliferation and metastasis [286]. Other alkaloid compounds were already successfully developed into FDA-approved chemotherapeutic drugs, such as camptothecin, vinblastine, and irinotecan [279]. Alkaloids belong to a diverse group of molecules, hence not every alkaloid presents anti-tumour activity [287], and several of these compounds display elevated toxicity [288]. Consistent with our data, PIP synergized with oxaliplatin *in vivo* to induce ROS in colorectal cancer and synergized with gemcitabine to induce apoptosis in KRAS mutant lung cancer. Doxorubicin can present cardiotoxicity at therapeutic levels. HAR synergized with doxorubicin to elicit apoptosis at non-toxic doses of doxorubicin in MCF7. HAR and gemcitabine synergistically inhibited cell proliferation and induced apoptosis in pancreatic cancer cells [286, 289-292].

Moreover, as HAR and PIP successfully reverted TRIB2 resistance through the reversal of the transcriptional signature of the cells, we confirmed the robustness of the cMAP tool to generate candidate compounds for experimental validation.

We hypothesized that HAR and PIP revert TRIB2 resistance by modulating FOXO activity. TRIB2 activates AKT, which leads to FOXO phosphorylation and subsequent translocation to the cytoplasm, rendering FOXO transcriptionally inactive [55]. Hence, it is a possibility that HAR and PIP exert their effects by decreasing the activity of the PI3K/AKT signalling pathway, leading to FOXO activation. We determined that both compounds act upstream of FOXO, modulating AKT activity and regulating FOXO subcellular localization and transcriptional activity. PIP was reported to inhibit CRM-1 in HeLa cells after 4H of treatment by binding covalently to a cysteine residue within the export receptor protein CRM-1 and preventing the interaction between CRM-1 and cargo proteins, thus inhibiting the nuclear export of proteins that

bear nuclear export sequences [293]. Hence, we assessed whether FOXO nuclear localization by HAR and PIP would result from CRM-1 inhibition. We treated a U2OS cell line expressing a fluorescent CRM-1 substrate reporter with HAR or PIP for 1H. The treatment of the reporter cells with HAR and PIP failed to affect CRM-1-mediated nuclear export. Our data suggest that the primary mechanism for FOXO nuclear translocation by HAR and PIP is not through the inhibition of CRM-1 but mainly due to modulation of AKT activity and preventing FOXO phosphorylation. Consistently, FOXO nuclear localization correlated with decreased phosphorylated AKT and FOXO, resulting in decreased AKT activity and increased FOXO activity. These results agree with other studies, in which PIP induced nuclear translocation of FOXO3, decreased FOXO3 phosphorylation and restored FOXO3 transcriptional activity via AKT activation [294]. Likewise, HAR was reported to decrease AKT and FOXO phosphorylation via inhibition of DYRK1A, preventing DYRK1A-mediated FOXO cytoplasmic translocation [284, 295]. Moreover, HAR and PIP also affected the total protein levels of AKT and FOXO in addition to the phosphorylation status, suggesting that these compounds may also decrease FOXO protein stability, independent of changes in FOXO transcription and translation processes that are known to take longer than 1H. Hence, HAR and PIP may modulate FOXO phosphorylation by inducing FOXO nuclear localization and degradation of phosphorylated FOXO. In agreement with our data, AKT induces ubiquitin degradation of cytoplasmic FOXO1 and FOXO3 following their export from the nucleus [296, 297].

In both osteosarcoma and melanoma cell lines, the presence of TRIB2 blunted the impact of BEZ235, HAR or PIP on AKT phosphorylation levels, indicating that this does not represent a cell line-specific effect. TRIB2 interferes with the efficacy of PI3K/AKT signalling pathway inhibitors but ultimately, HAR and PIP treatments culminated in the upregulation of FOXO target genes, confirming that FOXO regained its transcriptional activity in the nucleus. Others determined that HAR or PIP treatments in SW620 and HeLa cells, respectively, inhibited AKT, decreased phosphorylation of FOXO and affected the transcription of FOXO targets involved in apoptosis and cell cycle arrest [294, 295]. Hence HAR and PIP increased the transcriptional impact of BEZ235 in the presence of TRIB2, most likely via modulation of the PI3K/AKT signalling pathway. Interestingly, TRIB2 protein levels increased with

BEZ235 and HAR treatments. Previous data from our lab have shown that PI3K/AKT pathway inhibitors lead to the stabilization of TRIB2 protein levels. Indeed, Wang *et al*. reported that the mTOR inhibitor rapamycin impairs the proteasome-dependent TRIB2 degradation in liver cancer cells. The authors showed that p70S6K phosphorylates TRIB2, allowing Smurf1-mediated TRIB2 ubiquitination and degradation in liver cancer cells. Liver cancer is characterized by elevated expression of TRIB2 and stable TRIB2 protein compared with healthy tissue. They also demonstrated that rapamycin treatment inhibits p70S6K, thus preventing TRIB2 degradation. Furthermore, rapamycin treatment led to TRIB2 translocation from the nucleus to the cytoplasm, which the authors suggest is mediated by p70S6K activity [298]. In agreement with our data, PIP was previously reported to inhibit the PI3K/AKT axis in human triple breast cancer cells [299] and activate FOXO3, inducing FOXO nuclear translocation and expression of FOXO target gene BIM in HeLa cells [294]. PIP is found in long pepper fruit (Piper longum) and used in traditional Indian medicine to treat many diseases, including tumours [300]. In line with our data, PIP has been found to reverse chemotherapy resistance in several cancers [301-304]. PIP synergized with cisplatin to increase ROS levels and induce apoptosis in head and neck cancer cells *in vitro* and *in vivo* through PIP-mediated regulation of p53 target genes [301]. PIP improved the sensitivity of resistant human leukaemia cells to doxorubicin by reducing the expression of drug efflux pumps, upregulated genes involved with cell cycle and apoptosis, and decreased levels of phosphorylated AKT and NF-κB [302]. PIP increased the half-life of docetaxel in triple-negative breast cancer cells and downregulated BCL2 and survivin, improving docetaxel toxicity [303]. PIP restored the sensitivity of chemoresistant retinoblastoma cells to vincristine or carboplatin through decreased cell death, decreased expression of the efflux pumps MRP1 and MDR1, downregulation of genes involved with cell cycle regulation and survival, and decreased phosphorylated AKT and PI3K levels [304]. A recent study showed PIP to reverse resistance to Cisplatin in non-small cell lung cancer cells by inhibiting AKT phosphorylation [285]. Collectively, PIP displays no toxicity in normal cells but displays anti-tumour activity in cancer cells in combined treatment, improving the toxic effects of anti-cancer drugs. PIP impacts the activity of signalling pathways, such as PI3K/AKT, to modulate transcription of target genes that regulate cancer cell

proliferation and survival and decreasing drug efflux [302]. This observation is consistent with our results and suggests that the therapeutic effects of PIP in combined therapy could be helpful in various cancers with dysregulated prosurvival signalling, such as the PI3K/AKT pathway.

HAR is a fluorescent β-carboline alkaloid found in several plant species, including Banisteriopsis caapi vine and Peganum harmala. It has been shown to act as a reversible, selective inhibitor of monoamine oxidase (MAO)-A [305], a flavoenzyme that degrades amine neurotransmitters by oxidative deamination. It remains to determine if the enzymatic inhibition of MAO-A mediates the reversion of TRIB2-induced gene expression profile and synergic susceptibility observed upon HAR treatment. Reversible inhibitors of monoamine oxidase A (RIMAs) chemically unrelated to HAR such as Moclobemide, Brofaramine, Toloxatone or Befloxatone could be used to test this hypothesis. Conversely, HAR has been shown to potently and specifically inhibit DYRK1A kinase activity *in vitro* [306]. Interestingly, DYRK1A kinase is known to phosphorylate FOXO1 at S329 [307]. A more recent study shows that inhibition of DYRK1A decreased phosphorylation of FOXO3 on S253 by downregulation of AKT activity in head and neck squamous cell carcinoma cell lines [284]. In another study, Rüben *et al*. synthesized HAR analogues that retain DYRK1A inhibition but lost MAO-A inhibition. These compounds can be used to determine whether reversal of TRIB2-induced gene expression may result from MAO-A or DYRK1A [308, 309].

Our results indicate that HAR and PIP synergize with BEZ235 by inducing FOXO nuclear localization and transcriptional activity by modulating the PI3K/AKT signalling pathway in our *in vitro* models (Figure 3.51). As TRIB2 interacts with other substrates besides AKT, we cannot exclude alternative mechanisms for TRIB2-mediated resistance. In AML, TRIB2 increases the efflux pumps MDR1 and MRP1 expression by increasing phosphorylation of ERK and signal transducer and activator of transcription 3 (STAT3), generating resistance to doxorubicin [196, 265]. As such, further studies can be performed to characterize the full spectrum of TRIB2 effects in tumour progression and facilitate the discovery or repurposing of drugs to revert TRIB2 effects. Liang *et al.* developed a novel *in vivo* model to generate cisplatin-resistant cells and evaluate the impact of TRIB2 in this resistance [267]. Similar *in vivo*

experiments would be valuable to assess the clinical potential of combined treatment with HAR or PIP and standard chemotherapeutic agents. The *in vivo* anticancer activity of HAR or PIP combined with BEZ235 might be evaluated using our U2OS/TRIB2 cells xenografted into mice [310]. The resistance-reversal effect of HAR and PIP must be investigated in relevant clinical models and combined with standard therapeutic agents in cancers with TRIB2-induced resistance. A potential clinical model could be a melanoma patient-derived orthotopic xenograft (PDOX) mouse model derived from metastasis tissue from a melanoma patient with elevated expression of TRIB2, similar to other studies [311]. Ultimately, if HAR or PIP are successful, they can be incorporated into the standard treatment protocol for patients identified with suffering from cancers that present TRIB2-mediated resistance in a personalized medicine approach.

Taken together, our findings suggest that the natural alkaloids PIP and HAR might be beneficial in the clinic to overcome therapy resistance and improve the clinical outcome of treatments for patients with advanced melanoma and other tumour types.

5 Concluding remarks

Concluding remarks

Our lab has previously shown that the tumour suppressor FOXO is the central downstream transcriptional mediator of the PI3K/AKT pathway after PI3K inhibition, which is crucial for the anti-cancer action of several drugs, particularly PI3K pathway inhibitors, including BEZ235. Our lab previously established TRIB2 as an oncogenic protein that suppresses FOXO, and we hypothesized that TRIB2 mediates resistance to BEZ235 treatment by altering the gene expression profile of the cells, rendering them less sensitive to BEZ235 toxicity. We have confirmed that TRIB2 impacts cells at the transcriptional level by modulating genes involved with cancer progression, resulting in drug resistance.

Given the transcriptional changes resulting from TRIB2 overexpression that lead to a decrease in BEZ235 efficacy, we hypothesized that TRIB2 resistance effects could decrease with drugs that counteract these effects by reverting the gene expression signature of cells. We used the cMAP tool, a gene expression database, to identify candidate compounds that elicit transcriptional signatures opposite TRIB2. We discovered two compounds, HAR and PIP, that produce transcription signatures in cells opposite the TRIB2-induced transcriptional signature. This effect was enough to render cells sensitive to BEZ235 toxicity in the presence of TRIB2, ultimately reversing TRIB2-mediated resistance. Although this mechanism is still not fully characterized, we showed that HAR and PIP decrease the activity of the PI3K/AKT signalling pathway and reactivate FOXO transcriptional activity by inducing FOXO nuclear translocation. Considering that HAR and PIP successfully reverted TRIB2 resistance via reversal of transcriptional signature of the cells, we confirmed the robustness of the cMAP tool to generate candidate compounds for experimental validation.

Identifying molecular mechanisms involved in drug resistance or sensitization to targeted therapy is of enormous clinical importance. Therefore our results are the

proof of concept that TRIB2-mediated resistance can be pharmacologically targeted, using drugs that induce FOXO activation by modulating AKT activity.

Ultimately, our results might pave the way to a personalized clinical application to combine the treatment of tumours with high TRIB2 expression with agents such as HAR or PIP. Reducing the intrinsic and acquired resistance in TRIB2-induced resistant cancers may significantly improve the clinical outcome of anti-cancer therapies.

6 References

References

1. Green, P.H.R., B. Lebwohl, and R. Greywoode, *Celiac disease.* Journal of Allergy and Clinical Immunology, 2015. **135**(5): p. 1099-1106.
2. *Cancer*. 2018 [cited 2020 03.06.2020]; 12/09/2018:[Available from: https://www.who.int/news-room/fact-sheets/detail/cancer.
3. Vineis, P. and C.P. Wild, *Global cancer patterns: causes and prevention.* Lancet, 2014. **383**(9916): p. 549-57.
4. *Cancer Classification*. [cited 2020 23/06/2020]; Available from: https://training.seer.cancer.gov/disease/categories/classification.html.
5. *Cancer Treatment*. SEER Training Modules [cited 2020 23/06/2020]; Available from: https://training.seer.cancer.gov/treatment/.
6. Golemis, E.A., et al., *Molecular mechanisms of the preventable causes of cancer in the United States.* Genes Dev, 2018. **32**(13-14): p. 868-902.
7. Hanahan, D. and R.A. Weinberg, *Hallmarks of cancer: the next generation.* Cell, 2011. **144**(5): p. 646-74.
8. Sever, R. and J.S. Brugge, *Signal transduction in cancer.* Cold Spring Harbor perspectives in medicine, 2015. **5**(4): p. a006098.
9. Owen, K.L., N.K. Brockwell, and B.S. Parker, *JAK-STAT Signaling: A Double-Edged Sword of Immune Regulation and Cancer Progression.* Cancers, 2019. **11**(12): p. 2002.
10. Jung, Y.-S. and J.-I. Park, *Wnt signaling in cancer: therapeutic targeting of Wnt signaling beyond β-catenin and the destruction complex.* Experimental & Molecular Medicine, 2020. **52**(2): p. 183-191.
11. Weinberg, R.A., *The biology of cancer*. 2nd Edition ed. 2014: Garland Science, Taylor & Francis Group, LLC. 962.
12. Krishnamurthy, N. and R. Kurzrock, *Targeting the Wnt/beta-catenin pathway in cancer: Update on effectors and inhibitors.* Cancer Treatment Reviews, 2018. **62**: p. 50-60.
13. Jahangiri, A. and W.A. Weiss, *It Takes Two to Tango: Dual Inhibition of PI3K and MAPK in Rhabdomyosarcoma.* Clinical Cancer Research, 2013. **19**(21): p. 5811.
14. Du, Z. and C.M. Lovly, *Mechanisms of receptor tyrosine kinase activation in cancer.* Mol Cancer, 2018. **17**(1): p. 58.
15. Lemmon, M.A. and J. Schlessinger, *Cell signaling by receptor tyrosine kinases.* Cell, 2010. **141**(7): p. 1117-34.
16. Santarpia, L., S.M. Lippman, and A.K. El-Naggar, *Targeting the MAPK-RAS-RAF signaling pathway in cancer therapy.* Expert Opin Ther Targets, 2012. **16**(1): p. 103-19.
17. Frémin, C. and S. Meloche, *Fremin C, Meloche SFrom basic research to clinical development of MEK1/2 inhibitors for cancer therapy. J Hematol Oncol 3: 8.* Journal of hematology & oncology, 2010. **3**: p. 8.
18. Murugan, A.K., M. Grieco, and N. Tsuchida, *RAS mutations in human cancers: Roles in precision medicine.* Semin Cancer Biol, 2019. **59**: p. 23-35.
19. Niault, T.S. and M. Baccarini, *Targets of Raf in tumorigenesis.* Carcinogenesis, 2010. **31**(7): p. 1165-1174.
20. Castellano, E. and J. Downward, *RAS Interaction with PI3K: More Than Just Another Effector Pathway.* Genes & cancer, 2011. **2**(3): p. 261-274.
21. Hemmings, B.A. and D.F. Restuccia, *PI3K-PKB/Akt pathway.* Cold Spring Harbor perspectives in biology, 2012. **4**(9): p. a011189-a011189.

22. Janku, F., T.A. Yap, and F. Meric-Bernstam, *Targeting the PI3K pathway in cancer: are we making headway?* Nature Reviews Clinical Oncology, 2018. **15**(5): p. 273-291.
23. Thorpe, L.M., H. Yuzugullu, and J.J. Zhao, *PI3K in cancer: divergent roles of isoforms, modes of activation and therapeutic targeting.* Nature Reviews Cancer, 2015. **15**(1): p. 7-24.
24. Yang, J., et al., *Targeting PI3K in cancer: mechanisms and advances in clinical trials.* Molecular Cancer, 2019. **18**(1): p. 26.
25. Blind, R.D., et al., *The signaling phospholipid PIP₃ creates a new interaction surface on the nuclear receptor SF-1.* Proceedings of the National Academy of Sciences, 2014. **111**(42): p. 15054-15059.
26. Toker, A. and A.C. Newton, *Akt/Protein Kinase B Is Regulated by Autophosphorylation at the Hypothetical PDK-2 Site *.* Journal of Biological Chemistry, 2000. **275**(12): p. 8271-8274.
27. Nicholson, K.M. and N.G. Anderson, *The protein kinase B/Akt signalling pathway in human malignancy.* Cellular Signalling, 2002. **14**(5): p. 381-395.
28. Nitulescu, G.M., et al., *The Akt pathway in oncology therapy and beyond (Review).* Int J Oncol, 2018. **53**(6): p. 2319-2331.
29. Elghazi, L., N. Balcazar, and E. Bernal-Mizrachi, *Emerging role of protein kinase B/Akt signaling in pancreatic beta-cell mass and function.* Int J Biochem Cell Biol, 2006. **38**(2): p. 157-63.
30. Hinz, N. and M. Jücker, *Distinct functions of AKT isoforms in breast cancer: a comprehensive review.* Cell Commun Signal, 2019. **17**(1): p. 154.
31. Lv, D., et al., *PRAS40 signaling in tumor.* Oncotarget, 2017. **8**(40): p. 69076-69085.
32. Wang, L., et al., *Mammalian target of rapamycin complex 1 (mTORC1) activity is associated with phosphorylation of raptor by mTOR.* The Journal of biological chemistry, 2009. **284**(22): p. 14693-14697.
33. Hinz, N. and M. Jücker, *Distinct functions of AKT isoforms in breast cancer: a comprehensive review.* Cell Communication and Signaling, 2019. **17**(1): p. 154.
34. Rodier, G., et al., *p27 cytoplasmic localization is regulated by phosphorylation on Ser10 and is not a prerequisite for its proteolysis.* The EMBO journal, 2001. **20**(23): p. 6672-6682.
35. Chen, R., et al., *Phosphorylation of P27 by AKT is required for inhibition of cell cycle progression in cholangiocarcinoma.* Dig Liver Dis, 2018. **50**(5): p. 501-506.
36. Toker, A., *mTOR and Akt Signaling in Cancer: SGK Cycles In.* Molecular Cell, 2008. **31**(1): p. 6-8.
37. Chakraborty, S., et al., *Vimentin activation in early apoptotic cancer cells errands survival pathways during DNA damage inducer CPT treatment in colon carcinoma model.* Cell Death & Disease, 2019. **10**(6): p. 467.
38. Zhu, Q.S., et al., *Vimentin is a novel AKT1 target mediating motility and invasion.* Oncogene, 2011. **30**(4): p. 457-470.
39. Najm, P. and M. El-Sibai, *Palladin regulation of the actin structures needed for cancer invasion.* Cell adhesion & migration, 2014. **8**(1): p. 29-35.
40. Chin, Y.R. and A. Toker, *Akt2 regulates expression of the actin-bundling protein palladin.* FEBS letters, 2010. **584**(23): p. 4769-4774.
41. Kennedy, S.G., et al., *Akt/Protein kinase B inhibits cell death by preventing the release of cytochrome c from mitochondria.* Mol Cell Biol, 1999. **19**(8): p. 5800-10.
42. Altomare, D.A. and J.R. Testa, *Perturbations of the AKT signaling pathway in human cancer.* Oncogene, 2005. **24**(50): p. 7455-7464.
43. Hoxhaj, G. and B.D. Manning, *The PI3K-AKT network at the interface of oncogenic signalling and cancer metabolism.* Nat Rev Cancer, 2020. **20**(2): p. 74-88.
44. Madsen, R. and B. Vanhaesebroeck, *Cracking the context-specific PI3K signaling code.* Science Signaling, 2020. **13**: p. eaay2940.
45. Xu, F., et al., *Roles of the PI3K/AKT/mTOR signalling pathways in neurodegenerative diseases and tumours.* Cell & Bioscience, 2020. **10**(1): p. 54.

46. Hermida, M.A., J. Dinesh Kumar, and N.R. Leslie, *GSK3 and its interactions with the PI3K/AKT/mTOR signalling network.* Adv Biol Regul, 2017. **65**: p. 5-15.
47. Fu, W., et al., *MDM2 acts downstream of p53 as an E3 ligase to promote FOXO ubiquitination and degradation.* The Journal of biological chemistry, 2009. **284**(21): p. 13987-14000.
48. Ogawara, Y., et al., *Akt Enhances Mdm2-mediated Ubiquitination and Degradation of p53 *.* Journal of Biological Chemistry, 2002. **277**(24): p. 21843-21850.
49. Chibaya, L., et al., *Mdm2 phosphorylation by Akt regulates the p53 response to oxidative stress to promote cell proliferation and tumorigenesis.* Proceedings of the National Academy of Sciences, 2021. **118**(4): p. e2003193118.
50. Abraham, A.G. and E. O'Neill, *PI3K/Akt-mediated regulation of p53 in cancer.* Biochem Soc Trans, 2014. **42**(4): p. 798-803.
51. Takaishi, H., et al., *Regulation of nuclear translocation of forkhead transcription factor AFX by protein kinase B.* Proc Natl Acad Sci U S A, 1999. **96**(21): p. 11836-41.
52. Pan, C.W., et al., *AKT-phosphorylated FOXO1 suppresses ERK activation and chemoresistance by disrupting IQGAP1-MAPK interaction.* Embo j, 2017. **36**(8): p. 995-1010.
53. Brunet, A., et al., *Akt promotes cell survival by phosphorylating and inhibiting a Forkhead transcription factor.* Cell, 1999. **96**(6): p. 857-68.
54. Link, W., *Tribbles breaking bad: TRIB2 suppresses FOXO and acts as an oncogenic protein in melanoma.* Biochemical Society Transactions, 2015. **43**(5): p. 1085-1088.
55. Zanella, F., et al., *Human TRIB2 is a repressor of FOXO that contributes to the malignant phenotype of melanoma cells.* Oncogene, 2010. **29**(20): p. 2973-82.
56. Hill, R., et al., *TRIB2 confers resistance to anti-cancer therapy by activating the serine/threonine protein kinase AKT.* Nat Commun, 2017. **8**: p. 14687.
57. Hill, R., et al., *TRIB2 as a biomarker for diagnosis and progression of melanoma.* Carcinogenesis, 2015. **36**(4): p. 469-77.
58. Kozar, I., et al., *Many ways to resistance: How melanoma cells evade targeted therapies.* Biochimica et Biophysica Acta (BBA) - Reviews on Cancer, 2019. **1871**(2): p. 313-322.
59. Scolyer, R.A., G.V. Long, and J.F. Thompson, *Evolving concepts in melanoma classification and their relevance to multidisciplinary melanoma patient care.* Molecular oncology, 2011. **5**(2): p. 124-136.
60. Kalal, B., D. Upadhya, and V.R. Pai, *Chemotherapy Resistance Mechanisms in Advanced Skin Cancer.* Oncology Reviews, 2017. **11**: p. 326.
61. Lin, J.Y. and D.E. Fisher, *Melanocyte biology and skin pigmentation.* Nature, 2007. **445**(7130): p. 843-50.
62. Howlader N, N.A., Krapcho M, et al. *SEER Cancer Statistics Review, 1975-2016*. 2018 [cited 2020 05.10.2020]; Available from: https://seer.cancer.gov/archive/csr/1975_2016/.
63. Perera, E., et al., *Malignant Melanoma.* Healthcare, 2013. **2**: p. 1-19.
64. *Melanoma of Skin*. 2018 [cited 2020 05.10.2020]; Available from: https://gco.iarc.fr/today/data/factsheets/cancers/16-Melanoma-of-skin-fact-sheet.pdf.
65. *Cancer Today*. 2018 [cited 2020 05.10.2020]; Available from: https://gco.iarc.fr/today/online-analysis-multi-bars?v=2018&mode=cancer&mode_population=regions&population=900&populations=620&key=total&sex=0&cancer=39&type=0&statistic=5&prevalence=0&population_group=5&ages_group%5B%5D=0&ages_group%5B%5D=17&nb_items=20&group_cancer=0&include_nmsc=0&include_nmsc_other=1&type_multiple=%257B%2522inc%2522%253Atrue%252C%2522mort%2522%253Atrue%252C%2522prev%2522%253Afalse%257D&orientation=horizontal&type_sort=0&type_nb_items=%257B%2522top%2522%253Atrue%252C%2522bottom%2522%253Atrue%257D&population_group_list=8,40,112,56,70,100,191,203,208,233,246,250,276,300,348,352,372,380,428,440,442,470,499,578,616,620,498,642,643,688,703,705,724,752,756,528,807,804,826&population_group_globocan_id=908#collapse-group-1-5.

66. Austoker, J., *Melanoma: prevention and early diagnosis.* BMJ (Clinical research ed.), 1994. **308**(6945): p. 1682-1686.
67. Li, W.Q., et al., *Cutaneous nevi and risk of melanoma death in women and men: A prospective study.* J Am Acad Dermatol, 2019. **80**(5): p. 1284-1291.
68. Veierød, M.B., et al., *A prospective study of pigmentation, sun exposure, and risk of cutaneous malignant melanoma in women.* J Natl Cancer Inst, 2003. **95**(20): p. 1530-8.
69. Siskind, V., et al., *Nevi, family history, and fair skin increase the risk of second primary melanoma.* J Invest Dermatol, 2011. **131**(2): p. 461-7.
70. Kubica, A.W. and J.D. Brewer, *Melanoma in immunosuppressed patients.* Mayo Clin Proc, 2012. **87**(10): p. 991-1003.
71. Daniel Jensen, J. and B.E. Elewski, *The ABCDEF Rule: Combining the "ABCDE Rule" and the "Ugly Duckling Sign" in an Effort to Improve Patient Self-Screening Examinations.* The Journal of clinical and aesthetic dermatology, 2015. **8**(2): p. 15-15.
72. Miller, A.J. and M.C. Mihm, Jr., *Melanoma.* N Engl J Med, 2006. **355**(1): p. 51-65.
73. Vanni, I., et al., *Non-BRAF Mutant Melanoma: Molecular Features and Therapeutical Implications.* Frontiers in Molecular Biosciences, 2020. **7**(172).
74. Cheng, L., et al., *Molecular testing for BRAF mutations to inform melanoma treatment decisions: a move toward precision medicine.* Modern pathology : an official journal of the United States and Canadian Academy of Pathology, Inc, 2018. **31**(1): p. 24-38.
75. Irvine, M., et al., *Oncogenic PI3K/AKT promotes the step-wise evolution of combination BRAF/MEK inhibitor resistance in melanoma.* Oncogenesis, 2018. **7**(9): p. 72.
76. Iwabuchi, K. and L. Van Kaer, *Editorial: Role of CD1- and MR1-Restricted T Cells in Immunity and Disease.* Frontiers in Immunology, 2019. **10**(1837).
77. Mendonsa, A.M., T.-Y. Na, and B.M. Gumbiner, *E-cadherin in contact inhibition and cancer.* Oncogene, 2018. **37**(35): p. 4769-4780.
78. Guo, H., J.A. Carlson, and A. Slominski, *Role of TRPM in melanocytes and melanoma.* Experimental dermatology, 2012. **21**(9): p. 650-654.
79. Mrozik, K.M., et al., *N-cadherin in cancer metastasis, its emerging role in haematological malignancies and potential as a therapeutic target in cancer.* BMC cancer, 2018. **18**(1): p. 939-939.
80. Liu, Z., F. Wang, and X. Chen, *Integrin alpha(v)beta(3)-Targeted Cancer Therapy.* Drug development research, 2008. **69**(6): p. 329-339.
81. Li, H., et al., *The relationship between MMP-2 and MMP-9 expression levels with breast cancer incidence and prognosis.* Oncology letters, 2017. **14**(5): p. 5865-5870.
82. Jaiswal, P.K., A. Goel, and R.D. Mittal, *Survivin: A molecular biomarker in cancer.* The Indian journal of medical research, 2015. **141**(4): p. 389-397.
83. Tran, K.B., et al., *Diverse mechanisms activate the PI 3-kinase/mTOR pathway in melanomas: implications for the use of PI 3-kinase inhibitors to overcome resistance to inhibitors of BRAF and MEK.* BMC Cancer, 2021. **21**(1): p. 136.
84. Kwong, L.N. and M.A. Davies, *Navigating the therapeutic complexity of PI3K pathway inhibition in melanoma.* Clinical cancer research : an official journal of the American Association for Cancer Research, 2013. **19**(19): p. 5310-5319.
85. Domingues, B., et al., *Melanoma treatment in review.* ImmunoTargets and therapy, 2018. **7**: p. 35-49.
86. Graziani, G., L. Tentori, and P. Navarra, *Ipilimumab: a novel immunostimulatory monoclonal antibody for the treatment of cancer.* Pharmacol Res, 2012. **65**(1): p. 9-22.
87. Guo, L., H. Zhang, and B. Chen, *Nivolumab as Programmed Death-1 (PD-1) Inhibitor for Targeted Immunotherapy in Tumor.* Journal of Cancer, 2017. **8**(3): p. 410-416.
88. Garbe, C. and T.K. Eigentler, *Vemurafenib.* Recent Results Cancer Res, 2018. **211**: p. 77-89.
89. Dhillon, S., *Dabrafenib plus Trametinib: a Review in Advanced Melanoma with a BRAF (V600) Mutation.* Target Oncol, 2016. **11**(3): p. 417-28.

90. Gross, A.M., et al., *Selumetinib in Children with Inoperable Plexiform Neurofibromas.* N Engl J Med, 2020. **382**(15): p. 1430-1442.
91. Carvajal, R.D., et al., *Selumetinib in Combination With Dacarbazine in Patients With Metastatic Uveal Melanoma: A Phase III, Multicenter, Randomized Trial (SUMIT).* J Clin Oncol, 2018. **36**(12): p. 1232-1239.
92. Jiang, G., et al., *Dacarbazine combined targeted therapy versus dacarbazine alone in patients with malignant melanoma: a meta-analysis.* PloS one, 2014. **9**(12): p. e111920-e111920.
93. Quirt, I., et al., *Temozolomide for the Treatment of Metastatic Melanoma: A Systematic Review.* The oncologist, 2007. **12**: p. 1114-23.
94. Li, R.H., et al., *Temozolomide for Treating Malignant Melanoma.* J Coll Physicians Surg Pak, 2015. **25**(9): p. 680-8.
95. Quéreux, G. and B. Dréno, *Fotemustine for the treatment of melanoma.* Expert Opin Pharmacother, 2011. **12**(18): p. 2891-904.
96. Haferkamp, S., et al., *Patients with BRAF-Mutant Advanced/Metastatic Melanoma: Original Research on the Treatment Reality in Germany and Austria in the Era of Choice.* Advances in Therapy, 2020. **37**(8): p. 3619-3629.
97. Yu, C., et al., *Combination of Immunotherapy With Targeted Therapy: Theory and Practice in Metastatic Melanoma.* Frontiers in Immunology, 2019. **10**.
98. Sosman, J.A., et al., *Survival in BRAF V600-mutant advanced melanoma treated with vemurafenib.* The New England journal of medicine, 2012. **366**(8): p. 707-714.
99. Koelblinger, P., O. Thuerigen, and R. Dummer, *Development of encorafenib for BRAF-mutated advanced melanoma.* Current opinion in oncology, 2018. **30**(2): p. 125-133.
100. Robert, C., et al., *Five-Year Outcomes with Dabrafenib plus Trametinib in Metastatic Melanoma.* N Engl J Med, 2019. **381**(7): p. 626-636.
101. Lugowska, I., et al., *Trametinib: a MEK inhibitor for management of metastatic melanoma.* OncoTargets and therapy, 2015. **8**: p. 2251-2259.
102. Khunger, A., M. Khunger, and V. Velcheti, *Dabrafenib in combination with trametinib in the treatment of patients with BRAF V600-positive advanced or metastatic non-small cell lung cancer: clinical evidence and experience.* Ther Adv Respir Dis, 2018. **12**: p. 1753466618767611.
103. Larkin, J., et al., *Combined vemurafenib and cobimetinib in BRAF-mutated melanoma.* N Engl J Med, 2014. **371**(20): p. 1867-76.
104. Machado, S., et al., *Harmine and Piperlongumine Revert TRIB2-Mediated Drug Resistance.* Cancers (Basel), 2020. **12**(12).
105. Algazi, A.P., et al., *A dual pathway inhibition strategy using BKM120 combined with vemurafenib is poorly tolerated in BRAF V600E/K mutant advanced melanoma.* Pigment Cell & Melanoma Research, 2019. **32**(4): p. 603-606.
106. Mateo, J., et al., *A First-Time-in-Human Study of GSK2636771, a Phosphoinositide 3 Kinase Beta-Selective Inhibitor, in Patients with Advanced Solid Tumors.* Clinical Cancer Research, 2017. **23**(19): p. 5981-5992.
107. Coleman, M., et al., *Phase 2 study of parsaclisib (INCB050465), a highly selective, next-generation PI3Kδ inhibitor, in relapsed or refractory diffuse large B-cell lymphoma (CITADEL-202).* Leuk Lymphoma, 2021. **62**(2): p. 368-376.
108. Postow, M., et al., *434 Updated clinical data from the melanoma expansion cohort of an ongoing Ph1/1b Study of eganelisib (formerly IPI-549) in combination with nivolumab.* Journal for ImmunoTherapy of Cancer, 2020. **8**(Suppl 3): p. A264-A265.
109. Yap, T.A., et al., *First-in-Man Clinical Trial of the Oral Pan-AKT Inhibitor MK-2206 in Patients With Advanced Solid Tumors.* Journal of Clinical Oncology, 2011. **29**(35): p. 4688-4695.
110. Wright, S.C.E., et al., *Mechanisms of Resistance to PI3K Inhibitors in Cancer: Adaptive Responses, Drug Tolerance and Cellular Plasticity.* Cancers (Basel), 2021. **13**(7).

111. Khan, U., S.B. Kaushik, and R. Anvekar, *Recent Advances in Systemic Therapy for Malignant Melanoma.* SKIN The Journal of Cutaneous Medicine, 2020. **4**: p. 4.
112. Mucciolo, G., et al., *The dark side of immunotherapy: pancreatic cancer.* Cancer Drug Resistance, 2020. **3**(3): p. 491-520.
113. Ralli, M., et al., *Immunotherapy in the Treatment of Metastatic Melanoma: Current Knowledge and Future Directions.* Journal of immunology research, 2020. **2020**: p. 9235638-9235638.
114. Waldmann, T.A., *Cytokines in Cancer Immunotherapy.* Cold Spring Harb Perspect Biol, 2018. **10**(12).
115. Suarez-Kelly, L.P., et al., *A pilot study of interferon-alpha-2b dose reduction in the adjuvant therapy of high-risk melanoma.* Cancer immunology, immunotherapy : CII, 2019. **68**(4): p. 619-629.
116. Kumar, P., et al., *Recent advances with Treg depleting fusion protein toxins for cancer immunotherapy.* Immunotherapy, 2019. **11**(13): p. 1117-1128.
117. Harrington, K.J., et al., *Clinical development of talimogene laherparepvec (T-VEC): a modified herpes simplex virus type-1-derived oncolytic immunotherapy.* Expert Rev Anticancer Ther, 2015. **15**(12): p. 1389-403.
118. Morotti, M., et al., *Promises and challenges of adoptive T-cell therapies for solid tumours.* British Journal of Cancer, 2021.
119. Gide, T.N., et al., *Primary and Acquired Resistance to Immune Checkpoint Inhibitors in Metastatic Melanoma.* Clinical Cancer Research, 2018. **24**(6): p. 1260-1270.
120. Savoia, P., et al., *Targeting the ERK Signaling Pathway in Melanoma.* Int J Mol Sci, 2019. **20**(6).
121. Garcia-Alvarez, A., C. Ortiz, and E. Muñoz-Couselo, *Current Perspectives and Novel Strategies of NRAS-Mutant Melanoma.* OncoTargets and therapy, 2021. **14**: p. 3709-3719.
122. Grogan, N., et al., *Toxicities with targeted therapies after immunotherapy in metastatic melanoma.* Melanoma research, 2018. **28**(6): p. 600-604.
123. Meier, F., et al., *The RAS/RAF/MEK/ERK and PI3K/AKT signaling pathways present molecular targets for the effective treatment of advanced melanoma.* Front Biosci, 2005. **10**: p. 2986-3001.
124. Nikolaou, M., et al., *The challenge of drug resistance in cancer treatment: a current overview.* Clinical & Experimental Metastasis, 2018. **35**(4): p. 309-318.
125. Zargar, A., et al., *Overcoming the challenges of cancer drug resistance through bacterial-mediated therapy.* Chronic Diseases and Translational Medicine, 2019. **5**(4): p. 258-266.
126. Wang, X., H. Zhang, and X. Chen, *Drug resistance and combating drug resistance in cancer.* Cancer Drug Resistance, 2019. **2**(2): p. 141-160.
127. Cree, I.A. and P. Charlton, *Molecular chess? Hallmarks of anti-cancer drug resistance.* BMC Cancer, 2017. **17**(1): p. 10.
128. Mansoori, B., et al., *The Different Mechanisms of Cancer Drug Resistance: A Brief Review.* Advanced pharmaceutical bulletin, 2017. **7**(3): p. 339-348.
129. Yang, L., J. Fang, and J. Chen, *Tumor cell senescence response produces aggressive variants.* Cell Death Discovery, 2017. **3**(1): p. 17049.
130. Winder, M. and A. Virós, *Mechanisms of Drug Resistance in Melanoma.* Handb Exp Pharmacol, 2018. **249**: p. 91-108.
131. Poulikakos, P.I., et al., *RAF inhibitor resistance is mediated by dimerization of aberrantly spliced BRAF(V600E).* Nature, 2011. **480**(7377): p. 387-390.
132. Czarnecka, A.M., et al., *Targeted Therapy in Melanoma and Mechanisms of Resistance.* International journal of molecular sciences, 2020. **21**(13): p. 4576.
133. Marjanovic, N., R. Weinberg, and C. Chaffer, *Cell Plasticity and Heterogeneity in Cancer.* Clinical chemistry, 2012. **59**.
134. Papaccio, F., et al., *HGF/MET and the Immune System: Relevance for Cancer Immunotherapy.* International journal of molecular sciences, 2018. **19**(11): p. 3595.

135. Ko, B., et al., *MET/HGF pathway activation as a paradigm of resistance to targeted therapies.* Annals of translational medicine, 2017. **5**(1): p. 4-4.
136. Young, H.L., et al., *An adaptive signaling network in melanoma inflammatory niches confers tolerance to MAPK signaling inhibition.* The Journal of experimental medicine, 2017. **214**(6): p. 1691-1710.
137. Kaur, A., et al., *Remodeling of the Collagen Matrix in Aging Skin Promotes Melanoma Metastasis and Affects Immune Cell Motility.* Cancer Discovery, 2019. **9**(1): p. 64-81.
138. Gonzalez, H., C. Hagerling, and Z. Werb, *Roles of the immune system in cancer: from tumor initiation to metastatic progression.* Genes & development, 2018. **32**(19-20): p. 1267-1284.
139. Hugo, W., et al., *Genomic and Transcriptomic Features of Response to Anti-PD-1 Therapy in Metastatic Melanoma.* Cell, 2016. **165**(1): p. 35-44.
140. Zaidi, M.R., *The Interferon-Gamma Paradox in Cancer.* Journal of interferon & cytokine research : the official journal of the International Society for Interferon and Cytokine Research, 2019. **39**(1): p. 30-38.
141. Guo, J. and X. Zhou, *Regulatory T cells turn pathogenic.* Cellular & Molecular Immunology, 2015. **12**(5): p. 525-532.
142. Schmitt-Ney, M., *The FOXO's Advantages of Being a Family: Considerations on Function and Evolution.* Cells, 2020. **9**(3): p. 787.
143. Farhan, M., et al., *FOXO Signaling Pathways as Therapeutic Targets in Cancer.* International Journal of Biological Sciences, 2017. **13**(7): p. 815-827.
144. Calissi, G., E.W. Lam, and W. Link, *Therapeutic strategies targeting FOXO transcription factors.* Nat Rev Drug Discov, 2020.
145. Zhao, Y., et al., *Cytosolic FoxO1 is essential for the induction of autophagy and tumour suppressor activity.* Nature Cell Biology, 2010. **12**(7): p. 665-675.
146. Fasano, C., et al., *FOXO3a from the Nucleus to the Mitochondria: A Round Trip in Cellular Stress Response.* Cells, 2019. **8**(9).
147. Link, W., *Introduction to FOXO Biology.* Methods Mol Biol, 2019. **1890**: p. 1-9.
148. Link, W. and P.J. Fernandez-Marcos, *FOXO transcription factors at the interface of metabolism and cancer.* International Journal of Cancer, 2017. **141**(12): p. 2379-2391.
149. Yang, J.-Y., et al., *ERK promotes tumorigenesis by inhibiting FOXO3a via MDM2-mediated degradation.* Nature cell biology, 2008. **10**(2): p. 138-148.
150. Klotz, L.-O., et al., *Redox regulation of FoxO transcription factors.* Redox biology, 2015. **6**: p. 51-72.
151. Shats, I., et al., *FOXO transcription factors control E2F1 transcriptional specificity and apoptotic function.* Cancer research, 2013. **73**(19): p. 6056-6067.
152. Liu, Y., et al., *Critical role of FOXO3a in carcinogenesis.* Molecular Cancer, 2018. **17**(1): p. 104.
153. Paik, J.-H., et al., *FoxOs are lineage-restricted redundant tumor suppressors and regulate endothelial cell homeostasis.* Cell, 2007. **128**(2): p. 309-323.
154. Miller, T.W., et al., *Mutations in the phosphatidylinositol 3-kinase pathway: role in tumor progression and therapeutic implications in breast cancer.* Breast Cancer Research, 2011. **13**(6): p. 224.
155. Perri, F., S. Pisconti, and G. Della Vittoria Scarpati, *P53 mutations and cancer: a tight linkage.* Annals of translational medicine, 2016. **4**(24): p. 522-522.
156. Lambert, M., et al., *Targeting Transcription Factors for Cancer Treatment.* Molecules (Basel, Switzerland), 2018. **23**(6): p. 1479.
157. Patel, M.N., et al., *Objective assessment of cancer genes for drug discovery.* Nat Rev Drug Discov, 2013. **12**(1): p. 35-50.
158. Zanella, F., et al., *Chemical genetic analysis of FOXO nuclear-cytoplasmic shuttling by using image-based cell screening.* Chembiochem, 2008. **9**(14): p. 2229-37.
159. Ferreira, B.I., et al., *Small Molecule Inhibitors of CRM1.* Frontiers in Pharmacology, 2020. **11**(625).

160. Machado, S., et al., *Image-based Identification of Chemical Compounds Capable of Trapping FOXO in the Cell Nucleus.* Methods Mol Biol, 2019. **1890**: p. 163-170.
161. Cautain, B., et al., *Discovery of a Novel, Isothiazolonaphthoquinone-Based Small Molecule Activator of FOXO Nuclear-Cytoplasmic Shuttling.* PloS one, 2016. **11**(12): p. e0167491-e0167491.
162. Rahmani, K. and D.A. Dean, *Leptomycin B alters the subcellular distribution of CRM1 (Exportin 1).* Biochem Biophys Res Commun, 2017. **488**(2): p. 253-258.
163. Azizian, N.G. and Y. Li, *XPO1-dependent nuclear export as a target for cancer therapy.* Journal of Hematology & Oncology, 2020. **13**(1): p. 61.
164. Hornsveld, M., et al., *Re-evaluating the role of FOXOs in cancer.* Seminars in Cancer Biology, 2018. **50**: p. 90-100.
165. Lang, F., et al., *A phase I study of a dual PI3-kinase/mTOR inhibitor BEZ235 in adult patients with relapsed or refractory acute leukemia.* BMC Pharmacology and Toxicology, 2020. **21**(1): p. 70.
166. Cao, P., et al., *Activity of a novel, dual PI3-kinase/mTor inhibitor NVP-BEZ235 against primary human pancreatic cancers grown as orthotopic xenografts.* British Journal of Cancer, 2009. **100**(8): p. 1267-1276.
167. Simioni, C., et al., *Targeting the phosphatidylinositol 3-kinase/Akt/mechanistic target of rapamycin signaling pathway in B-lineage acute lymphoblastic leukemia: An update.* J Cell Physiol, 2018. **233**(10): p. 6440-6454.
168. Eyers, P.A., K. Keeshan, and N. Kannan, *Tribbles in the 21st Century: The Evolving Roles of Tribbles Pseudokinases in Biology and Disease.* Trends in Cell Biology, 2017. **27**(4): p. 284-298.
169. Ardito, F., et al., *The crucial role of protein phosphorylation in cell signaling and its use as targeted therapy (Review).* International journal of molecular medicine, 2017. **40**(2): p. 271-280.
170. Richmond, L. and K. Keeshan, *Pseudokinases: a tribble-edged sword.* The FEBS Journal, 2020. **287**(19): p. 4170-4182.
171. Chen, E.Y. and D.M. Clarke, *The PEST sequence does not contribute to the stability of the cystic fibrosis transmembrane conductance regulator.* BMC Biochemistry, 2002. **3**(1): p. 29.
172. Murphy, J.M., et al., *Molecular Mechanism of CCAAT-Enhancer Binding Protein Recruitment by the TRIB1 Pseudokinase.* Structure, 2015. **23**(11): p. 2111-21.
173. Li, K., et al., *TRIB3 Promotes APL Progression through Stabilization of the Oncoprotein PML-RARα and Inhibition of p53-Mediated Senescence.* Cancer Cell, 2017. **31**(5): p. 697-710.e7.
174. Salomé, M., L. Hopcroft, and K. Keeshan, *Inverse and correlative relationships between TRIBBLES genes indicate non-redundant functions during normal and malignant hemopoiesis.* Exp Hematol, 2018. **66**: p. 63-78.e13.
175. Keeshan, K., et al., *Tribbles homolog 2 inactivates C/EBPalpha and causes acute myelogenous leukemia.* Cancer Cell, 2006. **10**(5): p. 401-11.
176. Du, K., et al., *TRB3: a tribbles homolog that inhibits Akt/PKB activation by insulin in liver.* Science, 2003. **300**(5625): p. 1574-7.
177. Bailey, F.P., et al., *The Tribbles 2 (TRB2) pseudokinase binds to ATP and autophosphorylates in a metal-independent manner.* Biochem J, 2015. **467**(1): p. 47-62.
178. Murphy, J.M., et al., *A robust methodology to subclassify pseudokinases based on their nucleotide-binding properties.* Biochem J, 2014. **457**(2): p. 323-34.
179. Yoshino, S., et al., *Trib1 promotes acute myeloid leukemia progression by modulating the transcriptional programs of Hoxa9.* Blood, 2021. **137**(1): p. 75-88.
180. Keeshan, K., et al., *Transformation by Tribbles homolog 2 (Trib2) requires both the Trib2 kinase domain and COP1 binding.* Blood, 2010. **116**(23): p. 4948-57.
181. Yokoyama, T., et al., *Trib1 links the MEK1/ERK pathway in myeloid leukemogenesis.* Blood, 2010. **116**(15): p. 2768-2775.

182. Qu, J., et al., *TRIB3 suppresses proliferation and invasion and promotes apoptosis of endometrial cancer cells by regulating the AKT signaling pathway.* Onco Targets Ther, 2019. **12**: p. 2235-2245.
183. Wennemers, M., et al., *Tribbles homolog 3 denotes a poor prognosis in breast cancer and is involved in hypoxia response.* Breast Cancer Res, 2011. **13**(4): p. R82.
184. Wennemers, M., et al., *TRIB3 protein denotes a good prognosis in breast cancer patients and is associated with hypoxia sensitivity.* Radiother Oncol, 2011. **101**(1): p. 198-202.
185. O'Connor, C., et al., *Trib2 expression in granulocyte-monocyte progenitors drives a highly drug resistant acute myeloid leukaemia linked to elevated Bcl2.* Oncotarget, 2018. **9**(19): p. 14977-14992.
186. Campbell, K.J. and S.W.G. Tait, *Targeting BCL-2 regulated apoptosis in cancer.* Open biology, 2018. **8**(5): p. 180002.
187. García-Aranda, M., E. Pérez-Ruiz, and M. Redondo, *Bcl-2 Inhibition to Overcome Resistance to Chemo- and Immunotherapy.* International journal of molecular sciences, 2018. **19**(12): p. 3950.
188. Byrne, D.P., D.M. Foulkes, and P.A. Eyers, *Pseudokinases: update on their functions and evaluation as new drug targets.* Future Medicinal Chemistry, 2017. **9**(2): p. 245-265.
189. Foulkes, D.M., et al., *Covalent inhibitors of EGFR family protein kinases induce degradation of human Tribbles 2 (TRIB2) pseudokinase in cancer cells.* Science signaling, 2018. **11**(549): p. eaat7951.
190. Jamieson, S.A., et al., *Substrate binding allosterically relieves autoinhibition of the pseudokinase TRIB1.* Science Signaling, 2018. **11**(549): p. eaau0597.
191. Cortés, H., et al., *Repurposing of Drug Candidates for Treatment of Skin Cancer.* Frontiers in oncology, 2021. **10**: p. 605714-605714.
192. Otsuki, L. and A.H. Brand, *Cell cycle heterogeneity directs the timing of neural stem cell activation from quiescence.* Science, 2018. **360**(6384): p. 99-102.
193. Link, W., *Tribbles breaking bad: TRIB2 suppresses FOXO and acts as an oncogenic protein in melanoma.* Biochem Soc Trans, 2015. **43**(5): p. 1085-8.
194. Fang, Y., et al., *Tribbles homolog 2 (Trib2), a pseudo serine/threonine kinase in tumorigenesis and stem cell fate decisions.* Cell Communication and Signaling, 2021. **19**(1): p. 41.
195. Salome, M., et al., *A Trib2-p38 axis controls myeloid leukaemia cell cycle and stress response signalling.* Cell Death Dis, 2018. **9**(5): p. 443.
196. Ma, X., et al., *TRIB2 knockdown as a regulator of chemotherapy resistance and proliferation via the ERK/STAT3 signaling pathway in human chronic myelogenous leukemia K562/ADM cells.* Oncol Rep, 2018. **39**(4): p. 1910-1918.
197. O'Connor, C., et al., *The presence of C/EBPα and its degradation are both required for TRIB2-mediated leukaemia.* Oncogene, 2016. **35**(40): p. 5272-5281.
198. Wang, J., et al., *TRIB2 acts downstream of Wnt/TCF in liver cancer cells to regulate YAP and C/EBPα function.* Molecular cell, 2013. **51**(2): p. 211-225.
199. Guo, S., et al., *TRIB2 modulates proteasome function to reduce ubiquitin stability and protect liver cancer cells against oxidative stress.* Cell Death & Disease, 2021. **12**(1): p. 42.
200. Grandinetti, K.B., et al., *Overexpression of TRIB2 in human lung cancers contributes to tumorigenesis through downregulation of C/EBPα.* Oncogene, 2011. **30**(30): p. 3328-3335.
201. Hou, Z., et al., *TRIB2 functions as novel oncogene in colorectal cancer by blocking cellular senescence through AP4/p21 signaling.* Mol Cancer, 2018. **17**(1): p. 172.
202. Wang, J., et al., *Combined elevation of TRIB2 and MAP3K1 indicates poor prognosis and chemoresistance to temozolomide in glioblastoma.* CNS Neurosci Ther, 2020. **26**(3): p. 297-308.
203. Chen, Z., et al., *Knockdown of circ_0084043 suppresses the development of human melanoma cells through miR-429/tribbles homolog 2 axis and Wnt/β-catenin pathway.* Life Sci, 2020. **243**: p. 117323.

204. Wei, G., et al., *LncRNA ZEB1-AS1 promotes pancreatic cancer progression by regulating miR-505-3p/TRIB2 axis.* Biochemical and Biophysical Research Communications, 2020. **528**(4): p. 644-649.
205. Liu, C., et al., *LncRNA XIST promotes the progression of laryngeal squamous cell carcinoma via sponging miR-125b-5p to modulate TRIB2.* Bioscience reports, 2020. **40**(4): p. BSR20193172.
206. Jiang, C., et al., *TRIM21 causes abnormal expression of IL-6 in oral lichen planus via the TRIB2-MAPK signal axis.* American journal of translational research, 2020. **12**(8): p. 4648-4658.
207. Foulkes, D.M., et al., *Covalent inhibitors of EGFR family protein kinases induce degradation of human Tribbles 2 (TRIB2) pseudokinase in cancer cells.* Sci Signal, 2018. **11**(549).
208. Zhang, C., et al., *miR-511 and miR-1297 Inhibit Human Lung Adenocarcinoma Cell Proliferation by Targeting Oncogene TRIB2.* PloS one, 2012. **7**: p. e46090.
209. Zhang, Y.-X., et al., *Smad3-related miRNAs regulated oncogenic TRIB2 promoter activity to effectively suppress lung adenocarcinoma growth.* Cell Death and Disease, 2016. **7**: p. e2528.
210. Guo, J., et al., *miR-509-5p Inhibits the Proliferation and Invasion of Osteosarcoma by Targeting TRIB2.* BioMed Research International, 2019. **2019**: p. 2523032.
211. Zakrzewski, W., et al., *Stem cells: past, present, and future.* Stem cell research & therapy, 2019. **10**(1): p. 68-68.
212. Do, E.K., et al., *Trib2 regulates the pluripotency of embryonic stem cells and enhances reprogramming efficiency.* Experimental & molecular medicine, 2017. **49**(11): p. e401-e401.
213. Naiki, T., et al., *Naiki, T, Saijou, E, Miyaoka, Y, Sekine, K and Miyajima, A. TRB2, a mouse Tribbles ortholog, suppresses adipocyte differentiation by inhibiting AKT and C/EBPbeta. J Biol Chem 282: 24075-24082.* The Journal of biological chemistry, 2007. **282**: p. 24075-82.
214. Kim, H.S., et al., *TRIB2 regulates the differentiation of MLL-TET1 transduced myeloid progenitor cells.* J Mol Med (Berl), 2018. **96**(11): p. 1267-1277.
215. You, D., et al., *Long non-coding RNA MEG3 inhibits chondrogenic differentiation of synovium-derived mesenchymal stem cells by epigenetically inhibiting TRIB2 via methyltransferase EZH2.* Cell Signal, 2019. **63**: p. 109379.
216. Zanella, F., et al., *An HTS approach to screen for antagonists of the nuclear export machinery using high content cell-based assays.* Assay Drug Dev Technol, 2007. **5**(3): p. 333-41.
217. Tarrado-Castellarnau, M., et al., *Methylseleninic acid promotes antitumour effects via nuclear FOXO3a translocation through Akt inhibition.* Pharmacological Research, 2015. **102**: p. 218-234.
218. Martin, M., *Cutadapt removes adapter sequences from high-throughput sequencing reads.* 2011, 2011. **17**(1): p. 3.
219. Li, B. and C.N. Dewey, *RSEM: accurate transcript quantification from RNA-Seq data with or without a reference genome.* BMC Bioinformatics, 2011. **12**: p. 323.
220. Robinson, M.D., D.J. McCarthy, and G.K. Smyth, *edgeR: a Bioconductor package for differential expression analysis of digital gene expression data.* Bioinformatics, 2010. **26**(1): p. 139-40.
221. Chen, E.Y., et al., *Enrichr: interactive and collaborative HTML5 gene list enrichment analysis tool.* BMC Bioinformatics, 2013. **14**: p. 128.
222. Kuleshov, M.V., et al., *Enrichr: a comprehensive gene set enrichment analysis web server 2016 update.* Nucleic Acids Res, 2016. **44**(W1): p. W90-7.
223. Suarez-Arnedo, A., et al., *An image J plugin for the high throughput image analysis of in vitro scratch wound healing assays.* PLoS One, 2020. **15**(7): p. e0232565.
224. Mueller, J.K., et al., *Transcriptional regulation of the human KiSS1 gene.* Molecular and cellular endocrinology, 2011. **342**(1-2): p. 8-19.
225. Candi, E., et al., *Differential roles of p63 isoforms in epidermal development: selective genetic complementation in p63 null mice.* Cell Death Differ, 2006. **13**(6): p. 1037-47.

226. Lamb, J., *The Connectivity Map: a new tool for biomedical research.* Nat Rev Cancer, 2007. **7**(1): p. 54-60.
227. Lamb, J., et al., *The Connectivity Map: using gene-expression signatures to connect small molecules, genes, and disease.* Science, 2006. **313**(5795): p. 1929-35.
228. Musa, A., et al., *A review of connectivity map and computational approaches in pharmacogenomics.* Briefings in bioinformatics, 2018. **19**(3): p. 506-523.
229. Subramanian, A., et al., *Gene set enrichment analysis: a knowledge-based approach for interpreting genome-wide expression profiles.* Proceedings of the National Academy of Sciences of the United States of America, 2005. **102**(43): p. 15545-15550.
230. Livak, K.J. and T.D. Schmittgen, *Analysis of relative gene expression data using real-time quantitative PCR and the 2(-Delta Delta C(T)) Method.* Methods, 2001. **25**(4): p. 402-8.
231. Chou, T.C., *Drug combination studies and their synergy quantification using the Chou-Talalay method.* Cancer Res, 2010. **70**(2): p. 440-6.
232. Strober, W., *Trypan Blue Exclusion Test of Cell Viability.* Current protocols in immunology, 2015. **111**: p. A3.B.1-A3.B.3.
233. Song, G., et al., *Regulation of the C/EBPα signaling pathway in acute myeloid leukemia (Review).* Oncol Rep, 2015. **33**(5): p. 2099-2106.
234. Wang, X., et al., *KRT14 promoting invasion and migration of lung cancer cells through ROCK-1 signaling pathway.* International Journal of Clinical and Experimental Pathology, 2017. **10**: p. 795-803.
235. Schaefer, T., R. Steiner, and C. Lengerke, *SOX2 and p53 Expression Control Converges in PI3K/AKT Signaling with Versatile Implications for Stemness and Cancer.* Int J Mol Sci, 2020. **21**(14).
236. Li, Y., et al., *Inhibition of formin like 2 promotes the transition of ectopic endometrial stromal cells to epithelial cells in adenomyosis through a MET-like process.* Gene, 2019. **710**: p. 186-192.
237. Liu, Z., et al., *Direct Activation of Bax Protein for Cancer Therapy.* Medicinal research reviews, 2016. **36**(2): p. 313-341.
238. Wong, S.H.M., et al., *The TRAIL to cancer therapy: Hindrances and potential solutions.* Crit Rev Oncol Hematol, 2019. **143**: p. 81-94.
239. Wilhelmson, A.S. and B.T. Porse, *CCAAT enhancer binding protein alpha (CEBPA) biallelic acute myeloid leukaemia: cooperating lesions, molecular mechanisms and clinical relevance.* Br J Haematol, 2020.
240. Liu, K., et al., *BIRC7 promotes epithelial-mesenchymal transition and metastasis in papillary thyroid carcinoma through restraining autophagy.* Am J Cancer Res, 2020. **10**(1): p. 78-94.
241. Ly, T., S. Harihar, and D.R. Welch, *KISS1 in metastatic cancer research and treatment: potential and paradoxes.* Cancer Metastasis Rev, 2020.
242. Pasha, M., et al., *Sestrin2 as a Novel Biomarker and Therapeutic Target for Various Diseases.* Oxid Med Cell Longev, 2017. **2017**: p. 3296294.
243. Yoshida, G.J., *Beyond the Warburg Effect: N-Myc Contributes to Metabolic Reprogramming in Cancer Cells.* Front Oncol, 2020. **10**: p. 791.
244. Yu, J. and L. Zhang, *PUMA, a potent killer with or without p53.* Oncogene, 2008. **27 Suppl 1**(Suppl 1): p. S71-S83.
245. Yang, J., et al., *Statistical Methods for Identifying Differentially Expressed Genes in Replicated cDNA Microarray Experiments.* Statistica Sinica, 2000. **12**.
246. Hsu, C.-M., et al., *NVP-BEZ235 Attenuated Cell Proliferation and Migration in the Squamous Cell Carcinoma of Oral Cavities and p70S6K Inhibition Mimics its Effect.* International journal of molecular sciences, 2018. **19**(11): p. 3546.
247. Deng, L., et al., *The PI3K/mTOR dual inhibitor BEZ235 suppresses proliferation and migration and reverses multidrug resistance in acute myeloid leukemia.* Acta Pharmacologica Sinica, 2017. **38**(3): p. 382-391.

248. He, D., et al., *Effects of harmine, an acetylcholinesterase inhibitor, on spatial learning and memory of APP/PS1 transgenic mice and scopolamine-induced memory impairment mice.* Eur J Pharmacol, 2015. **768**: p. 96-107.
249. Prejanò, M., T. Marino, and N. Russo, *On the Inhibition Mechanism of Glutathione Transferase P1 by Piperlongumine. Insight From Theory.* Frontiers in Chemistry, 2018. **6**(606).
250. Mathijssen, R.H., et al., *Pharmacology of topoisomerase I inhibitors irinotecan (CPT-11) and topotecan.* Curr Cancer Drug Targets, 2002. **2**(2): p. 103-23.
251. Palomer, A., et al., *Identification of novel cyclooxygenase-2 selective inhibitors using pharmacophore models.* J Med Chem, 2002. **45**(7): p. 1402-11.
252. Zheng, G., et al., *Exploring the Inhibitory Mechanism of Approved Selective Norepinephrine Reuptake Inhibitors and Reboxetine Enantiomers by Molecular Dynamics Study.* Scientific Reports, 2016. **6**(1): p. 26883.
253. Bakowski, D., A.J. Wood, and A.B. Parekh, *Sequi Ad Maius Bonum; Targeting Ion Channels in the Lung.* Function (Oxf), 2021. **2**(1): p. zqaa045.
254. Khan, M., et al., *Oral administration of cytosolic PLA2 inhibitor arachidonyl trifluoromethyl ketone ameliorates cauda equina compression injury in rats.* J Neuroinflammation, 2015. **12**: p. 94.
255. Brierley, D.I. and C. Davidson, *Developments in harmine pharmacology--implications for ayahuasca use and drug-dependence treatment.* Prog Neuropsychopharmacol Biol Psychiatry, 2012. **39**(2): p. 263-72.
256. Piska, K., et al., *Piperlongumine (piplartine) as a lead compound for anticancer agents - Synthesis and properties of analogues: A mini-review.* Eur J Med Chem, 2018. **156**: p. 13-20.
257. Ishikawa, C., M. Senba, and N. Mori, *Effects of NVP-BEZ235, a dual phosphatidylinositol 3-kinase/mammalian target of rapamycin inhibitor, on HTLV-1-infected T-cell lines.* Oncology letters, 2018. **15**(4): p. 5311-5317.
258. Uhl, K.L., et al., *Harmine, a dual-specificity tyrosine phosphorylation-regulated kinase (DYRK) inhibitor induces caspase-mediated apoptosis in neuroblastoma.* Cancer Cell International, 2018. **18**(1): p. 82.
259. Yamaguchi, Y., T. Kasukabe, and S. Kumakura, *Piperlongumine rapidly induces the death of human pancreatic cancer cells mainly through the induction of ferroptosis.* Int J Oncol, 2018. **52**(3): p. 1011-1022.
260. Seoane, J., et al., *Integration of Smad and forkhead pathways in the control of neuroepithelial and glioblastoma cell proliferation.* Cell, 2004. **117**(2): p. 211-23.
261. You, H., et al., *FOXO3a-dependent regulation of Puma in response to cytokine/growth factor withdrawal.* J Exp Med, 2006. **203**(7): p. 1657-63.
262. Razavipour, S.F., K.B. Harikumar, and J.M. Slingerland, *p27 as a Transcriptional Regulator: New Roles in Development and Cancer.* Cancer Research, 2020. **80**(17): p. 3451-3458.
263. Rossin, A., G. Miloro, and A.-O. Hueber, *TRAIL and FasL Functions in Cancer and Autoimmune Diseases: Towards an Increasing Complexity.* Cancers, 2019. **11**(5): p. 639.
264. Hill, R., et al., *A novel phosphatidylinositol 3-kinase (PI3K) inhibitor directs a potent FOXO-dependent, p53-independent cell cycle arrest phenotype characterized by the differential induction of a subset of FOXO-regulated genes.* Breast Cancer Res, 2014. **16**(6): p. 482.
265. Mayoral-Varo, V., L. Jiménez, and W. Link, *The Critical Role of TRIB2 in Cancer and Therapy Resistance.* Cancers, 2021. **13**(11): p. 2701.
266. Rosich, L., et al., *Dual PI3K/mTOR inhibition is required to effectively impair microenvironment survival signals in mantle cell lymphoma.* Oncotarget, 2014. **5**(16): p. 6788-6800.
267. Liang, Y., et al., *TRIB2 contributes to cisplatin resistance in small cell lung cancer.* Oncotarget, 2017. **8**(65): p. 109596-109608.
268. KIM, J.N., et al., *Kisspeptin Inhibits Colorectal Cancer Cell Invasiveness by Activating PKR and PP2A.* Anticancer Research, 2018. **38**(10): p. 5791-5798.

269. Monga, J., et al., *Tribbles 2 confers enzalutamide resistance in prostate cancer by promoting lineage plasticity.* bioRxiv, 2021: p. 2021.03.26.437250.
270. Chen, D., et al., *Dual PI3K/mTOR inhibitor BEZ235 as a promising therapeutic strategy against paclitaxel-resistant gastric cancer via targeting PI3K/Akt/mTOR pathway.* Cell Death & Disease, 2018. **9**(2): p. 123.
271. Zhao, X., et al., *Transcriptional programming drives Ibrutinib-resistance evolution in mantle cell lymphoma.* Cell Reports, 2021. **34**(11).
272. Xu, S., et al., *TRIB2 inhibits Wnt/β-Catenin/TCF4 signaling through its associated ubiquitin E3 ligases, β-TrCP, COP1 and Smurf1, in liver cancer cells.* FEBS Letters, 2014. **588**(23): p. 4334-4341.
273. Xin, J.-X., et al., *miR-99 inhibits cervical carcinoma cell proliferation by targeting TRIB2.* Oncology letters, 2013. **6**(4): p. 1025-1030.
274. Broderick, J.A. and P.D. Zamore, *MicroRNA therapeutics.* Gene Therapy, 2011. **18**(12): p. 1104-1110.
275. Sakamoto, K.M., *Protacs for treatment of cancer.* Pediatric research, 2010. **67**(5): p. 505-508.
276. Lim, S.M., et al., *Development of small molecules targeting the pseudokinase Her3.* Bioorg Med Chem Lett, 2015. **25**(16): p. 3382-9.
277. Sun, X., et al., *PROTACs: great opportunities for academia and industry.* Signal Transduction and Targeted Therapy, 2019. **4**(1): p. 64.
278. Wang, Y., et al., *Degradation of proteins by PROTACs and other strategies.* Acta Pharmaceutica Sinica B, 2020. **10**(2): p. 207-238.
279. Jarada, T.N., J.G. Rokne, and R. Alhajj, *A review of computational drug repositioning: strategies, approaches, opportunities, challenges, and directions.* Journal of Cheminformatics, 2020. **12**(1): p. 46.
280. Chen, B., et al., *Reversal of cancer gene expression correlates with drug efficacy and reveals therapeutic targets.* Nature Communications, 2017. **8**(1): p. 16022.
281. Zerbini, L.F., et al., *Computational Repositioning and Preclinical Validation of Pentamidine for Renal Cell Cancer.* Molecular Cancer Therapeutics, 2014. **13**(7): p. 1929-1941.
282. van Noort, V., et al., *Novel drug candidates for the treatment of metastatic colorectal cancer through global inverse gene-expression profiling.* Cancer Res, 2014. **74**(20): p. 5690-9.
283. Subramanian, A., et al., *A Next Generation Connectivity Map: L1000 Platform and the First 1,000,000 Profiles.* Cell, 2017. **171**(6): p. 1437-1452.e17.
284. Radhakrishnan, A., et al., *A dual specificity kinase, DYRK1A, as a potential therapeutic target for head and neck squamous cell carcinoma.* Scientific Reports, 2016. **6**(1): p. 36132.
285. Zhang, C., et al., *Piperlongumine Inhibits Akt Phosphorylation to Reverse Resistance to Cisplatin in Human Non-Small Cell Lung Cancer Cells via ROS Regulation.* Front Pharmacol, 2019. **10**: p. 1178.
286. Hałas-Wiśniewska, M., et al., *The Synergistic Effect of Piperlongumine and Sanguinarine on the Non-Small Lung Cancer.* Molecules, 2020. **25**(13).
287. Lu, J.-J., et al., *Alkaloids Isolated from Natural Herbs as the Anticancer Agents.* Evidence-Based Complementary and Alternative Medicine, 2012. **2012**: p. 485042.
288. Garcia-Oliveira, P., et al., *Status and Challenges of Plant-Anticancer Compounds in Cancer Treatment.* Pharmaceuticals (Basel), 2021. **14**(2).
289. Chen, W., et al., *The synergistic effects of oxaliplatin and piperlongumine on colorectal cancer are mediated by oxidative stress.* Cell Death & Disease, 2019. **10**(8): p. 600.
290. Ye, W., et al., *Synergistic effects of piperlongumine and gemcitabine against KRAS mutant lung cancer.* Tumori, 2021. **107**(2): p. 119-124.
291. Atteya, R., et al., *Chemical screening identifies the β-Carboline alkaloid harmine to be synergistically lethal with doxorubicin.* Mechanisms of Ageing and Development, 2017. **161**: p. 141-148.

292. Wu, L.-W., et al., *Harmine suppresses the proliferation of pancreatic cancer cells and sensitizes pancreatic cancer to gemcitabine treatment.* OncoTargets and therapy, 2019. **12**: p. 4585-4593.
293. Niu, M., et al., *Piperlongumine is a novel nuclear export inhibitor with potent anticancer activity.* Chem Biol Interact, 2015. **237**: p. 66-72.
294. Liu, Z., et al., *Piperlongumine-induced nuclear translocation of the FOXO3A transcription factor triggers BIM-mediated apoptosis in cancer cells.* Biochem Pharmacol, 2019. **163**: p. 101-110.
295. Liu, J., et al., *Harmine induces cell cycle arrest and mitochondrial pathway-mediated cellular apoptosis in SW620 cells via inhibition of the Akt and ERK signaling pathways.* Oncol Rep, 2016. **35**(6): p. 3363-3370.
296. Greer, E.L. and A. Brunet, *FOXO transcription factors at the interface between longevity and tumor suppression.* Oncogene, 2005. **24**(50): p. 7410-7425.
297. Huang, H. and D.J. Tindall, *Regulation of FOXO protein stability via ubiquitination and proteasome degradation.* Biochimica et biophysica acta, 2011. **1813**(11): p. 1961-1964.
298. Wang, J., et al., *Impaired phosphorylation and ubiquitination by p70 S6 kinase (p70S6K) and Smad ubiquitination regulatory factor 1 (Smurf1) promote tribbles homolog 2 (TRIB2) stability and carcinogenic property in liver cancer.* J Biol Chem, 2013. **288**(47): p. 33667-33681.
299. Shrivastava, S., et al., *Piperlongumine, an alkaloid causes inhibition of PI3 K/Akt/mTOR signaling axis to induce caspase-dependent apoptosis in human triple-negative breast cancer cells.* Apoptosis, 2014. **19**(7): p. 1148-1164.
300. Bezerra, D.P., et al., *Overview of the therapeutic potential of piplartine (piperlongumine).* Eur J Pharm Sci, 2013. **48**(3): p. 453-63.
301. Roh, J.L., et al., *Piperlongumine selectively kills cancer cells and increases cisplatin antitumor activity in head and neck cancer.* Oncotarget, 2014. **5**(19): p. 9227-38.
302. Kang, Q. and S. Yan, *Piperlongumine reverses doxorubicin resistance through the PI3K/Akt signaling pathway in K562/A02 human leukemia cells.* Experimental and therapeutic medicine, 2015. **9**(4): p. 1345-1350.
303. Patel, K., et al., *Piperlongumine for Enhancing Oral Bioavailability and Cytotoxicity of Docetaxel in Triple-Negative Breast Cancer.* J Pharm Sci, 2015. **104**(12): p. 4417-4426.
304. Wang, X.-Q., et al. *Effect of piperlongumine on drug resistance reversal in human retinoblastoma HXO-RB44/VCR and SO-Rb50/CBP cell lines*. International journal of clinical and experimental pathology, 2015. **8**, 2525-2534.
305. Kim, H., S.O. Sablin, and R.R. Ramsay, *Inhibition of Monoamine Oxidase A by β-Carboline Derivatives.* Archives of Biochemistry and Biophysics, 1997. **337**(1): p. 137-142.
306. Göckler, N., et al., *Harmine specifically inhibits protein kinase DYRK1A and interferes with neurite formation.* The FEBS Journal, 2009. **276**(21): p. 6324-6337.
307. Woods, Y.L., et al., *The kinase DYRK1A phosphorylates the transcription factor FKHR at Ser329 in vitro, a novel in vivo phosphorylation site.* Biochem J, 2001. **355**(Pt 3): p. 597-607.
308. Rüben, K., et al., *Selectivity Profiling and Biological Activity of Novel β-Carbolines as Potent and Selective DYRK1 Kinase Inhibitors.* PLoS ONE, 2015. **10**: p. e0132453.
309. Wurzlbauer, A., et al., *How to Separate Kinase Inhibition from Undesired Monoamine Oxidase A Inhibition-The Development of the DYRK1A Inhibitor AnnH75 from the Alkaloid Harmine.* Molecules, 2020. **25**.
310. Zhu, Y.-R., et al., *The anti-cancer activity of the mTORC1/2 dual inhibitor XL388 in preclinical osteosarcoma models.* Oncotarget, 2016. **7**.
311. Yamamoto, M., et al., *Efficacy of Tumor-Targeting Salmonella A1-R on a Melanoma Patient-Derived Orthotopic Xenograft (PDOX) Nude-Mouse Model.* PLOS ONE, 2016. **11**(8): p. e0160882.